NIKHEF NATIONAL INSTITUTE FOR NUCLEAR PHYSICS AND HIGH-ENERGY PHYSICS

2003

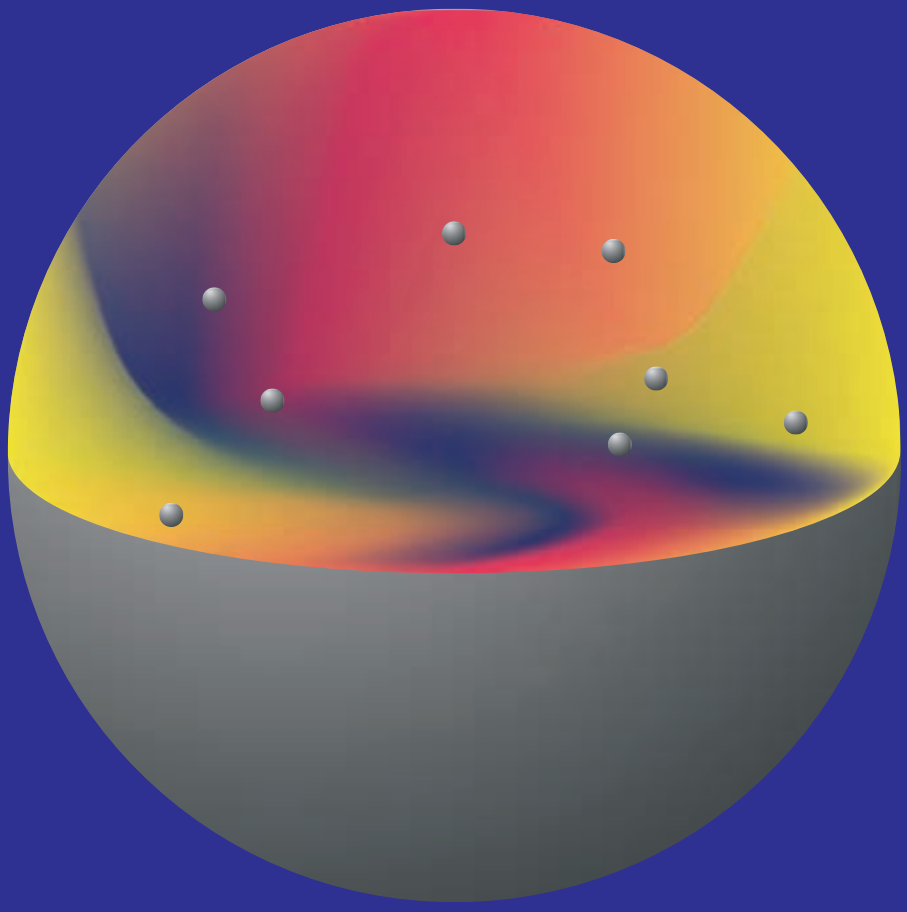

ANNUAL REPORT

NIKHEF

NATIONAL INSTITUTE FOR NUCLEAR PHYSICS AND HIGH-ENERGY PHYSICS

ANNUAL REPORT

2003

Kruislaan 409, 1098 SJ Amsterdam
P.O. Box 41882, 1009 DB Amsterdam

Colofon

Publication edited for NIKHEF:

Address:	Postbus 41882, 1009 DB Amsterdam Kruislaan 409, 1098 SJ Amsterdam
Phone:	+31 20 592 2000
Fax:	+31 20 592 5155
E-mail:	directie@nikhef.nl

Editors:	Louk Lapikás, Marcel Vreeswijk & Auke-Pieter Colijn
Layout & art-work:	Kees Huyser
Cover Photograph:	Relativistic fluid mechanics: impression of a fluid current moving on a sphere where scalar fields live.
URL:	`http://www.nikhef.nl`

NIKHEF is the National Institute for Nuclear Physics and High-Energy Physics in the Netherlands, in which the Foundation for Fundamental Research on Matter (FOM), the Universiteit van Amsterdam (UvA), the Vrije Universiteit Amsterdam (VUA), the Katholieke Universiteit Nijmegen (KUN) and the Universiteit Utrecht (UU) collaborate. NIKHEF co-ordinates and supports all activities in experimental subatomic (high-energy) physics in the Netherlands.

NIKHEF participates in the preparation of experiments at the Large Hadron Collider at CERN, notably Atlas, LHCb and Alice. NIKHEF is actively involved in experiments in the USA (D∅ at Fermilab, BaBar at SLAC and STAR at RHIC), in Germany at DESY (Zeus, Hermes and Hera-b) and at CERN (Delphi, L3 and the heavy-ion fixed-target programme). Furthermore astroparticle physics is part of NIKHEF's scientific programme, in particular through participation in the ANTARES project: a detector to be built in the Mediterranean. Detector R&D, design and construction of detectors and the data-analysis take place at the laboratory located in Sciencepark Amsterdam as well as at the participating universities. NIKHEF has a theory group with both its own research program and close contacts with the experimental groups.

Contents

Preface 1

A Experimental Programmes 3

1 The ATLAS Experiment 3

1.1 ATLAS experiment 3

1.2 DØ experiment 9

2 The B-Physics Programme 13

2.1 Introduction 13

2.2 Status of HERA-B 13

2.3 Status of the BaBar Experiment 13

2.4 The LHCb Vertex detector 15

2.5 Level-0 Pile-Up Veto System 18

2.6 The Outer Tracker of LHCb 18

2.7 Reconstruction and Physics Studies 22

3 Heavy Ion Physics 25

3.1 Introduction 25

3.2 Results from SPS experiments 25

3.3 Jet production and jet quenching studied in STAR 26

3.4 The Alice experiment at CERN 27

4 ANTARES 29

4.1 Introduction 29

4.2 Prototype Sector Line 29

4.3 On-shore data processing 30

4.4 Analysis methods 30

4.5 Outlook 31

5 ZEUS **33**

5.1 Introduction 33

5.2 ZEUS beats HERA beam background 33

5.3 Analysis HERA-I from 1991-2000 33

5.4 Performance of the ZEUS vertex detector 34

6 HERMES **37**

6.1 Introduction 37

6.2 Data taking 38

6.3 Physics analysis 38

6.4 Instrumentation 41

6.5 Outlook 43

7 DELPHI **45**

7.1 DELPHI programme and Detector exhibit 45

7.2 Publications 45

7.3 B physics 45

7.4 QCD 46

7.5 Standard Model Electroweak results 46

8 L3 **49**

8.1 Introduction 49

8.2 Searches 49

8.3 W and Z physics 49

8.4 QCD 51

8.5 L3+Cosmics 51

B Transition Programme **53**

1 New Detector R&D at NIKHEF **53**

1.1 Introduction 53

1.2 The readout of drift chambers with the Time-Pix-Grid 53

1.3 CMOS-based pixel detectors 55

1.4 X-ray imaging pixel detectors 55

2 Grid Projects **57**

2.1 Introduction 57

2.2 Local Facilities 57

2.3 The LHC Computing Grid Project 57
2.4 The DataGrid Project 57
2.5 AliEn 60
2.6 DØ Grid 60
2.7 EGEE 60
2.8 Virtual Laboratory for eScience 60

3 Experiments abroad 61
3.1 Proton-neutron knockout from ^{3}He induced by virtual photons 61

C Theoretical Physics 63

1 Theoretical Physics Group 63
1.1 Introduction 63
1.2 Physics of the standard model 63
1.3 Beyond the standard model 64
1.4 Cosmology, astrophysics and quantum gravity 64

D Technical Departments 67

1 Computer Technology 67
1.1 Computer system management 67
1.2 Project support 69

2 Electronics Technology 73
2.1 Introduction 73
2.2 Department developments 73
2.3 Projects 73

3 Engineering Department 79
3.1 ATLAS 79
3.2 LHCb 80
3.3 Alice Inner Tracking System 81
3.4 ANTARES 81
3.5 Alpha Magnetic Spectrometer 81
3.6 IdePhix 82

4 Mechanical Workshop 83

4.1 Introduction 83
4.2 Projects 83

E Publications, Theses and Talks 87

1 Publications 87

2 PhD Theses 98

3 Invited Talks 99

F Resources and Personnel 105

1 Resources 105

2 Membership of Councils and Committees during 2003 106

3 Personnel as of December 31, 2003 109

Preface

The CERN LHC program will start in 2007. This is an important date for many physicists worldwide and certainly also for NIKHEF and its scientific and technical staff. The construction of the various components of the large detectors ATLAS, LHCb and ALICE or instead sees steady progress. During 2003 we saw completion of 75 out of 96 muon chambers for ATLAS. NIKHEF scientists contributed in an important way to the H8 testbeam which validated many aspects of the ATLAS muon System. In LHCb an important achievement was the production of the first prototype secondary vacuum box. The LHCb outer tracker project has passed all necessary steps to enter the production phase. The ALICE experiment is also entering the production phase. NIKHEF contributes to electronics and readout. Together with industry, tooling has been developed for the positioning of the silicon ladders.

These preparations for the LHC program form an enormous challenge for the technical departments of NIKHEF. Their work is essential in the execution of the scientific program of NIKHEF, and in the preparation for future activities. At this point, with a deep sense of loss, I recall the decease of Paul Rewiersma of the electronics technology department. Paul started his work at NIKHEF with design work for the ACCMOR collaboration. His last contributions were to the ANTARES experiment.

The design and construction of detectors is only one activity towards the LHC program. In parallel, NIKHEF physicists participate in the DØ experiment at Fermilab, BaBar at SLAC and the STAR collaboration at Brookhaven. The aim is to be involved in frontline experimental research as well as to prepare for the many analysis tasks at similar LHC experiments.

The DØ experiment has performed a thorough analysis of the properties of the top-quark, with the important result that the value of the top-quarks mass is now $179.0 \pm 3.5 \pm 3.8$ GeV. This value is higher than the results from previous analyses. In combination with LEP data it means that the prediction for the Higgs mass is now also higher. A NIKHEF group joined BaBar at the end of the year 2002. These physicists have concentrated on the measurement of the angle γ, one of the parameters expressing CP-violation in the B system. The BaBar collaboration found the new charmed meson $D_s(2317)$ and discovered the decay $B \rightarrow \pi^0\pi^0$. Its branching fraction is an important input in further CP-violation studies. The STAR collaboration has obtained interesting results on the behavior of jets produced in heavy-ion collisions. These results are important for the ALICE Program.

In order to investigate phenomena like the Higgs mechanism or CP-violation, sound theoretical predictions are necessary. The NIKHEF theory group has been working on many aspects of the standard model and beyond. Here it remains clear that the algebra program FORM is an indispensable tool in this theoretical work. The theory group entered the field of astroparticle physics, a relatively new area of research.

From the start of LHC operations, the experimental group will have to deal with massive amounts of data at an unprecedented level. The development of the required grid technology is now well underway. NIKHEF plays a major role in the development of several grid technologies and its implementation in several grid projects such as VL-E and EGEE. The NIKHEF participation in DØ and other experiments provides good opportunities to test the grid for high-energy physics applications.

On the 17th of March 2003 the ANTARES collaboration successfully put the first data and control lines on the bottom of the Mediterranean Sea and connected the equipment to the junction box so that signals were available on shore on the same day. Although there was a problem with the reference clock, many aspects of the design could be validated. The completion of this neutrino telescope is foreseen in 2006.

The LEP program has officially come to an end in 2003; the enormous contribution of the LEP program to our current understanding of the standard model will be in the textbooks for many years to come. The NIKHEF program at the HERA collider has been the subject of

an extensive review by a panel chaired by J. Dainton. The committee underlined the high quality of the scientific work and made strong recommendations for the final stages and completion of the program at HERA.

Jos Engelen

During the year 2003 it became clear that Jos Engelen would not complete his five year term as director of NIKHEF. He was appointed by the CERN council as Chief Scientific Officer and deputy Director General of CERN. The NIKHEF community congratulates him with this great personal and scientific honor.

Karel Gaemers

A Experimental Programmes

1 The ATLAS Experiment

1.1 ATLAS experiment

A view of the ATLAS detector is shown in Figure 1.1. NIKHEF has significant detector construction responsibilities for the muon spectrometer (the outermost shells of the ATLAS detector; see Section 1.1) and for the central tracker (the part of the ATLAS detector nearest to the beam line; see Section 1.1). The preparations which should lead to a prominent presence in ATLAS data analysis can be found in Section 1.1. The progress regarding our participation in the DØ experiment at Fermilab is presented in Section 1.2.

One of the highlights in 2003 was the H8 test beam program at CERN with NIKHEF physicists taking an active part in the validation of the ATLAS muon spectrometer and silicon tracker detector hardware, readout electronics and data analysis. With the ATLAS detector construction work well underway, the efforts continue to shift to reconstruction software and physics performance studies. This led to major Dutch contributions to recent software releases. In December 2003, the Dutch ATLAS group organized a 3-day workshop in Lunteren to discuss the preparations leading to physics data analysis. This workshop was very successful and will be repeated in 2004. In 2003, five PhD theses were completed including the thesis of our first PhD student on the DØ experiment.

Muon spectrometer

The ATLAS muon spectrometer consists of a barrel and two end-caps. In the barrel region the muon track is measured by three concentric shells of muon chambers based on the Monitored Drift Tube (MDT) principle. In the end-caps the muon track is measured by three disks covered with MDT chambers. In the barrel region the magnetic field is generated by a huge superconducting toroid with eight coils. The magnetic field in the end-cap regions is generated by smaller superconducting toroids. NIKHEF is responsible for many components in the ATLAS muon spectrometer: the 96 Barrel Outer Large (BOL) MDT chambers; the barrel (RASNIK) alignment system; the complete detector monitoring (temperature and magnetic field) and control (initialization of the front-end electronics) and the highest level of the data acquisition system (the Muon Read-Out Driver or MROD). In addition Dutch industries construct the two large end-cap toroids.

The NIKHEF muon spectrometer detector construction responsibilities are near completion. As a consequence, most physicists are working on the analysis of H8 test beam data and the development of simulation and reconstruction software for the full ATLAS muon spectrometer. The only muon related hardware project remaining in the development phase is the precise calibration (order 0.01%) of 1200 magnetic field probes. This project is a collaboration between CERN and NIKHEF.

MDT chamber production

At the end of 2003, 75 of the 96 large BOL MDT chambers were completed at NIKHEF. During 2003, we gained extensive experience in equipping these chambers with services like alignment, temperature monitoring, gas distribution, front-end electronics cards and Faraday cages. The earlier difficulties with malfunctioning gas pipes have been solved. At this moment the only missing component is the so-called Chamber Service Module (CSM) which collects all data from the front-end electronics cards and sends them on a single fiber to the higher level data acquisition electronics (the MROD, see section 1.1 for more details). The CSMs are provided by our American colleagues and should be available in 2005. At NIKHEF we have already six prototype CSMs to operate the large cosmic-ray stand to test the 96 BOL MDT chambers under real operation conditions.

In agreement with the schedule, all 96 BOL MDT chambers will be transported to CERN in the fall of

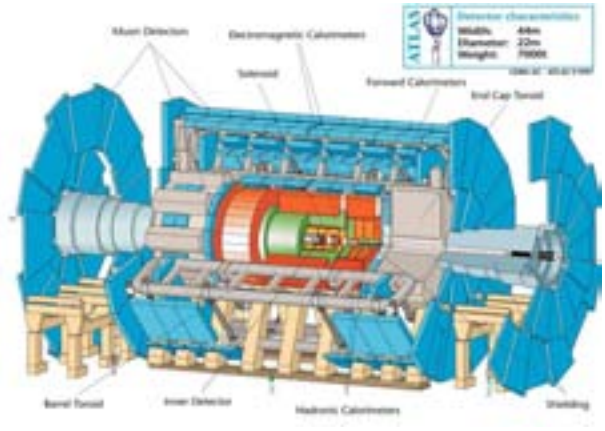

Figure 1.1: *Artist impression of the ATLAS detector.*

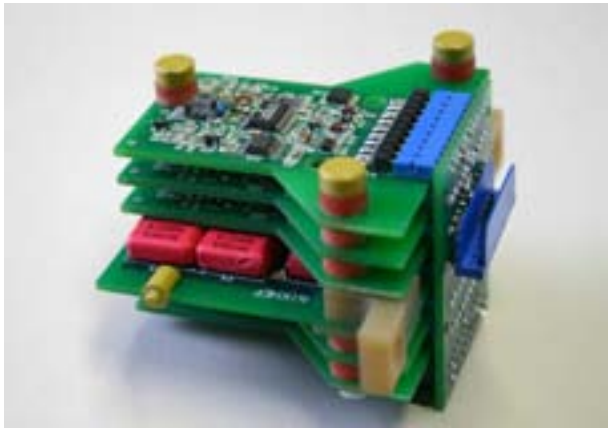

Figure 1.2: *The assembly of four magnetic field sensors and at the center one coil calibration card.*

Figure 1.3: *The magnetic field calibrator in the dipole magnet at CERN.*

2004 to be integrated with the resistive plate trigger chambers (RPCs) prior to their installation into the ATLAS cavern in 2005. The preparation of the MDT-RPC integration, including the construction of the common MDT-RPC mounting fixtures, was started in 2003 and apart from the worrisome RPC production schedule no other problems are foreseen.

RASNIK alignment status

In 2003 the calibration bench for the important so-called projective RASNIK alignment system was developed and demonstrated to be able to reach a precision of 4 μm, well below the target precision of 15 μm. Also in 2003 the next level in the multiplexed RASNIK readout scheme, the MasterMux, was designed, tested and submitted for serial production. This leaves, in accord with the schedule, for 2004 the design of the final USA15Mux as the last RASNIK related task to be completed.

Detector control system

The detector control system (DCS) for the ATLAS muon spectrometer is entirely developed by NIKHEF and comprises: temperature monitoring, magnetic field monitoring, initialization of the MDT front-end electronics and the monitoring of the voltages and temperatures on the MDT front-end electronics cards. The design of the system was completed in 2003 and, apart from the magnetic field sensors, all components are either available or are in production.

The magnetic field sensors make use of the Hall effect: on each sensor three orthogonally mounted Hall sensors are used to measure the value and the direction of the local magnetic field. The crucial aspect of these sensors is their calibration to a precision of 0.01%. This is realized by means of an ingenuous calibration bench (and procedure) originally developed by a group at CERN. This CERN device demonstrated the feasibility of the 0.01% precision. However, in 2002 it became clear that the CERN bench was not suitable for the serial calibration of the large number (1200) of ATLAS magnetic field probes and NIKHEF was asked to realize a robust and easy to operate calibration bench based on the CERN principle. As a concerted effort of the NIKHEF technical departments a state-of-the-art calibration tool was realized.

Figure 1.2 shows the calibration head with four magnetic field cards and one so-called coil card. The calibration principle requires the head to rotate uniformly in a very homogeneous (0.001%) magnetic field available at CERN. The magnitude of the homogeneous magnetic field itself is continuously monitored by an NMR probe. The magnetic induction in the coils is used to determine the instantaneous orientation of the head which allows to calibrate the three Hall sensors on each of the four magnetic field cards. Alternatively, the head can be moved in a stop-and-go mode in which case the instantaneous head position is taken from decoders mounted onto the two orthogonal rotation axes. Trial runs began late 2003 and revealed some defects which are under investigation at the moment. So far a precision of 0.1% was reached compared to the expected 0.01% precision. The installation of the calibrator in the gap of the dipole magnet at CERN is shown in Figure 1.3.

H8 test beam

As in the summer of 2002, also in the summer of 2003 the H8 muon spectrometer test beam setup was

the focal point of many NIKHEF activities. In 2003, a crucial new component in the test beam was the NIKHEF designed and constructed Muon Read-Out Driver (MROD) electronics card. The MRODs are the last stage in the muon data acquisition chain, each MROD serves the read-out of six MDT chambers. The commissioning of the MRODs in H8 proved less easy than anticipated. Nevertheless, little beam time was lost because during the first month of test beam running the CERN accelerator complex suffered from repeated breakdowns allowing ample time for MROD debugging. During the second half of the test beam period the MROD performance met the specifications thereby validating the full MDT read-out chain to be used in the complete ATLAS muon spectrometer. As in 2002, also in 2003 the detector control and alignment components and read-out electronics, provided by NIKHEF, operated as specified.

From the data analysis point of view the test beam provides a stimulating play-ground for in particular our PhD students. Significant progress was achieved in the simulation of the detailed muon induced signals in the individual muon drift tubes. Similarly the full potential of the front-end electronics (notably the time-slewing correction) was employed to further improve the resolution to a level below the original specification in the Muon Technical Design Report.

End-cap toroids

The two cold masses (CMs) are manufactured by Brush-HMA in Ridderkerk. Both CM's were due to be delivered and assembled at CERN in fall 2002. This schedule was shifted to a delivery end of 2003 for the first CM and end of 2004 for the second one. This scheme still matched the revised ATLAS time line. Winding of all 16 coils was completed end of 2003 and eight coils were impregnated by that time (all coils for one CM). Also eight keystone boxes were available after welding and machining at a subcontractor. Realization of the cooling circuits failed due to persistent problems in qualifying for the (manual) welding of the aluminum cooling pipes. This work was subcontracted. After many trials and despite expert advise the subcontractor concluded that these welds could only be realized successfully by orbital welding. The company had no experience with this type of welding and claimed extra costs for acquisition of the equipment, training of the welders and a partial replacement of the aluminum circuitry by stainless steel. Also the aluminum extrusions were not appropriate for orbital welding because of variations in the wall thickness. The last few years the CERN workshop acquired a lot of experience in orbital welding of aluminum pipes and fortunately it appeared possible to realize the cooling circuits at CERN. End of 2003 an agreement was reached to transfer the welding of the cooling circuits to CERN.

Central tracker

The central tracker employs three technologies for the measurements of charged tracks: nearest to the interaction point several layers with silicon pixel elements (the PIXEL detector); subsequently several layers with silicon strip detectors (the SCT detector[1]) and finally an arrangements of drift tubes (the TRT detector[2]). The complete central tracking volume sits within a large solenoid which provides a 2 T magnetic field.

NIKHEF is involved in the silicon strip detector, SCT, project and in particular in the construction of one of the two SCT end-caps. NIKHEF's main responsibility is the procurement of 2×9 high-precision carbon-fiber disks which are used to hold the many silicon detector modules. In addition NIKHEF constructs 80 silicon detector modules and at NIKHEF one complete end-cap is built and tested. The other end-cap is built in England. In 2003 excellent progress was made in this very difficult, multi-disciplinary and international project. Construction is in full swing at NIKHEF and the schedule is very tight for in-time delivery of the complete end-cap to CERN for installation in the ATLAS cavern in 2006.

SCT production

All 20 (including two spares) carbon-fiber disks which hold the silicon strip modules have now been delivered to NIKHEF. Early in the year, the manufacturer had difficulty meeting our stringent flatness requirements of 0.5 mm over the 1.2 m diameter. They refined their processing several times so that finally they could reliably achieve all specifications.

Before mounting services and modules on the disk, several access holes have to be machined, followed by the gluing of hundreds of plastic mounting pads. The tooling for this was developed early in the year, with delivery to England (RAL) of a prototype disk in January.

In order to position modules precisely and without risk of clashes, the mounting pads have to be the correct height. Machining them to a variation of less than 0.1 mm over the whole disk proved challenging. The method involves attaching the relatively floppy disk to a

[1] SCT is the acronym for Semi-Conductor Tracker.
[2] TRT is the acronym for Transition Radiation Tracker.

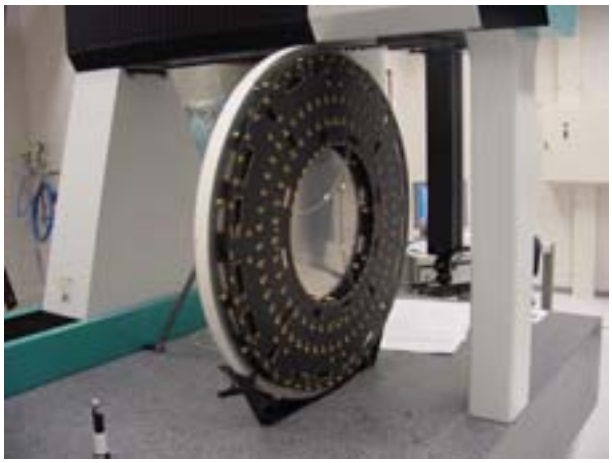

Figure 1.4: *Photo of a carbon-fiber support disk during verification of the mechanical accuracy using the 3D metrology measurement machine at NIKHEF.*

precise and stiff tool-plate, without distorting the disk. The mounting points can then be machined flat without the disk bending or vibrating. Finally the required precision was achieved when we realized the temperature had to be controlled to better than 0.5 ^{o}C to prevent the tool-plate from distorting. Figure 1.4 shows the final metrology inspection of a disk. The first production disk was delivered to England in October 2003.

NIKHEF will produce 80 of the 4000 modules in the SCT. These consist of two silicon-strip sensors glued together with better than 5 μm precision, with each of the 1536 strips bonded to its readout electronics. Assembly was delayed by the late delivery of version K5 of the hybrid containing the readout electronics, but at last in June production began of five "qualification" modules. These were completed and tested, exceeding specifications. This led to NIKHEF site-qualification in October and subsequently NIKHEF started mass production at the end of the year, reaching a peak rate of four modules per week. NIKHEF module assembly is expected to be completed late in 2004.

NIKHEF will equip nine disks with services and modules (total 1000), and assemble the disks into a carbon-fiber cylinder to complete one of the two SCT end-caps. The tooling for placing modules was well on its way to completion at the end of 2003. This has a rotating disk-holder and a module grabber with cameras and micrometer adjustment stages to align the module to the mounting pins on the disk. The modules have to be tested after mounting. The infrastructure for this includes cooling plant which was delivered in June, and a large test-box which was started at the end of the year.

The first disks should be assembled into the cylinder in 2004. The tooling design for this made major advances in 2003, with the main components ordered toward the end of the year.

Trigger, data-acquisition & detector control

The submission of the ATLAS trigger, data-acquisition (DAQ) and detector control system (DCS) Technical Design Report (TDR) at the end of June constituted an important milestone for the project. NIKHEF contributed in particular results from "paper" and "computer" models. Some further development of the existing computer model was required. The modeling results clearly show that the design presented in the report in principle can satisfy the performance requirements. The TDR has been formally approved.

The ROBIn prototype, a PCI board able to receive and buffer two 160 MByte/s data streams and with a Gigabit Ethernet network interface has become available for testing in 2003. The board is the result of a common project, in which the University of Mannheim, University of London (Royal Holloway) and NIKHEF participate. In the course of the year it was decided that the ROBIn boards will be located in rack-mounted PCs in the USA15 underground area. At the end of the year it was also decided that a new version of the board, able to receive and buffer three 160 MByte/s data streams and also with a Gigabit Ethernet network interface, will be designed. During the year, configuration code for the FPGA of the current prototype has been developed.

Muon Read-Out Driver

In the summer of 2003 the MROD, the Read-Out Driver for the muon chambers (MDTs), was deployed at the H8 test beam at CERN (see also Section 1.1). Two MROD modules were used successfully for reading out 12 MDTs. These modules use an older version of the ADSP-21160 SHARC processor of Analog Devices. Using the same design, for evaluation purposes a new module was built with the most recent version of this processor. It has been found that some problems have been solved, but reliable communication between the processors is still only possible at half of the specified speed (40 MByte/s in stead of 80 MByte/s per communication link with a 80 MHz processor clock). The "CSMUX" modules, originally developed as temporary facility for sending data from the TDCs on the chambers in the cosmic ray test stand to the MROD, have been converted into data generators. A CSMUX mod-

Figure 1.5: *Photo of the MROD test setup. The 9U VME crate at the left contains two MROD prototype modules. CSMUX modules in the crate at the right send simulated event data, formatted in the same way as data output by the Chamber Service Modules (CSMs) on the muon chambers, to the MROD under test.*

ule can now emulate the data produced by a chamber and send these to the MROD via an optical fiber. With the modules performance tests with realistic data are possible. A test setup is shown in Figure 1.5.

Operation of the MROD prototype above the maximum event rate of 100 kHz has been demonstrated for small events. For events with realistic sizes it is expected that this rate can also be sustained, but more complex software has to be developed to demonstrate this[3]. In view of the limited headroom of the current design and on the basis of recommendations by a review panel, in 2004 work on an upgrade of the design will be started, with the new Xilinx Virtex-II Pro FPGAs replacing the Altera FPGAs used in the prototypes. In first instance operation in the same way as the current prototype is foreseen. However, the new design will have a built-in upgrade possibility, as data transport via the communication links of the SHARC processors can be replaced by transport via the up to 3 Gbit/s serial links of the Xilinx FPGAs. This will result in a higher internal bandwidth of the MROD and reduce the processing load of the processors.

Detector Control System

In the detector control system (DCS) the Embedded Local Monitor Board (ELMB) plays an important role as the main building block of the DCS front-end I/O of the ATLAS sub detectors. The ELMB is also used in other LHC experiments. In total nearly 10,000 of these boards are being produced. In 2003 the software which is delivered with the ELMB has been developed further by NIKHEF. This software enables the ELMB to be used "off-the-shelf", or may be customized with limited effort in case of special requirements. The software has several features aimed at minimizing the effect of radiation induced bit flips in memories and registers. The tolerance of the hardware for radiation and the effectiveness of these features has been studied in several radiation tests with satisfactory results.

From simulation to reconstruction to physics analysis

The ATLAS software suite has matured considerably during the last year. The core software, called Athena, allows processing of events using detector services, conditional data, persistence etc. in a very modular fashion based on C++. Proton collision events can be generated with numerous event generators and single particle guns. Detector response is available using parameterizations (fast Monte Carlo) of the generated final state particles as well as by detailed detector simulation based on Geant4. Enormous effort was put in validating the Geant4 program and work is ongoing to reach correct simulation and digitization of all aspects of the ATLAS detector. Reconstruction algorithms are subsequently run in the same Athena environment, completing the chain between generation of simulated events and full reconstruction.

The most important tests of this complete software suite are the 'computing data challenges and a series of test beams. In 2003 NIKHEF was actively involved in the SCT and muon test beams at CERN as well as in the upcoming data challenge in 2004 (data challenge 2 or DC2).

In the ATLAS community the commissioning of the detector, both prior to data taking and during the first running periods, receive a lot of attention. A few months before the first proton collisions many subdetectors will be tested, calibrated and aligned using cosmic muons, whereas during the first running periods a number of 'standard' physics channels will provide indispensable tools for these tasks.

Inner tracker and muon spectrometer software

NIKHEF is playing a major role in developing and delivering key components of the inner detector software and bringing it into a production quality state for DC2

[3] This is due to the 40 MByte/s in stead of 80 MByte/s bandwidth available per SHARC communication link, making it necessary to transport the data across more links than in the tests done. Fortunately the MROD prototype offers support for this.

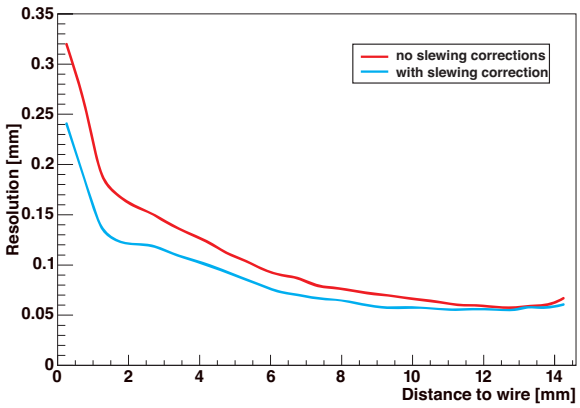

Figure 1.6: *The resolution of a Monitored Drift Tube (MDT) as a function of the distance to the wire with and without the time-slewing correction.*

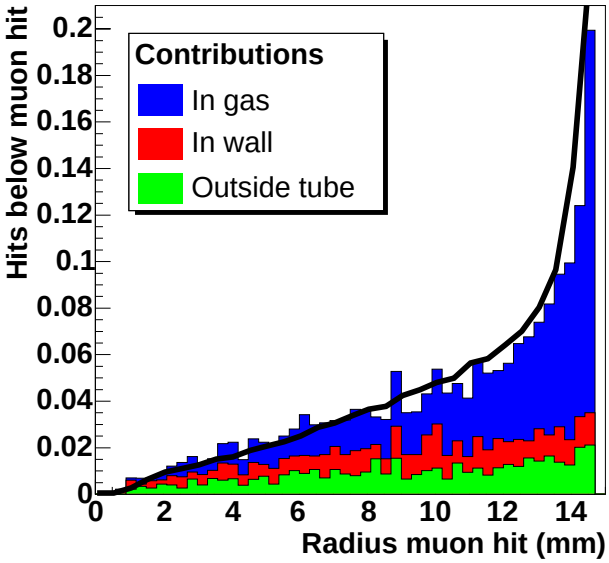

Figure 1.7: *The fraction of hits in a Monitored Drift Tube (MDT) obscured by a δ-electron as a function of the distance to the wire.*

and combined test beam running. NIKHEF is coordinating the developments of the detector description software for the inner detector and providing the geometry for the SCT and interface to reconstruction for the pixel and SCT detectors. We have reached the goal of using a common source for detector description (GeoModel) for Geant4 simulation, digitization and reconstruction and the full chain is operational. This detector description also includes the possibility of introducing alignment corrections and we have demonstrated this for the Pixel and SCT detectors. We continue to work on improving the realism of the SCT simulation and working on improvements to the SCT digitization.

The same software infrastructure used in the full ATLAS detector is also being used for the combined test beam. We have successfully demonstrated the use of common software components to simulate and reconstruct tracks in the test beam. During the test beam periods we actively participated in the data taking of the SCT, alignment of the modules, and straight track reconstruction. In particular we investigated the effect of inserting various targets in the beam-line, to induce a production vertex in the beam-line. Simulation of the set-up allowed to cross check the resolution of the space points and indicated the detector alignment was correctly understood. Reconstruction of track segments in the SCT system including pattern recognition, using ATLAS standard software tools, is ongoing.

NIKHEF is also actively involved in the Muon subsystem software, where we contribute to calibration, simulation, digitization and track reconstruction. We are coordinating the efforts to set up and implement in the Athena framework the calibration software for the complete muon spectrometer. We will also provide an implementation of the MDT calibration software, which is the most complicated calibration of the four detector technologies used in the muon system. We participated in the CERN H8 test-beam this summer, where (among other things) a new feature in the MDT read-out electronics, the so-called charge measurement, was introduced. With this charge measurement the time-slewing of the electronics can be corrected, and the resolution can be improved. The NIKHEF calibration software was extended to include this new measurement.

Figure 1.6 shows the MDT resolution as a function of the distance to the wire with and without this new time-slewing correction. The average resolution improves from 90 micron to 70 micron by using this new feature. For the simulation of the MDTs we improved the handling of δ-electrons, which are the main cause of inefficiency. Figure 1.7 shows the fraction of MDT hits that are hidden by δ-electrons, as a function of the distance to the wire. The various contributions to δ-electrons as generated in the Monte Carlo, after our improvements, sum up to the values as measured in our cosmic ray test set-up.

Effort is still ongoing in the MDT digitization, where a more detailed description of the MDT response is modeled. In particular, the new charge measurement and its correlation with the timing measurement is modeled by generating the full signal shape. The current

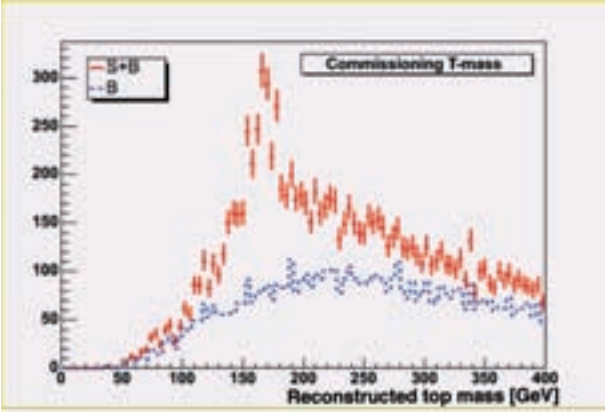

Figure 1.8: *Simulation of the top-quark signal in $t\bar{t}$ production at the LHC with one top quark decaying semi-leptonically.*

muon reconstruction software is not suited to reconstruct muons from cosmic origin, because it assumes that muons originate from the interaction point and this assumption is not valid for these cosmic muons. NIKHEF has started to develop muon reconstruction software that can cope with muons that do not come from the interaction point, in order to fully benefit from the detector commissioning period.

Physics studies

One of our primary interests in ATLAS is the discovery of the Higgs particle, and we have performed various studies on the Higgs particle in ATLAS. For example, after discovery of the Higgs particle we showed that its CP state can be determined from its decay to τ-lepton pairs. We also estimated Higgs production uncertainties originating from uncertainties in the underlying parton densities.

In addition our group focuses on top physics for a number of reasons. We have experience in top physics from the D$\emptyset$ experiment, top quark properties provide interesting checks on the Standard Model, the top quark production cross section is huge and will be used for calibration studies and provides feed-back on the detector during the commissioning period, it provides an excellent starting point for more involved Higgs studies, and NIKHEF plays a key role in theoretical aspects of (single) top quark physics.

NIKHEF is coordinating the validation of many generators for top production and background events, and we are responsible for event production in DC2. We will observe the top signal within a few days of data taking and are testing the measurement robustness against various detector commissioning stages.

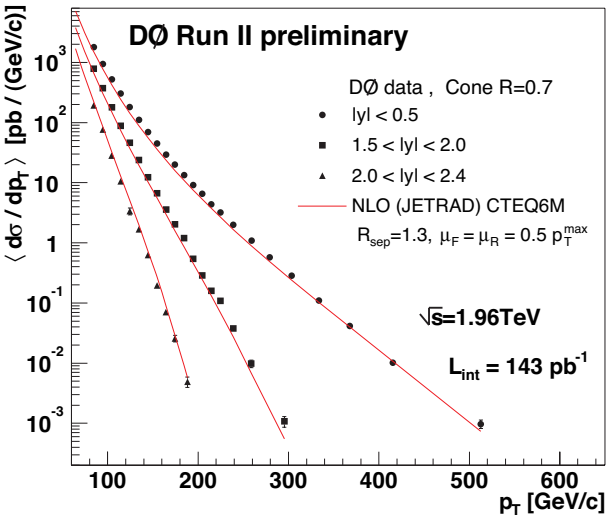

Figure 1.9: *Cross section for jet production (cone algorithm with $R = 0.7$), as a function of jet p_T, in various ranges of jet rapidity y, and a comparison to a NLO calculation.*

For example, in Figure 1.8 we show the single-leptonic top signal using MC@NLO with background coming from W plus 4 additional jets using the AlpGen generator, after a couple of days of data taking. In this figure no b-tagging is assumed to be present, as a pessimistic scenario for the startup period. We are involved in the mass determination of the top quark, and the observation of single top events in order to determine the Kobayashi-Maskawa matrix element V_{tb}. Furthermore we are in the process of developing strategies for the unexpected at ATLAS. We are studying the exciting possibility that with additional extra dimensions gravity becomes strong at the TeV scale, observable in graviton excitations in the TeV range.

1.2 D$\emptyset$ experiment

Run II of the Tevatron is aimed at collecting an integrated luminosity of at least 2 fb^{-1} before first LHC collisions. During 2003, the performance of the Tevatron has further improved upon the 2002 performance, and D$\emptyset$ collected data corresponding to an integrated luminosity of 150 pb^{-1}, which combined with the 2002 data gives more than 200 pb^{-1} for physics analysis. Further accelerator work is going on to improve performance, in particular the inclusion of the recycler for increased anti-proton storage capacity.

Detector hardware

The detector is complete and largely commissioned, and taking data with 85% efficiency. In 2003, a Level 1

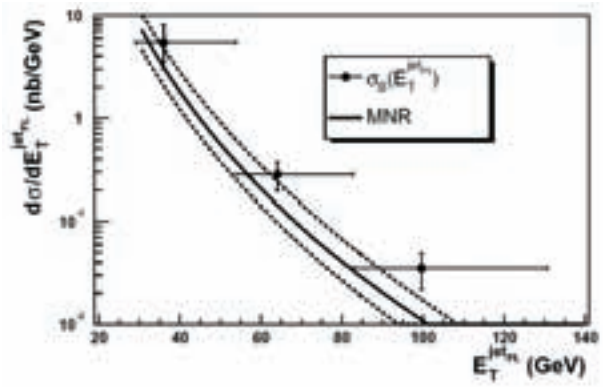

Figure 1.10: *Measured cross section for the production of b-quark jets as a function of jet E_T, and comparison to a NLO calculation (MNR). The uncertainty on the NLO calculation is shown as dashed lines.*

track trigger, CTT, became operational, and commissioning was started for a Level 2 displaced track trigger, STT. This trigger should be of significant help in triggering on particles containing bottom quarks. The performance of the tracker system (silicon strips and scintillating fibers) is good, and progress has been made in track reconstruction software. The calorimeter is operational, but has been suffering in 2003 from noise induced in the precision readout, leading to a non-optimal energy resolution and occasional fake jets. Extensive studies are going on to cure this in hardware and software.

The NIKHEF hardware responsibilities, a radiation monitor for the silicon tracker, a beam loss monitor system, and a Hall probe magnetic field monitoring system, have operated stably. The forward proton detectors, for which NIKHEF has designed and made positioning components, are now operational during data taking.

DØ computing

The NIKHEF group plays a role in pursuing full-scale data analysis outside Fermilab. With a much-improved event reconstruction program, all DØ Run II data taken up to September 2003 have been reprocessed in the last months of 2003, partly on NIKHEF computers. In order to achieve this, the DØ software was adapted to work on the European DataGrid, and the DØ data reprocessing has been a first real data test of that Grid system. In 2003, some seven million fully simulated Monte Carlo events were requested and produced. Data transfer to and from the DØ data management system SAM is automatic.

The DØ agenda server that has been setup in Nijmegen

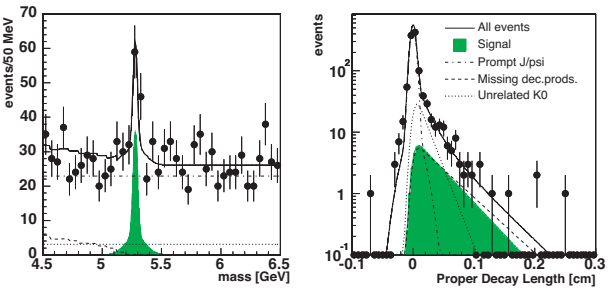

Figure 1.11: *Distribution of mass (left) and proper decay length (right) for reconstructed J/ψ K^0_S combinations, and the result of a combined mass-lifetime fit. The $B_d \to J/\psi\ K^0_S$ component resulting from the fit is shown as the shaded histogram.*

to allow for a homogeneous interface to all of DØś meetings and to facilitate posting of relevant documentation is widely used.

DØ software and physics analysis

Interesting physics results from Run I data are still appearing. Noteworthy is a new measurement of the top quark mass in the lepton plus jets decay channel, which combined with the other decay channels leads to the new DØ result $m_t = 179.0 \pm 3.5 \pm 3.8$ GeV. This is the most precise individual measurement of the top quark mass. The new top quark mass result is somewhat higher than the previous result, leading to an upward shift in the allowed Higgs boson mass range in Standard Model fits.

Physics analysis of Run II data has progressed well in 2003, boosted by the data reprocessing effort. Many analyzes now surpass the precision of the Run I analyzes, and some are new for DØ. Results have been submitted to conferences on searches for new particles and phenomena, W and Z boson production and decay, jet production (see Figure 1.9), B-meson production and lifetimes, and top quark production.

The NIKHEF group is interested in pursuing top physics and Higgs-boson searches, and look for new physics. In order to do so, students and staff are involved in the development of software for b-quark-tagging, jet identification, and lepton reconstruction. These tools have been used in 2003 for electroweak and top and bottom quark physics.

An important milestone in 2003 was the successful defense of the first dutch DØ PhD-thesis. The production of b-quarks can be recognized by secondary vertex reconstruction, track impact parameter tagging, and soft lepton tagging ($b \to c\ell\nu$). A NIKHEF PhD-student

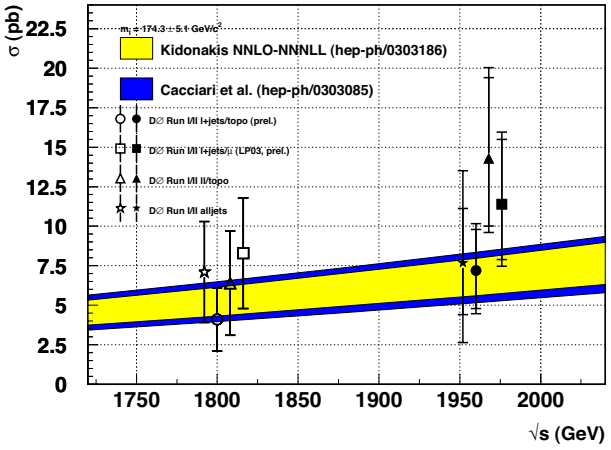

Figure 1.12: *Measured cross section for $t\bar{t}$ production in various final states, in Run I ($\sqrt{s} = 1.8$ TeV) and in Run II ($\sqrt{s} = 1.96$ TeV).*

has measured the cross section for the production of b-quark jets in the first Run II data, using soft muon tagging. The measured b-jet production cross section is shown in Figure 1.10 as a function of jet E_T, and is on the high side, but not incompatible with, a NLO calculation.

Algorithms have been developed for track impact parameter tagging, where signed impact parameters are used to calculate probabilities for tracks to originate from the primary vertex. These algorithms are being used to measure the dynamics of b-quark production, with the aim to disentangle the contributing processes of flavor creation, flavor excitation and gluon splitting. Also, the algorithms are used to search for $Z \rightarrow b\bar{b}$, an obvious prelude to Higgs-boson searches.

A further analysis focuses on an exclusive b-decay mode, namely $B_d \rightarrow J/\psi K^0_S$, which is one of a number of decays that are interesting for studies of CP violation in the B system. In Amsterdam, a PhD-student has reconstructed events in this decay mode and optimized the selection. The B_d lifetime was measured in these events from reconstructed B decay vertexes, as shown in Figure 1.11, as a first step toward CP violation measurements in DØ.

A b-tagging algorithm based on secondary vertex probabilities has been used for the study of top-quark-pair ($t\bar{t}$) production, and their hadronic decay into (at least) six jets. A first measurement of the $t\bar{t}$ production cross section in this all-hadronic decay mode has been made.

One PhD-student has finalized a NLO calculation of the single top quark production cross section, and has measured the $t\bar{t}$ production cross section in the electron plus jets decay mode. In this decay mode, and in the muon plus jets decay mode, likelihood discriminants are constructed to separate signal and background. The $t\bar{t}$ cross section measurements are summarized in Figure 1.12.

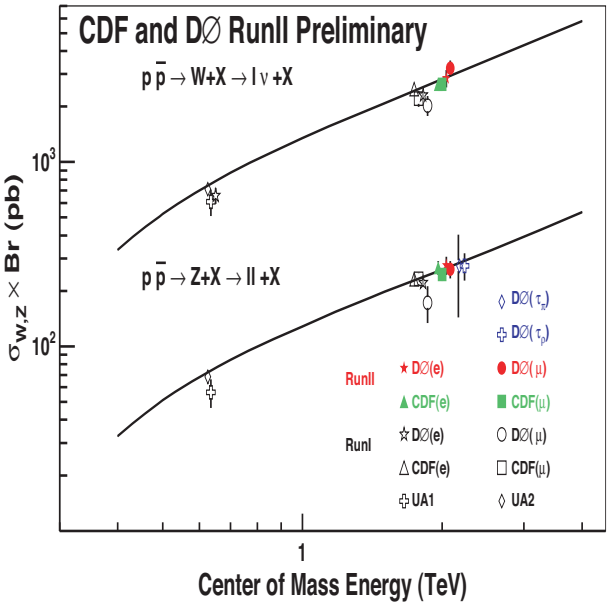

Figure 1.13: *Cross section for W and Z production and decay into electrons, muons, and taus final states.*

Further focus is placed on the identification of τ leptons using tracking and calorimetry. In Nijmegen, a PhD-student has measured the $p\bar{p} \rightarrow Z \rightarrow \tau^+\tau^-$ cross section, using a final state in which one τ decays to a muon and neutrino's, and the other τ hadronically into $\pi^{\pm}\nu$ or $\pi^{\pm}\pi^0\nu$. The result, together with other measurements of Z and W production and decay into electrons and muons, is shown in Figure 1.13. Furthermore, students are looking to improve the trigger for τ's and jets.

For 2004, the Tevatron foresees an additional 300 pb^{-1} of data, and a total of 5-8 fb^{-1} of data is expected to have been delivered by 2009. In 2003 it was decided that the DØ trigger system will be upgraded to cope with the higher luminosities foreseen, but that DØ will remain operating the current silicon micro-vertex detector until the end of Run II. A new inner layer of silicon strip detectors (Layer 0) will be installed in 2005, to improve the impact parameter resolution and counterbalance the radiation damage expected to occur in Layer 1.

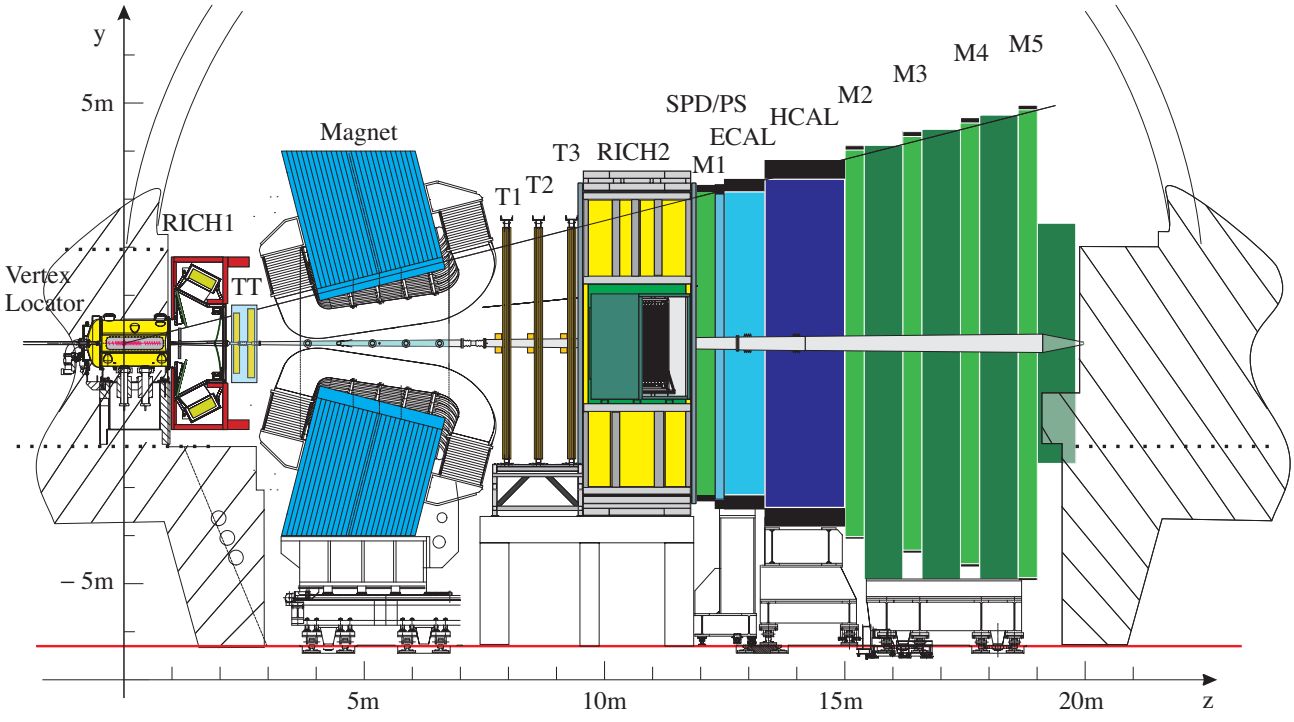

The LHCb detector layout.

2 The B-Physics Programme

2.1 Introduction

The main focus of the B physics group of NIKHEF is the participation in the LHCb experiment at CERN. The group is also active in the Hera-B experiment at DESY and the BaBar experiment at the Stanford Linear Accelerator Center (SLAC) in Palo Alto, U.S.A. Given the limited performance of both the experiment and the HERA accelerator, Hera-B will not contribute in a significant manner to our understanding of $\mathcal{CP}$ violation in the B system. Consequently, the NIKHEF group has decided to end its contributions toward Hera-B. In order to participate in a leading experiment on $\mathcal{CP}$ violation in the B system, NIKHEF joined the BaBar experiment at SLAC. Various accurate measurements to pinpoint the origin of $\mathcal{CP}$ violation can be made by BaBar, in this way preparing the group for measurements in LHCb. The LHCb experiment at the LHC collider of CERN, is planned to come into operation in April 2007. The development of the detector components for LHCb is generally proceeding on schedule. The same is true for software development and the study of data analysis methods.

2.2 Status of HERA-B

After a decision of the directorate of DESY, Hera-B has been shutdown by March 3rd, 2003. Until this moment, much less beam time has been available than was originally allotted to Hera-B. In fact, only about between 10 and 20 % of the envisaged data sample could be recorded in the period between November 2002, when HERA operation was stable enough for regular data taking with Hera-B, and beginning of March 2003, when HERA was shut down for the luminosity upgrade.

Nevertheless, this amounts to about 300,000 J/ψ events and about 220 million minimum bias events. The data are being analysed under many different aspects, but none of these analyses has yet been finalized. We give here an (incomplete) list of the subjects which are at present under work:

1. J/ψ polarization and differential distributions in the muon channel;
2. the $b - \bar{b}$ production cross section through detached $J/\psi \rightarrow \mu\mu$ events;
3. analysis of double semi-leptonic B-decays.
4. hyperon production, including $\Sigma(1385)$, Ξ, Λ_{1520}, Ξ^*_{1530}, and others ;
5. double-ϕ production;
6. D-meson production;
7. A-dependence and x_F-dependence of J/ψ production;
8. ratio of J/ψ and ψ' production;
9. Υ production;
10. Bose-Einstein correlations;
11. upper limit on $D^0 \rightarrow \mu\mu$. Our result appears to be 2 to 3 times more sensitive than the present upper limit.
12. Pentaquark analysis, including searches for Θ^+ and Ξ^{--}. Until now, we can only place upper limits on production cross sections, which are competitive in the light of the cross sections reported by other experiments.
13. χ_c - production ratio of $\chi_c \rightarrow J/\psi+\gamma$ with respect to. direct J/ψ production.

It is worthwhile to mention that the detector has been well under control after the commissioning period preceding the data taking period. This concerns the efficiencies and reliability of the different subsystems, and especially the understanding and operation of the First Level and Second Level triggers, which worked better than expected. At present, a major effort is invested in a better understanding of the efficiency map of the FLT, which is vital for the extraction of absolute cross sections.

2.3 Status of the BaBar Experiment

Introduction

At the end of 2002, NIKHEF joined the BaBar experiment (shown in Figure 2.1) at the Stanford Linear Accelerator Center in Palo Alto, U.S.A.

During 2003, the integrated luminosity recorded by the experiment increased by 57 fb^{-1} to a total of 152 fb^{-1}. Part of the large increase is due to the introduction in the second half of the year of the almost continuous (or 'trickle') injection into the low-energy ring of the PEP-II accelerator. Plans for next year include the same 'trickle' injection into the high-energy ring of the accelerator. Not only does this procedure bring the average

Figure 2.1: *Front view of the BaBar detector during maintenance.*

luminosity closer to the peak luminosity, but it also insures more stable running conditions of the accelerator. This in turn helps to increase the overall running efficiency, and thus the collected integrated luminosity. As a result, current extrapolations predict that by 2007 a sample of 500 fb^{-1} can be collected.

The increased luminosity collected during 2003 makes it possible to consider various new analysis opportunities. This is also clear from the record number of 25 papers published in refereed journals during 2003, bringing the total number of such papers to 49.

Physics Results

Even though the emphasis of the BaBar experiment is on the measurements of *CP* asymmetries in *B* decays, one of the surprises of 2003 was the discovery of a new charmed meson, the $D_s(2317)$. The mass of this excited state is lower than models had predicted. As a result, it has dropped below the threshold for the decay mode expected to dominate, leading in turn to a greatly reduced width. This discovery spawned renewed (theoretical) interest in the modeling of the *D* meson system. In addition to this discovery, BaBar also published new limits on *D* mixing.

Another first observation was that of the decay of $B \to \pi^0\pi^0$. The importance of this mode lies in the fact that the magnitude of the branching fraction of this mode determines how well one can relate the measured *CP* asymmetry in the decay $B \to \pi^{\pm}\pi^{\mp}$ to the CKM angle α. Unfortunately, although small in absolute terms, the relatively large value of this branching ratio, $(2.1 \pm 0.6 \pm 0.3) \cdot 10^{-6}$, only allows one to constrain the difference

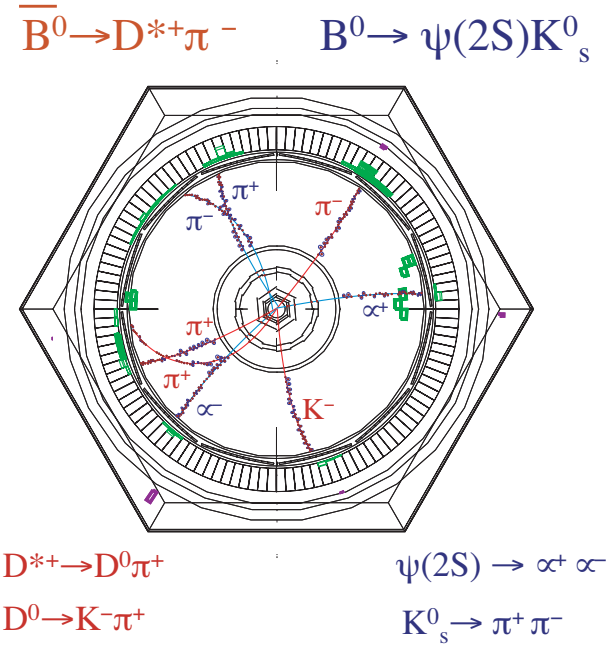

Figure 2.2: *A fully reconstructed event as seen by the BaBar detector. One of the B mesons has decayed through the decay chain* $B^0 \to J/\psi K^0_S$ *, followed by* $J/\psi \to \mu^+\mu^-$ *and* $K^0_S \to \pi^+\pi^-$ *, while the other B has been reconstructed as the decay* $\bar{B}^0 \to D^{*+}\pi^-$ *, with* $D^{*+} \to D^0\pi^+$ *with the subsequent decay* $D^0 \to K^-\pi^+$.

between the observed 'effective' angle and the CKM angle to be less than 47° at 90% CL.

Fortunately, the same construction also holds for the modes $B \to \rho^0\rho^0$ and $B \to \rho^+\rho^-$. In this case there is still only an upper limit on the branching ratio of $\mathcal{B}(B \to \rho^0\rho^0)$ of $2.1 \cdot 10^{-6}$, which implies the much stronger constraint that the angle α deviates less than 17° at 90%CL from the observed effective angle, making the determination of the *CP* asymmetry in $B \to \rho^+\rho^-$ a priority for next year.

The NIKHEF group has focused its interest on measurements which constrain the *CP* angle γ. The first step in this program is the measurement of *CP* asymmetry in the mode $B \to D^{(*)\mp}\pi^{\pm}$, where the decay is fully reconstructed. An example of such a reconstructed decay is shown in Figure 2.2. The *CP* asymmetry in this mode is proportional to $\sin(2\beta+\gamma)$, and, as $\sin 2\beta$ is well known from previous BaBar measurements, this measurement will thus constrain γ. The sensitivity to $\sin(2\beta+\gamma)$ originates from the interfer-

ence between the two amplitudes which contribute to this decay. The difficulty of this analysis lies in the fact that the *CP* asymmetry is not only proportional to $\sin(2\beta+\gamma)$, but also to *r*, the ratio of the two interfering amplitudes. Unfortunately *r* is too small to be measured directly in the foreseeable future, and must be obtained from other measurements and theoretical arguments. An additional complication is due to the coherent production of B and $\bar{B}$ at BaBar: the possibility of *CP* violation in the decay of the 'other' B meson produced simultaneously with the signal decay must be taken into account.

Notwithstanding these challenges, the first direct constraints on the angle γ could be set (see Figure 2.3), and a paper was submitted to Phys.Rev.Lett.

The next step in this program will be to use the decay $B \to D^{*\mp}\rho^{\pm}$. Due to the fact that the final state consists of two vector mesons, there are several amplitudes that contribute to this decay, depending on the helicity of the final state. The additional observables thus generated make the analysis more complicated, but do allow the determination the ratio of the amplitudes required to extract $\sin(2\beta+\gamma)$ without relying on theoretical assumptions which would otherwise limit the attainable accuracy.

2.4 The LHCb Vertex detector

This year significant progress was made on the production of the mechanical components for the vertex detector. An important achievement was the production of the first prototype secondary vacuum box for the detectors shown in Fig. 2.4. The top, side and end foils were produced with the hot-metal-gas forming method, in which an 0.3 mm thick AlMg3 foil (an aluminum alloy with 3% magnesium) is heated in a special mold in 4 hours to 350°C, after which the foil is pressed by heated gas into the mold. A start has been made with the verification of the required shape on a 3D measuring machine.
Also the first prototype of the rectangular bellow has been produced. The bellow consists of two sets of 20 stainless steel shells. The fully welded assembly is shown in Fig. 2.5.

A large amount of production drawings for the mechanical components of the Vertex detector have been submitted to the EDMS system at CERN. The drawings for the pipe frame stand, the Y-translation frame, the center frame and the detector support have been approved. Several other ones are under approval.

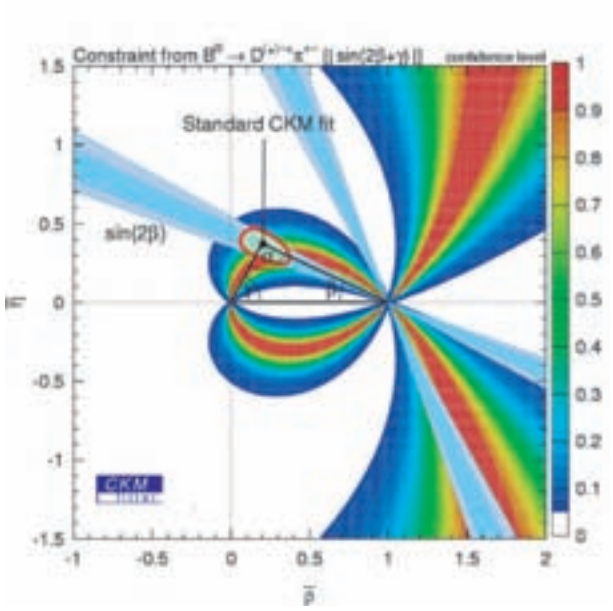

Figure 2.3: *Constraints on the plane spanned by the ρ and η parameters which appear in the Wolfenstein parameterization of the CKM matrix. The definitions of the three CP angles α, β and γ are indicated. The constraints from the analysis of fully reconstructed $B \to D^{(*)\mp}\pi^{\pm}$, combined with the results from partially reconstructed $B \to D^{*\mp}\pi^{\pm}$ are shown in colour according to their confidence level. In addition, the constraints on the angle β from the measurements of CP asymmetries in the 'golden' CP modes like $B \to J/\psi K^0_S$ are indicated. The region allowed by these two measurements of CP asymmetries is consistent with the area obtained from the Standard CKM fit.*

One of the principal components is the vacuum vessel. The results of the Finite Element Analysis have been approved by TIS (the Technical Inspection and Safety Department at CERN).
An issue that is still under discussion is if a Viton O-ring can be applied between the detector vacuum and the beam vacuum. In the present design such a ring with small compression forces is required to avoid deformation of the flanges, and consequently of the detector housing. If the system needs to be vented for detector maintenance the permeation through such an O-ring might saturate the NEG material in the beam pipe. Both CERN and NIKHEF have therefore performed permeation measurements. From the NIKHEF results we concluded that the amount of gas that permeates through the O-rings can considerably be reduced if both the beam vacuum and detector

Figure 2.4: *The first completed secondary vacuum box.*

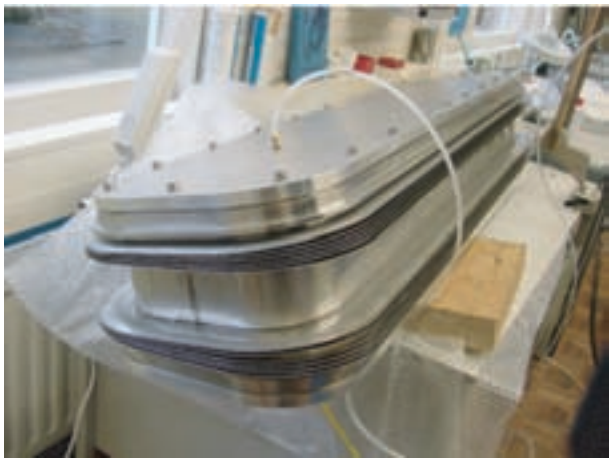

Figure 2.5: *The prototype rectangular bellow.*

vacuum will be vented with ultra-pure neon, and if the access to the detector system can be limited to 50 hours. Under those conditions the detectors can be accessed about 20 times before the NEG material has

Figure 2.6: *The pipe frame stand and the Y-translation frame have been placed in the South hall of the former PIMU building. Here, the complete system will be assembled and tested.*

to be reactivated.
From the approved items, the machine shops at NIKHEF and the VU have produced the pipe frame stand and the Y-translation frame. The center frame undergoes its final machining. The detector support is under construction. The whole system will be assembled in the South hall of the former PIMU-hall. The pipe frame stand and the Y-translation frame have been installed already, as shown in Fig. 2.6.

The VU has also produced several cylindrical vacuum vessels, shown in Fig. 2.7. They will provide realistic volumes (1900 l for the primary vacuum system, 500 l for the secondary one) to perform evacuation and venting simulation tests in order to optimize the evacuation and venting procedures. The vessels will also be used for integral leak tests of the secondary vacuum boxes and the bellows. Furthermore, two of them will be used as container for coating the outside of the secondary vacuum boxes with a layer of NEG material. This process will be performed at CERN.
For controlling the venting and evacuation processes, membrane switches will be used. The reliability of these devices has been checked: their behavior remained constant within 0.1 mbar over 20,000 switching cycles. This roughly corresponds with 800 evacuations. The switches have been modified at NIKHEF in order to equip them with all-metal seals at the beam vacuum side. The complete set of switches that will be used in LHCb is shown in Fig. 2.8.

Figure 2.7: *Test vessels for the evacuation and venting simulations. The complete volume is comparable to the volumes in the actual set-up. With this system the evacuation and venting tests can be performed with realistic volumes.*

Figure 2.8: *Membrane switch assembly to be used to control the evacuation and venting procedures at LHCb.*

A service agreement between the LHC vacuum group (AT-VAC) and NIKHEF is being worked on. CERN will take the operational responsibility, NIKHEF will perform maintenance tasks. A functional specification document from the AT-VAC is under discussion.

The kapton cables, that transport the signals from the silicon sensors to the trigger electronics, have undergone mechanical stress tests. The set-up is shown in Fig. 2.9. The end parts of the cable were translated

Figure 2.9: *Set-up for endurance tests of the flat cables that will be used in the vacuum system. The 30 mm displacement corresponds with the expected movement during injection of the LHC beams.*

Figure 2.10: *The optimized wakefield suppressor which produces an almost perfect rf match between the beam pipe and the detector vacuum boxes, both in open and closed position.*

over 30 mm. In part of the tests the end parts were also moved by 5 mm in the vertical direction. This corresponds to the expected displacement during injection of the LHC beams. After 40,000 cycles with only the horizontal displacement and another series of 30,000 cycles with the combined one no cracks or other damage was observed.
The optimized wake field suppressor as shown in Fig. 2.10 eliminates almost all resonances, both in

open and closed position of the detector halves. Also the endurance tests for this wake field suppressor have been performed. Opening the wake field suppressor by 30 mm (as required during injection) and a perpendicular displacement over 5 mm resulted in no damage after 30,000 cycles.
Extensive measurements have been done on the outgassing from all components of the detector system. Therefore, samples have been tested from the kapton cables and the components of the detector module (hybrid, TPG material, paddle base and heat connector interface). The dominant contribution comes from the paddle base and the flat cable connectors. The total pressure in the detector vacuum is estimated to be 3×10^{-5} mbar. This is quite acceptable for the secondary detector vacuum.
A start has been made with the construction of a CO_2 cooling set-up. The water cooling and the freon cooling system have been installed. With this system the properties and cooling performance will be studied. Also extensive heat transfer model calculations have been performed. A first indication is that the TPG material is sufficient to cool the detector, but that the heat connection interface needs a considerable improvement. The contribution from the rf heating of the secondary vacuum box is quite small. This is especially due to the fact that the torlon coating at the inside of the secondary vacuum box strongly improves the emissivity of the box.

Development of a radiation hard front-end chip for the vertex detector of LHCb

The development of a radiation hard front-end chip in 0.25 μm CMOS technology for the vertex detector of LHCb is approaching its final stage. In a collaboration between the ASIC-lab in Heidelberg and NIKHEF new submissions have been prepared and produced. Presently, the 128 channel 40 MHz full-size chip *Beetle*1.3, is under investigation in laboratory tests at Heidelberg, Zürich, CERN, Lausanne and NIKHEF. Beam tests and measurements with a radioactive source are performed on silicon sensor and hybrid prototypes, equipped with *Beetle*1.2 and *Beetle*1.3 chips. It has been decided that one more iteration will be made, i.e., a *Beetle*1.4 is going to be produced, while the production schedule remains within the overall VELO planning.

2.5 Level-0 Pile-Up Veto System

The Level-0 Pile-Up Veto System is designed to reject crossings with multiple interactions at the first trigger level of LHCb. An LHCb Trigger Trigger Design Report (TDR) with a description of the Pile-Up system has been submitted in September, the approval of the TDR by the LHCC followed later.

Crucial elements of the system for which a close collaboration with other institutes within LHCb now exists, are

- The Beetle chip for the readout of 2 planes of silicon strip detectors. The 1.3 version Beetle chip has been tested extensively with respect to the comparator part for which NIKHEF is responsible
- The optical digital transfer of signals from the detector to the processor system. A common project has started concerning all optical links within LHCb.

At NIKHEF tests of the prototype of the processor board have been concluded: it fulfills the requirements of being able to run at 40 MHz. The work is now focused on the second submit of the Pile-Up hybrid (since the first submit failed) and on the optical data transfer system.

2.6 The Outer Tracker of LHCb

The Outer Tracker project has gone through all phases leading to the launch of the mass production of the detector modules:

- the engineering design of the detector has been finalised, presented to the LHCb collaboration and reviewed by an external panel in the Engineering Design Review (EDR) in May 2003;
- production tools have been designed and realized and shipped to all production sites;
- contracts for the production of all detector material and parts have been signed and quality assurance plans drafted. The flow of most materials toward the production centers passes through NIKHEF;
- many detector prototypes have been constructed and tested. On the basis of those results, the production has been launched. Work instructions and Quality Assurance (QA) plans for the production have been written up and will be reviewed in the Production Readiness Review (PRR) of May 2004.

Considerable progress in the Front-End Electronics, entirely NIKHEF responsibility, was made: two full pro-

Figure 2.11: *Straw Preparation Tool.*

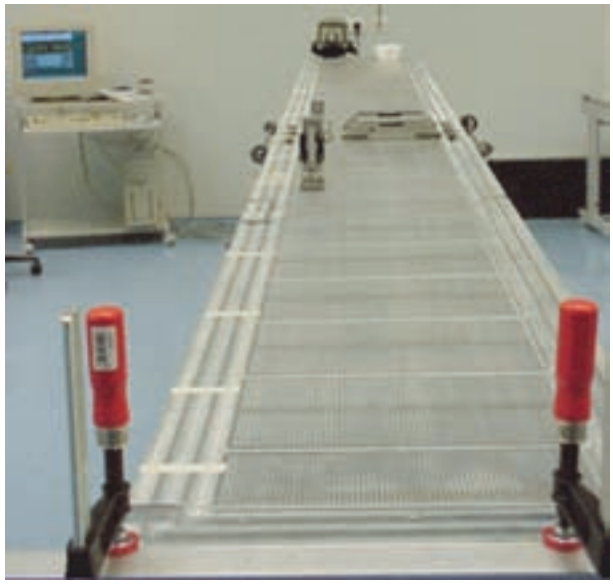

Figure 2.12: *Straw Template Tool aligned with laser interferometry.*

totypes of the FE Electronics boxes have been constructed and tested at NIKHEF. Moreover, the engineering design of the detector infrastructure (support frames, detector services, etc.) has been started and foresees the assembly of 1/4 station (two layers of modules, FE Electronics, frames and services) at NIKHEF before the end of 2004.

OT Module Production

Once the engineering design of the detector modules was reviewed and approved, of crucial importance became the completion of production and QA tools. NIKHEF played a central role, being responsible for the design, production and commissioning of two of the main production tools, the Straw Preparation Tool (SPT) and the Straw Template Tool (STT), as well as of the Wire Tension Meter, HV testing, and source scanning QA tools.

The SPT is used to "prepare" straws by cutting them to length, inserting wire locators, preparing a piece of straw at one end ("tongue") for GND connection and soldering this tongue ultrasonically. Three SPTs were designed and produced by the VU group, and delivered and commissioned to all production centers.

The STT is essentially an alignment jig, where all 64 straws forming a mono-layer are accurately aligned next to each other, to be later glued to their supporting panel. The high intrinsic resolution of the drift-cells (about 200 μm) requires very tight mechanical tolerances (of the order of $\pm$50 μm) in the straw-alignment pattern. The STT also plays a crucial role in defining the detector planarity; this results in the request of a jig planarity tolerance of $\pm$100 μm, by no means a trivial requirement for objects about 40 cm wide and up to 5 m long. The High Tech Aerospace unit of the Philips Enabling Technologies Group produced 5 STTs (3 of 5m and 2 of 2.5m) based on the design of the Engineering Department of NIKHEF. These jigs were aligned to the required accuracies with the help of laser interferometry, as shown in Figs. 2.12 and 2.13.

Once production tools were ready, a long period of prototype production and QA tests followed, at the end of which the first full-size (5m) modules, shown in Fig. 2.14, were produced at NIKHEF.

At that stage of the project, we concentrated on controlling the quality of the production in a stable and reliable way. The Wire Tension Meter (WTM) tool, shown in Fig. 2.15, was designed and produced at NIKHEF: the tensions of the strung wires is measured by inducing a mechanical oscillation in each wire by means of a short electrical pulse, and measuring the main resonance frequency of the wire in a magnetic field. We commissioned three of these devices and delivered them to all production centers; the details can be found in the

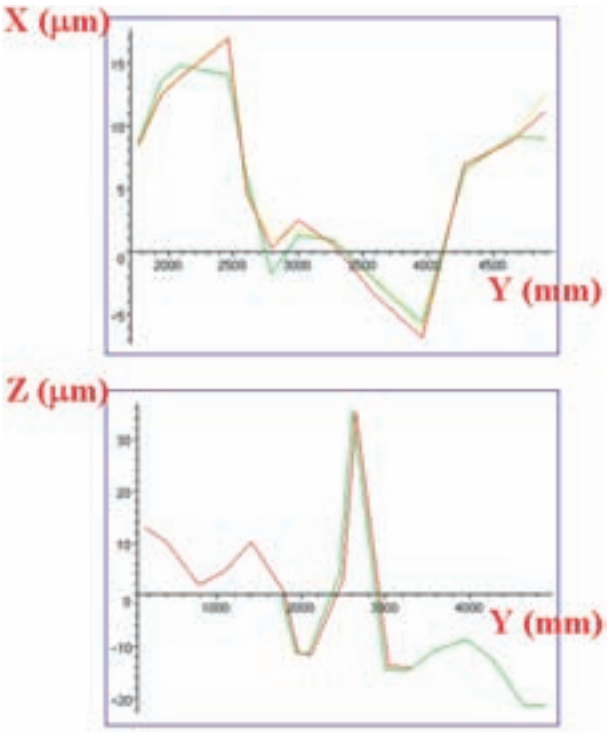

Figure 2.13: *Alignment precision of the STT along the wire coordinate (top) and flatness (bottom) achieved through laser interferometry.*

Figure 2.14: *Gluing of the two mono-layers of an OT module (top); finishing of an OT module (bottom).*

LHCb Note LHCb-2004-034. Prior to closing a module gas box, the quality of all strung wires in a mono-layer is controlled by checking that the tension measured with the WTM falls in within a few grams from the nominal value (70 gr); wires outside this acceptance window are then replaced.

Once the tension of all strung wires is checked, each anode wire in a mono-layer is brought to high voltage (about 1600 V) in air and the leakage current (of the order of 1 nA) of each wire is measured as a function of increasing HV with a precise computer-controlled current meter designed and realized at NIKHEF. A distribution of measured currents for a mono-layer is shown in Fig. 2.16; wires showing currents above few tens of nA are then replaced.

Prior to gluing two straw mono-layers into a module, the wire pitch is checked at four positions for all 64 wires in a mono-layer with the aid of a special computer-controlled tool developed at NIKHEF. After some initial problems encountered with the first few module prototypes, a precision in the pitch distribution of the order of $\sigma_{\rm PITCH} \simeq 30\mu{\rm m}$ was achieved. In the pitch distribution in Fig. 2.17 practically all wire pitches fall in a window of ± 50 μm around the nominal (5.25 mm) value.

Two straw mono-layers are then glued into a module and the gas box is sealed. After a curing time of about 19 hours at 20 ^{o}C, the module is filled with gas and the gas tightness of the module is checked; at the end of the procedure, volume losses below 10^{-6} l/s are obtained (significantly better than the specified 5% loss per volume exchange).

After modules are flushed with the counting gas for a few days, they are systematically tested by scanning their entire surface with a ^{90}Sr source and measuring the resulting leakage current. A current distribution from the ^{90}Sr scan over the surface of a half module is

Figure 2.15: *Wire Tension Meter measuring the wire tensions of a straw mono-layer.*

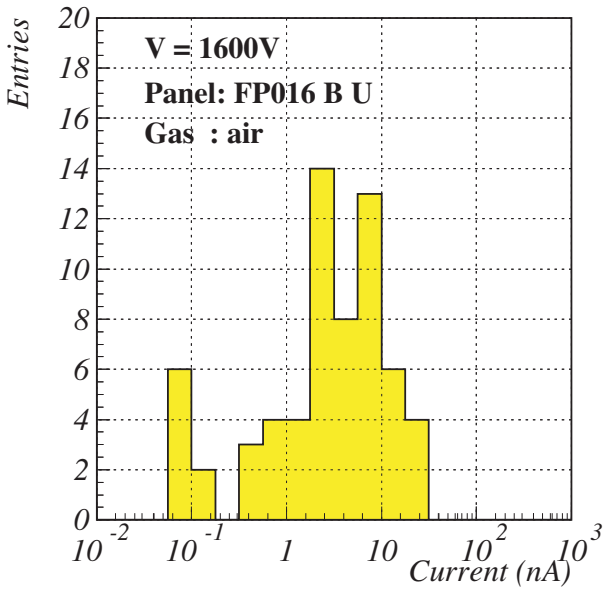

Figure 2.16: *Distribution of measured currents of a mono-layer in air, at HV = 1600 V.*

shown in in Fig. 2.18: the typical patterns due to the presence of the wire locators are easily recognized.

In addition, dedicated investigation of the pulse height distribution from an ^{55}Fe source are carried out for given sub-portions of the module surface. The gain of each straw channel can thus be determined, as shown in Fig. 2.19.

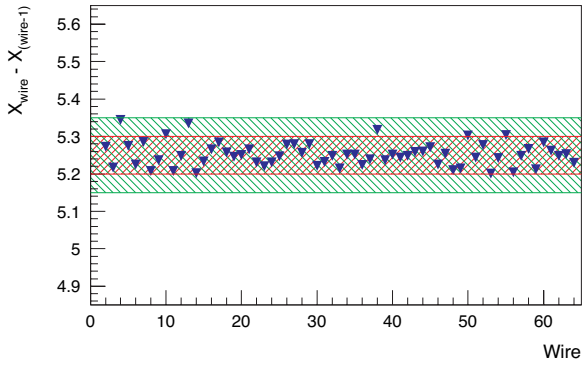

Figure 2.17: *Wire pitch distribution of a straw mono-layer: the red band is ± 50 μm, and the green one ± 100 μm.*

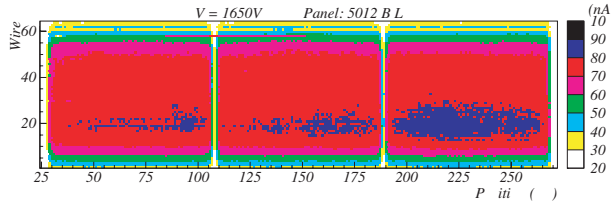

Figure 2.18: *Leakage current over the surface of a half module from a ^{90}Sr scan at HV = 1650 V.*

Front-End Electronics

The extremely compact design of the FE Electronics foresees the complete digitisation of the drift-time data to take place on board the FE Electronics, where data are also serialized and optically transmitted on optical fibres to the readout electronics in the counting room. NIKHEF is responsible for the design, production and commissioning of the Outer Tracker FE Electronics, as well as for the design and realization of all related services: Timing and Fast Control (TFC), Electronic Control System (ECS), Low and High Voltages supply (LV and HV), analog monitoring etc.

We completed the design of the FE Electronics, which is to be globally reviewed by an independent panel in April 2004. We also constructed two complete prototypes of the whole FE Electronics box, shown in Fig. 2.20, including among the others:

- HV boards, containing the HV-decoupling capacitors buried in the PCB layers;
- the ASDBLR service boards, where the small straw

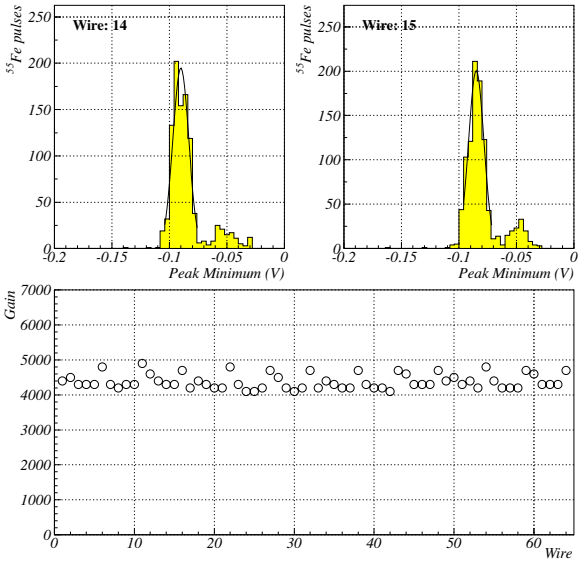

Figure 2.19: *Pulse height distribution from two anode wires measured with an ^{55}Fe source (top); channel gains of a straw mono-layer (bottom).*

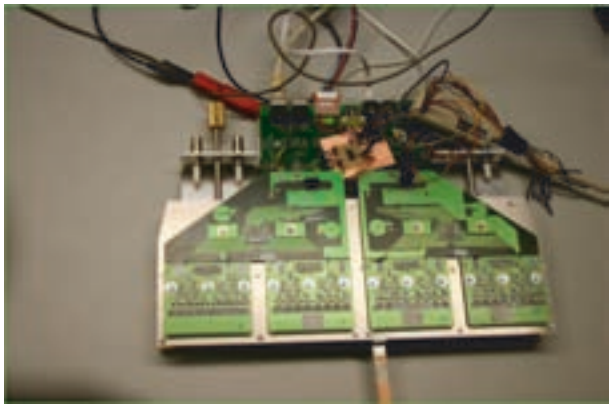

Figure 2.20: *Prototype FE Electronics box mounted on its support and cooling chassis.*

pulses get amplified and discriminated by the ASDBLR ASICs;

- the OTIS service boards, where the time delay between the digital straw signals passing over a certain threshold (typically of few thousands electron charges) and the LHC experimental clock gets digitised by the OTIS ASICs;
- the mechanical support and cooling frame and the shielding aluminum box.

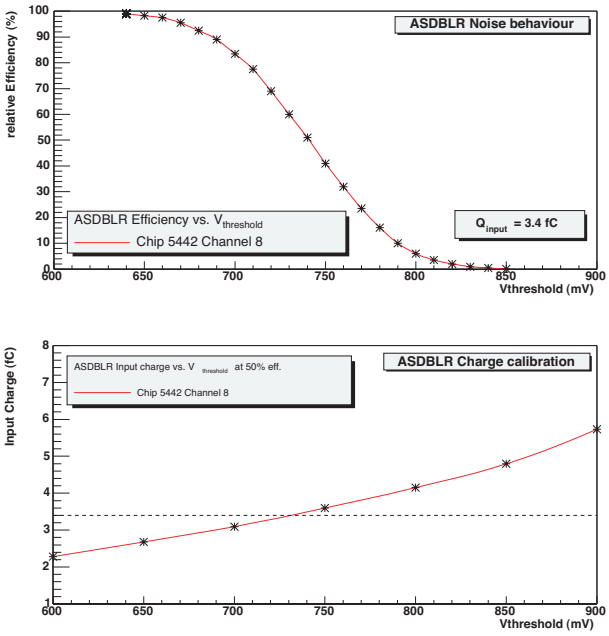

Figure 2.21: *Threshold (top) and gain curve (bottom) of a readout channel.*

All boards were tested and qualified. E.g. in Fig. 2.21, the measured threshold and the gain curve of a straw channel is shown, from which the electronics Equivalent Noise Charge (ENC) can be determined.

2.7 Reconstruction and Physics Studies

Detailed Monte Carlo simulation studies are carried out with a twofold purpose:

- to develop reconstruction algorithms for future real data,
- to validate the final modifications in the proposed LHCb detector set-up.

The final layout of the experiment is shown in the figure on page 12.

Event Generator and Detector Simulation

Minimum bias proton-proton interactions at a center-of-mass energy of $\sqrt{s} = 14\mathrm{TeV}$ are generated with the PYTHIA program. A sample of $b\bar{b}$-events is obtained by selecting events with at least one b or $\bar{b}$ hadron in the final state. The decay of all unstable particles is performed with the QQ program developed by the CLEO collaboration. In this procedure both the PYTHIA and

QQ parameters have been tuned using available published data in order to reproduce the expected environment of the LHCb machine in the LHCb interaction point.

Generated particles are subsequently traced through the LHCb detector using the GEANT package, simulating all interactions between these final state particles and the detector materials. In the simulation program the entrance and exit points of each particle traversing a sensitive detector layer are registered, together with the energy loss in that layer. This information is then used to mimic the detector "raw data", taking into account the details of the sensitivity and response of each detector, including detection inefficiencies and electronic noise.

Reconstruction

In the track reconstruction program the registered hits of the VELO, the TT, the IT and the OT detectors are combined to form particle trajectories across the detector. For efficient track finding two complementary approaches have been used. In the first approach a track candidate is searched in the VELO and extrapolated to the T stations where hits matching the track are added. In the second approach an independent track seed is searched in the T stations which is matched to unused track in the VELO detector. The overall procedure leads to an efficiency of 95% for B decay tracks with a corresponding ghost-track rate of 9%. The quality of the reconstructed tracks is indicated by their momentum resolution and their impact parameter mismatch at the track vertex. Distributions for these parameters are shown in Fig. 2.22. For B decay tracks the average resolutions are $< \sigma_{IP} >= 40$ μm and $< \delta p/p >= 0.37\%$.

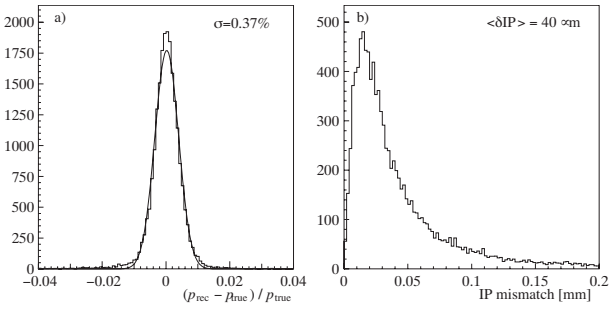

Figure 2.22: *(a) Momentum resolution with a Gaussian fit, and (b) impact parameter precision, for B-decay tracks.*

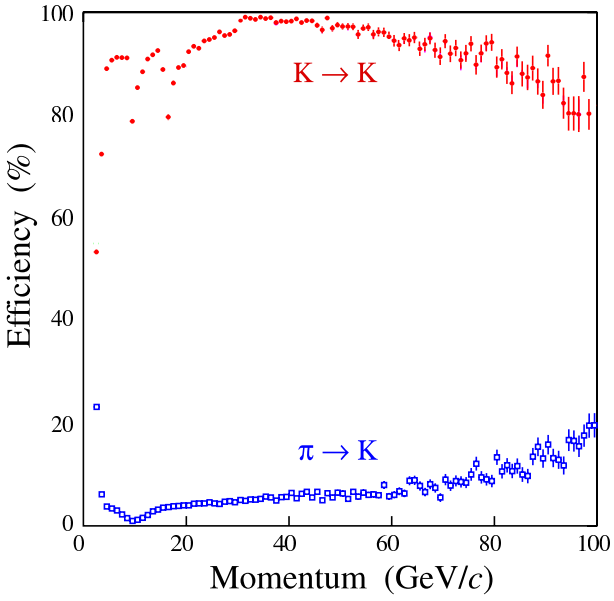

Figure 2.23: *(a) Kaon identification efficiency (solid points) and pion misidentification rate (open points) as a function of momentum.*

Particle identification within LHCb is provided by the two RICH detectors (pion, kaon and proton identification), the Calorimeter system (electron and photon identification) and the Muon Detector (muon identification). A full pattern reconstruction procedure is also put in place for these detectors. For all reconstructed particles likelihoods are defined for each particle hypothesis. The performance of the kaon identification, the most difficult task, is plotted in Fig. 2.23.

Event Selection

The main challenge in the offline selection of B decay final states is to maintain a high efficiency for the signal B decay events, while providing a very large rejection factor for the combinatorial background. The offline selections of a large number of B^0 and B_s decay channels are studied in detail using the simulated events. In general the selection criteria make use of:

- a precise invariant mass requirement of reconstructed B mesons,
- a high resolution measurement of the B decay vertex that is inconsistent with the primary event vertex,
- a particle identification consistent with the required decay particles.

Channel (c.c included)	efficiency	yield
$B^0 \to \pi^+\pi^-$	0.69%	26k
$B_s^0 \to D_s^-\pi^+$	0.34%	80k
$B_s^0 \to D_s^\mp K^\pm$	0.27%	5.4k
$B_s^0 \to J/\psi(\mu^+\mu^-)\phi$	1.67%	100k

Table 2.1: *Estimates for the total efficiencies and the annual yields of benchmark b-hadron decays for the re-optimized LHCb detector.*

Table 2.1 lists the total efficiency and the expected yearly event yield for four benchmark B decay channels.

In order to demonstrate the robustness of the simulation and reconstruction, the whole procedure has been repeated by using conservative settings of all resolution and efficiency parameters simultaneously in the program. The expected loss of events as compared to the standard procedure is $\sim 30\%$, which is considered acceptable for this unlikely hypothetical situation.

CP Sensitivity

The expected sensitivities to CP observables have been assessed with "fast Monte Carlo" programs, using the efficiency and resolution parameters obtained by the full simulation procedure.

The NIKHEF group focused on three benchmark decays of the B_s meson:

- the decay channel $B_s \to D_s^-\pi^+$; a flavor specific decay that can be used to measure the mass difference (Δm_s) between the CP-even and CP-odd eigenstates of the B_s meson. This decay mode is also used as a calibration channel to determine the experimental mis-tag fraction ω_{tag} directly from the data. The expected decay time distributions for one year data-taking are shown in Fig. 2.24. The highest value of Δm_s that can be observed with 5σ statistical significance is 68 ps^{-1}, far beyond the expected value in the Standard Model.

- the decay channel $B_s \to D_s^\mp K^\pm$; a decay in which a large CP violation observation is expected. A measurement of the time dependent asymmetries, as shown for simulated events in Fig. 2.25, leads to a determination of the unitary parameter $\gamma' = \gamma - 2\chi$.

- the decay channel $B_s \to J/\psi\phi$; a decay in which the Standard Model predicts no CP violation. A non-zero observation of CP violation, labeled by the parameter 2χ, would indicate the presence of new flavor changing interactions.

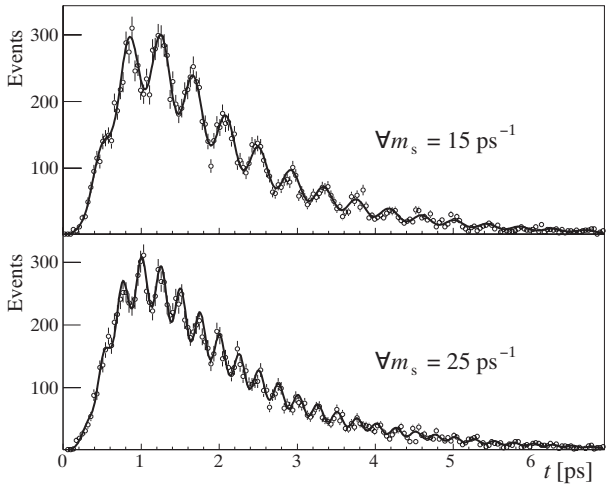

Figure 2.24: *Proper-time distribution of simulated $D_s \to D_s^-\pi^+$ candidates, for two different values of Δm_s. The data points represent one year of data, while the curves correspond to the maximized likelihood.*

A measurement of the time dependent asymmetries of these three decay modes results in a measurement of the CKM parameter γ with an expected error of 14 degrees after one year of data-taking, without theoretical uncertainty.

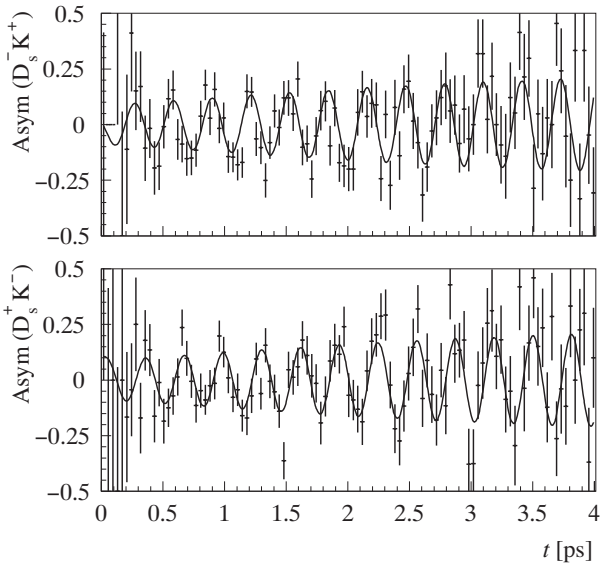

Figure 2.25: *Time-dependent $\overline{B_s}$-B_s asymmetry of simulated $D_s^- K^+$ (top) and $D_s^+ K^-$ (bottom) candidates for a value of $\Delta m_s = 20 ps^{-1}$ and $\gamma' = 65$ degrees.*

3 Heavy Ion Physics

3.1 Introduction

The strong interaction is one of the four fundamental forces in Nature. Quantum Chromo Dynamics (QCD), part of the standard model of particle physics, is a very successful microscopic theory of the strong interaction. It successfully describes the "zoo" of observed hadrons and, at large momentum transfer, the interactions of their constituent quarks and gluons. However, despite intense experimental efforts no free quarks or gluons have ever been observed. This so called confinement of quarks and gluons inside a hadron is one of the most interesting and puzzling properties of the strong interaction and is one of the features of QCD that from first principles is still poorly understood. At an energy density larger than in a proton, QCD predicts the existence of a deconfined form of matter, called a Quark Gluon Plasma (QGP), where the quark and gluon degrees of freedom are liberated instead of being confined within hadrons. The transition between confinement at low temperature and deconfinement at high temperature may provide better understanding of the fundamental properties of the strong interaction. Colliding heavy-ions at the highest energies available is expected to be the best possibility to create and study such a large high temperature system in the laboratory.

NIKHEF has been actively involved in fixed target experiments at the CERN SPS (WA98, NA49, and NA57), which still bear new results. The major focus of the experimental activity in the field has, however, shifted to the Relativistic Heavy Ion collider (RHIC) at Brookhaven National Laboratory. The NIKHEF heavy ion group is actively participating in data taking and analysis in the STAR experiment. Moreover, the group continues its effort in the preparation of the ALICE detector at the future LHC collider. In this report highlights of all these activities will be summarized.

3.2 Results from SPS experiments

The WA98 experiment has been able to extract the first direct photon measurement in heavy ion collisions, which created a lot of theoretical interest, because direct photon spectra contain unique information about the early dense phase of the reaction. The systematic uncertainties allowed a reliable extraction only at relatively high transverse momentum. Now interferometric methods have been used to estimate the yield of direct photons at low transverse momenta [1]. The measured source radii are similar to those obtained with charged pions, which is consistent with an emission of

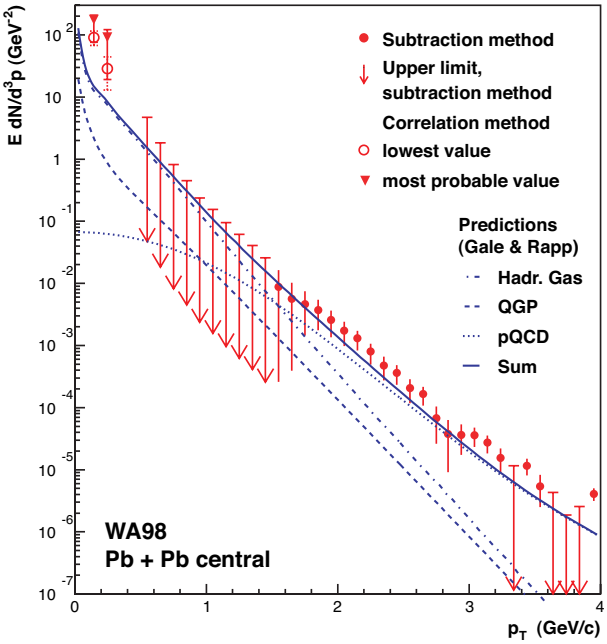

Figure 3.1: *Direct photon yields extracted from intensity interferometry measurements in central Pb-Pb collisions at 158AGeV studied in the WA98 experiment.*

these photons from the hadronic phase. In Fig. 3.1 the estimated yields are compared to those obtained from the earlier measurement (subtraction method). Also shown are theoretical calculations including both QCD prompt photons and thermal photons emitted from a hadron gas or a QGP. While these calculations can relatively well describe the data at intermediate and high transverse momenta p_t, they are considerably below the new low-p_t results.

To search for possible signals of the onset of deconfinement, the NA49 experiment has taken central Pb-Pb data at five different energies in the years 1996–2002. Preliminary results from the 2002 runs at 20 and 30 *A*GeV supplement those from 40, 80 and 158 *A*GeV published earlier [2]. The new data confirm the sharp maximum at about 30 *A*GeV in the ratio of K^+/π^+ yields as shown in Fig. 3.2. The curves in this figure show predictions from a statistical hadron-gas model [3] and from two microscopic transport models [4, 5]. It is clear that, at least at present, hadronic models fail to describe the data. More results from this energy scan have been obtained, e.g. it is observed that the inverse slope of kaon spectra is constant in the energy range of the SPS. The ratio of Λ/π, also measured by NA49

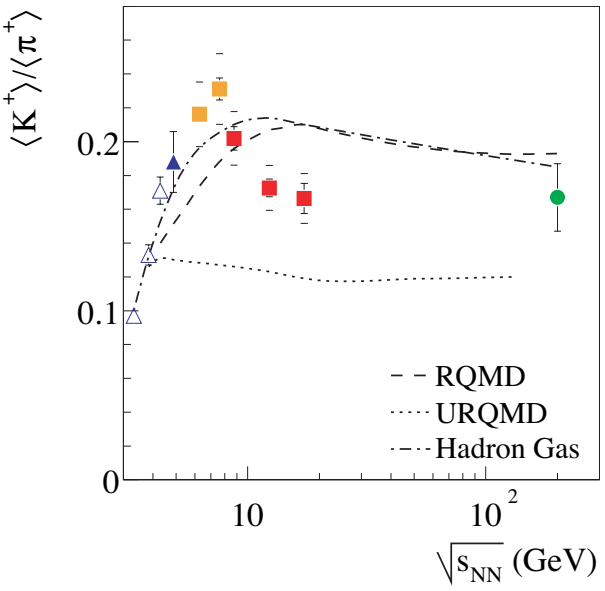

Figure 3.2: *Energy dependence of the ratio K^+/π^+ in central Pb-Pb collisions from AGS (triangles), NA49 (squares) and RHIC (Au-Au collisions). The curves show predictions from three different hadronic models.*

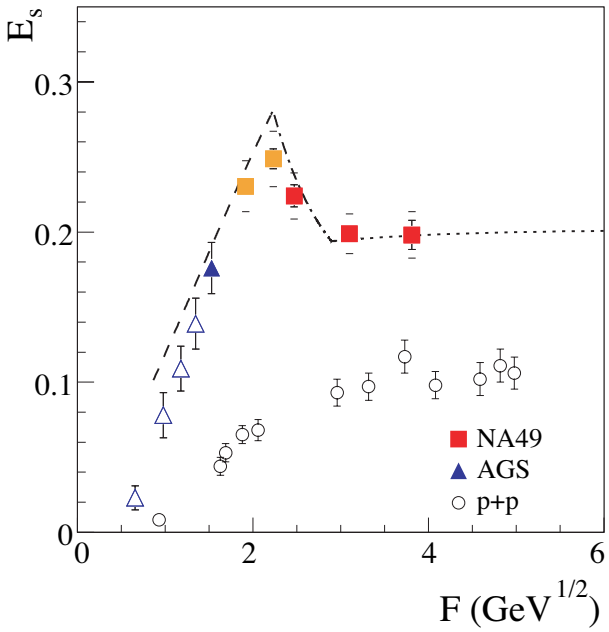

Figure 3.3: *Energy dependence ($F \approx s^{1/4}$) of the ratio E_s of strangeness to pion yields in Pb-Pb collisions. The curve is the prediction from the SMES model. Proton data (open symbols) are shown for comparison.*

[6], shows a similar energy dependence as the K^+/π^+ ratio.

Figure 3.3 shows the ratio E_s of total strangeness (Kaon plus Lambda) to pion yields versus the Fermi energy measure $F \approx s^{1/4}$. Also plotted is the prediction from the SMES model [7] which assumes a phase transition to the QGP at SPS energies. The data are in fair agreement with this model.

If the anomalies observed by NA49 do indeed indicate a phase transition at SPS energies or that they can just be explained in a hadronic scenario is still an open question.

3.3 Jet production and jet quenching studied in STAR

High-p_t partons are produced in the very early stage of a collision. When traversing a dense system they are exposed to the color charges in the medium. Similar to QED bremsstrahlung the partons will lose energy, a phenomenon called jet-quenching. This makes them an ideal probe to study the initial condition of heavy-ion collisions. Because the jets resulting from these high-p_t partons are difficult to isolate from the soft background in an heavy-ion collision, it was proposed to measure the leading particles which typically take about half the energy of the jet. In fact, one of the earliest observations at RHIC was the suppression of the yield of high momentum hadrons, which was in line with the expectations from jet quenching.

Possible signatures of the QGP from single inclusive particle observables in heavy-ion collisions, like the measurement of the suppression of single hadrons cited above, require reference measurements from proton-proton and proton-nucleus collisions. However, observables from heavy-ion collisions do allow for a self-normalization when utilizing the collision geometry. Fig. 3.4 shows an illustration of a non-central heavy-ion collision. The observed anisotropy in particle yields versus the reaction plane – the plane spanned by the beam-axis and the impact parameter – is a self-normalizing observable. The particle yield can be characterized by:

$$\frac{\mathrm{d}^3N}{\mathrm{d}p_t^2\mathrm{d}\phi\mathrm{d}y} = \frac{\mathrm{d}^2N}{2\pi\mathrm{d}p_t^2\mathrm{d}y}[1 + 2\sum_n v_n \cos(n(\phi - \Psi_R))],$$

where p_t is the transverse momentum of the particle, ϕ is its azimuthal angle, y is the rapidity and Ψ_R the reaction plane angle, see Fig. 3.4. The second coefficient, v_2, of this Fourier series is called *elliptic flow* and is, due to the ellipsoidal shape of the collision region, the dominant coefficient.

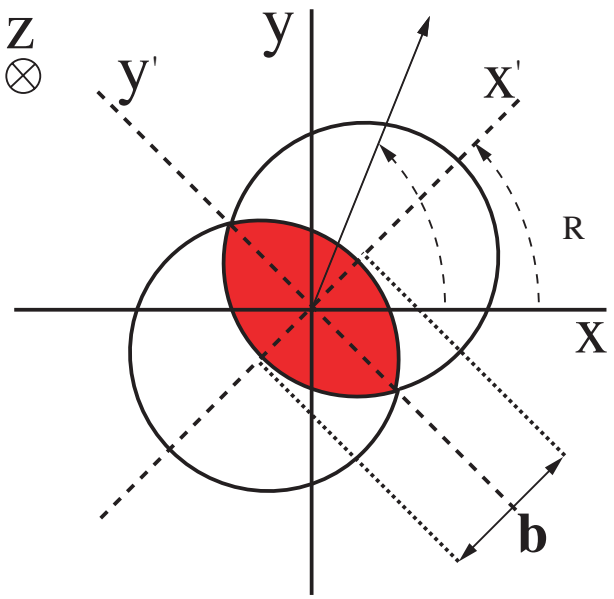

Figure 3.4: *Schematic view of a nucleus-nucleus collision in the transverse plane.*

Detailed QCD calculations indicate that the amount of energy loss depends on the parton density of the created system and the path length. In a non-central heavy-ion collisions, a high-p_t parton moving in the direction perpendicular to the reaction plane (longer path through medium) will loose more energy than when moving in the reaction plane, thereby creating an asymmetry v_2 in the particle emission pattern. A larger difference in energy loss leads to a larger corresponding v_2. In the absence of jet quenching, the azimuthal distribution of high-p_t particles even in a non-central heavy-ion collision would be isotropic and therefore v_2 equal to zero. Figure 3.5 shows the v_2 of charged particles up to $p_t = 12$ GeV/c[8]. The triangles represent the v_2 obtained using the traditional two particle correlation methods while the stars are the v_2 obtained using multiple particle correlations and are considered a lower limit on the true v_2. The large v_2 observed above 6 GeV/c is consistent with expectations from jet energy loss.

Two-particle distributions in the relative azimuthal angle of charged high-p_t particles measured in $p + p$, d+Au, and Au+Au collisions at RHIC exhibit a jet-like correlation characterized by the peaks at $\Delta\phi = 0$ (near-side correlations) and at $\Delta\phi = \pi$ (back-to-back). As expected for large jet energy loss, the back-to-back jets are found to be strongly suppressed in Au+Au collisions compared to $p + p$ and d+Au collisions. A self-normalizing extension of these measurements is studying these correlations with respect to the reaction plane orientation. Figure 3.6 shows that the near-side jet-like correlations measured in Au+Au are similar to those measured in $p+p$ collisions. The back-to-back (around $\Delta\phi = \pi$) correlations measured in Au+Au collisions for in-plane trigger particles are suppressed compared to $p + p$, and even more suppressed for the out-of-plane trigger particles[8]. The observed dependence of the suppression of the back-to-back correlations on the orientation relative to the reaction plane is consistent with jet-quenching scenario where the energy loss of a parton is proportional to the distance traveled through the dense medium.

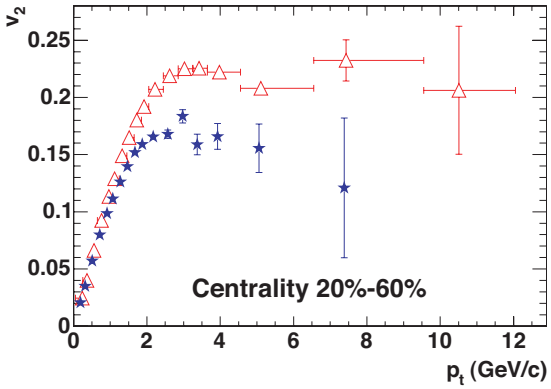

Figure 3.5: *High-p_t azimuthal particle correlations.*

The measurements at RHIC have provided a large number of new observations, the most striking ones being the observed strong particle suppression at high-p_t and the mass dependence of the elliptic flow, together with the new measurements shown here. These observations are consistent with the creation of a very dense and strongly interacting system in heavy-ion collisions at RHIC energies. The new dataset from the 2003–2004 run at RHIC provides a factor ≈ 20 increase in integrated luminosity. This dataset was taken with most of the EMC in STAR available and will allow for di-"jet" correlation measurements in the true perturbative range and investigations of the flavor dependences of these.

3.4 The Alice experiment at CERN

The Alice experiment is now in its construction phase. After contributing significantly to the design and development of many parts of the outer two layers (SSD) of the Alice inner tracking system (ITS), the Dutch group is now concentrating on the production of the EndCaps and the read-out electronics. In addition the final assembly of the SSD system will be done in the

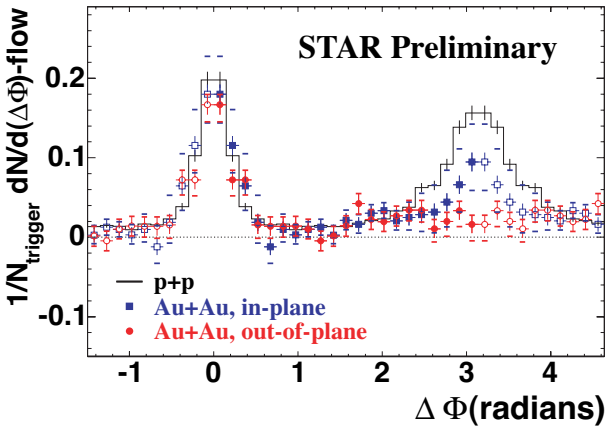

Figure 3.6: *Di-"jet" correlations in in-plane (out-of-plane) Au-Au collisions compared to those in pp collisions.*

Netherlands.

The EndCap modules isolate the front-end modules, which operate at the sensor bias potential, from the read-out electronics at ground potential. Two chips (ALABUF and ALCAPONE) were designed, produced and tested. Protoype boards with all the functionality of the EndCaps were successfully used in combination with Alice front-end modules in two beamtests during 2003. About 150 EndCaps, containing nearly 2000 electronic boards, will be produced and tested in 2004 and 2005.

The design of the front-end read-out module system (FEROM) is now completed. This system will be able to digitize the analog signals from all 2000 front-end modules in parallel at 10 MHz. Since each module produces 1536 samples, the total conversion time is comfortably within the 200 μs required for the *pp* trigger in the Alice experiment. Prototype boards will be used during a beamtest in 2004.

In both SSD layers of the inner tracking system the front-end modules are supported by light weight carbon fibre structures. The sensors are mounted on these structures such that the active areas overlap. The supports with front-end modules attached are called ladders. The ladders are mounted in each layer in the ITS at two different radii, creating an overlap of the active area in the azimuthal direction. The gaps between the sensors are small in order to maximize the geometrical acceptance of the system. In addition the position of each sensor within the assembly should be well known in order to simplify the alignment. As a result, the accuracy of the ladder assembly process needs to be better than 10 μm for some of the coordinates [11]. In addition the electronics is sensitive to electro-static discharge. Therefore the assembly process will be highly automated.

An assembly machine automatically positions all the modules for one ladder, after which the modules are glued to the support frame. Thus, the machine takes care of the most critical actions without direct human manipulation. This machine was designed and built in cooperation between NIKHEF and an industrial company. The assembly machine is currently being tested.

References

[1] M. M. Aggarwal et al. [WA98 Collaboration], "Interferometry of Direct Photons in Central ^{208}Pb+^{208}Pb Collisions at 158A GeV," submitted to Phys. Rev. Lett., arXiv:nucl-ex/0310022.

[2] S. Afanasiev et al. [NA49 Collaboration, Phys. Rev. **C66** (2002) 054902.

[3] P. Braun-Munziger et al., Nucl. Phys. **A697** (2002) 902.

[4] H. Sorge et al., Nucl. Phys. **A498** (1989) 567c, Phys. Rev. **C52** (1995) 3291.

[5] UrQMD Collab., S. Bass et al., Prog. Part. Nucl. Phys. **41** (1998) 255.

[6] T. Anticic et al. [NA49 Collaboration], "Λ and $\bar{\Lambda}$ in Central Pb-Pb Collisions at 40, 80, and 158A GeV," submitted to Phys. Rev. Lett., arXiv:nucl-ex/0311024.

[7] M. Gaździcki and M. Gorenstein, Acta Phys. Polon. **B30** (1999) 2705. Phys. Lett. **B518** (2001) 41.

[8] A. H. Tang [STAR Collaboration], "Azimuthal anisotropy and correlations in p + p, d + Au and Au + Au collisions at 200-GeV," arXiv:nucl-ex/0403018.

[9] M. Gyulassy, "The QGP discovered at RHIC," arXiv:nucl-th/0403032.

[10] http://www.cerncourier.com/main/article/44/3/17; http://qm2004.lbl.gov/

[11] Alice Technical Design report 4, Inner Tracking System, CERN/LHCC 99-12.

4 ANTARES

4.1 Introduction

The ANTARES collaboration is building a deep underwater detector for high energy (¿ 10 GeV) cosmic neutrinos, which may be produced through e.g. pp or $p\gamma$ interactions at the acceleration sites of high energy cosmic rays. Neutrino detection is based on the registration of Cherenkov light associated with muons originating from charged current neutrino scattering in or near the instrumented volume. At high energies, the muon direction is closely correlated to the neutrino direction. It can be reconstructed from the arrival times of the Cherenkov photons at the photosensors of the detector.

4.2 Prototype Sector Line

By the fall of 2002, a prototype line, consisting of five floors with three photomultipliers each (a so-called sector), had been assembled and deployed at the foreseen site at a depth of 2.4 km. The French submarine "Nautile" had been booked to connect the prototype detector to the so-called junction box. This would establish the contact between the detector and the shore via the

Figure 4.1: *Deployment of the submarine "Nautile".*

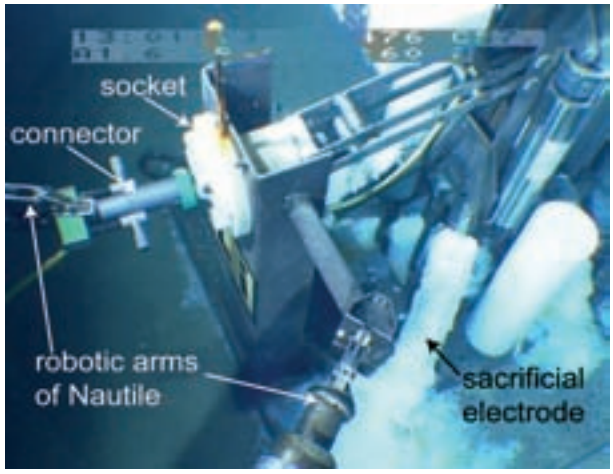

Figure 4.2: *Connection of the prototype sector line by means of a wet-mateable connector, which is inserted into a socket at the botton of the line by two robotic arms at the front of Nautile.*

40 km long cable, which has been in place since October 2001. However, the submarine was needed to prevent a major ecological disaster due to the spilling of oil from the wreck of the "Prestige". Finally, on the 17th of March 2003, the long awaited connection was made; see figures 4.1 and 4.2. The first signals from the deep-sea were recorded the same day. This offered immediate validation of the products developed at NIKHEF:

- the data read-out system, using Gb/s optical fibre communication based on Dense Wavelength Division Multiplexing (DWDM) opto-electronics,
- the on-shore data processing and archiving software,
- the in-sea power modules for the detector electronics,
- the cooling system of the in-sea electronics,
- the run control system and
- the online data monitoring and archiving software.

Apart from functioning from day one, these systems have proved to be stable over the full data taking period of about four months.

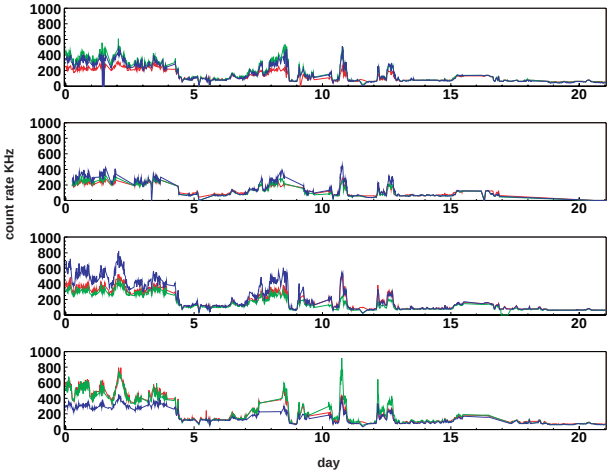

Figure 4.3: *Measured count rates of the photomultiplier tubes as a function of time on four different floors. The different colours represent the three photomultipliers on each floor.*

A problem with the distribution of the reference clock signal prevented us from reaching the ns time accuracy required for the reconstruction of (atmospheric) muons. Fortunately, the timing accuracy had already been verified beforehand in the lab to be of the order of 1 ns (see NIKHEF annual report 2002). After recovery of the line, the problem was found to be caused by a flaw in the design of the string cable. The cable manufacturer has supplied an improved cable, which will be used when the prototype line will be re-deployed in the fall of 2004.

The optical background rates have been measured for the full period. A small fraction of the total data is summarised in figure 4.3. Beside a stable contribution from natural radio-activity, there is an important contribution from bioluminescent life forms, which shows fluctuations on times scales from seconds to weeks. From an analysis of the data, it has been shown that the bioluminescence activity is partly correlated to the magnitude of the sea current.

4.3 On-shore data processing

All data produced by the detector are sent to shore, without the intervention of an off-shore trigger. On shore, a computer farm serves to filter the physics events from the optical background. Apart from ongoing development of faster algorithms, studies have been carried out to identify filter settings which can be used during the periods of high optical background, as have been observed with the prototype sector line.

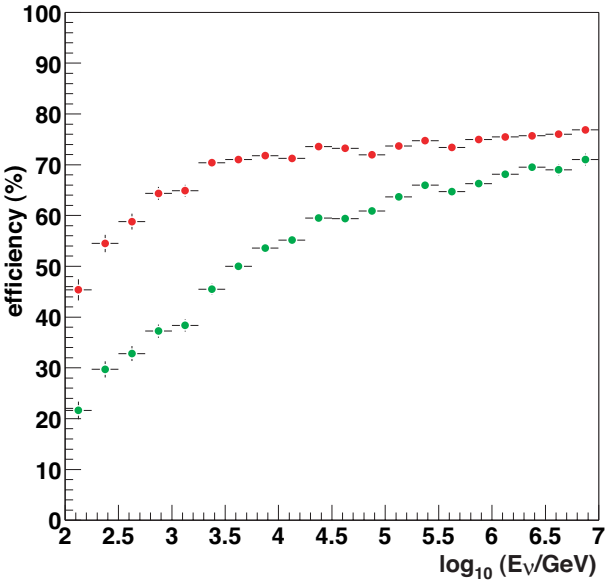

Figure 4.4: *Trigger efficiency (for events with at least six signal hits) as a function of the neutrino energy for the standard trigger (green dots) and for the off-line GRB analysis (red dots), which uses directional information provided by the GCN.*

Simulations show that we can cope with background rates up to a few hundred kHz, while retaining much of the trigger efficiency and reconstruction accuracy for high energy events.

A case study has been made to investigate the possibility to detect neutrinos from Gamma Ray Bursts (GRBs). By interfacing the Data AcQuisition (DAQ) system of ANTARES with the GRB Coordinate Network (GCN), alerts from the GCN can be used as an external trigger. The alerts will typically arrive several tens of seconds after a satellite has detected a GRB. This will trigger the DAQ system to write a snapshot of several minutes of buffered, unfiltered data to disk. In this way, all data from a time window ranging from a few minutes before to a few minutes after the time of the GRB will be available for off-line analysis. This analysis can make use of the directional information provided by the GCN, thereby improving the signal to noise ratio compared to the standard triggering scheme. This results in an improvement of the detection efficiency by about a factor of two in the sub-TeV energy range, as is shown in figure 4.4. By selecting only the events which are compatible with the GRB coordinates and time, the analysis becomes virtually background free, which make GRBs one of the most promising signals for ANTARES.

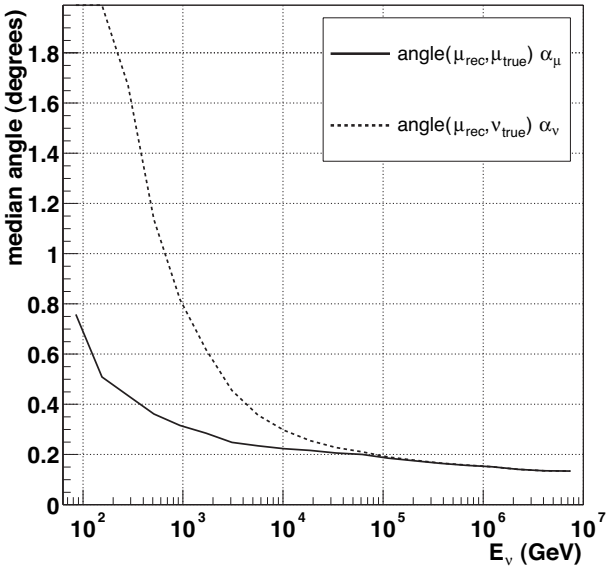

Figure 4.5: *Angular resolution of the muon and of the neutrino direction as a function of the neutrino energy. The resolution is defined as the median of the angular error. For energies below 10 TeV it is dominated by the physics of the neutrino interaction. For higher energies, the accuracy of the muon track measurement is the limiting factor.*

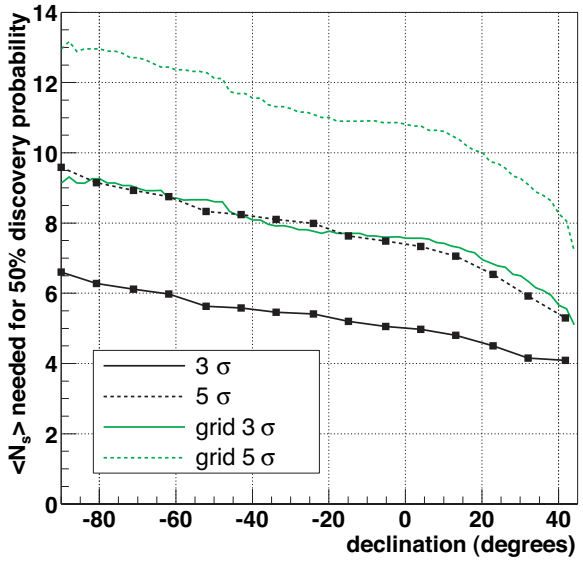

Figure 4.6: *Discovery potential of a search for point-like neutrino sources after one-year of data taking with ANTARES. The result is expressed mean number of events a source must produce in the detector to yield a 50% chance of discovering it at the indicated confidence levels.*

4.4 Analysis methods

A new method was developed to search for point-sources of cosmic neutrinos. After selection of well-reconstructed upward-going muon events, the (irreducible) background is due to atmospheric muon-neutrinos, which will be detected at a rate of about 10 per day. A cosmic point source of neutrinos will show up as a cluster of events (i.e. a local excess above the expected background) in the direction of the source. The angular resolution of the detector is clearly a crucial parameter in distinguishing signal clusters from random background clusters. Ongoing work on reconstruction methods has led to improvements in the angular resolution (see figure 4.5), while also increasing the detection efficiency.

In order to distinguish clusters caused by a neutrino point source from random background clusters, a new search method, based on an unbinned likelihood ratio test, has been developed In this method, the knowledge of the angular resolution, energy resolution and detector acceptance is incorporated, while all available information on the angular spread and energy of the events is used without loosing information to binning effects. In figure 4.6 the performance of this method is compared to a more conventional 'grid' method, which is based only on counting the events in the cells of a grid covering the observable sky. The new method results in a significant increase in the discovery potential. On average, a neutrino point source which yields a 3σ effect in the conventional method, can be discovered at the 5σ confidence level using the new method.

The sensitivity of a point source search with ANTARES is shown in figure 4.7, which shows the neutrino flux that is needed for a 5σ discovery and the average 90% confidence level upper limit that ANTARES expects to set after one year of data taking. For comparison, this figure also shows upper limits that have been obtained by the MACRO and AMANDA-II experiments, and the one that the IceCube detector expects to set in 2009. Furthermore, theoretical flux predictions are shown for two types of sources: microquasars and GRBs (for which a specialised search method will be used to further increase the sensitivity, see section 1.3). The currently existing limits for the southern hemisphere do not rule out a discovery with ANTARES. In case no discovery is made, ANTARES will improve these limits by about an order of magnitude after one year of data taking.

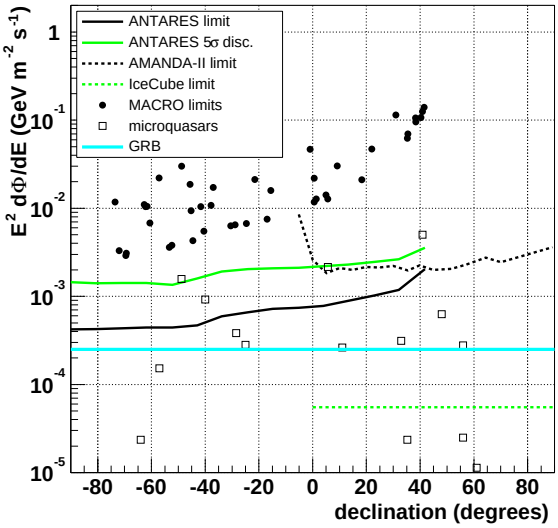

Figure 4.7: *Sensitivity of ANTARES to point sources of neutrinos with a spectrum proportional to E^{-2} as a function of declination, compared to the limits (expected to be) set by other experiments and to models of neutrino production in microquasars and GRBs. Established 90% confidence level limits are shown from MACRO (for 51 selected source candidates, 6.3 years of data taking) and AMANDA-II (average limit, 197 days). For ANTARES and IceCube the limits expected after one year of data taking are shown. The flux needed for a 5σ discovery with ANTARES after one year of data taking is also shown.*

4.5 Outlook

The mass production of the final detector strings is well underway. The power modules required for the full detector have been produced and the mass production in industry of the DWDM data read-out electronics has been started. In Saclay, all 900 phototubes have been delivered and the production of the optical modules is on schedule. The launch of the first full detector string is planned for March 2005. The completion of the full 12 string ANTARES detector is foreseen in 2006.

5 ZEUS

5.1 Introduction

The ZEUS experiment looks at interactions from electrons with protons, provided by the HERA collider in Hamburg. After this collider was refashioned in 2001, the restart was disappointing. Interactions of the particle beams with rest gas in the vacuum pipe were causing unacceptable background signals in the ZEUS experiment itself. During 2003 still a lot of time was devoted to these background problems but fortunately this resulted in solving the main problems. In addition, the analysis of data that has been acquired until 2001 has now been finalised and prepared for publication. As an ongoing activity, the performance from the new vertex detector in ZEUS was studied. In the following we report on these three main topics.

5.2 ZEUS beats HERA beam background

Since the reconfiguration of the accelator elements near the interaction region to achieve a sharper focus of the particle beams, the HERA experiments suffered from large backgrounds. In a joint effort with the other HERA experiments, ZEUS physicists successfully worked to understand the deeper reasons for this unexpected high background. A detailed simulation of all accelerator elements up to 100 meters away from the experimental region proved to be necessary before making a proposal to solve the problem. NIKHEF has played a major role in this simulation program with one of its post docs. In march 2003 a new shutdown of the accelerator allowed intervention to make the necessary modifications to the accelerator and improve the shielding near the ZEUS experiment.

As a result of this accelerator shutdown that lasted until September there is no large new data volume available for analysis. In spite of the fact that soon after the restart we could see that the cause of background problem is solved, it still requires a very good vacuum to have stable running. This is in accordance with what was expected but unfortunately several incidents (like power failures) caused leaks and instable running conditions.

At present the pressure has finally reached stable vacuum conditions and the machine is now ready for its final run toward a high intensity. To ensure the delivery of the number of collisions that was foreseen at the time of the upgrade, the HERA running period has officially been extended with one year until the end of 2006.

5.3 Analysis HERA-I from 1991-2000

Before the accelerator upgrade, HERA delivered luminosity until the fall of 2000. Generally this run is called HERA-I and in the last three years of running 17 pb^{-1} of electron-proton and 67 pb^{-1} of positron-proton collisions were collected by the ZEUS experiment.

The major topic of HERA-I was the measurement of the electron-proton deep inelastic scattering process. The mechanisms underlying this process can be split in the interaction through a neutral or a charged boson. The neutral current cross sections were already published in recent years but in 2003 the analysis of the charged current interactions was finalised and published. This analysis is described in a PhD thesis of one of the NIKHEF students. In figure 5.1 the cross section of the charged current reaction is shown.

In addition the data from both measurements were combined and the results are compared by a model that relies on a fixed number of free parameters. In previous years these fits had to include results from fixed tar-

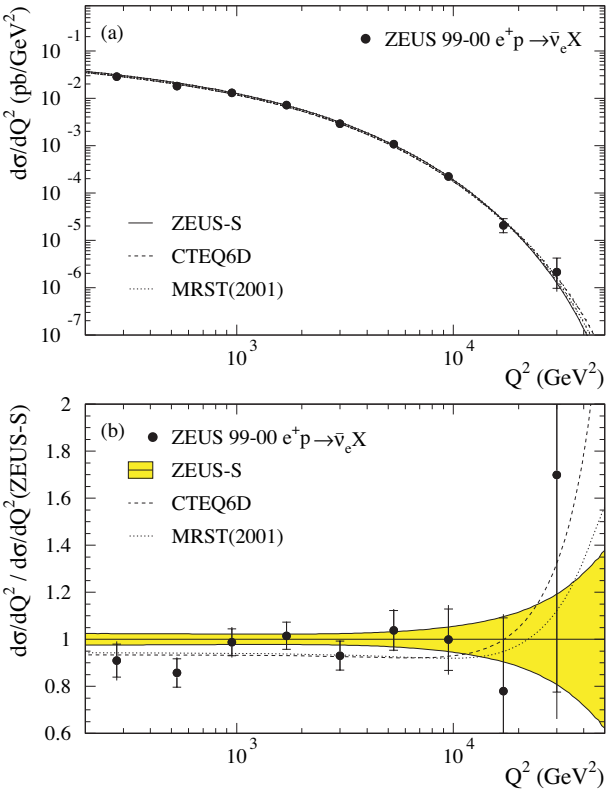

Figure 5.1: *Charged current cross section.*

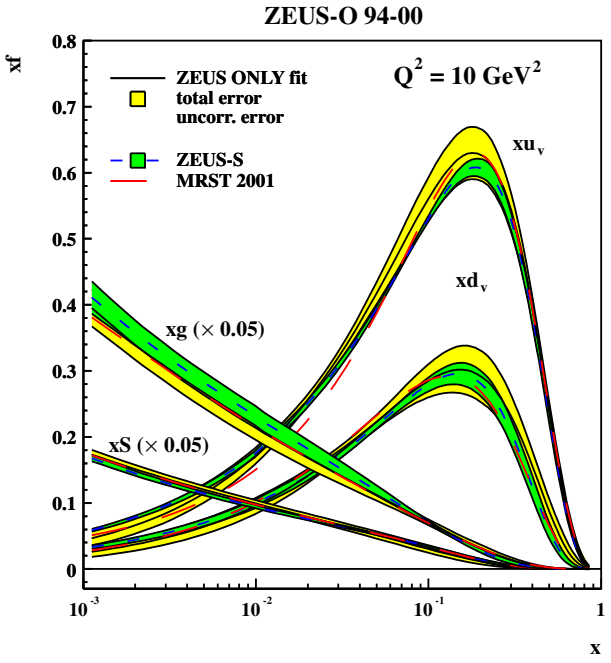

Figure 5.2: *Quark and gluon densities extracted from ZEUS data only compared with fits including fixed target data.*

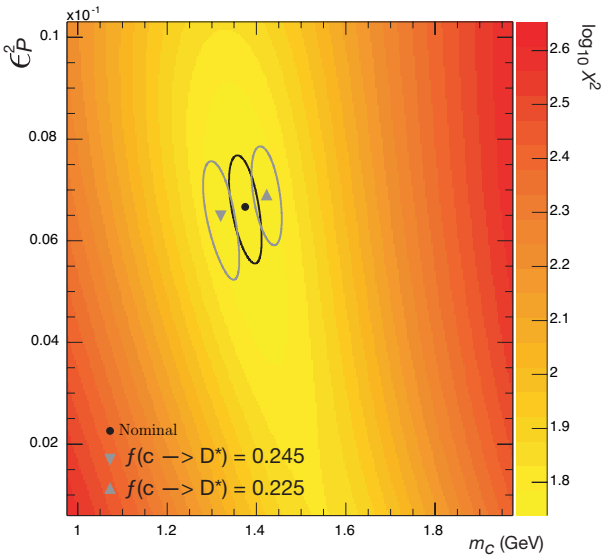

Figure 5.3: *Fitting both the charm mass and the Peterson fragmentation function.*

get experiments at other accelerators to constrain the parameters.

When all HERA-I data, taken by the ZEUS experiment only, are collected and added we are now able to fit all parameters and get constraints on each one of them. The results agree well with previous models and fit results. It all leads to a beautiful graph that shows in great detail how the structure of a proton can be broken down into contribution of the three valence quarks, the gluon density and the quark-anti-quark pairs in the so called sea. This proton structure is best illustrated with the momentum density as show in Figure 5.2. It shows a comparison of the extraction of the quark densities using the fixed target data and with those extracted using ZEUS data alone.

A different look inside the proton can be done with the study of heavy quarks like charm and beauty. With the HERA-I data one of the NIKHEF PhD students studied the charm content of the proton. In the comparison of such data with theory it is important to know the charm mass and to understand how a charm quark forms the hadron that is observable in the detector. This process, the so called fragmentation, can be parametrised with a function. Although more than one function is used in the literature, the one proposed by Peterson is used frequently. This function has one free parameter ϵ. In the thesis of S. Schagen it is shown how a fit procedure can be constructed that allows to extract the charm mass and the fragmentation parameter simultaneously. The results of the fit are shown in figure 5.3. From the cross section of the D*-production the charm mass is extracted as $m_{charm} = 1.37 \pm 0.04 \pm 0.08$ GeV.

5.4 Performance of the ZEUS vertex detector

In last years report we concluded from a small amount of data taken before this shutdown, that the ZEUS experiment itself was performing well. In particular the vertex detector, a new component to which NIKHEF members invested a major part of their attention over the last years, showed very promising results.

In 2003 three major steps forward were made. First of all the fine tuning of the detector calibration has improved the data quality with respect to data from 2002. This fine tuning lies mainly the synchronization of the signal sampling with the HERA bunch passing frequency. Although a rough calibration (still in the 10 ns region) had been done it now has been improved to 1 ns!

Secondly the precision of the alignment of the vertex detector with respect to the rest of the ZEUS track-

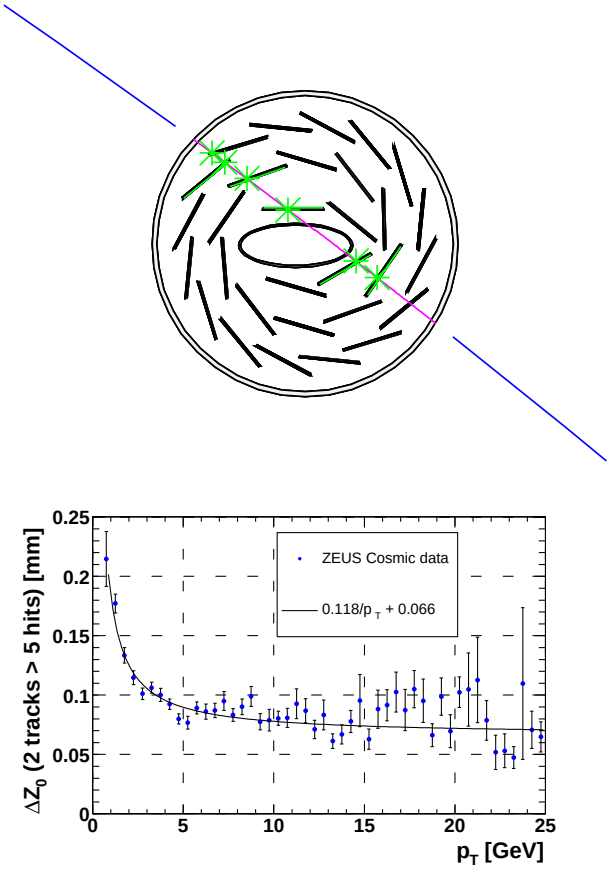

Figure 5.4: *On the top plot an example of a cosmic ray seen in ZEUS. In the bottom plot the miss distance between two segments of cosmic tracks. Dividing by a $\sqrt{2}$ gives the impact parameter resolution as a function of the momentum of the particle.*

ing detector has improved. The position of the major detector elements (these are the so called ladders, the detector is built with 30 ladders) is now corrected so that the deviations from the actual position are on average smaller than 0.01 mm!

The trackfit package that includes the data from our new vertex detector has been developed at NIKHEF. In 2003 when HERA started to deliver high intensity beams (albeit for short periods) it proved that the reconstruction code was too slow. We managed to reduce the CPU time of the tracking package with a factor of five!

The progress in the commissioning of the vertex detector is best showed in the impact parameter resolution. A set of particle tracks generated by cosmic rays has been recorded during the time that the accelerator is idle. With these tracks the performance can be studied very precisely. The momentum of these muon tracks is measured by the central tracking detector and therefore effects of multiple scattering can be separated from real detector effects. The estimated impact parameter resolution that can be derived from the this muon track sample is shown in figure 5.4 as a function of momentum. The resolution at high particle momenta is actually a factor of two better than foreseen in the detector proposal.

Wiring of the lead glass calorimeter in HERMES. (©DESY Hamburg)

6 HERMES

6.1 Introduction

The objective of the HERMES experiment at DESY is the study of the origin of proton spin. By scattering polarized high-energy electrons (or positrons) from polarized targets, the amount of spin carried by the various quark types can be measured. The same experiment also gives access to various related subjects on the quark-gluon structure of matter. In particular, the role of partonic correlations in the nucleon and the possible existence of novel multi-quark states have received considerable attention recently.

In the year 2003 only a limited amount of data was collected by the HERMES experiment due to an extended shut-down period of the HERA electron-proton collider at DESY, and considerable beam tuning efforts that were needed to reduce the unwanted backgrounds for the other HERA experiments. Fortunately, all of this has resulted in a considerably improved situation, which was reflected by two months of regular data taking near the end of the year.

During this relatively brief period the single piece of new HERMES instrumentation, the Lambda Wheels, went into routine operation. This wheel-shaped array of silicon counters was largely developed and constructed by our group at NIKHEF. The problem encountered last year, which was related to an unfortunate interference between the much larger than expected fringe field of the magnet used to orient the target spins and the readout electronics which are locally connected to the Lambda Wheels, was completely solved. Lambda-Wheel data are now included in the standard HERMES data stream.

The NIKHEF group is also partially responsible for the operation of the (longitudinal) polarimeter, which monitors the polarization of the stored lepton beam in HERA. With this instrument, polarizations up to about 50% were measured in 2003. This is the first time that such high polarizations have been observed since the large upgrade of the HERA facility in 2001. On average, beam polarizations of 30% to 40% are now reached.

The analysis of data collected in previous years has led to two remarkable results in 2003. The first one concerns the observation of a narrow baryon state with one unit of strangeness near a mass value of 1.53 GeV. This observation came shortly after similar reports were received from several other experiments in Japan, Russia, the United States and Germany. The state is commonly interpreted as being the first example of an entirely new type of particle containing 5 valence quarks, the so-called pentaquark. The second important result that was released by the HERMES collaboration in 2003 concerns the first measurement ever made of a single-spin asymmetry in semi-inclusive deep-inelastic lepton scattering from a transversely polarized target. These data make it possible to study the spin-structure of the nucleon while "switching off" the gluon contribution. More details on these new results are given in Sect. 6.3.

In the fall of 2003 the research work of the NIKHEF group in the HERMES collaboration was subject to a mid-term review organized by the funding agency FOM. An international review committee judged the research as being "challenging and of fundamental importance", and strongly endorsed the continued support of the NIKHEF group in HERMES until the end of HERA Run II.

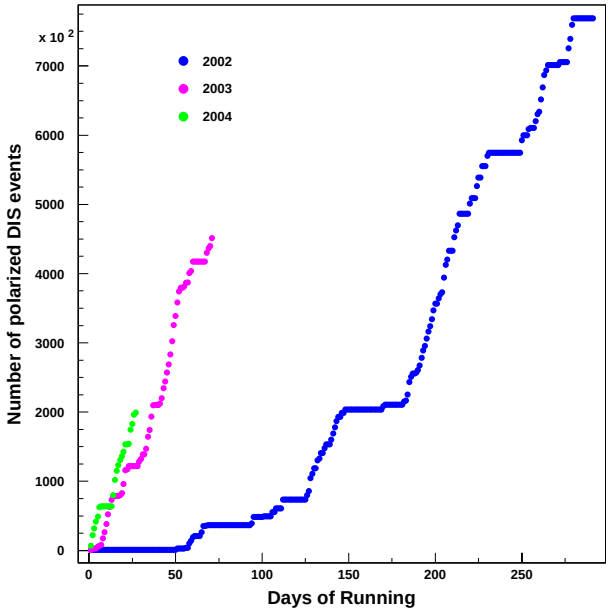

Figure 6.1: *Integrated number of deep-inelastic scattering events collected by the HERMES experiment at DESY since the beginning of HERA Run II in 2002. The data obtained in each year are labeled by a different color. The data collected in the beginning of 2003 before the extended HERA shut-down are included in the 2002 data set.*

In the coming years the group will receive additional support from the 6^{th} Framework Programme of the European Commission, because the "I3HP" integrated infrastructure project on hadron physics was approved recently. Within this project the NIKHEF group is participating in a Joint Research Activity (JRA) on generalized parton distributions and an EU-Network on transverse spin phenomena.

6.2 Data taking

Following the highly successful data-taking period from 1995 to 2000 (usually referred to as HERA Run I), a second data taking period was started in the year 2002. Unfortunately, due to severe background problems encountered by the other experiments that make use of the HERA collider only a modest amount of data has been collected in HERA Run II so far. In fact, an additional shut-down period had to be scheduled at HERA (from March to August, 2003) in order to allow for appreciable modifications to both the accelerator and the collider experiments. After a brief recommissioning period, actual data-taking started in October 2003.

In Figure 6.1 the integrated number of deep-inelastic scattering events is displayed for each year of HERMES Run II. The data are plotted in a cumulative fashion as a function of the day since the beginning of the run. Only a limited number of polarized deep-inelastic scattering events has been collected in 2003, due mainly to the rather short duration of the run period. Otherwise, the data taking efficiency was good, as reflected by the steep slope of the curve.

The data collected in 2003 have been obtained with a transversely polarized hydrogen target. These data are used to study the transverse polarization of quarks in the nucleon, a subject on which no data exist so far. First results are presented in the next section.

6.3 Physics analysis

In 2003 several interesting physics results were released by the HERMES collaboration. In the following subsections some examples are given including the first results based on data obtained in HERA Run II (on transverse spin asymmetries).

Pentaquarks

Recently, first indications have been reported for an exotic baryon resonance with strangeness $S = +1$ at a mass of about 1.54 GeV. The first data were presented by the LEPS collaboration studying the reaction $\gamma \rightarrow K^-(K^+X)$ at the Spring-8 synchrotron facility in Japan. Later, similar reports were issued by the CLAS

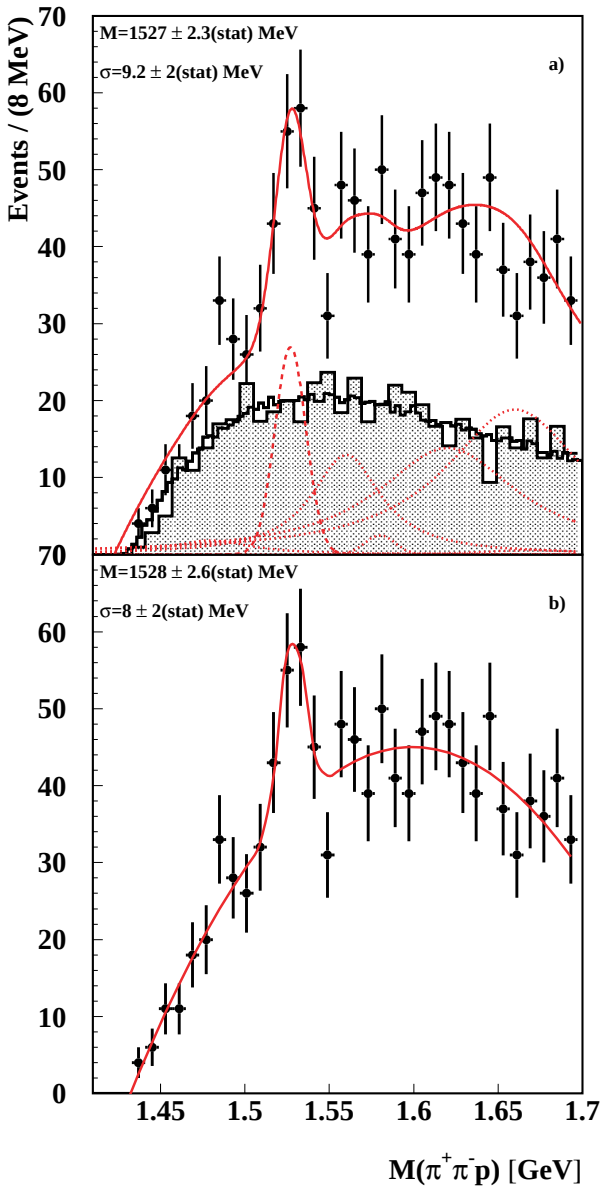

Figure 6.2: *Invariant-mass spectrum for $K_s p$ events. In the upper panel the gray shaded histogram represents the result of a Monte-Carlo simulation of the non-resonant background, while the fine-binned histogram has been obtained from a mixed-event analysis. The fitted curve is based on the simulation of the background in combination with a set of known Σ^{*+} resonances (dotted curves) and a free Gaussian (dashed). In the lower panel a fit to the data of a free Gaussian plus a third-order polynomial is shown. The masses and widths shown in each panel are the result of the fits.*

collaboration at Jefferson Lab, and groups from ITEP and Bonn, mostly focussing on the K^+n channel. The resonance, which is named Θ^+, corresponds to an isosinglet state with quark configuration ($uudd\bar{s}$). Such pentaquark states were predicted 25 year ago to exist in QCD.

At HERMES a search for this baryon resonance was also initiated. Quasi-real photoproduction data obtained on a deuterium target were used to identify the new state through the decay $\Theta^+ \to K^0_s p \to \pi^+\pi^- p$. Various selection criteria have been applied to the data to enhance the number of $\pi^+\pi^- p$ events with respect to the background. The invariant mass spectrum gives evidence for the existence of a narrow state at 1.53 GeV as illustrated in Figure 6.2. In this figure, two different methods of treating the background are presented. In the upper panel the $\pi^+\pi^- p$ spectrum is described as the sum of a non-resonant part and a fit that includes the positions and widths of the known Σ^{*+} resonances in the spectrum. The non-resonant part was taken from a Monte-Carlo simulation, of which the shape was verified by a spectrum constructed from combinations of kaons and protons from different events ("mixed-events"). In the lower panel of Figure 6.2, the $\pi^+\pi^- p$ spectrum is described by a third-order polynomial plus a Gaussian, which is the method used by the other experiments that have claimed the observation of the Θ^+ state. It is gratifying to see that both methods yield consistent results, i.e. a surprisingly narrow peak is obtained at a mass value where no other resonances are known to exist.

The width of the peak at 1.53 GeV is only slightly larger than the experimental resolution of the HERMES spectrometer ($\sigma \approx 7$ MeV). The $4-6\ \sigma$ significance of the pentaquark observation at HERMES is similar to what has been claimed by the other experiments.

Transversity

The chiral-soliton (instanton) model and lattice gauge calculations both predict that the tensor charge of the nucleon ($\delta\Sigma_q$), which can be derived from the *transversity* distribution function $h_1(x)$, is considerably larger than the longitudinal quark spin contribution $\Delta\Sigma_q$, which is derived from data on the longitudinal spin-dependent structure function $g_1(x)$. The difference between $\delta\Sigma_q$ and $\Delta\Sigma_q$ is caused by the absence of gluon-splitting contributions in the transverse case, which is also expected to result in a relatively weak Q^2 dependence of $h_1(x)$. Unfortunately, because $h_1(x)$ is chirally odd inclusive deep-inelastic scattering cannot be used to measure it. In semi-inclusive deep-inelastic scatter-

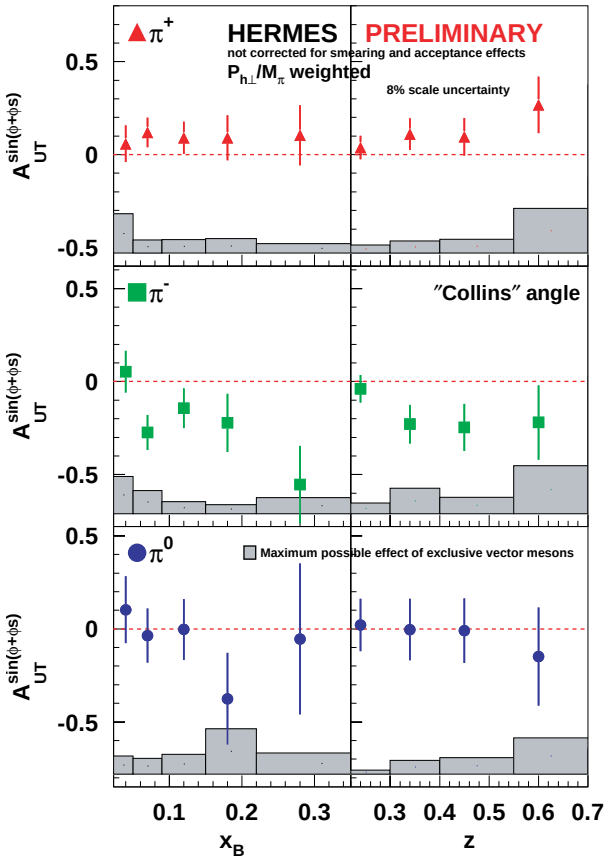

Figure 6.3: *Azimuthal target-spin asymmetry as a function of the variables x_B (left column) and z (right column) for semi-inclusive deep inelastic scattering off a transversely polarized hydrogen target. Data for semi-inclusive π^+ (upper panels), π^- (middle panels) and π^0 (lower panels) are shown. The "Collins" azimuthal angle, which is defined as the sum of the azimuthal angle of the pion and that of the target spin vector, has been used in evaluating these data. The results have been weighted by the factor $p_{\perp,\pi}/M_\pi$. The hatched area represents the systematic uncertainty on the data, which is largely dominated by possible contaminations of exclusive vector meson production.*

ing information on $h_1(x)$ can only be obtained in processes that are governed by a chirally odd fragmentation function. This can be achieved by measuring the azimuthal distribution of pions produced in semi-inclusive deep-inelastic scattering off transversely polarized nucleons, a process which depends on the chiral-odd Collins fragmentation function. By comparing the yield for two transverse spin orientations a so-called sin-

gle (target) spin asymmetry (SSA) is obtained, which is directly related to the size of $h_1(x)$.

First results on single-spin asymmetries obtained on a transversely polarized target are shown in Figure 6.3. The amplitude of the azimuthal dependence (or the $\sin\phi_C$ moment) is shown as a function of the Bjorken scaling variable x_B and the pion energy fraction $z = E_\pi/\nu$. Data are shown for π^+, π^0 and π^- mesons. The $\sin\phi_C$ moment is evaluated with respect to the azimuthal angle ϕ_C, which is defined as the sum of the azimuthal angles of the pion and the target polarization vector (with respect to the lepton scattering plane).

The data in Figure 6.3 show that there is evidence for non-zero values of the transversity distribution $h_1(x)$. It came as a surprise, however, that the π^- data showed a larger (negative) asymmetry than the small (positive) asymmetry observed for the π^+ data, whereas the opposite had been expected.

In order to arrive at a better understanding of these results considerably more data are needed. This is the reason that the HERMES experiment continues to take data on a transversely polarized hydrogen target in the coming year. Moreover, other reaction channels that are potentially sensitive to transverse spin effects, such as azimuthal asymmetries in two-pion production, are explored as well.

Exclusive two-pion production

Studies of the quark-gluon structure of the nucleon are usually limited to inclusive and semi-inclusive deep inelastic scattering experiments, from which parton distribution functions can be extracted. Our understanding of quark-gluon dynamics can be extended considerably if information could be obtained on the so-called Generalized Parton Distributions (GPDs), which take into account the dynamical correlations between partons with different momenta. Experimentally, GPDs can be investigated in hard exclusive production of mesons by longitudinally polarized virtual photons. Under these conditions the amplitude factorizes into a hard part governed by perturbative QCD and two soft parts given by the GPDs, and Generalized Distribution Amplitudes for hadron formation, respectively. Additional information on GPDs can be obtained from hard exclusive electroproduction of $\pi^+\pi^-$-pairs, which process is sensitive to the interference between the two isospin channels involved and thus provides a unique window on hadron structure.

At HERMES this hard exclusive electroproduction of $\pi^+\pi^-$ pairs has been studied on hydrogen and deuterium targets. From the angular distribution of the pion pairs the first-order Legendre moment $\langle P_1(\cos\theta)\rangle$ has been determined, where θ is defined as the production angle of the π^+ meson with respect to the direction opposite to the the recoiling target in the $\pi^+\pi^-$ center of mass. The dependence of this first-order Legendre moment on the $\pi^+\pi^-$ invariant mass $m_{\pi\pi}$ is shown in Figure 6.4 for hydrogen. The data are compared to a calculation based on the GPD framework (due to M. Polyakov). Within this model, the non-trivial dependence of the data on $m_{\pi\pi}$ can be understood as being due to the interference between pion pairs in relative

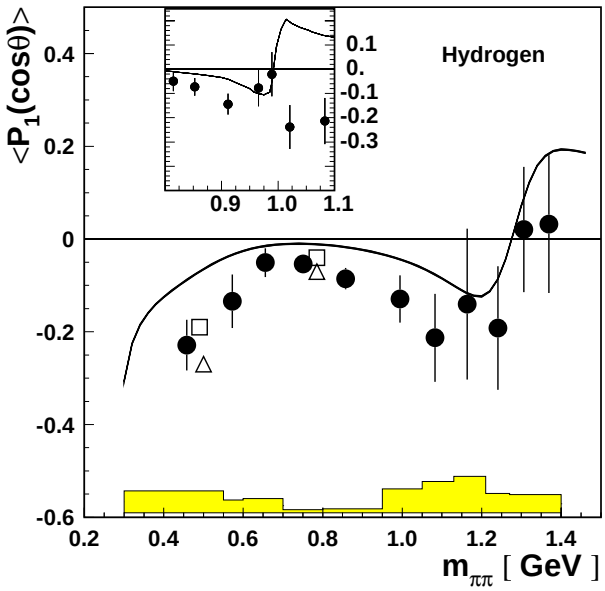

Figure 6.4: *The dependence of the first-order Legendre moment $\langle P_1(\cos\theta)\rangle$ on the invariant two-pion mass $m_{\pi\pi}$ for exclusive two-pion electroproduction on hydrogen. The curve represents a leading-twist prediction for hydrogen in the Generalized Parton Distribution framework. While the solid curve includes a two-gluon exchange contribution, the open squares (at $x_B = 0.1$) and open triangles (at $x_B = 0.2$) represent isolated calculations without the gluon exchange contribution. In the these calculations, the f_0 scalar meson contribution was not included. Instead, the region $0.8 < m_{\pi\pi} < 1.1$ GeV is separately considered in the inset to investigate possible contributions from the narrow $f_0(980)$ scalar meson. The curve in the inset represents a different GPD calculation that includes the f_0 contribution. All experimental data are centered at $\langle x\rangle = 0.16$ and $\langle Q^2\rangle = 3$ GeV^2. The systematic uncertainty is represented by the hatched area.*

P-wave (isovector channel) and S, D-waves (isoscalar channel) states.

By studying these and other (combinations of) Legendre moments, and their dependence on the Bjorken scaling variable x_B, the relative importance of quark and gluon exchange in two pion production, and the role of higher-twist effects can be assessed. The present results already provide some evidence for contributions due to higher twist or transverse virtual photon polarization. Possible contributions from $f_0(980)$ scalar meson production are likely to be small (see inset in Fig. 6.4.)

Deep-inelastic scattering from nuclei

During selected (brief) periods the HERMES experiment operates with unpolarised (gaseous) nuclear targets. Data were obtained on H, D, He, N, Ne and Kr targets, mostly at 27 GeV, but also at 12 GeV. These data were used to study the effect of the nuclear medium on inclusive deep-inelastic scattering, the attenuation of hadrons produced inside nuclei and coherence length effects in vector meson production. Many of these results have been discussed in previous annual reports.

Because HERMES data for the ratio of deep-inelastic scattering cross sections, $(\sigma_A/A)/(\sigma_D/2)$ suffer from fairly large statistical and systematic uncertainties, the group decided to participate in a dedicated experiment carried out in Hall C at Jefferson Laboratory (JLab) in Newport News, Virginia, in which these cross sections can be determined with very high precision. The purpose of this experiment is (among others) to measure the ratio R of longitudinal to transverse DIS cross sections, $R = \sigma_L/\sigma_T$ down to very low values of the four-momentum transfer squared Q^2 for various nuclei. Such data will provide first measurements of R in the low Q^2 domain, where R should go to zero for $Q^2 \to 0$ because of current conservation. In this domain large non-perturbative effects are anticipated, which could be enhanced in the nuclear medium.

In the JLab experiment, inclusive deep-inelastic scattering data were obtained at beam energies of 5.65, 3.43 and 2.31 GeV at various scattering angles for targets of H, D, C, Al, Cu and Au. This makes a Rosenbluth separation possible, in which the longitudinal and transverse DIS cross sections are determined separately. Since the radiative corrections in these data at low final electron energies are rather large (due to hard photon emission followed by nuclear elastic scattering at low Q^2), special attention is being given to an accurate description of both internal and external radiative corrections. The

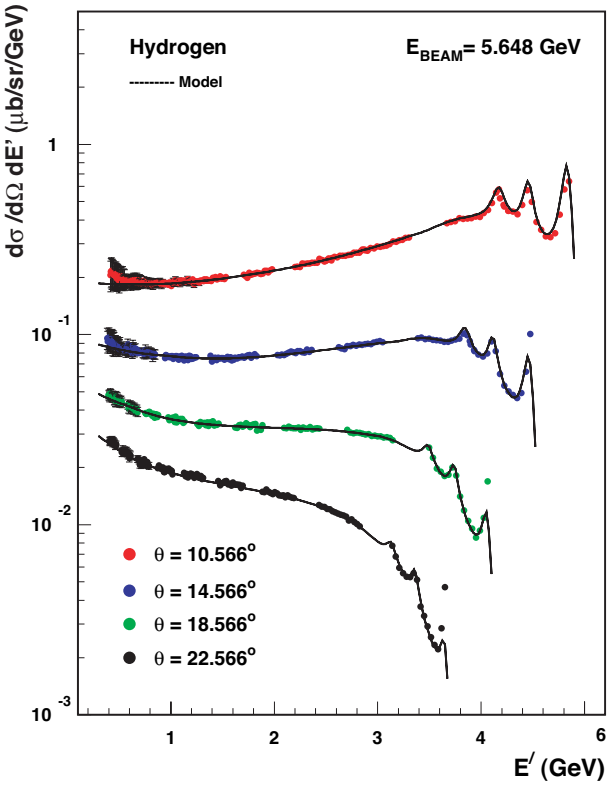

Figure 6.5: *Differential cross section for deep inelastic scattering from hydrogen as a function of the energy of the scattered electron. The data have been collected in Hall C at JLab at four different scattering angles. The data are described by calculations that include all known information on form factors, the nucleon resonance region, deep inelastic scattering and radiative corrections.*

JLab data are not only being used to extract the ratio R for various nuclei, but also to extend the data base of the structure function F_2 and to measure the EMC effect at low values of Q^2.

A first result of the JLab measurements is shown in Figure 6.5, where the measured differential cross section is plotted as a function of the energy of the scattered electron for four different angle settings of the spectrometer. The data are of very high quality, and are well-described by a calculation that includes all relevant contribution in this energy domain: form factors, nucleon resonances, structure functions and radiative effects. The precision of the data obtained is essential for carrying out longitudinal-transverse separations and for extracting information on the dependence of R and the EMC effect on nuclear mass. This analysis will be finalized in the coming year.

6.4 Instrumentation

The HERMES detector is a forward-angle spectrometer in which both scattered positrons (or electrons) and produced hadrons are detected within an angular acceptance of $\pm$ 170 mrad horizontally, and $\pm$ (40 – 140) mrad vertically. The NIKHEF group is partially responsible for the longitudinal polarimeter, the wheel-shaped silicon detector in the front region (the Lambda Wheels), the Pb-glass calorimeter (driving mechanism) and the beam-loss monitor. Because the longitudinal polarimeter and the Lambda Wheels required most of our attention, only those two subjects are discussed below.

The Lambda Wheels

The Lambda Wheels are two wheel-shaped arrays of silicon strip counters that are mounted inside the HERA electron beam vacuum approximately 50 cm downstream of the HERMES internal target. The Lambda Wheels enlarge the acceptance for the detection of slowly-decaying hadrons produced in various semi-inclusive reaction channels by a factor of two to four. Moreover, the precision by which the polarisation of the Λ^0 hyperon can be determined is greatly improved, because the false asymmetry (which is large if the standard HERMES acceptance is used) vanishes when the Lambda Wheels are employed.

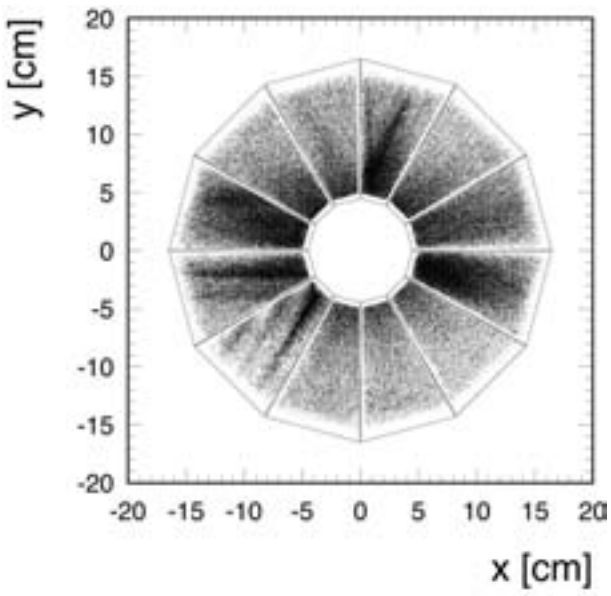

Figure 6.6: *Position of hits recorded in the Lambda Wheels in 2003. The threshold used for this plot is set at 30 % of the signal produced by a minimum ionizing particle (i.e. 0.3 MIP). The outline of the modules, and the entire detector is also shown.*

The detector consists of 12 modules, and has an outer diameter of about 33 cm. Each module has two double-sided wedge-shaped silicon counters, cut out of 6″ wafers, with accompanying readout electronics based on the HELIX-2.2 chip. Cooling is provided by a closed loop filled with ethanol, which in turn is cooled by a set of Peltier elements.

Following the upgrade and recommissioning of HERA (in 2001-2002), the Lambda Wheels were installed. Unfortunately, the commissioning of the Lambda Wheels in 2002 was hampered by the unexpectedly high fringe field of the newly installed transverse-target magnet. During the HERA shut-down period of 2003, all modules were modified in order to operate them in relatively high magnetic fields. In the fall of 2003 this operation proved to be successful, and since then the Lambda Wheels have been fully operational and the data have been included in the HERMES data stream. The hit pattern of events recorded with the Lambda Wheels is displayed in Figure 6.6.

The Longitudinal Polarimeter

The longitudinal polarimeter (LPOL) at HERA exploits the asymmetry in the Compton cross section by scattering circularly polarized photons off longitudinally polarized electrons. The interaction point is located 39 m downstream from the center of the HERMES target. The backscattered photons are detected in a calorimeter that measures the total energy of the photons. Due to their very large boost almost all photons are scattered into a very small cone around 180° in the laboratory frame and travel along the electron beam. In order to separate the photons from the electron beam a dipole magnet is used to bend the electrons by 0.54 mrad. This is enough to extract the photons from the beam line 16 m downstream of this bend.

The backscattered photons are detected using a crystal calorimeter made from four independent crystal detectors, which allow the simultaneous determination of the energy and position of the scattered photon on the face of the detector. In Figure 6.7 the results obtained with the longitudinal polarimeter are compared to those of the transverse HERA polarimeter (TPOL), which is located at a different position in the HERA storage ring. Without special tuning efforts the beam polarization obtained in 2003 was usually between 30 and 40%. Figure 6.7 shows that a dedicated tuning effort can raise

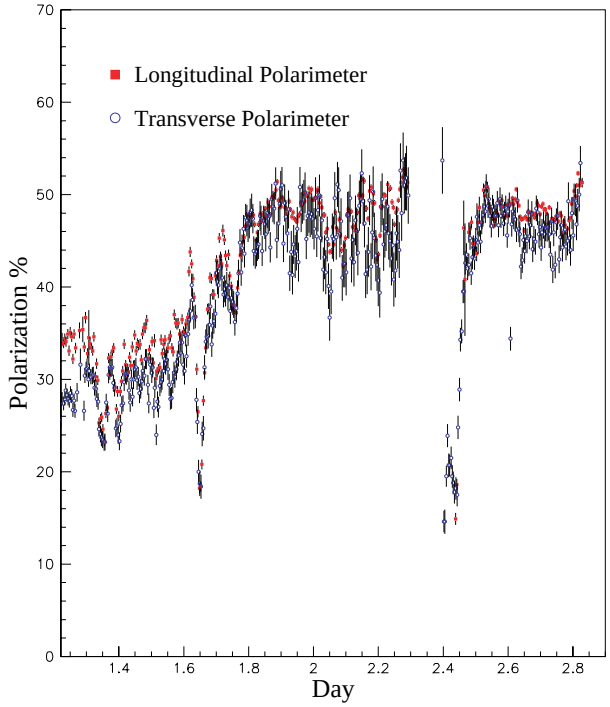

Figure 6.7: *Polarization of the HERA positron beam as measured in March 2003. After a dedicated tuning effort a polarization of 50% was obtained.*

the polarization to about 50%. This is important for various measurements in the near future at HERMES.

6.5 Outlook

In the year 2004 data taking with the transversely polarized target will continue at higher beam currents. Hence, the statistics for the transverse target-spin asymmetries are expected to be increased by a factor 4, which will substantially improve the significance of the data shown in Figure 6.3.

Late in 2004 (or early 2005) a new large-angle recoil detector will be installed at HERMES. With this detector and the now operational Lambda Wheels, the acceptance for the detection of recoil particles is very large. This will make it possible to study exclusive processes that give access to the Generalized Parton Distributions introduced in Sect. 6.3.

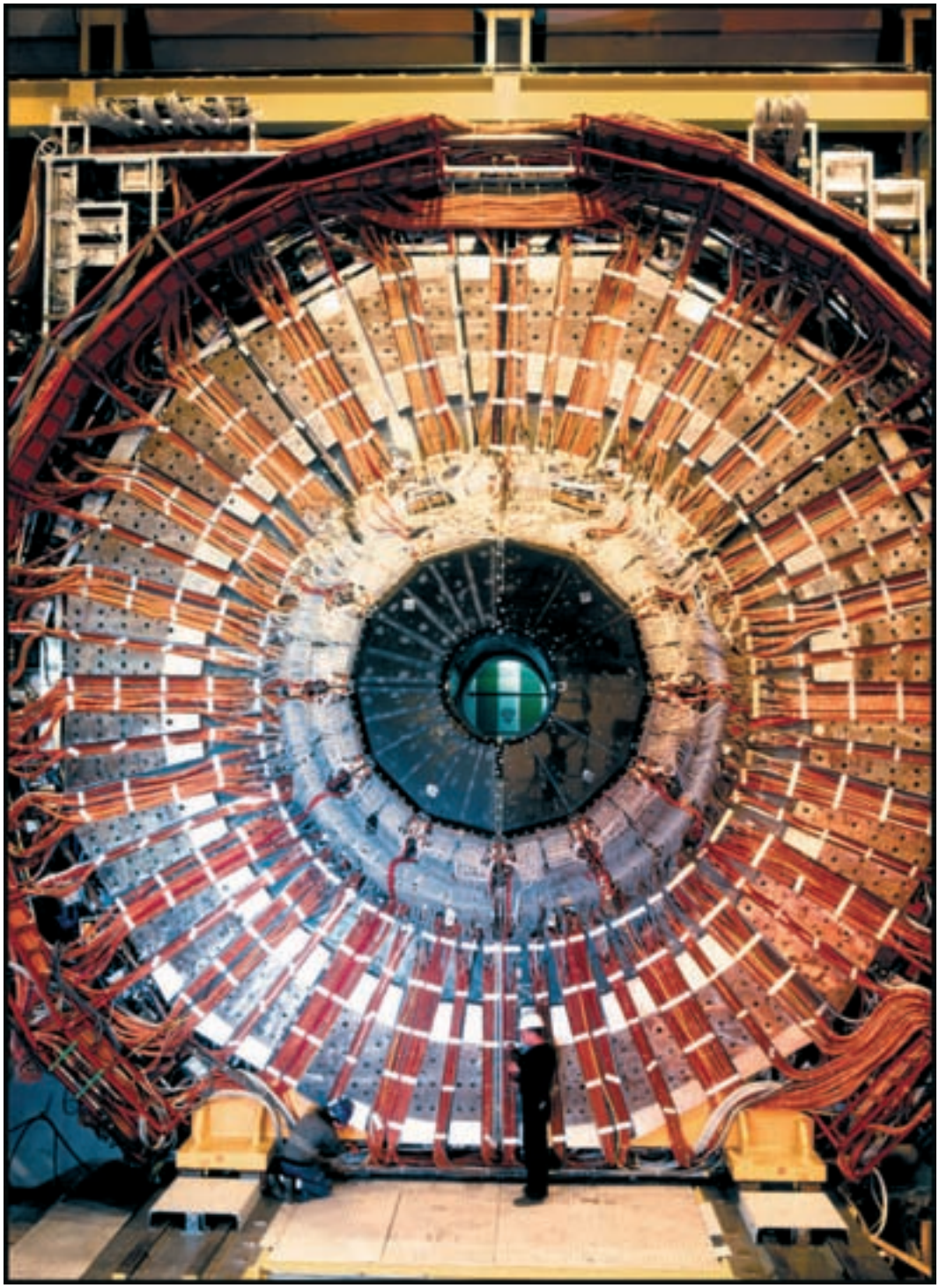

The DELPHI Detector during dismantling. (©CERN photo 0012034)

7 DELPHI

7.1 DELPHI programme and Detector exhibit

The DELPHI detector stopped data taking at the end of the year 2000. This year the LEP FOM programme ended. A final evaluation report of the LEP programme has been prepared and will be submitted to the FOM council.

The barrel part of the DELPHI detector is being prepared as a permanent exposition for CERN visitors. It has been moved to its final position in pit 8, compatible with the spatial arrangement of the LHCb counting houses. A visitors platform has been installed. Several sub-detectors are being prepared to allow viewing of internal construction details. It is foreseen to make the detector exhibit available to the public from summer 2004 onwards.

7.2 Publications

During the year 2003 the DELPHI Collaboration continued the analysis of data collected both at the Z peak (LEP1) and at centre-of-mass energies 161-209 GeV (LEP2). Many analyses were finalised. A total of 15 papers were published or accepted for publication in refereed journals in 2003 and an additional 12 papers were submitted for publication. Out of these, 9 papers are based on LEP1 data and covered mainly B and τ physics topics. A further 16 papers are in preparation and it is expected that ongoing analyses will lead to another 25 papers in 2004-2005.

A total of 47 contributions were submitted to the HEP-EPS Conference in Aachen and the Lepton-Photon Symposium at Fermilab.

The NIKHEF group contributed to B physics, W physics and Tri-linear Gauge Couplings (TGC's). One PhD thesis was finished on single W production and TGC's.

7.3 B physics

Using high performance neural network techniques, precise measurements of B^+, B^0 and mean b-hadron lifetimes have been obtained:
$\tau_{B^+} = 1.624 \pm 0.014(stat) \pm 0.018(syst)$ ps,
$\tau_{B^0} = 1.531 \pm 0.021(stat) \pm 0.031(syst)$ ps or
$\frac{\tau_{B^\pm}}{\tau_{B^0}} = 1.060 \pm 0.021(stat) \pm 0.024(syst)$ ps, and
$\tau_b = 1.570 \pm 0.005(stat) \pm 0.008(syst)$ ps.
The B^+ and average b-hadron lifetime are - despite the competition from the experiments BABAR and BELLE at the B factories - the most accurate to date. These precise measurements allow to test - and confirm - the predictions of the Heavy Quark Effective Theory (HQET) for the charged to neutral B lifetime ratio to a precision of about 3%.

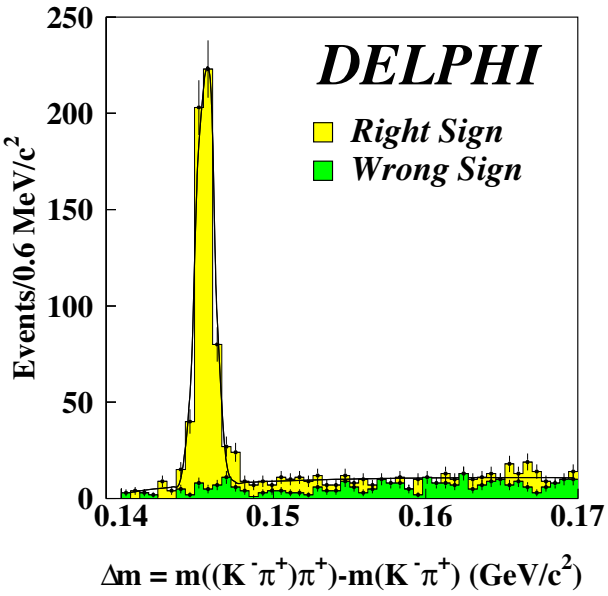

Figure 7.1: *Mass difference Δm of $(K\pi)\pi$ and $K\pi$ showing a D^* signal.*

The CKM matrix element $|V_{cb}|$ has been measured from the decays $\overline{B^0_d} \rightarrow D^{*+} l^- \bar{\nu}_l$ using exclusively reconstructed D^{*+} decays. The invariant mass distribution for the $(K\pi)\pi$ channel is shown in Fig. 7.1.

Using HQET, the branching ratio for this decay can be expressed as the product of a known form factor times $F(1)^2_{D^*}|V_{cb}|^2$. The function $F(1)_{D^*}$ is the Isgur-Wise function at zero recoil, and it is estimated to be 0.91 ± 0.04. Combining this measurement with a more inclusive measurement, previously published by DELPHI, yields $|V_{cb}| = 0.0414 \pm 0.0012(stat) \pm 0.0021(syst) \pm 0.0018(theor)$. Thus, $|V_{cb}|$ is determined with a 7 percent error.

The CKM matrix can be parametrised - the so-called Wolfenstein parametrisation - with four free parameters: λ, A, ρ and η. The λ parameter is accurately determined from Kaon decays. The second parameter A is most precisely determined from $|V_{cb}|$ measurements.

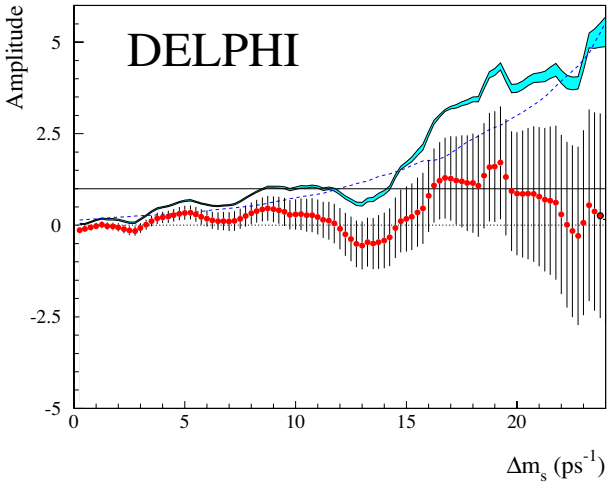

Figure 7.2: *Measured amplitude as a function of the oscillation frequency shown as points with error bars. The dashed line shows the sensitivity or expected upper limit at 95% CL, the solid lines represent the actual upper limit with and without including the systematic errors.*

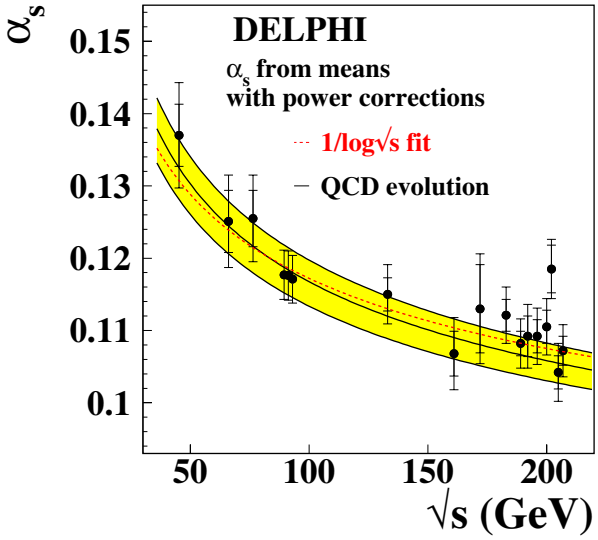

Figure 7.3: *Energy dependence of α_s as obtained from event shape distributions. The total and statistical (inner error bars) uncertainties are shown. The band displays the average values of these measurements when extrapolated according to the QCD prediction. The dashed lines show the result of the $1/\log\sqrt{s}$ fit.*

This element is therefore important in present and future precision tests of the CKM matrix.

In the last four years, a large effort was put into the search for $B_s^0 - \overline{B_s^0}$ oscillations. On the basis of fits to the CKM matrix it was was expected that the $B_s^0 - \overline{B_s^0}$ oscillation frequency should be less than 40 times faster than the B_d^0 oscillation frequency. New analyses were performed optimised to search for fast oscillations. In DELPHI five analyses were published using: exclusive B_s events, D_s-lepton and -hadron events, events with high transverse momentum p_t leptons and fully inclusive B events. The combined result of the measured oscillation amplitude A as a function of the oscillation frequency Δm_s is shown in Fig. 7.2. An amplitude A value equal to 1 would correspond to the hypothesis of $B_s^0 - \overline{B_s^0}$ oscillations. No clear signal for $B_s^0 - \overline{B_s^0}$ oscillations was found and a limit on the oscillation frequency was set at $\Delta m_s > 8.5\ ps^{-1}$, with a sensitivity at 12.0 ps^{-1}. The combined results from the LEP and SLD experiments (plus CDF) are published in the PDG 2004 and set a limit at $\Delta m_s > 14.4\ ps^{-1}$, with a sensitivity at 17.8 ps^{-1}. Unfortunately, no oscillations are yet observed, although a hint of a signal could be present around 15-20 ps^{-1}. The Tevatron experiments - and future experiments at the Large Hadron Collider - will continue the search.

Final papers on orbitally excited B particles, the b fragmentation function, and B leptonic and hadronic moments are being prepared.

7.4 QCD

The measurement of five event shape distributions and their means at energies from 183 to 207 GeV have been compared with QCD predictions. From the mean values the strong coupling constant α_s was determined using four different methods. The running of α_s with energy - a basic prediction from QCD - is verified, as shown in Fig. 7.3. Combining the results with those obtained at lower energies, including the results obtained around the Z peak, gives $\alpha_s(M_Z) = 0.1157 \pm 0.0033$ and the QCD β function is described by $\frac{\mathrm{d}\alpha_s^{-1}}{\mathrm{d}\log\sqrt{s}} = 1.11 \pm 0.09(stat) \pm 0.19(syst)$ to be compared with the QCD expectation of 1.27.

7.5 Standard Model Electroweak results

In 2003 several final results on four-fermion production processes were published. The *WW* production cross-section as a function of the centre-of-mass energy is shown in Fig. 7.4. These measurements are a tremendous confirmation of the Standard Model (SM)

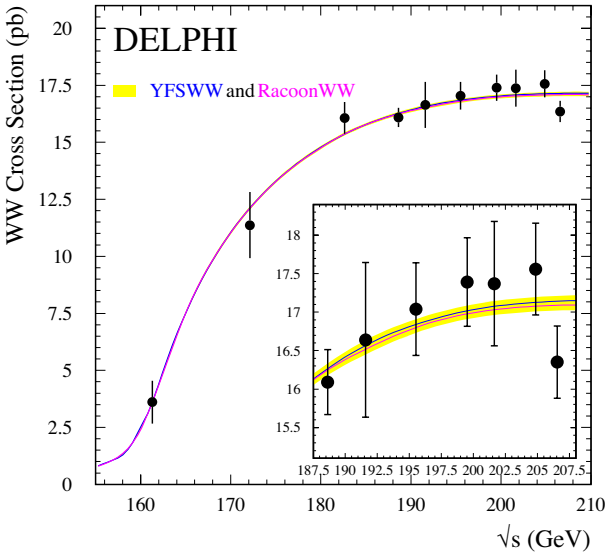

Figure 7.4: *Measurements of the WW cross-section as a function of the centre-of-mass energy compared with the Standard Model prediction given by the YFSWW and RacoonWW programs. The shaded band represents the uncertainty on the theoretical calculations.*

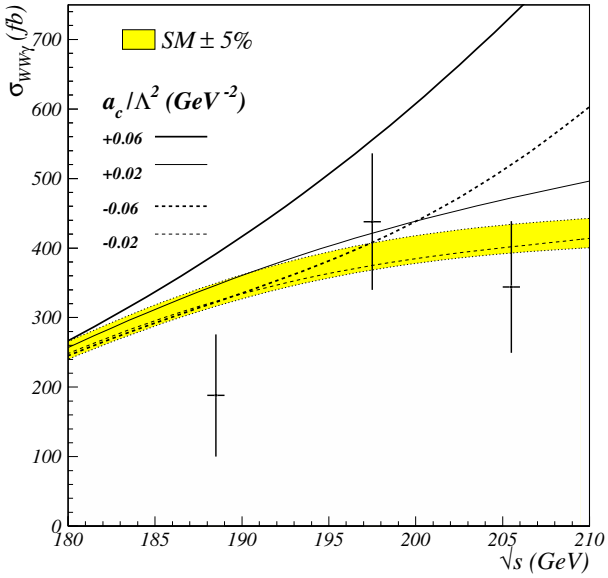

Figure 7.5: *$W^+W^-\gamma$ cross-section as a function of the centre-of-mass energy. The measured cross-sections (crosses) are compared to the SM prediction from WPHACT/YFSWW. The cross-sections obtained with EEWWG for indicative values of the anomalous parameter a_c/Λ^2 (in GeV^{-2}) are also shown.*

prediction, where large cancellations of the three tree-level Feynman diagrams occur. The measured cross-sections, when compared to the latest theoretical calculations that include full $O(\alpha)$ corrections to the three tree-level processes, and combined over all energies give a ratio $exp./theory = 1.001 \pm 0.015$.

Also the branching ratio for the leptonic decay of the W boson is measured and its value, averaged over the three lepton species, is $Br(W \to l\nu_l) = (10.85 \pm 0.14(stat) \pm 0.08(syst))\%$, in good agreement with the SM expectation of 10.83%. From this measurement the value of the CKM matrix element $|V_{cs}|$ can be derived: $|V_{cs}| = 0.973 \pm 0.019 \pm 0.012$. Further analysis of the production and decay angular distributions of the W boson show no evidence for the presence of anomalous TGC couplings between the gauge bosons.

Another process studied by DELPHI is $e^+e^- \to W^+W^-\gamma$, which involves the coupling of four gauge bosons. The expected cross-section from the SM at LEP2 energies is small. The measured cross-sections are in agreement with the SM expectation (see Fig. 7.5) and are used to establish limits on anomalous couplings among the four gauge bosons $WW\gamma\gamma$ and $WW\gamma Z$, e.g. $-0.063\ GeV^{-2} < a_c/\Lambda^2 < +0.032\ GeV^{-2}$.

Final papers on the measurements of the W mass, TGC's, single boson (Z, W) and $Z\gamma^*$ production are in preparation.

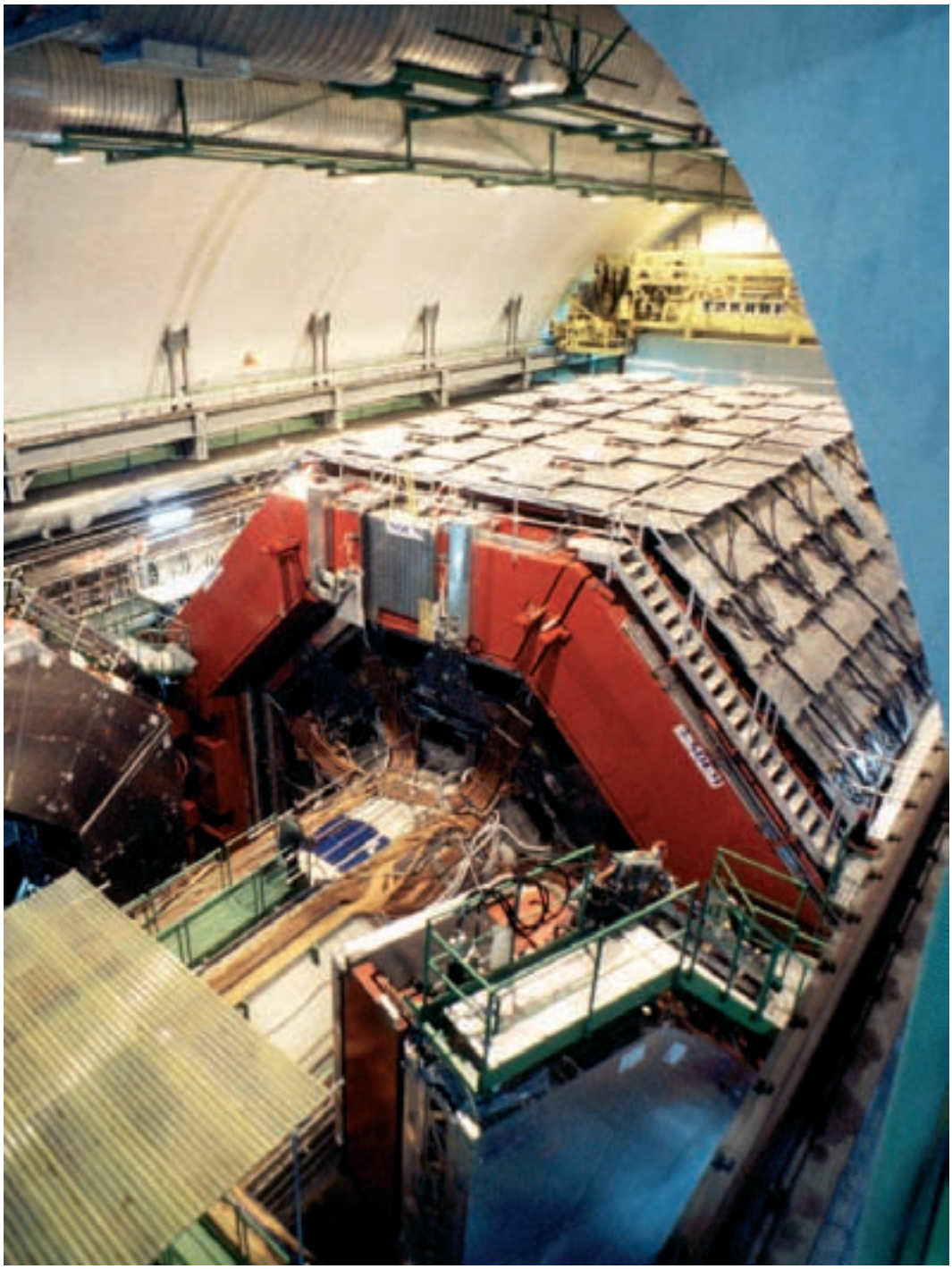

The L3 experiment with cosmic ray detector. (©CERN photo 0003004)

8 L3

8.1 Introduction

L3 was a general purpose detector designed with good spatial and energy resolution of electrons, photons, muons and jets produced in e^+e^- reactions.

The closure of LEP at the end of 2000 ended the yearly data-taking which began in 1989. Effort in 2003 concentrated on completion of analyses and their publication. In 2003 12 papers were published, and a large number of contributions were made to conferences, e.g., 56 to the EPS Conference on High Energy Physics in Aachen. About 30 additional papers are in preparation.

The number of physicists working on L3 further declined in 2003. In The Netherlands, one Ph.D. degree was granted on L3 analysis; five additional Ph.D. degrees are expected in coming years.

NIKHEF physicists contribute primarily to analyses of the mass and couplings of the W-boson, QCD, and the cosmic ray muon flux. The Ph.D. thesis defended in 2003 was on cosmic ray muons.

8.2 Searches

Following the publication, as first of the LEP experiments, of final results on the search for the Standard Model Higgs boson in 2001, the results were combined with those of the other LEP experiments. The final result is a lower bound on the Standard Model Higgs mass of 114.4 GeV at 95% confidence level. Although the Standard Model Higgs boson was not found, the possibility remained that Higgs bosons predicted in various extensions of the Standard Model could be detected, since some of these hypothetical Higgs bosons should have a mass smaller than that of the Standard Model Higgs. Examples are the charged Higgs bosons expected in two-Higgs doublet models and doubly-charged Higgs bosons in Higgs-triplet and left-right symmetric models. No such Higgs bosons were observed, and lower limits were set on their masses, typically around 80 GeV for the singly-charged and 100 GeV for the doubly-charged Higgs boson.

Excited leptons are predicted in composite models where leptons and quarks have substructure. They were searched for in both pair and single production in a variety of decay modes. No excited leptons were found and limits were set on their masses, typically of the order of 100 GeV. An example of the results is shown in Figure 8.1.

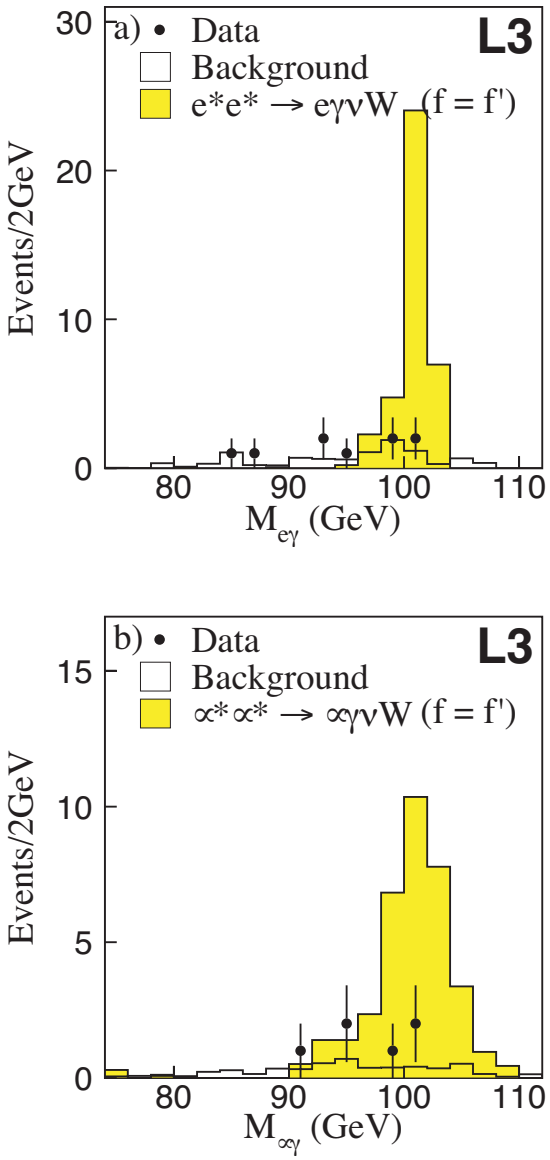

Figure 8.1: *The electron-photon (a) and muon-photon (b) invariant mass in $e\gamma\nu W$ and $\mu\gamma\nu W$ final states, respectively. The expected signal for excited leptons of mass 101 GeV is shown together with the data and the expected Standard Model background.*

8.3 W and Z physics

One of the main goals of the LEP program is the measurement of the properties of the W-boson and its cou-

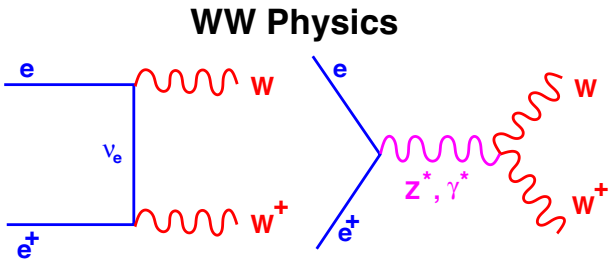

Figure 8.2: *Tree-level Feynman diagrams for the reaction* $e^+e^- \to W^+W^-$.

plings to other gauge bosons. In total some 10000 $e^+e^- \to W^+W^-$ candidate events have been selected.

The existence of triple-gauge-boson vertices is a consequence of the non-Abelian gauge structure of the electroweak theory. To lowest order, three Feynman diagrams contribute to W-pair production, as shown in Figure 8.2. The two s-channel graphs involve such vertices, namely γWW and ZWW. In general each is parametrised in terms of seven triple-gauge-boson couplings (TGCs). Retaining only CP-conserving couplings and assuming electromagnetic gauge invariance, gives six couplings. At tree level in the Standard Model they have the values $\kappa_\gamma = \kappa_Z = g_1^Z = 1$ and $\lambda_\gamma = \lambda_Z = g_5^Z = 0$. The distribution of the W production angle and the polar and azimuthal decay angles of the W^+ and W^- in their rest frames, as well as the W^+W^- production cross section depend on the values of these TGCs. From an analysis of these distributions the values of the TGCs are extracted. The cross section for $e^+e^- \to e\nu W$ depends on κ_γ and λ_γ. These TGCs are also measured in this channel and can be combined with the results of the W^+W^- analysis. An example of these results is shown in Figure 8.3. The TGCs are found to be consistent with the Standard Model expectations.

ZZ production has also been studied. The Standard Model cross section for ZZ production is an order of magnitude smaller than that of WW. The measured cross section is found to be in good agreement with the Standard Model (see Figure 8.4), and the distribution of the resulting jets and leptons in phase space is consistent with that expected from the Standard Model TGCs for $ZZ\gamma$ and ZZZ.

Final results on the mass and width of the W are expected in 2004. In 2003 progress was made on reducing the systematic uncertainties in these measurements. The dominant systematic uncertainty on the measurement of the W mass and width in the four-quark chan-

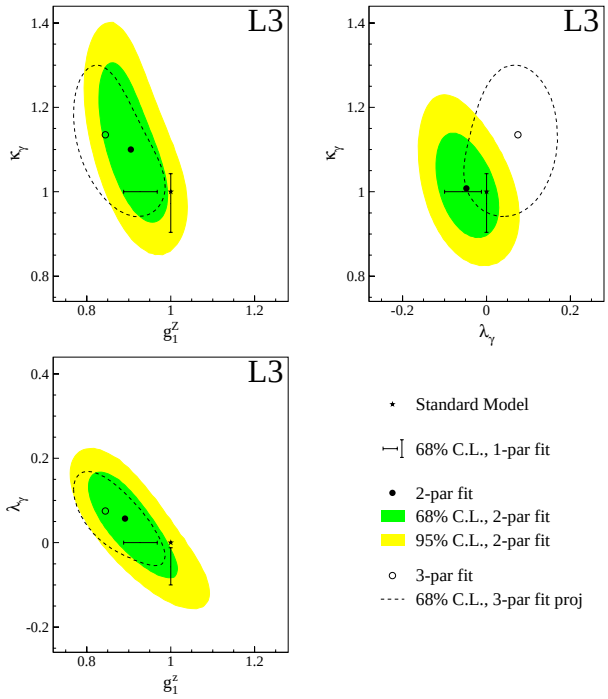

Figure 8.3: *Confidence limits on the ZWW and* γWW *TGCs* λ_γ, κ_γ *and* g_1^Z.

nel arises from theoretical uncertainty on two QCD effects. One is Bose-Einstein correlations (BEC) between identical bosons from different W bosons. Lack of theoretical understanding limits the precision of Monte Carlo modeling of these correlations, which in turn leads to uncertainty in the fit of the W resonance shape to the data. The L3 results on Bose-Einstein correlations were published in 2002 and indicated that they had little effect on the W mass measurement.

The other effect is the amount and nature of colour flow between gluons arising in the hadronisation of the $q\bar{q}$ from one W, *e.g.*, $W^- \to d\bar{u}$, and those from the other W, *e.g.*, $W^+ \to \bar{s}c$. This is usually referred to as colour reconnection.

Preliminary results have ruled out the most extreme models of colour reconnection. In 2003 L3 published its final result on colour reconnection. The study examines the ratio of the energy- and particle-flow between jets from the same W to that between jets from different W's. This ratio is compared (Figure 8.5) to various models of colour reconnection. It is also compared to the flow in the semi-hadronic channels, i.e., where one W decays leptonically and one hadronically. The results are consistent with no colour reconnection, and limits

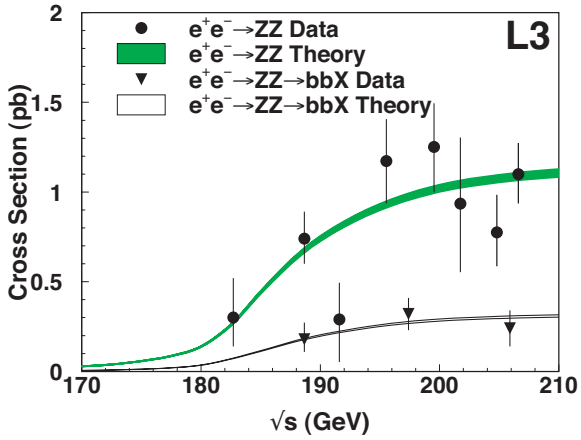

Figure 8.4: *Measurements and predictions for $e^+e^- \to ZZ$ and $e^+e^- \to ZZ \to b\bar{b}X$ cross sections as function of the centre-of-mass energy.*

are set on the amount of colour reconnection in various models. Unfortunately, the systematic uncertainty on the W mass from this source remains rather large. It is hoped that combination of the L3 colour reconnection results with those from other experiments will further reduce this uncertainty.

A LEP-wide working group plans to combine the results of all experiments on both colour reconnection and inter-W BEC in order to reduce the systematic uncertainties on the LEP-wide combination of W mass and width.

8.4 QCD

L3 has also studied colour reconnection in 3-jet Z decays, where colour flow is from the quark via the gluon to the anti-quark. Colour reconnection effects could alter this flow, creating a colour-flow "gap" within the gluon jet. This is related to the rapidity gap events observed in ep and $p\bar{p}$ events. The colour flow was studied in terms of asymmetries constructed from the difference in particle flow between quark and gluon jets and that between the quark and anti-quark jets. One such asymmetry is shown in Figure 8.6 where it is compared to the expectations in models with and without colour reconnection. No evidence for colour reconnection is found, which results in limits on the colour reconnection model of ARIADNE and on the Generalized Area Law as incorporated in JETSET. Interestingly, HERWIG disagrees with the data without colour reconnection as well as with colour reconnection.

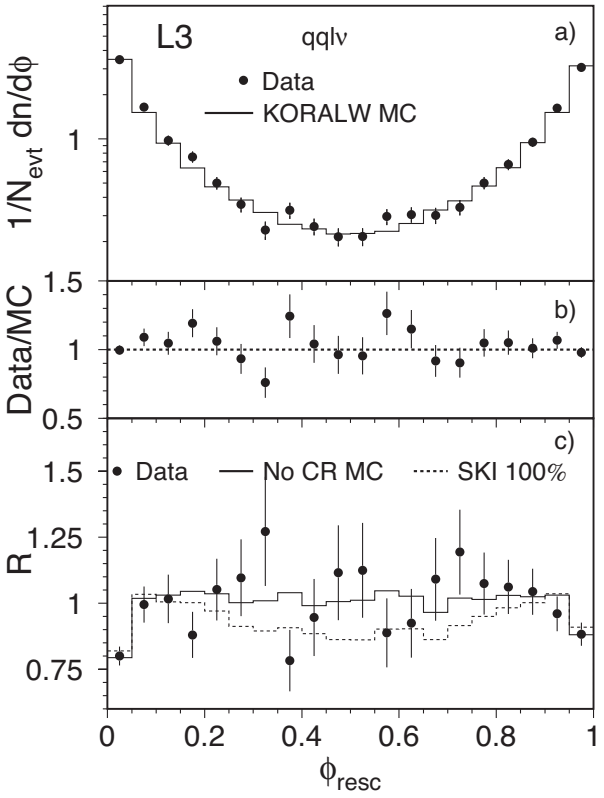

Figure 8.5: *(a) Particle flow distributions as a function of the rescaled angle for the semi-hadronic W decays for data and the KORALW prediction. (b) Ratio of data and MC as a function of the rescaled angle. (c) R, the particle flow in hadronic events divided by twice that of semileptonic events compared to MC with no colour reconnection and to MC using the SKI model of colour reconnection.*

Various results from $\gamma\gamma$ collisions were published. An example, is a study $\gamma\gamma \to p\bar{p}$, which provides data of higher statistical precision and at higher $W_{\gamma\gamma}$ than previously available. These data should be of use in making predictions for other baryon-antibaryon channels. The data are in agreement with the quark-diquark model predictions, as were the previous L3 results on $\Lambda\bar{\Lambda}$ and $\Sigma^0\bar{\Sigma}^0$ production.

8.5 L3+Cosmics

The vertical spectrum for cosmic ray induced muons with momenta greater than 20 GeV has been analysed by several groups using several methods. The results are in excellent agreement, as can been seen in Figure 8.7. The systematic uncertainty on the vertical spectrum is less than 2.5% at a muon momentum of 100 GeV. Next to the vertical spectrum, the muon charge

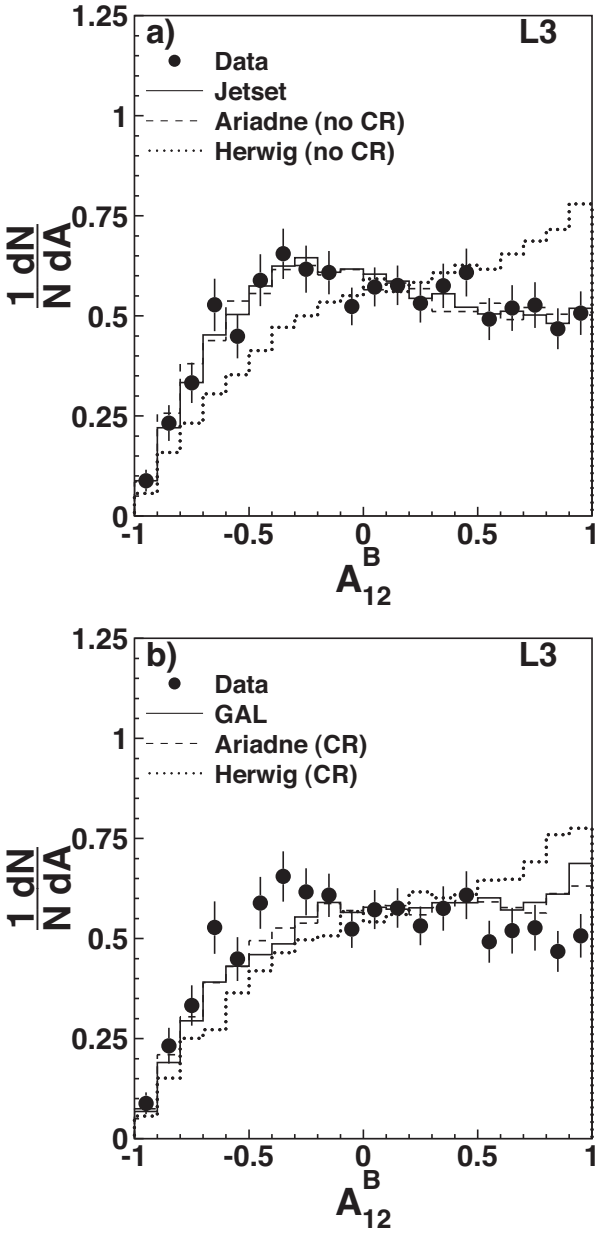

Figure 8.6: *Colour flow asymmetry compared to models without (a) and with (b) colour reconnection.*

ratio has been measured with high accuracy (the systematic uncertainty is about 1.5%). The effect of potential misalignments of the muon detector were studied in great detail during the past year, since this greatly influences the charge ratio.

Not only the vertical spectrum and charge ratio, but also the zenith dependence of these quantities has been measured, in eight bins in cosine zenith extending down

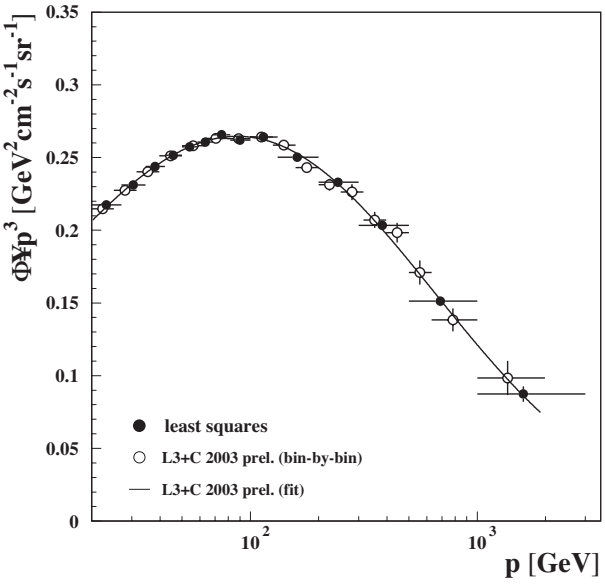

Figure 8.7: *Vertical cosmic ray muon spectrum.*

to cosine zenith values of 0.525. This is the first such measurement at high energies. A paper on the vertical spectrum and charge ratio, as well as the zenith dependence is expected to be published in 2004.

In 2003 a thesis on the combination of air shower data and muon data was defended. This thesis has been circulated to the model builders of air shower simulations (in particular CORSIKA). The results show that the number of high energy muons in the simulation is not well understood. Several improvements to the simulation have been suggested, and more work on this topic will be done before publishing the results.

In addition to searches for steady point sources and Gamma Ray Bursts, a search for high energy signals originating from pulsating sources (pulsars) has been started. A power spectrum of the muon signal originating from the direction of the pulsar will be made. A difficulty in this search is that the distance between pulsar and earth fluctuates in time (due to relative motion of earth and pulsar), thus resulting in a time dependent pulsating frequency. A solution to this problem has been provided to us by the astrophysics community, and implementation of this solution is taking place.

B Transition Programme

1 New Detector R&D at NIKHEF

1.1 Introduction

In 2003 a new project was started at NIKHEF on detector research and development for future experiments in particle physics. The project was set-up having in mind both the long-term perspectives of high-energy physics and the infrastructure available at the institute.

The most prominent long-term perspectives in the field include possible upgrades of the LHC experiments and the construction of a new e^+e^- collider operating at a center-of-mass energy of 500 GeV or higher. Moreover, it is of importance to carry out such an R&D project while considering possible applications of novel detector technologies outside the field of high-energy physics at the same time.

As a starting point, i.e. to define the basic specifications of a new detector, the foreseen (central) experiment at a future global linear collider (GLC) was chosen. The interest in such an experiment is largely driven by the wish to measure detailed properties (such as mass, spin, branching ratios, etc.) of the Higgs particle(s) and other particles that will possibly be discovered at the LHC. As such discoveries will open a new realm of physics beyond the Standard Model, high precision measurements are needed to distinguish between the many different theories that have been proposed so far.

Using the characteristics of the linear collider, the global layout of a future e^+e^- experiment can be defined. The present R&D project intends to contribute to the development of two detector systems for such an experiment. Together with a third activity that is aimed at the development of X-ray detectors for various applications, this has led to the following three main R&D topics investigated within this project:

- Time-Pix-Grid: the development of a wireless time-projection chamber (TPC) that is directly readout by specially developed multipixel CMOS chips with a fully integrated gas-gain grid;
- CMOS-based pixel detectors: the development of monolithic CMOS-based pixel detectors in which the sensor and readout parts have been integrated for use in vertex detector systems;
- X-ray imaging: the development of hybrid CMOS pixel detectors for X-ray imaging applications outside high-energy physics.

The last subject, which is the continuation of the already existing MediPix project in NIKHEF, has been incorporated in the present activities in view of the large overlap in the employed technologies, the possible synergetic effects, and the potential importance of these technologies for LHC detector upgrades.

As the year 2003 marks the beginning of this new project at NIKHEF, the progress varies considerable among the various subprojects. While the X-ray imaging work has matured such that one technology transfer contract with an industrial partner has been negotiated and a second one is being arranged, the work on CMOS-based pixel detectors was barely started near the end of the year. These differences are reflected by the length of the separate reports on each of these activities that are given below.

Apart from the research and development work itself, members of the group participated in the organization of two workshops:

- In April 2003, the 4-th ECFA-DESY workshop on the physics and detectors for a 90 - 800 GeV linear e^+e^- collider was organized at NIKHEF. The workshop attracted more than 200 participants from all over the world.
- In October 2003, a workshop was co-organized on the topic of "High-density Detector Processing and Interconnect" at the IEEE-Nuclear Science Symposium in Portland (USA).

Moreover, a member of the group served as guest-editor of the proceedings of the 4th International Symposium on Radiation Imaging Detectors (IWORID2002).

1.2 The readout of drift chambers with the Time-Pix-Grid

Wire chambers are widely used in high energy physics. The most advanced type is the Time Projection Chamber (TPC). It consists of a gas-filled drift space in which a homogeneous electric field is created by electrodes on a field cage. The electrons, left by the passage of a charged particle crossing the chamber volume, drift towards one end of the chamber where they reach a plane of parallel anode wires. Close to the wire, the strong electric field causes the electrons to gain enough energy to release 'secondary' electrons. The position of the electron avalanches, and their induced charge on the

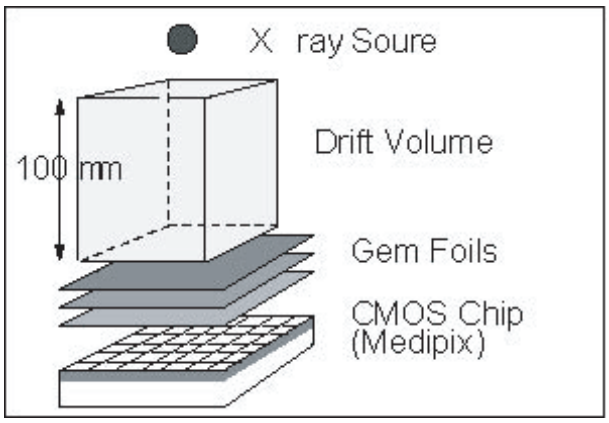

Figure 1.1: *Lay-out of the test chamber used to study whether a set of GEM foils in combination with the MediPix pixel array can be operated successfully.*

cathode pads behind the anode wires, is then measured in two spatial dimensions. The measured pattern of the induced charge corresponds to the projection, along the drift direction of the drift space, of the track on the wire plane. The distance between track segments and the wire plane can be deduced from the recorded drift times. Together, this enables a three dimensional reconstruction of the track position and curvature. Large, accurate and successful TPCs have been used, for instance, in the ALEPH and DELPHI experiments at the LEP-collider at CERN.

In 1996, F. Sauli replaced the anode wire plane by a Gas Electron Multiplier (GEM) foil. It consists of a 50 μm insulating Kapton foil, covered with 5 μm copper at both sides. Holes are etched in both copper layers using a standard photolithography procedure. Special attention is paid to the alignment of the holes in the two layers which have to face one another accurately, forming hole pairs. The foil is then exposed to a liquid that dissolves Kapton and leaves the copper unaffected. In this way the Kapton between the hole pairs is removed, leaving (gas-filled) tubes in the Kapton foil. Applying a potential difference of about 400 V between the two copper layers results in gas multiplication in the tubes.

The avalanche charge is picked up by anode pads under the GEM foil. In the case of a wire plane readout, the signals on the (cathode) pads are actually induced by the positive ion space charge, left in the avalanche, while drifting along a local field line towards the cathode. This charge signal is spread over several cathode pads, enabling the accurate measurement of the centre-of-gravity of the avalanche position. In the case of a GEM, the electrons are extracted from the hole in which

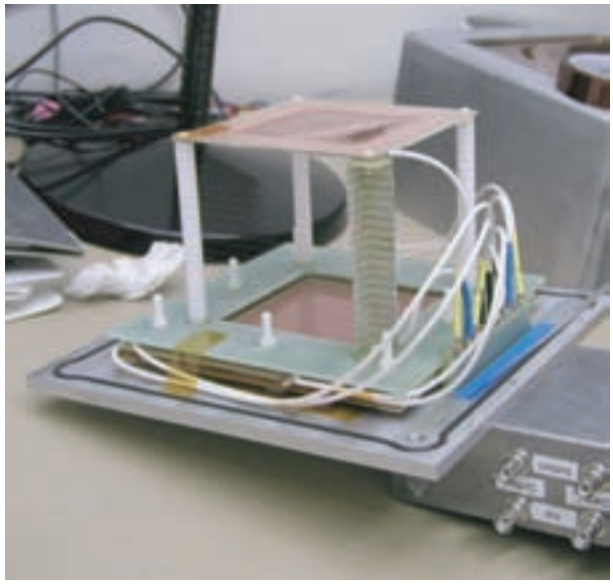

Figure 1.2: *Picture of the test chamber used to study the combination of a set of GEM foils and a MediPix pixel array. The cover of the chamber is seen in the back of the photograph.*

they were created, and they will drift towards the local anode pad. The avalanche position can be measured accurately if the pads are small. As ultimate limit, the pad size equals the size of the region associated with a GEM hole.

In conventional TPCs, each pad is equipped with a preamplifier, followed by a (digital) signal sampling circuit. This is not practical for very small (thus many) pads. We propose to develop, by means of state-of-the-art integrated circuit technology, a new monolithic sensor that includes a CMOS pixel chip and a metal grid. This device will replace the front-end wiring and readout electronics of traditional wire chambers. Gas multiplication occurs in the gap between the grid and the pixel chip, and the sensitivity of the circuitry enables the arrival time and position of single drifting electrons to be determined. The new 'wireless' gaseous detector allows to construct lighter, cheaper, simpler and more precise particle detection systems. It can also be applied in other fields like X-ray and neutron (diffraction) spectroscopy, tomography and imaging.

For a proof-of-principle we constructed the chamber depicted in figures 1.1 and 1.2. It consists of a drift volume of 100 x 100 x 100 mm^3, followed by a gas multiplication stage consisting of three cascaded GEM foils. Below the last GEM foil, the MediPix2 CMOS pixel array is placed (described below).

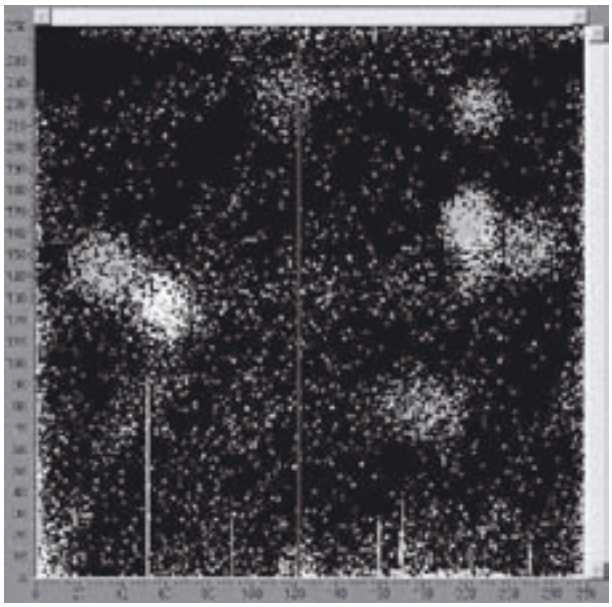

Figure 1.3: *Readout of the MediPix pixel array, while it is operated in conjunction with the GEM foils in the set-up shown in figures 1.1 and 1.2. The test chamber was irradiated with a ^{55}Fe source.*

We applied the 'naked' MediPix chip, without X-ray converter, as readout sensor for the electron charges leaving the GEM holes. In figure 1.3, an image is shown from the chamber being irradiated with X-ray quanta from a ^{55}Fe source. Such a quantum ejects one or more electrons from a gas atom, which creates a small local cloud of primary electrons. Due to diffusion during the drift process, the cloud width increases, resulting in the typical shape of the events seen in figure 1.3.

We have shown that the 'pixel segmented direct anode' is a feasible technique which can be applied in drift chambers, where it replaces wires, feed throughs, cables and readout electronics.

1.3 CMOS-based pixel detectors

In recent years significant progress has been made in the development of vertex detectors for large collider experiments. The purpose of such detectors is a very precise measurement of the location of the collision and the position in space where a particle produced in the collision decayed. As compared to existing detectors, a new type of vertex detectors is now under development in which a microchip is used without a separate detection medium. The charge that is generated by a particle inside the electronics circuit represents the actual signal.

An advantage of this novel technique is that very small structures can be built, which is in pace with the miniaturization trend that is pursued by chip manufacturers. In addition the chips can also be thinned down, which has the important advantage that multiple scattering effects in the detector can be reduced significantly.

Although the principle of such new detector systems has been demonstrated to work quite satisfactory there are several important issues that require further research and development. The power consumption of these sensors, for instance, is still higher than that of other comparable systems. It is presently being studied whether a modified readout sequence can reduce the power consumption. Alternatively, it is being tried whether it is feasible to power off the detector during periods of inactivity.

The research and development on such monolithic detector systems is being conducted in an international working group, in which NIKHEF participates together with groups from (a.o.) Strasbourg, DESY and Liverpool. The design of this so-called active chip has been made in Strasbourg and is known under the name MIMOSA. In the NIKHEF group in Nijmegen one PhD student is working on this project. He has been able to build a test system for the readout of the MIMOSA chip.

1.4 X-ray imaging pixel detectors

Expertise and know-how, obtained by designing semiconducting pixel detectors for high-energy physics, has been used to develop a novel type of X-ray imagers for use in medical, biological and industrial applications. Using these new technologies, it becomes possible to directly detect and measure the ionization caused by the absorption of an X-ray photon in a suitable semiconductor, instead of first converting the X-rays into visible light and detecting the integrated signal of many primary X-ray photons.

This so-called "Quantum Imaging Method" is not only much more sensitive than current methods based on photographic emulsions or on scintillators with CCDs, but it also holds promise for completely new image enhancing methods, such as contrast enhancement by energy-dependent weighting, end even a real "Colour X-ray camera", which will be able to recognize different chemical elements in an image by their characteristic K-line fluorescence.

The X-ray imaging group participates in interdisciplinary research projects in the field of semi-conducting Pixel Detectors. These activities centre on the MediPix

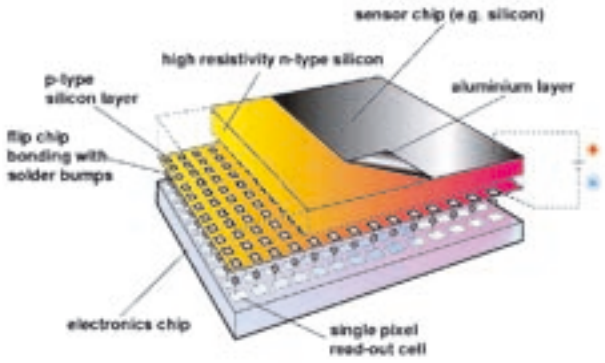

Figure 1.4: *Hybrid pixel detectors consist of a CMOS readout chip bump-bonded to a semi conducting sensor chip. Where high-energy ionizing particles are to be detected the sensor material chosen is generally high-resistivity silicon for reasons of cost and uniformity of response. For X-ray detection higher-Z sensor materials are often preferred.*

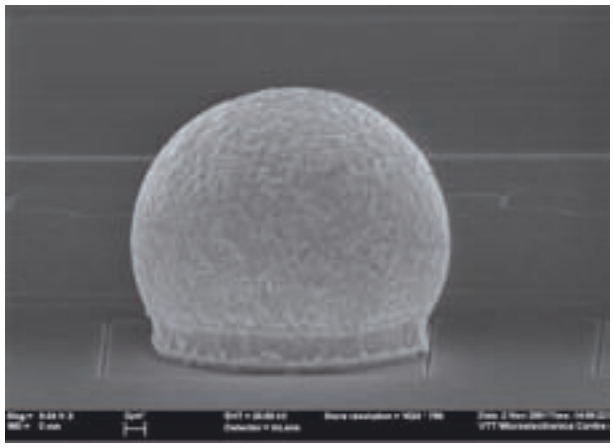

Figure 1.5: *A key enabling technology is high-density bump bonding to connect each sensitive detection pixel to its unique CMOS processing circuit. The SEM photo above is of a 25 μm diameter eutectic solder bump. (courtesy of VTT, Finland.)*

collaboration, an R&D project endorsed by the CERN division for Education and Technology Transfer (ETT). It bundles the research of 17 European groups and one American R&D group. Strong contacts already exist and are actively pursued with European Industries, to commercially exploit these new results.

Within the Netherlands, the group has close bilateral contacts with the MESA+ research institute at the University of Twente, Enschede. With them we share two PhD positions in deep submicron chip-design. One such position was funded, until September 2003, from a EU-TMR grant by the European Union, and the second was granted by FOM in the framework of "Projectruimte 2002". In these projects we develop novel CMOS circuits in 250 and 130 nanometer technology, to be used in future generations of "Medipix-like" pixel readout chips (see figure 1.4). In order to develop such chips, analogue and digital circuits are designed and tested in so-called multi-project wafer submits based on the 130 nm CMOS technology. The costs for such engineering runs are substantial, and are mainly financed through technology transfer contracts with Dutch Industry.

One of our activities concerns the design of extremely small and ultra-low power Analog to Digital Converters, to be used inside every pixel. The other project aims at developing ultra-high rate transmission over copper cables, using clever electronics to compensate for attenuation and dispersion in such cables at frequencies above 10 GHz. Both projects, when successful, will produce know-how that is also of high interest for future detectors and detector upgrades in High-Energy Physics experiments.

NIKHEF has designed and built the MUROS-2 interface unit, based on a Field Programmable Logic Array (FPLA). This circuit converts between parallel and serial transmission at speeds up to 200 MHz, and performs the needed signal level conversions. Already 24 such systems have been delivered to the Medipix collaboration, as well as to our industrial partner, and a new series production of 40 of such interfaces has now been started.

In collaboration with the Electronic engineering department at NIKHEF a 2 by 4 Multi-chip carrier has been designed, to carry a tiled array of 8 Medipix-2 chips, making it possible to build an X-ray imager with a fully sensitive area of 28 x 56 mm^2. It uses cutting edge high-density interconnect technology (HDI), with a ten-layer printed wire board in stacked micro-via build-up technology. As a first step, four Medipix-2 chips have been bumped on a single silicon sensor matrix (see figure 1.5), to obtain an imaging area of 28 x 26 mm^2 and a total of 0.25 million pixels. To increase the area of such tiled arrays, new wafer-scale post-processing technologies must be used, such as the plasma reactive ion etching of vias through the silicon substrate of our CMOS readout circuits. In this way, 4-side tile-able detectors will be developed.

2 Grid Projects

2.1 Introduction

The LHC experiments at CERN are adopting the Grid Computing paradigm for their main work of Monte-Carlo event production, data distribution and access, and later for reconstruction and data analysis. Grid Computing works with advanced authorization and authentication methods to allow the HEP software, data, and task execution to be fully distributed among participating institutes. The LHC data and computing centers will no longer be centrally located at CERN but will be distributed across the world. The scheme also has advantages locally, since an institute such as NIKHEF will have substantial local power which can be deployed according to institute priorities.

NIKHEF plays a major role in several Grid projects:

- we are one of the core sites for the LHC Computing Grid;
- we are one of the five main sites for the European DataGrid project;
- we are a major participant in the Dutch National e-Science infrastructure projects (BASIK/VL-E);
- we will play a leading role in the software development arm of the European sixth-framework EGEE (Enabling Grids for E-science in Europe) project.

2.2 Local Facilities

Approximately 280 CPUs are dedicated to Grid computing services at NIKHEF. An additional 15 machines supply Grid administrative functions like site information services, Grid user databases, distributed file storage, network monitoring, and control of access to local resources by remote Grid users. Local storage amounts to about 3.5 terabyte, most of which is carried by high-performance RAID arrays deployed in 2003. We have access to 12 terabyte of Grid-based storage at SARA in the next building.

Roughly half of the CPUs come from the NCF Grid Fabric Research Cluster. The cooling problems with these machines, reported last year, were solved and these machines are currently deployed in the LCG-2 cluster.

2.3 The LHC Computing Grid Project

The LHC Computing Grid (LCG) project began construction of a global computing grid in the second half of 2003. NIKHEF joined in October, and throughout the rest of 2003 NIKHEF had more computing resources than any other single site in LCG (including CERN). NIKHEF functions as a "core" site in LCG. Core sites are distinguished by two criterion:

1. Grid deployment at core sites is not limited to computing resources (worker nodes); a core site deploys other grid-wide services such as a workload management system ("resource brokers") or grid file-system catalogs ("replica location servers").
2. Core sites have enough in-house expertise that they do not require substantial assistance from the LCG project with installation, maintenance, and troubleshooting — the core sites often provide such assistance to smaller local sites such as universities.

Aside from its function as a core site, NIKHEF makes several other important contributions to LCG. Some of them are described under the DataGrid section below; in particular, in the areas of Virtual Organization services and Certificate Authority services, we play the same role in LCG as in EDG. Two areas specific to the LCG project are described below.

The Grid Applications Group

The Grid Applications Group or "GAG" is the arm of the LCG project charged with steering the development of grid software to ensure that it meets the needs of the LHC community. NIKHEF has been part of the GAG since its inception. The GAG's major accomplishment during 2003 was to produce the HEPCAL-II document (High Energy Physics Common Application Layer). This document presents requirements from the four LHC experiments regarding HEP analysis activities on grid resources, and makes suggestions for how grid software development projects might implement these requirements in a scalable fashion. J. Templon (NIKHEF) was co-editor of HEPCAL-II. It was accepted by the CERN SC2 as an official requirements document of the LCG project.

Fabric Management Project

The NIKHEF grid group capitalized on its expertise in fabric management, accumulated during the EDG project, by landing a major role in the LCG fabric management working group. Fabric Management refers to the installation, configuration, and monitoring of large grid computing clusters. Work will begin in earnest on this effort in 2004.

2.4 The DataGrid Project

The European DataGrid (EDG) is a project funded by the European Union with the aim of setting up a computational and data-intensive grid of resources for the analysis of data coming from scientific exploration. NIKHEF is one of the five "core sites" of the European DataGrid.

NIKHEF runs both a "production" and a "development" cluster. We also operate virtual-organization servers (databases mapping people onto their experiment organizations for accounting and security purpose) and data catalog servers.

We summarize below the local contribution to the various tasks ("work packages") in EDG.

Data Management

NIKHEF staff made extensive local and remote tests of the EDG Data Management subsystem in 2003. The data-storage product deployed in summer 2003 was deemed unusable, so NIKHEF staff collaborated with a small group at CERN to deploy an alternate storage system. This system remained in use throughout 2003, and in particular was used for grid reprocessing of DØ data from FNAL.

Fabric Management

NIKHEF continued development work on the LCAS system, reported on last year. This system ensures that resources, for example compute clusters, are only available to users that are properly authorized. This year, NIKHEF released the more advanced system LCMAPS, which adds capabilities such as recognizing experiment membership and roles within the experiments ("MC Production Manager"). This system has been successfully deployed on the EDG testbed in 2003, and is scheduled for take-up by the LCG project in 2004.

In order for the Grid to effectively distribute computational work across the participating computer centers, the centers need to provide some estimate of how available their site is. The current practice is for a site to provide an "estimated traversal time" which indicates that if the queue were to accept a job now, how long will it be before it actually starts to execute. This is a tough problem when there are multiple groups accessing the same pool of queues, and scheduled according to some local policy. H. Li finished his Masters' thesis project in this area in 2003. A prototype estimation facility has been produced as a part of the project, and a paper reporting on the results has been accepted for presentation at the International Symposium on Cluster Computing and the Grid (CCGrid) in April 2004.

Testbed Integration

NIKHEF is one of the five core sites in the EDG project. The NIKHEF development testbed (five machines) is usually (together with Rutherford Lab in the UK) the first site to deploy a new EDG software release after it has been tested at CERN. NIKHEF has provided many bug fixes to these releases. NIKHEF staff also provide support to both local and remote users in diagnosing run-time problems with computational tasks submitted on the EDG. J. Templon served as head of the EDG Integration Team for a short term in 2003 (substituting during an extended vacation by the normal leader).

This effort also provides central services for Grid "virtual organization" membership to all Grid sites. Furthermore we provide the Grid file-catalog service for the DØ, LHCb and Alice experiments, as well as to members of the biomedical and earth-observation communities.

Security services

When interconnecting a multitude of systems worldwide with high-speed connectivity, such a system will instantly become a valuable target for abuse. It is therefore important to do strong authentication of the users of such a system, and to make sure that authorization reflects usage policies.

The user authentication in the Grid is based on public-key cryptography and an associated Public Key Infrastructure (PKI) to distribute the keys. This system is well known from its role in e-commerce transactions, where sensitive financial data (credit card numbers) are encrypted such that only the intended recipient (the web trader) can read it. The Grid takes this technique one step further, and has also the individual end-users authenticate in this way. Using limited-lifetime "proxies", it has been successfully leveraged to provide "single sign-on" for all users on the Grid: you only need to type your pass phrase once at the beginning of the day, and all grid resources can be used without further hassle.

The DutchGrid Certification Authority, run by NIKHEF, provides trusted services to all users in the Netherlands and its statements are trusted world-wide. To promote interoperability between the various counties, in particular with the advance of LHC computing, the DutchGrid CA has worked on definition of common requirements and procedures within the Global Grid Forum.

Impression of the 7th EU DataGrid Internal Project Conference, 26.09 - 01.10 2003 Heidelberg/Germany.

HEP Applications

During the latter half of 2003, the group mounted a major effort to perform reprocessing of DØ data on EDG resources. The effort was successful in two respects:

- actual HEP experimental data were successfully reprocessed, for the first time, on a generic grid infrastructure;
- the activity provided many insights into what is right and wrong about the current state of grid computing systems for high-energy physics.

A paper presenting the experiences has been submitted to the Journal of Grid Computing, and the insights have been used to advance the state of HEP grid computing in the context of many meetings within the LCG and EGEE projects.

2.5 AliEn

AliEn is a grid prototype constructed by members of the Alice Collaboration at CERN. NIKHEF was the first site (outside of CERN) on which AliEn was successfully installed and this experience contributed valuable corrections to the AliEn design. NIKHEF has continued to contribute one CPU to AliEn production and tests throughout 2003.

2.6 DØ Grid

The 104-CPU DØ farm ran efficiently up until the fourth quarter of 2003, when it was dismantled and the CPUs transferred to the EDG testbed in support of the DØ reprocessing effort mentioned above. At the close of this effort, most of the CPUs were transferred to the LCG-2 cluster. The DØ computing activities will from now on take place using grid resources.

2.7 EGEE

Because of the success of the DataGrid project the EC has accepted as follow-up the sixth-framework EGEE project. This is a 32 Meuro project approved initially for two years with an optional two-year extension. The project has 70 funded partners, and counting also the un-funded partners well over a hundred institutes collaborate. The EGEE project is to deploy a Europe-wide grid infrastructure for sciences. HEP is the leading application; however the project is intended to be applicable to all sciences in Europe. One third of the budget for EGEE is for research and deployment, one third for the operation and one third to port other applications to use the grid. From The Netherlands, NIKHEF, SARA and the University of Amsterdam are partners in EGEE. NIKHEF specifically will contribute to the grid operations activity (in partnership with SARA); in authorization, access, and authentication research and development (in partnership with the UvA); and in applications deployment (bringing scientific activity to the Grid). These activities mesh well with group expertise accumulated during the EDG project.

2.8 Virtual Laboratory for eScience

The Virtual Lab for eScience (VL-E) is a Dutch project financed by the Dutch ministry of economic affairs from the ICES-KIS budget. Participants come from universities, institutes, and industrial groups across the Netherlands. VL-E is primarily a Computer Science project, but it has a quite strong application part as well. NIKHEF participates in the programs for Data Intensive Sciences (DISC), and in the Scaling and Validation. The petabyte-scale activities of HEP experiments certainly fall into the "data intensive science" category; aside from HEP, DISC also encompasses astrophysics (ASTRON) and Earth Observation (KNMI), and complements our other activities in LCG and EGEE. The Scaling and Validation activity meshes well with our large-scale cluster deployment activities within the LCG project, since what is really needed to test "scaling" are big sites running large quantities of computing and data-access tasks.

3 Experiments abroad

3.1 Proton-neutron knockout from ^{3}He induced by virtual photons

(MAMI Proposal A1/4-98; with the Universities of Mainz, Tübingen and Glasgow)

The ^{3}He nucleus is a suitable target to obtain information on short range nucleon-nucleon correlations and two-body hadronic currents by means of an electromagnetic probe. In addition, theoretical predictions on knockout reactions off ^{3}He are available from calculations employing realistic NN potentials within the Faddeev framework. Data of the reaction $^3\mathrm{He}(e,e'pp)$ were taken at AmPS, NIKHEF. The results from its analysis stimulated to perform an experiment of the complementary reaction $^3\mathrm{He}(e,e'pn)$. The combination of results from both experiments allows to investigate the relative importance of *pp* and *pn* correlations in the three-nucleon system.

The present $^3\mathrm{He}(e,e'pn)$ experiment was performed by the A1 collaboration at Mainz. It represents the first observation of an $(e,e'pn)$ reaction. The scattered electrons were detected in the magnetic Spectrometer B (Fig. 3.1), proton detection was performed with the highly segmented scintillator array HADRON3 (Fig. 3.2), provided by NIKHEF, while the neutrons were detected in three time of flight units.

Data are taken in five kinematical configurations defined by the four-momentum transfer q and the energy transfer ω. These configurations are indicated by the shaded areas in Fig. 3.3. The energy transfer ranges from $\omega = 170$ MeV to $\omega = 320$ MeV. The four-momentum transfer has central values at q =300, 330, 375 and 445 MeV/c. These points range from the so called 'dip region' (A1 and Y1) towards the delta resonance (B2, A2 and Z2), also shown in Fig. 3.3.

The tasks of NIKHEF in this experiment are focused on the HADRON3 detector and the data analysis. The

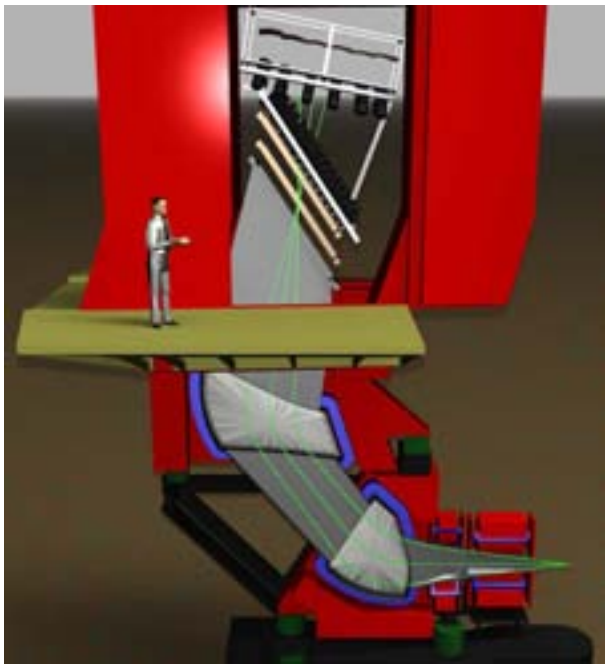

Figure 3.1: *The magnetic SpectrometerB covers a solid angle of 5.6 msr. It has a momentum acceptance of 15% and a vertex resolution of 1 mm.*

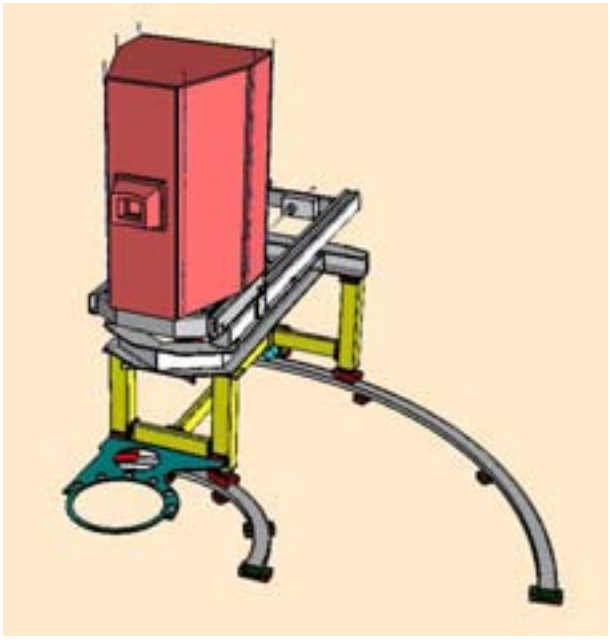

Figure 3.2: *The Hadron3 detector is a highly segmented scintillator array. Its effective opening angle of 28° in both directions corresponds to a solid angle of 230 msr. It has an energy resolution of 2.7% FWHM in the acceptance from 70 to 250 MeV.*

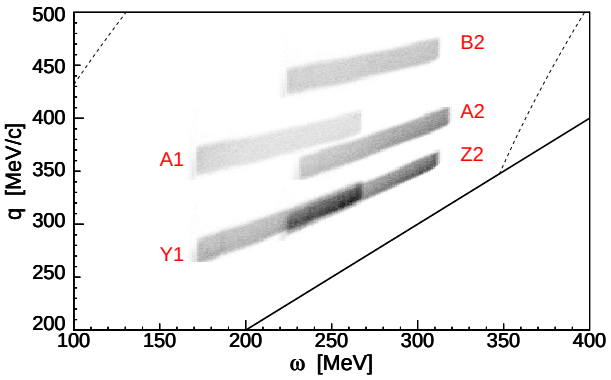

Figure 3.3: *Momentum transfer q vs. energy transfer ω measured in the $^3He(e,e'pn)$ experiment. The left and right dashed lines indicate the centroids of the peaks corresponding to quasi-elastic electron scattering and Δ-excitation, respectively. The solid line indicates the kinematics for real photon induced np knockout.*

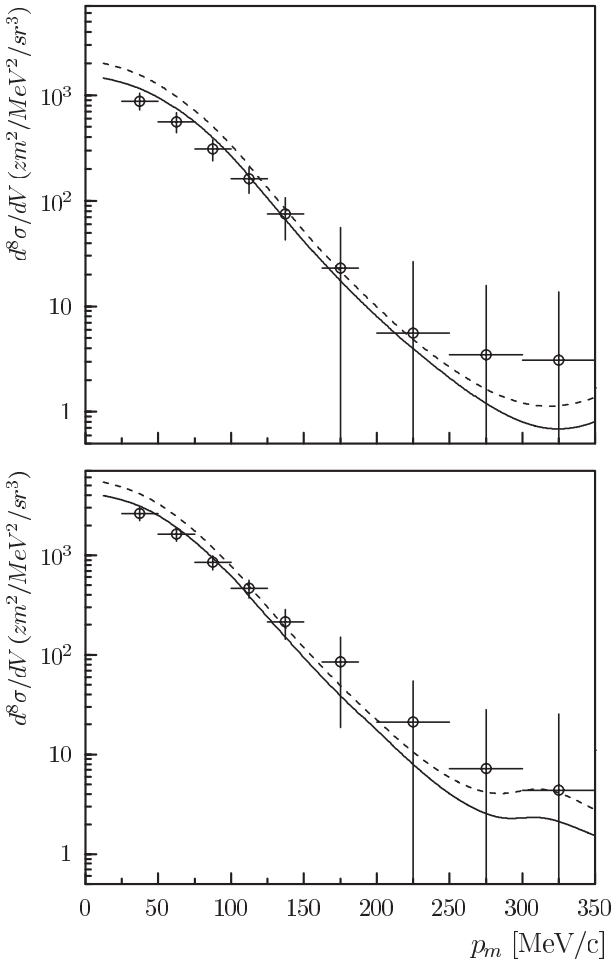

Figure 3.4: *Missing momentum dependence of the preliminary $^3He(e,e'pn)$ cross sections for the (ω,q) kinematics at (270,375) and (220,300) in the upper and lower panels, respectively. The solid lines represent the predictions of continuum Faddeev calculations, using the Bonn-B NN potential, from one-body currents, while in the dashed lines meson exchange currents are included.*

detector calibrations have been completed and dedicated analysis code for the HADRON3 arm data has been implemented in the software package of the collaboration. The new combination of detectors during the ^{3}He$(e,e'pn)$ experiment required new procedures in the data processing and analysis. For this purpose, a method developed at NIKHEF for analyzing $(e,e'pp)$ data, was adapted for $(e,e'pn)$ data.

So far, the data taken at the (ω[MeV], q[MeV/c]) configurations (220, 375), (220, 300) and (270, 375) have been analysed. In Fig. 3.4, preliminary ^{3}He$(e,e'pn)$ cross sections obtained for the two domains in (ω, q) at (220, 300) and (270, 375) are shown as a function of p_m, the missing momentum. They are compared to the theoretical predictions obtained from continuum Faddeev calculations using the Bonn-B NN potential.

In the p_m range up to 150 MeV/c, the slope of the data is less steep than the theoretical prediction and shows a better agreement with calculation employing one-body currents only. At high p_m, the statistical precision of the data limits the possibility to draw firm conclusions on the necessity to include two-body currents in the calculation.

Once final corrections and improvements are applied to the present data analysis, the data taken in the remaining kinematic configuration will be analysed as well. The obtained ^{3}He$(e,e'pn)$ cross sections will then be compared to those of the complementary ^{3}He$(e,e'pp)$ reaction and to theoretical predictions that involve the isospin dependence of hadronic currents and nucleon-nucleon correlations in the three-nucleon system.

C Theoretical Physics

1 Theoretical Physics Group

1.1 Introduction

Subatomic physics aims to find out the fundamental degrees of freedom, like particles and interactions, that are relevant to the description of the world at the shortest scales we can probe. This includes the properties and dynamics of quarks and gluons inside the proton and other hadronic particles, or the production and propagation of neutrinos in nuclear processes, e.g. in stars and supernovae.

To discover what the relevant degrees of freedom are, particles like electrons, protons or neutrinos are produced in accelerators and scattered at high energies from each other or from some fixed target. Theoretical physics provides the framework for the analysis and interpretation of such experiments. The development of quantitative models requires theories to be formulated in a sometimes rather abstract mathematical language. As a result, research in theoretical physics encompasses the development of new mathematical methods as well as their application to specific physical models.

1.2 Physics of the standard model

The ultimate building blocks of atoms and nuclei are leptons, such as the electron, and quarks of either charge $2/3$ (u-quarks) or charge $-1/3$ (d-quarks). Quarks interact through the strong color force to form protons, neutrons and nuclei; nuclei and electrons are bound into atoms by the electromagnetic force. In addition to these two types of interactions, there are two other forces acting on subatomic matter. The first one, the weak interaction, transforms particles of different kind into each other, as in β-decay and other forms of radioactivity. The other one is gravity, which is only known and understood at the macroscopic level, and in the universe at large. Quarks, leptons and their interactions are described to great accuracy by the theory known as the standard model.

Each type of quark and lepton known, happens to exist in three different mass states: besides electrons we find muons and τ-particles, with exactly the same properties except for their mass; similarly, there are three types of neutrinos, and three types of u- and d-quarks. The reason why there are three, and only three, of such families is not understood. It is one of the challenges for theoretical physics to come up with a reasonable explanation.

An essential ingredient of the standard model is, that at the most fundamental level (at very short distances and in very high-energy interactions) quarks and leptons are massless. The particle masses that we actually observe are the result of dynamical processes, which impede light-speed propagation of these particles even in the vacuum. There are two separate mechanisms at work; both are characterized by the violation of some symmetry inherent to the theory. The first broken symmetry is the so-called chiral symmetry of the strong color interactions; obviously this mechanism only applies to quarks. The other one is the violation of the weak isospin symmetry of quarks and leptons, which contributes to the generation of mass for all matter particles.

A fundamental difference between these two dynamical processes is, that the violation of weak isospin symmetry is believed to result from a scalar field with which quarks and leptons interact, and which takes a non-zero constant value in the vacuum, throughout the universe. In the case of chiral symmetry breaking no such scalar field is present; instead, the origin of the phenomenon is a condensate of quarks in the vacuum, like the presence of a condensate of Cooper pairs in superconductors.

If the breaking of weak isospin symmetry is indeed due to a fundamental scalar field, this field should leave an observable trace in the form of the so-called Higgs particle, a heavy neutral spin-0 particle which should be produced in certain weak interactions, but which has so far eluded observation. Discovery of the Higgs particle, if it exists, is one of the major physics goals for the LHC, under construction at CERN.

The interpretation of the data that will come out of the LHC experiments, is a major challenge to theoretical and experimental physicists alike. In the LHC protons will collide with protons, and these collisions will probe their deep inner structure in terms of quarks and gluons, the quanta of the color field. An accurate parametrization of this structure is indispensable for the detailed analysis of the collisions. The NIKHEF theory group is one of the leading groups in the world able to do the kind of calculations needed for this purpose.

1.3 Beyond the standard model

The standard model provides a very successful and precise description of subatomic phenomena. Nevertheless there are a number of reasons to believe that there exist new particles and/or new types of interactions when we extend our explorations in the subatomic domain.

First, it has been found that neutrinos are massive, but their masses are very tiny. They are at least a million times lighter than the electron, the lightest particle known so far. A natural explanation arises if at the same time we suppose there is another mass scale, at least a million times heavier than the heaviest lepton (the τ), associated with the new (right-handed) neutrino states that exist if neutrinos possess mass. This mass scale is way beyond that characterizing the standard weak interactions

Second, it has been observed that the strength of the electro-magnetic, weak and color interactions varies with energy, and inversely with the distance scale at which it is probed, in such a way that they reach a common value when extrapolated to energy scales of the order of 10^{15} GeV. This could be a sign of unification of these forces at this scale.

Third, observations of the motions of stars and galaxies, and an an analysis of the precision measurement of the cosmic microwave background point to the existence of large amounts of non-baryonic dark matter in the universe. Whatever the nature of this matter, it can not consist of quarks, and neither of any of the known leptons.

One conjecture as to the nature of this dark matter is supersymmetry. Supersymmetry is a principle associating a scalar particle with each fermion in the standard model, with the same electric and color charges; it also associates fermions with the same charges to the Higgs and vector bosons: the gluons, the photon and the massive weak vector bosons $W^{\pm}$ and Z^0. Supersymmetry naturally comes out of models of quantum gravity, but it also improves the mathematical properties of the standard model. For the latter property to hold, it is however required that the masses of the extra particles predicted by supersymmetry do not exceed values of the order of 1-2 TeV. A stable massive neutral particle arising due to supersymmetry could explain the nature of dark matter. In this scenario supersymmetric particles should be observable at the LHC as well. The NIKHEF theory programme includes studies of supersymmetric models, especially in the context of unification and quantum gravity. Some of these models can be tested at the LHC.

1.4 Cosmology, astrophysics and quantum gravity

As the discussion of dark matter shows, particle physics and astrophysics have common fields of interest. In fact, much can be learned about the universe by observing more than only light and radio waves from distant stars and galaxies. Neutrinos are particularly suited to collect information about highly energetic astrophysical processes from distant sources, because owing to their weak interactions they can travel large distance at the speed of light without being deflected or losing energy. The ANTARES programme at NIKHEF is directed toward the development of a neutrino telescope in the Mediterranean. In a related effort the theory group at NIKHEF has taken up the modelling of the astrophysical production of high-energy neutrinos and other particles from various sources, and their propagation and observable effects like mixing and oscillations in the vacuum as well as in dense matter.

Relativistic plasmas and fluids are an important element in the development of cosmological models of the early universe. An important branch of such studies concerns the plasma of quarks and gluons, which is expected to exist at high temperatures and densities such as in the early universe. In the laboratory it may be possible to create such a plasma in heavy ion collisions. The properties of this plasma, and the approach to this regime at increasing temperature, need to be understood and modelled; studies in this direction are carried out in collaboration with the group in Bielefeld (Germany).

Relativistic fluids can be described in the non-dissipative limit by effective relativistic field theories. A new development in the NIKHEF theory programme has been the extension of such effective field theories for relativistic fluids allowing to include supersymmetry.

The gravitational force has never been observed to play a role at the subatomic level. However, as gravitational interactions become stronger at shorter distances, extrapolation of known physics leads us to assume that a quantum theory of gravity should become relevant at the latest at the Planck scale, associated with energies of the order of 10^{19} GeV. This scale also characterizes the physics of the earliest epoch in the history of the observed universe. Furthermore, quantum gravity may also be essential to an accurate description of the physics of black holes.

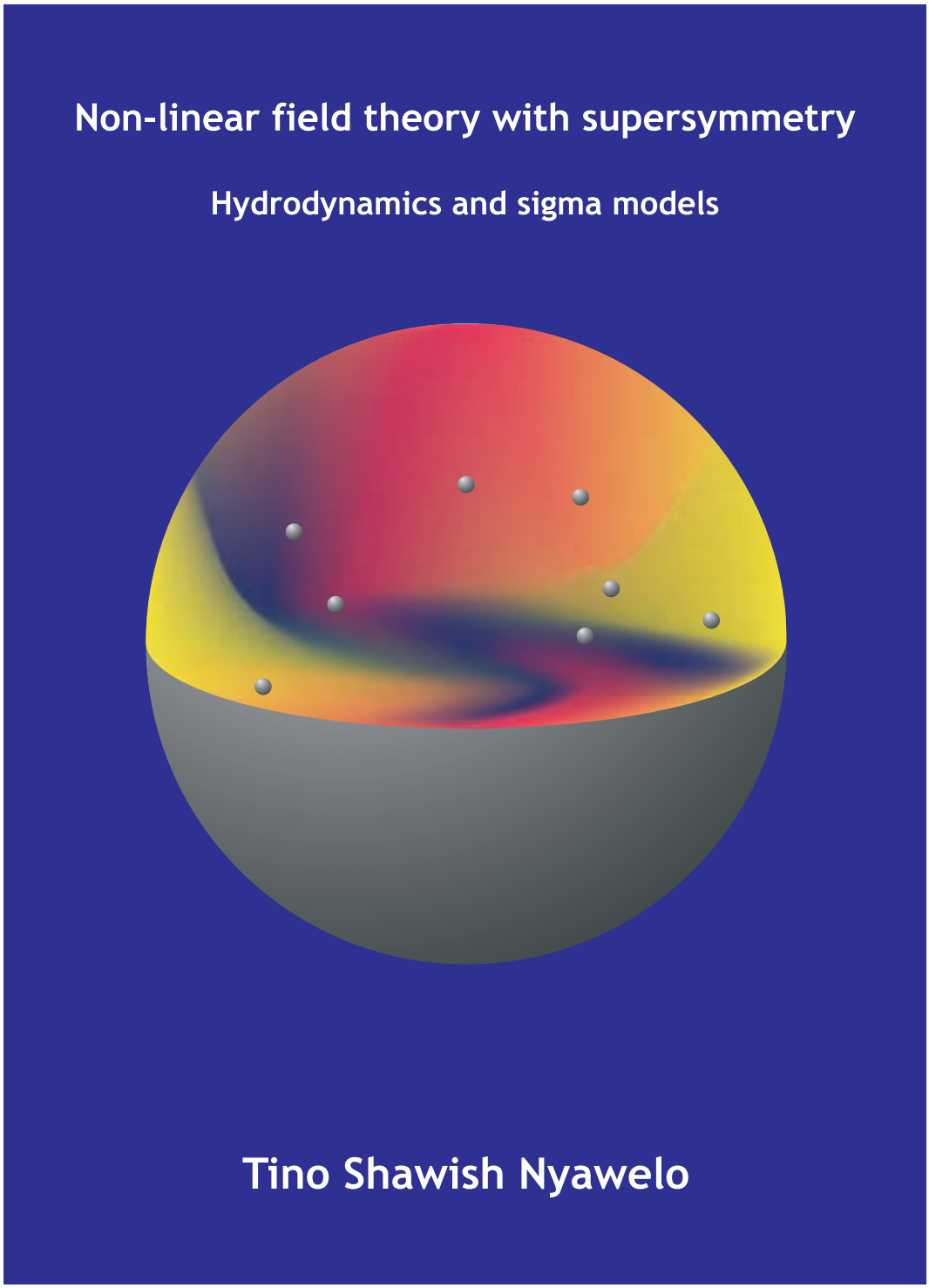

Cover of Tino Nyawelo's PhD thesis.

The main candidate we posses for a theory of quantum gravity is string theory. The elementary objects described by this theory are tiny quantum strings moving in 10 or 11 space-time dimensions. All particles and forces should be manifestations of some properties of these strings. Although it may seem far fetched, many remarkable results have come out of string theory; for example, it predicts the existence of gravity, rather than postulating it as a separate ingredient. Also, the quantum theory of strings seems to be much better behaved mathematically than other theories of quantum gravity.

Therefore it is desirable to see if not just gravity, but the full standard model living in 4-d space-time can somehow be obtained from string theory. A substantial effort in this direction in the Netherlands is carried out in the context of the FOM programme FP 57, in which the NIKHEF theory group also participates.

From left to right: Tim Jones, co-author of the 2-loop β function, David Gross, co-author of the 1-loop β function, Oleg Tarasov, co-author of the 3-loop β function and Jos Vermaseren (NIKHEF), co-author of the 4-loop β function of QCD, calculated with Vermaseren's FORM program.

D Technical Departments

1 Computer Technology

1.1 Computer system management

MS Windows

In 1997 we started building the infrastructure for a Microsoft Windows Domain at NIKHEF. At that time Windows-NT Server version 4.0 just became available and was the logical choice to run on our Windows server systems. During the following years the number of Windows clients increased to about 200 systems and additional services like application and file services have been implemented on the NT servers. Microsoft released Windows 2000 in the year 2002 as the successor of Windows NT and advertised more stability and flexibility as the major improvements compared to the NT server software

At NIKHEF we started the preparations for the migration from the NT server to the 2000 server infrastructure in the first quarter of 2003. First we sent a system manager to a training course and built a small standalone test bed, where we were able to get familiar with the new system and exercise possible migration scenarios. During the year a newer version, Windows 2003 server, became available and we decided to migrate directly to this version at the end of this year. We decided to follow the migration scenario based on the 'native mode', which, distinct from the 'mixed mode', is a step by step irreversible replacement of the existing NT services by 2003 services. The actual migration to the new software and partial to new hardware as well, took place in the Christmas holidays and caused only a limited interruption of the services for our users.

After the update, the following services are provided by MS Windows 2003 servers in the nikhef.nl domain:

- Redundant Windows Domain Controller.
- Central managed Antivirus software for server and client systems.
- Software update services (SUS) for MS Windows.
- Home and project directory file service with backup and quota administration.
- Windows application server for non Windows users (like Linux clients).

MS Windows systems are vulnerable for viruses and other kind of attacks as initiated continuously from many different sources in the internet and even from sources in the internal network, like infected lap tops. In August this year some of our systems were polluted by the Blaster virus. After this incident we automated the update of server and desktop systems using the Software Update Server (SUS). Now the security patches are fully automatically installed as soon as they become available. However the owners of the Windows laptops are responsible for doing these updates themselves.

In the course of this year Windows XP Professional has been installed as the default for the desktop systems. Older systems still run Windows 2000 Professional and in incidental cases even Windows NT still has been supported for legacy reasons, such as the systems for the control of the MDT chamber production in the clean room. In total about 200 desktop PC's run the MS Windows client software.

Linux

Red Hat 7.3 is the Linux version that has been installed on all Linux server systems, on the grid compute nodes and on the majority of the Linux desktop systems. Only a limited number of desktop systems still operate for legacy reasons under the Red Hat 6 version and for compatibility reasons the SUSE Linux distribution (HERMES). To fulfill a special request from our theory department we have installed the Red Hat version 9 to be able to optimize the performance for the FORM application.

In 2003 Red Hat announced a rather drastic change in its license policy, which is supposed to have an impact for all high-energy physics institutes. A license for the Red Hat distribution used to be available at no costs. This is no longer the case whenever the new policy will be implemented for the so called Red Hat Enterprise Edition. The consequences of this change in policy were subject of discussions on the major HEP institutes. For obvious reasons we have made the decision to follow the strategy that CERN will define for the coming years. However at the end of 2003 this strategy has not been defined yet. For the time being we will stay with the Red Hat 7.3 version and only perform minor updates which are required from a security point of view. From a user perspective, the 7.3 version offers a stable and complete system, compatible within the collaborations and without any urgent need to update to a new version.

Figure 1.1: *Linux file servers with Tbyte capacity*

Other Unix platforms

The SGI server 'pake' was removed in the first quarter of this year. This marked the end of a period of many years where the SGI IRIX platform was used for collaborations from DESY like HERMES and ZEUS and for the I-DEAS application at the mechanical design department.

The trend to replace Sun Solaris systems by Linux operated systems continued. However the major server in the network 'ajax' runs Solaris and has performed stable and according to our needs. The generic Solaris login server has been taken out of operation at the end of the year and replaced by a Linux server.

File service

To be able to fulfill the increasing demand for central file storage we have installed two Linux servers connected with a dual Ultra SCSI interface to a redundant array of parallel IDE disks.

The server 'gimli' with a bruto capacity of 2.4 Tbyte, has been installed in the third quarter of this year and is dedicated to storage of all kind of experimental data as it is produced by detectors and simulation programs (see Figure 1.1). These data disk partitions are accessible for all client systems in the nikhef.nl domain using a global name scheme like `/data/antares` or `/data/dzero`.

The second file server 'pepijn' has been installed in the last quarter of the year and has a bruto capacity of 3 Tbyte. This server is fully dedicated to what is generally known as 'project disk service' and is distinguished from the data server by the fact that all files on this server are part of the daily incremental backup scheme. Just like the data server, the project disks can be referenced for all clients systems according to a global name scheme like `/project/atlas` or `/project/antares`.

The very same server configurations have been installed as 'storage elements' in the grid infrastructure as well. This kind of file servers have an excellent price-performance ratio compared to the more traditional systems (cheap Linux server, IDE disks instead of SCSI disks) and redundancy because of hot-swappable disk units and on-the-shelve spare parts. The 1 Gb/s connection per server to a (copper) port of the network backbones, guarantees an optimal transport speed of the data into the local area network.

Mail service

A substantial and increasing part of the incoming electronic mails can be characterized as being unsollicited mail. Statistics taken during 24 hours showed that only about one third of the incoming mails has been accepted by our mail filters, this implies that two third of these mails were rejected or were tagged as SPAM. The total number of incoming mail handled by the 'smtp.nikhef.nl' mail server is over 20.000 per day. To be able to process this large number of incoming mails we had to replace our two existing single processor mail servers with two more powerful dual-processor Linux servers. A third mail server has been installed as a secondary mail server in case of a failure of a primary server.

The measures taken to prevent the delivery of unwanted mails to our end users are the following. The first step is to check whether the domain or IP address of the sender is present on a 'black list'. We consult a static black list maintained by ourselves and one or more dynamic black lists maintained by third parties in the internet. In case of a positive hit, we simply reject and bounce the e-mail back to the sender. The next step checks whether the addressed user at nikhef.nl exists, if not the mail is again rejected and bounced back. Next the incoming mail will be accepted and processed by a virus scanner and a SPAM filter. The definition files of the virus scanner and the SPAM filter are updated regularly to keep in line with the actual viruses and SPAM strategies. Mails tagged as SPAM are delivered to the end user; it is up this user to decide how to handle SPAM mail.

We have made available a web-based mail client. NIKHEF computer users, who are outside NIKHEF, can use this mail client to read and send their electronic mail from any other location in the world with an internet connection.

Figure 1.2: *The AMS-IX overhead fiber cabling system.*

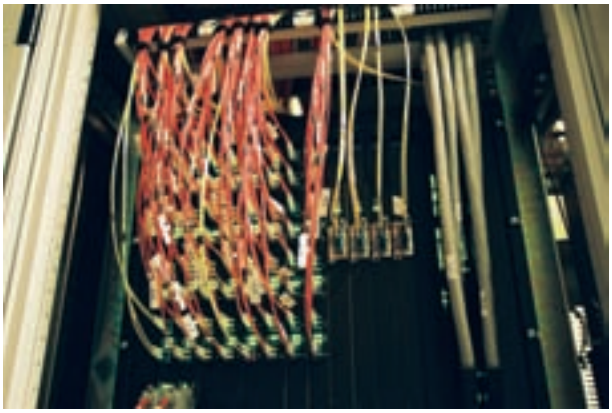

Figure 1.3: *Core switch of the AMS-IX backbone*

Network infrastructure

The backbone of our local area network and the filter to the external networks are implemented in a Foundry BigIron 8000, a network device with capabilities for high-speed routing and switching IP traffic. We have extended this device with a module with eight ports, enabling 1Gb/s transmission each over a 'copper' UTP connection. These ports are used to connect the new Linux servers (mail, file, etc) directly to the network backbone.

The wireless LAN has been extended to cover all meeting rooms and public spaces at NIKHEF. The WLAN is very much appreciated by NIKHEF users and visitors who connect their laptop to the 'guestnet' segment of the local area network.

In collaboration with the partners on the WTCW campus we have started a pilot project with 802.1X authentication on a WLAN. This pilot project has been initiated and partly financed by SURFnet. The idea behind this initiative is that SURFnet builds a hierarchical network with 802.X authentication in the Netherlands that enables staff employees and students of SURFnet member institutes to login with their own account and password, wherever this network is available.

Video conferencing service

The ISDN connected videoconferencing hardware has been replaced by a new setup that enables both ISDN and IP connected videoconferencing sessions. This setup consists of a TV set and a Polycom ViewStation with a high-quality camera and microphone, an IP addressable system (video.nikhef.nl) and an adapter for the ISDN connection.

Amsterdam Internet Exchange

In the past years NIKHEF has invested substantially to upgrade its facilities to the current professional level. On 31 January 2003, following the AMS-IX tech meeting, NIKHEF together with SARA celebrated the deliverance of our no-break installations. In April a new NIKHEF entrance protocol came into force and a website was launched with all relevant information about our facilities (`http://www.nikhef.nl/ams-ix/`). Further in 2003 NIKHEF installed an overhead fiber cabling system and streamlined its fiber management (see Figure 1.2).

The number of customers and racks in use continued to grow. NIKHEF welcomed the first steps in the upgrade of the AMS-IX backbone infrastructure (see Figure 1.3). NIKHEF values the innovative approach taken by AMS-IX. In preparation SARA and NIKHEF have installed additional fiber infrastructure between both our facilities.

Conference support

In the year 2003 the CT supported two conferences with IT facilities (the Linear Collider workshop in April and the LHC electronics conference in October) and organized the HEPix conference in May. This conference is organized twice a year and its purpose is to present and discuss the IT status and strategy of the HEP institutes all around the world. The about 60 participants of this conference are in general members of the IT groups.

1.2 Project support

Introduction

This chapter gives a summary of the contributions of the members of the Computer Technology Group to the

LHC and other projects at NIKHEF. Refer to the relevant chapters in this Annual Report for more detailed information about the projects.

ATLAS detector

MDT sub-detector

We have focused most of our efforts this year on the production support of the chambers and on the integration of the subsystems.

The chamber production has been performed according to the schedule. The CT group has delivered support for the LabView automation tools and the quality assurance database.

We contributed to design and development of the software for the read-out chain for the MDT sub-detector. A set up has been made to read out 12 MDT chambers at the test beam facility at CERN. Much effort has been put in the hospitalization of the performance of the software in the MROD subsystem. This software has been implemented on embedded digital signal processors (Sharc DSP from Analogue Devices). By restructuring the software and optimizing the compilation of the code the requirement of 100 KHz event rate has just been met.

In the last quarter of this year we have started with the preparation of the DAQ system of the cosmic ray test set up at NIKHEF. The DAQ system is based on the software packages developed by the CERN Trigger/DAQ group, which is basically the same software that will be used in the final DAQ system for the ATLAS detector.

The Detector Control System (DCS) will be used for the initialization of the parameters of the front-end electronics in the MDT detector. This set up consists of a PVSS supervisory control module, a communication module to the embedded CAN field bus device (ELMB) and a conversion module to the serial JTAG interface which shifts the parameter bit streams into the front-end electronics.

The RASNIK alignment system has been integrated into the DCS. The stand-alone Windows application ICARAS has been converted to RASDIM, which includes the same functionality as ICARAS does, but adds to this the communication interface based on the DIM protocol to the PVSS supervisory control application. Apart from this integration effort, we have implemented the software for a new frame grabber module and added functionality like background subtraction to the imaging software.

Central Detector Control System

NIKHEF is responsible for the development and support of the 'standard' software for the Embedded Local Monitor Box (ELMB). This box has been implemented in a CAN field bus node and the communication with this device has been designed conform the standards of the CANopen protocol. Sensors for monitoring parameters like temperature and magnetic field can be connected to the ELMB. Moreover more specific functionality has been implemented like an interface to the serial JTAG interface.

About 9000 ELMB devices will be produced in the next year under direction of the ATLAS central DCS group. NIKHEF delivers the embedded software for most of these devices and provides support to the users. For this purpose a CANopen framework has been implemented that can be used as the basic building block for the embedded software.

We have supported radiation tests, which has been performed under well-defined conditions to measure the effect of radiation on the functioning of the hardware and the software. Software functionality has been added to be able to recover from single upset events (like flipping bits in memory locations). According to these tests we can be confident that the ELMB's will operate in the ATLAS detector for a sufficient long period.

ANTARES

The ANTARES collaboration performed tests with a prototype sector line and a prototype mini instrumentation line in the Mediterranean Sea. The set-up included the DAQ chain: the VxWorks front-end processors, the TCP-IP based network and the on-line cluster in the shore station. The CT group has been involved in some parts of the DAQ software and software for the shore station. From a software point of view the test runs were considered as being successful.

Grid computing

Introduction

In 2003 the grid computing for the LHC era started by initiating the LHC Grid Computing project (LCG) at CERN. NIKHEF started contributing this project in the last quarter of the year by installing hardware and services for the LCG-1 test bed (see Figure 1.4). The LCG grid services are based on the middleware as it has been developed for the European DataGrid project (EDG). The EDG en LCG test beds at NIKHEF have provided resources for the data challenges of the LHC experiments and for data analysis for running experi-

Figure 1.4: *Picture of the LCG-1 test bed (left) and the DØ farm (right)*

ments like ANTARES and ZEUS. Preparations for new projects like the Enabling Grids for E-Science in Europe (EGEE) and the Dutch Virtual Laboratory for E-science have been started to be able to continue working on grid deployment and developments in the next years.

Grid middleware

NIKHEF contributed to security related components of the grid middleware. Security is an important issue whenever remote users want to have access to local grid resources. For this purpose we have designed and implemented LCAS, a module that handles authorization requests to local resources and LCMAPS to map grid credentials to local credentials needed to runs jobs on local resources. Dedicated plug-ins have been developed like the Posix and LDAP enforcement modules and the AFS access module. Grid user groups are administrated in Virtual Organizations (VO), like an ATLAS VO or a GridTutorial VO. A Job repository module has been developed as a plug-in for LCMAPS, to be able to keep track on the status and history of jobs with respect to logging, accounting and auditing. The modules mentioned here have been integrated into the EDG Software version 2.1 in the last quarter of 2003.

Grid infrastructure

The grid infrastructure at NIKHEF has been expanded in 2003 with compute nodes (CE), Storage capacity (SE), grid server nodes and with gigabit network capacity.

The NCF cluster has a capacity of 66 dual-processor Linux compute nodes. This cluster has been assembled and installed in the last quarter of 2002. Unfortunately the processors in this cluster became overheated whenever intensive compute jobs were utilizing these processors. We have put much effort in optimizing the air flow through the 1-U high chassis and now we successfully keep the temperature under control.

In the last quarter of the year we have extended the grid compute capacity with 28 dual-processor compute nodes, with server systems to provide LCG services and with two storage elements of a capacity of 2.5 Tbyte each. The grid backbone network infrastructure, a Foundry BigIron switch/router has been extended with a module serving 16 x 1Gb/s ports with copper UTP connections.

Grid network research

In close collaboration with the UvA and SARA we have participated in network research in the context of the European DataTag project. For this purpose a Force-10 gigabit router/switch has been installed in the NIKHEF computer room to be able to set up a test environment for research on protocols for high-speed networking. With this set up we were able to utilize a 10 Gb/s 'light path' to a CERN router and achieved a memory-to-memory copy from NIKHEF to CERN with a speed of 5.6 Gb/s.

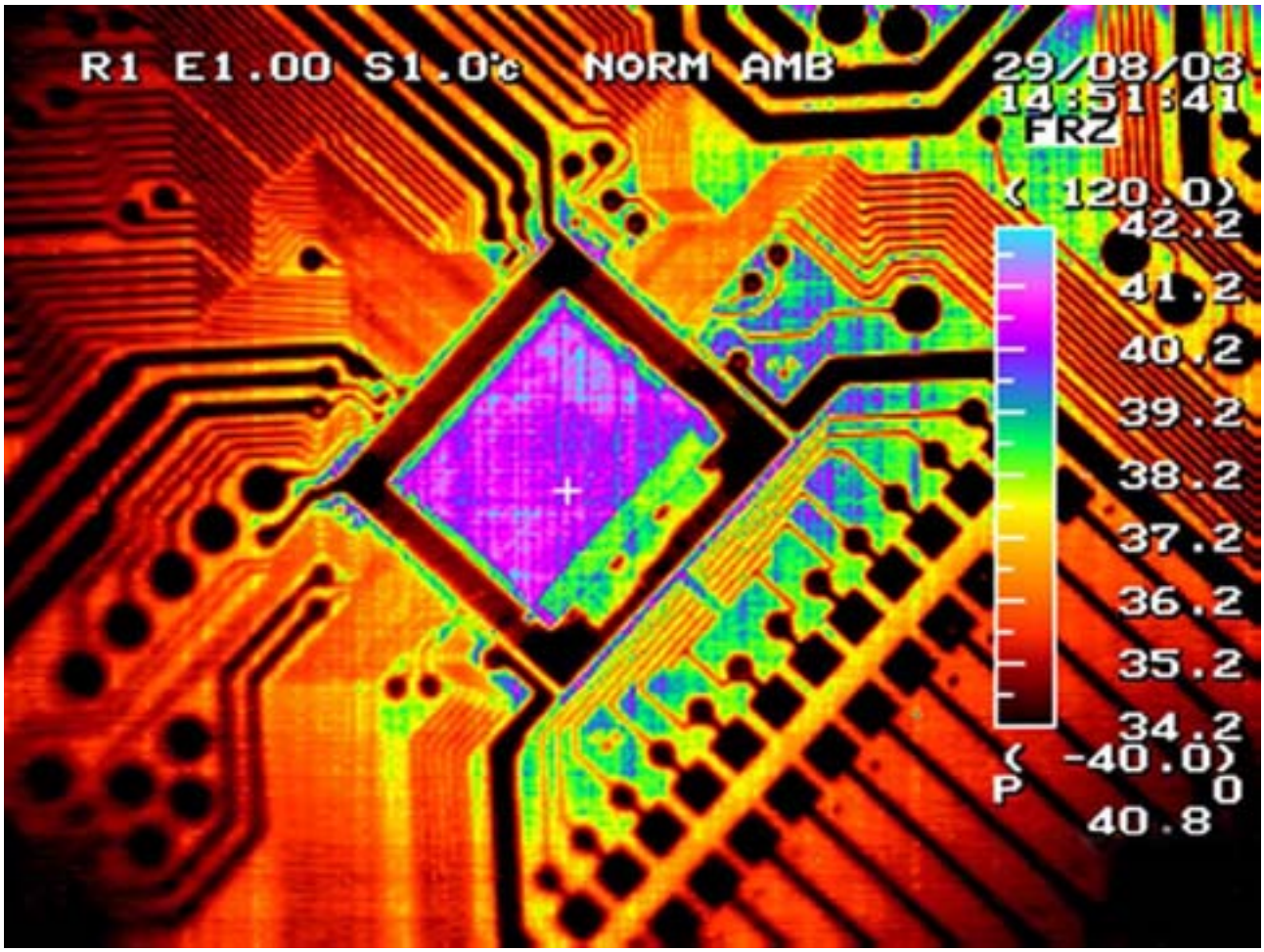

Thermal image of a chip used in a prototype vertex detector for LHCb. Each color represents a temperature, see vertical scale. The resolution of the photo is 50 μ.

2 Electronics Technology

2.1 Introduction

The electronic department has contributed to several projects in the experimental programs, which can be divided in three main streams:

- aftercare for the Zeus microvertex detector and the Hermes lambda-wheel detector at DESY;
- design of components, production of prototypes and preparation for the final production for detectors in the LHC experiments ATLAS, LHCb and ALICE;
- design and production for non-accelerator based experiments like ANTARES and Medipix.

Figure 2.1 shows the manpower consumption for projects in 2003.

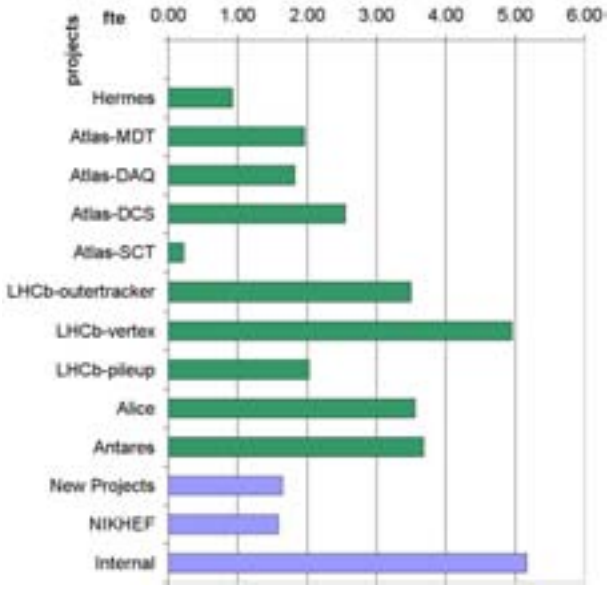

Figure 2.1: *ET manpower distribution in 2003*

2.2 Department developments

A wide area of expertise is important to meet the requirements of the modern digital and analogue electronic designs. Our group faces challenges in several fields; most notably are electromagnetic compatibility, noise handling, printed circuit board design, optical networks and microelectronics. For the micro electronics a start is made for future developments using a 0.13μ CMOS IC technology. This will be the "standard" technology for the coming years. Two circuits are being investigated, a stable current/voltage reference (bandgap) circuit and a Silicon detector amplifier. The motivation to use new technologies is higher radiation tolerance and higher integration density for more functionality near the sensors. This technology with 1.2Volt power supply voltage requires new design techniques and therefore early studies are necessary. Designing with the aid of software tools like VHDL, SPICE, MENTOR GRAPHICS become more and more a must. The Nikhef IC design facility has been updated. There are now 16 CADENCE (full custom IC design), 20 HSPICE (analog simulation), 1 DRACULA (physical verification) and 2 SYNOPSYS (logic synthesis) licenses. There are 5 specific workstations in the Nikhef network available for IC design work. The licenses are provided via the EuroPractice organization.

2.3 Projects

Most projects are characterized by a strong collaboration between people of the mechanics, computer technology and electronics groups from Nikhef. These multi disciplinary projects asked for a strong coordination and planning in the technical field. Several projects are in the stadium between prototype and production. In the scope of quality assurance and control, various dedicated calibration and test tools are designed. Some highlights in the electronic field are described below.

HERMES

In the HERA shutdown period, a quarter of the 'lambda wheels' was slightly modified to allow for running with the future HERMES target magnet. The modification replaced the part of the circuit that used inductive coupling with its capacitive counterpart. These modified lambda wheel modules have been operated successfully up to the maximum field of the target magnet. During the shutdown period of 2004, the remaining lambda wheel modules will be upgraded. A new version of the Beam Loss Monitor featuring an integrated radiation trigger, was tested and installed at the HERMES experiment. It showed reliable operation in the luminosity runs in the second half of 2004.

The helix2.2 chip used in the lambda wheels have a design flaw which results in a slow startup of the chips. Startup times of several minutes have been observed, which is significant compared to the total startup procedure of HERMES after at the beginning of the lu-

minosity runs. The helix chips are switched off during injection and ramping of the HERA lepton beam to reduce radiation damage. HERA beam is injected typically every 8 hours. The startup can be accelerated by illuminating the helix2.2 chips. A so called 'light fixture' was designed, tested and installed during the summer shutdown and the first results are promising.

ATLAS

Muon Readout Driver - MROD

The Muon Read-Out Driver Prototype-1 (MROD-1) supports six optical input links, each coming from the Chamber Service Module (CSM) on a Muon MDT chamber, and converts serial data-bits from at maximum 18 TDC's on a chamber into 32-bit data words. The MROD groups these data words for each TDC and checks whether the data words from all TDC's belonging to the same event number have arrived. The data from this event is formatted and send via an output link to the Read-Out Buffer (ROB) for further processing by the downstream Trigger and Data Acquisition (DAQ) system.

In the summer of 2003, two fully equipped MROD modules participated successfully in the H8 test-beam at CERN. Performance tests were done, which led to hardware/software optimizations. Tests show that improvement is still needed to run at the full 100 kHz trigger rate; there will not be much processor power left. In November, the MROD-1 had an "Intermediate Design Review" at CERN. The review committee made some valuable remarks on the design and was critical on the use of the digital signal processors with respect to the performance measured. The committee suggested to investigate an "all FPGA" solution[4] .

Read-Out-Buffer - ROBIN

The ATLAS Read-Out sub System (ROS) provides data access to events from the different subdetectors, which have been accepted by the first selection stage of the ATLAS Data Acquisition (DAQ) system (Level 1 trigger). A main hardware component of the ROS is an intelligent input module called RobIn, which accepts an input data stream of data fragments from the subdetectors. It provides temporary storage for these data fragments and delivers specific fragments upon request to the downstream system. Logically a total of 1600 RobIn's are required, each one dealing with a maximum input fragment rate of 100kHz and a maximum input bandwidth of 160MByte/s, delivered via a standard ATLAS optical link (S-Link). Output rate and bandwidth are in the order of 10% of the input values. The final DAQ architecture will assemble 3 logical RobIn modules into a single physical RobIn component with a Bus-Based (BB) output channel. An additional network connection will provide an option for increased scalability and the possibility study a Switch-Based (SB) architecture.

A first RobIn prototype series of 30 RobIn modules is developed and built by a joint effort of the ATLAS institutes: University of Mannheim, Royal Holloway University London and Nikhef. The prototype RobIn accepts data from 2 S-Link input channels and allows to investigate both the fully BB and SB architecture options of the RobIn.

The core of the RobIn prototype is build around two devices, a XILINX XC2V1500 FPGA, featuring 1.5 million gates and 528 I/O connections, and an IBM PowerPC405 running at maximum 266 MHz. The FPGA covers all high performance, time critical functions like S-Link input protocol handling, buffer memory access and high speed buffer management. VHDL is used to describe the functionality of the FPGA. A simulation environment of the FPGA has shown to be useful for both the development of the VHDL code and to debug errors found during tests. The PowerPC processor handles the requests from the downstream Trigger/DAQ system and performs the fragment bookkeeping. The PowerPC is programmed in C and runs embedded firmware. For each input channel 64MB of SD-RAM fragment buffer space is available. The PCI interface is build with a commercial 64bit/66MHz PCI bridge. The Ethernet interface is implemented via a dedicated gigabit Ethernet MAC and a PHY device supporting both optical and electrical media. The S-Link hardware is based on the HOLA S-Link implementation which uses 2.5 Gbit/s point-to-point data transmission technology via an optical fiber.

Performance tests have shown that the prototype RobIn satisfies the requirements but there are some stability issues to be solved. The performance is limited by the access speed of the onboard PowerPC to the FPGA and need some design improvements.

Detector control

The magnetic field in the ATLAS detector has to be monitored and checked during the operation of the detector. For this measurement system 1500 3D magnetic

[4]FPGA = Filed Programmable Array which is relatively fast but equipped for one dedicated task. The current design also uses DSPs Digital Signal Processors which are software controlled, but slower.

field sensors are envisaged. In order to measure not only the strength but also the direction of the magnetic field, each magnetic field probe consist of three hall sensors placed perpendicular to each other. Because of the strong temperature dependency of the Hall Effect, the temperature of the probe is measured too.

The electric signals of the hall sensors are very small, so a signal conditioner is placed on the same printed circuit board as the Hall sensors. The signal conditioner digitizes the analogue signals from the hall sensors and the temperature sensor.

These sensors are calibrated using a dedicated set-up at CERN. Five 3D sensors are calibrated at the same time by rotating them through a homogeneous magnetic field. To reduce the number of rotating wires, the five magnetic sensors are controlled by a microcontroller that is also rotating. The micro controller is read out via a four-wire CAN-bus. The sensors can be calibrated by adjusting the magnetic field and the temperature.

Rasnik

0-serie RASMUX

After last year's production of 5700 RasCaMs (sensor) and 6300 RasLeDs (light source), the last on-chamber component for the RasNik system the RasMux was produced and tested. These modules concentrate the signals onto a single cable and connect to the next stage of (off-chamber) multiplexing, the MasterMux. The 860 modules are assembled by an outside firm, which also performed some simple tests. Final and fully functional tests were performed at Nikhef. A prototype of the MasterMux has been build en tested. Production of this component (60 pcs.) starts next year.

B Physics

LHCb outer tracker

Sixteen prototypes of the front end board were made with the new ball grid array chip. Also a front end frame was designed for support of the boards and cooling of the chips. The front ends are not allowed to cool against air, because of heating up the hall, so they will be water cooled. Also eight first prototype Otis boards (time to digital conversion), still with bare bonded chips were made. Together with the Gol/aux board (optical/electrical communication board) made in Heidelberg, a complete front end prototype was available for testing end 2003. Testing devices for chamber-production were made like a wire tension meter in cooperation with a commercial firm and a scanning radiation source with two sensitive 64-channel current meters were made.

A lot of work is put into connecting the aluminum parts of the chamber. Straw wall and faraday cage have to be well connected to ground. Crimp connectors, welding devices and nickel plating were studied. Preproduction runs of all different boards used in the different sized chambers were started, while the chamber production start in 2004. The chamber construction and services (LV and HV supply, timing, control, cooling) were studied.

LHCb-Vertex and Pile up Veto electronics

A new version of the beetle chip for the LHCb vertex detector, silicon tracker and pile-up trigger has been submitted in June. The major modification for the pile-up project was the change in threshold circuitry of the comparators which enables a better tuning of the individual thresholds. To reduce the large offset spread of the comparators, the design was partly modified. Moreover, the range and resolution of the individual threshold adjustment was increased by changing a 3 bit DAC to a 5 bit version. Since the arrival of the beetle chip from the foundry, in October, extensive tests are ongoing. The offset variation is now under control and further tests are done to characterize the chip under all possible operating conditions.

Unfortunately, the prototype pile-up hybrid housing 16 beetle chips with its 256 binary outputs running a 80 Mbit/s, was not delivered. After several attempts and a waiting period of 10 months, it was clear that the envisaged production would not succeed. The main reason for the failure of the production was the quality and thickness of the top two Kapton layers. In the mean time the design is changed to adapt to the latest version of the beetle chip and production will start in early 2004.

The testing of the prototype vertex finder board has been finished. As a next step, the design of the optical link, needed to transport the binary signals of the beetle chip from the cavern to the counting house, is ongoing. Major parts of the VHDL code were written and prototype printed circuit board will be designed in the near future. Vacuum compatible flat cables have been designed, produced and tested. These Kapton cables consist of three layer; the outer layers are used both as shield and are also used to supply power to the hybrid. In the middle layer, differential strip-lines carry the analog and binary output signal as well as the digi-

Figure 2.2: *Frontside Wakefield surpressor*

tal control signals. The cables survived the mechanical stress test in which the cables were bent 50000 times. This is more than 5 times number of cycles needed for 10 year of LHCb running.

LHCb-Vertex RF measurements and shielding

During 2003 the setup in the mockup tank is modified for simulation measurements for the wake field supressor. The present setup consists of

- the detector box surfaces facing to the beam are now covered with the definitive pressed corrugated RF Aluminum foil of 300 micrometer;
- the Wakefield suppressor at the front side of the detector boxes is better shaped for the direction of the image currents in the open situation to 60 mm max. during beam fill time;
- the Wakefield suppressor at the exit foil side is still the type with the side-flap because it must fit in the mechanical exit foil construction at the beam center.

Fig. 2.2 shows the details of the frontside Wakefield suppressor and the corrugated Aluminum foil. Measurements gave good results for all the measured distances of the detector boxes 20, 40 and 60 mm.

In Fig. 2.3 the measurement results are given for the detector box distance of 60mm with the described setup. The Real and Imaginary coupling impedance are shown.

The earlier 850 MHz and now 900 MHz resonance is still present but is smaller then in the former measure-

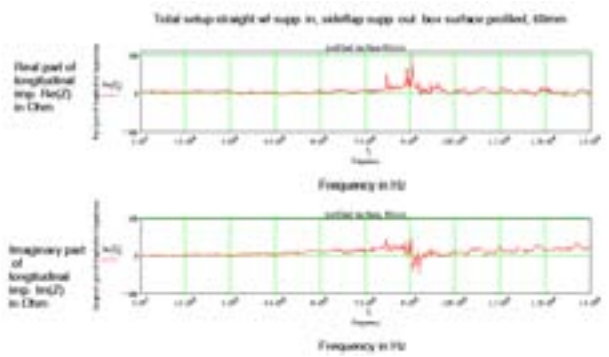

Figure 2.3: *RF impedance behavior of the detector box*

ment setup during 2002. This resonance is a complicate RF mode of which the mockup tank is part of the resonator. Because of the fact that the conductivity of the RF corrugated foil is $\frac{1}{3}$ of the conductivity of pure Aluminum the Q of this mode is lower in the present setup. The material of the tank in the realistic design is of stainless steel, which will again decrease the effective Q of this unwanted resonance.

ALICE

For ALICE we develop a control module for the front-end electronics. It will be placed close to the silicon sensors in te experiment. In total 168 modules must be produced. These modules of 5 x 5 x 7 cm each consist of 9 aluminum carriers on which kapton printed circuit boards will be glued. Aluminum is necessary for heat transfer to the cooling system.

A functional proto setup of the EndCap module has been build and tested (Fig. 2.4). It is equipped with 13 test boards which each 1 ASIC (ALCAPONE) that can control and drive the required signals to and from the

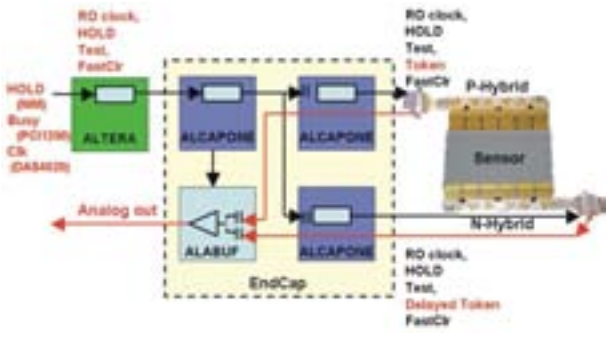

Figure 2.4: *Block diagram of Alice EndCap module*

Figure 2.5: *Complete beam test setup with pcb's and sensors (In black box)*

sensor module. Fig. 2.5 shows a picture of the whole setup with 13" large pcb's, and a black box containing the prototype silicon sensors. This setup was tested in a particle beam at CERN and the real behavior of the prototype system was verified and its functionality was demonstrated, and the performance could be studied and optimized.

The next step in the project is to design the real End-Cap module at the required dimensions. To be able to go down to the final dimensions the design of the ASIC's was mandatory. During the prototyping, the unpackaged ASIC's were wire bonded at Nikhef on special carriers to perform the electrical tests.

The ASIC's were developed using a 0.25μ CMOS IC technology, they are now in production. The ASIC's will be fabricated on 8-inch wafers, so wafer probing is necessary before dicing and the placement of the ASIC's on the pcb's. To prepare the production-test of the ASIC's, the electronics department of the Vrije Universiteit Amsterdam designed a specific chip tester on our specifications.

ANTARES

Optical network

The gigabit Ethernet (GbE) electric-optical conversion boards, DWDM-boards [5] , between the detector and the shore station and v.v. passed the last design iterations for optimizing the production of 180 boards. Every transmitter, a laser for a specified DWDM-band, a receiver and an APD [6], need particular tuning after the specifications of the item. The layout of the board permits placing of resister values for tuning and avoid the use of less fail save trimmers. This last version of GbE and the special 100 MHz version DWDM-board, with adapted pass band filters for the slow control part of the detector, have been tested successfully. All the components are at Nikhef and verified in order to start the production.

A special database of the optical component specifications is under development for the production and field service of the DWDM-boards in the scope of quality control. Testing the entire ANTARES optical network is difficult because of its topology and restricting optical multiplexing. Therefore a case study has been made for developing and constructing an OTDR (optical domain reflecto meter) within the working bandwidths of the optical (de)multiplexers). It is possible to construct such an OTDR with additional hardware and existing instruments.

Mechanics

There is paid a lot of attention to the mechanical form-factor of cooling bases, fiber trays and crates in collaboration with the mechanical department. The production of most elements is started.

[5] DWDM = Dense Wavelength Division Multiplexing.

[6] APD = Avalanche Photo Diode to converse optical signals on fibers to electrical signals on copper wire.

One of the two ATLAS End Cap Toroids during assembly at Brush-HMA in Ridderkerk.

3 Engineering Department

In 2003 the Engineering Afdeling had to deal with the peak of the engineering work for the four LHC projects. Most of the CAD-modeling work has been finished and a start was made with the many detailed design drawings and additional documentation. Tenders for major parts have been initiated. Concepts for tooling frames and support systems have been determined. Ahead lies the finishing of the documentation, processing and ordering of all the parts. Together with the MA a new Coordinate Measuring Machine (CMM) was installed and we have two modern automatically driven CMMs currently available for quality performance checks of all the various components to be made and delivered.

3.1 ATLAS

Semi-Conductor Tracker

All raw disks for the Semi-Conductor Tracker (SCT) were delivered in 2003. Half of them will eventually be delivered to RAL when finished at NIKHEF. The finishing process i.e. cutting holes, measuring flatness, gluing and milling the inserts and mounting the close-outs has been successfully developed in the end. Disk processing has become a routine job now and all disks will soon be ready for the next step: Services-to-Disk.

Tooling and testing equipment has been developed. Especially worth menrioning are:

- a cooling box with low temperature aggregate for testing entirely assembled disks ;
- a concept for equipment for module-to-disk assembly (Fig. 3.1);
- many other tools for assembling parts on disks

The current phase in assembling the tracker is the disk-to-cylinder processing. Development of the disk-to-cylinder tooling is almost ready. The parts for the base frame have been ordered (Fig. 3.2). The prototype of the transport boxes for disks was developed with special demands for shockproof handling and shipping disks. FEM-analysis was necessary to improve the box. The order for the production of the boxes was outsourced.

Figure 3.1: *ATLAS SCT equipment for modules-to-disk processing. Detector modules have to be positioned with an accuracy of 30μm. Due to large numbers of modules to be mounted on both sides of all the disks an efficient production method is crucial.*

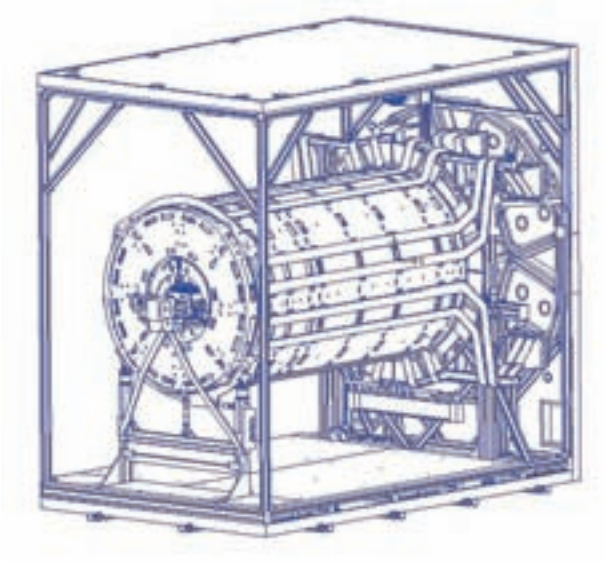

Figure 3.2: *For ATLAS SCT nine disks with detectors on both sides will be mounted in one cylinder. This equipment will assist the operators in handling the fragile but expensive finished disks with a minimum of risk for damage.*

Figure 3.3: *The common supports for the muon chambers of ATLAS MDT were designed with the help of FEM-simulation. The prototype behaved in accordance with simulations.*

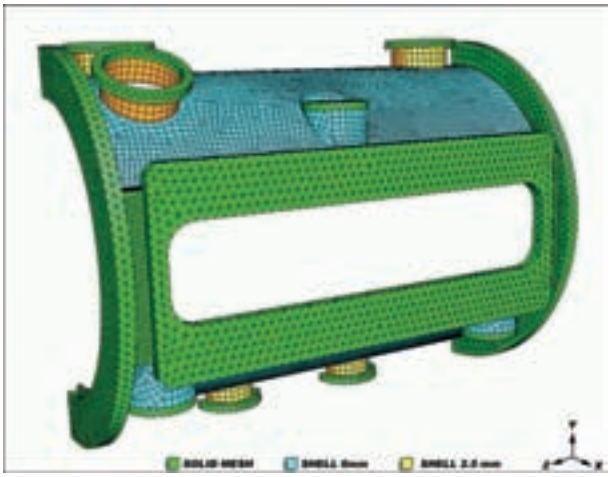

Figure 3.4: *An impression of the FEM-simulations made for the redesign of some critical areas of the secondary vacuum vessel of the LHCb vertex detector. Altering followed by immediate recalculating was very helpful in achieving the right shape after a few iterations.*

Monitored Drift Tubes

The engineering and design for Monitored Drift Tubes (MDT) was almost finished in 2002 and production was in full progress in 2003. Therefore, the main concern of the EA was the detailed design drawings and the engineering of the common support (Fig. 3.3) as well as the tooling, e.g. the lifting frames for the muon chambers. Many drawings were approved for EDMS archiving.

End Cap Toroids

Superconducting magnets for the end cap toroids (ECT) are produced by Brush HMA. The supervising of the work is a NIKHEF responsibility. The EA was involved in the impregnation process of the magnet coils with resin under vacuum.

3.2 LHCb

Vertex

The drawings of the vacuum vessel have been finished. FEM-analyses showed some critical places in the construction of the vessel. The FEM-model (Fig. 3.4) was very helpful in improving the vessel design. TIS-approval was achieved by the end of 2003 and tendering was started immediately. A paper has been written for NEVAC, the journal of the Dutch Vacuum Society, about the design of the vacuum vessel.

Support structures for the vessel, the stand, Y-translation frame and centre frame, were delivered and installed in the testing area (PIMU). FEM-analyses for the lifting points of the stand were made and approved by TIS.

A prototype for the RF-boxes was constructed together with the MA. Especially forming and welding of the ultra thin foil to the box turned out to be a major challenge. Performance tests are being done right now and show promising results. The final boxes are expected to be finished in 2004.

The conceptual design of the Detector vacuum system was finished. Special attention was paid to the safety of the primary accelerator vacuum which will have to be guaranteed under all circumstances. Small scale tests on components were started. A set of valves for the vacuum system has been welded at Shell laboratory. Prototype design of the system was started.

Cooling system prototyping and test infra structure was installed in the test area where the vertex CO_2-cooling system will be developed (VTCS). The dissipation from the silicon detectors and the readout electronics generate heat in the detector vacuum, near the accelerator vacuum. The heat will be removed with the VTCS.

The drawings for all items under production have been approved in the EDMS. The drawings for detector support have been submitted. Production will start as soon as the drawings have been approved.

Figure 3.5: *Station design of the LHCb outer tracker straw modules. The detector straw panels will be mounted on frames guided on rails to enable sideward movement away from the detector. The problem was to find a place for all components and electronic boxes as well as routing all services needed within the small available envelope.*

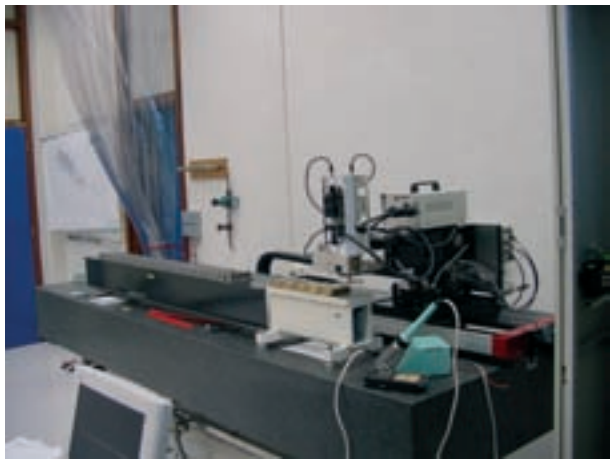

Figure 3.6: *For the Alice inner tracker system the modules, i.e. hybrids joined with the actual silicon strip detectors and connected via a specially folded flat cables, 32 modules will have to be mounted very accurately on a space frame bridge (not visible on the photo). The 5 degrees of freedom robot device will automatically assemble a few hundred of these so called detector ladders.*

Outer tracker

This year the production of 120 panels for the straw modules started in the newly built clean room. Most difficulties in producing templates for the panels by Philips machine factories were solved with the support of our Wenzel CMM. The sucking method for the straws to the panels had to be improved and is now working fine after all. Very accurate aligning of the templates with laser interferometry was achieved eventually. Templates for Warsaw were delivered and measured. Templates for Heidelberg were turnkey delivered at the end of 2003. The last series of templates were ordered for delivery early in 2004.

The engineering of the support structures (stations) for the detector modules including the routing of gas tubes and the water cooling of the electronics (Fig. 3.5) has been almost finished in 2003. Since dissipation of heat is again an issue in operating the straw modules, flow cooling simulations with FEM were performed.

3.3 Alice Inner Tracking System

The pick and place robot for high precision positioning silicon strip detector (SSD) modules on carbon fiber space frames was outsourced and approved for delivery (Fig. 3.6). A folding tool for flat cable to pre-assemble the hybrid with the actual SSD was developed. A prototype of the folding tool has been tested. A series of these tools will be outsourced in 2004. The conceptual design for the carbon fiber support cones was modeled in CAD. The engineering will be done in close cooperation with our Utrecht colleagues in the Alice inner tracker project.

3.4 ANTARES

Submersible electronic housing boxes for ANTARES were designed by the electronic department. The production drawings of the housings were outsourced to a well skilled engineering firm. Their task was to provide a set of drawings that enabled manufacturing of the housings in any machine factory without further assistance or instructions.

3.5 Alpha Magnetic Spectrometer

The cooling circuit (Tracker Thermal Control System) for the super conducting magnet for the spectrometers silicon tracker was developed in good cooperation with the NLR. This cooling system has much in common with the VTCS of the Vertex detector. Basic principle is the CO^2 cooling method which has the ability to distribute cold. This functionality is especially useful

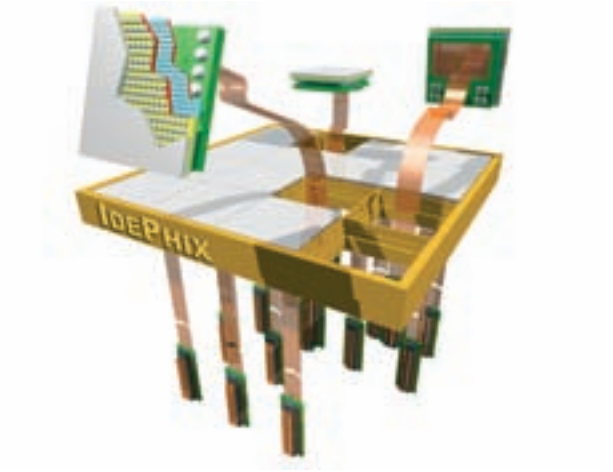

Figure 3.7: *Impression of an array of buttoned X-ray detector modules for the Idephix proposal.*

when there is little place for cooling devices. In 2003 the drawings were finished. The MA will soon start the manufacture of all the parts. This project is not part of a NIKHEF scientific program and will be shut down in 2004.

3.6 IdePhix

IdePhix modules are a spin off from X-ray pixel detectors. They can be used in X-ray diagnostics for medical purposes. Therefore modules have to be positioned in a two dimensional array. A module frame will allow an array of 4 x 4 IdePhix modules to be positioned and operated. Important specifications for the design are the mechanical and thermal stability and the repositioning accuracy for the modules which should be better than 10 μm. For a proposal to get European money we made a preliminary design study an a photo realistic picture for the cover of the proposal (Fig. 3.7).

4 Mechanical Workshop

4.1 Introduction

At present work in the mechanical workshop consists mainly of the development of tooling for production, and the production of the detectors itself; prototyping is becoming less important. Since the end dates of several projects that contain a large amount of mechanical production, are rapidly approaching, and since the engineering work has almost been done, the working-pressure on the mechanical workshop is becoming severe. This workload has required to double the amount of employed manpower in the past two years.

In 2003 a total of 9 trainees from, and in collaboration with, local schools had the opportunity to learn and improve their skills in the mechanical workshop.

4.2 Projects

ATLAS Muon Chambers

The Muon-Chamber production for ATLAS is running smoothly. For the gluing process of the smaller chambers (1440 and 1680 mm width) tools had to be changed, which has all been done without delaying the production. The first large amount of usable stainless steel inlet tubes arrived at the last quarter of 2003; approximately 20 Muon Chambers have now been made gas tight. At present our weekly production rate is to make almost 2 Muon Chambers gas tight and mount their Faraday cages. Nearly all further mechanical components necessary for finishing the Muon Chambers are presently available.

After restricting the gas flow during the gas-tightness test, breaking of wires did not occur anymore. Since we have not encountered any further significant problems during 2003, it seems likely that all Muon Chambers will be finished in time (October 2004).

ATLAS Semi-Conductor Tracker (SCT)

The manufacturer of the bare discs for the SCT changed his tooling last year. Hence, all discs are now delivered with flatness within specifications. Several tests have been done for the preparation of gluing the inserts onto the discs (see Fig. 4.1).

In the beginning of 2003 another prototype disc has been prepared completely in order to test once more all procedures; everything went well, and now the production of the SCT-discs is proceeding. In between the steps in the machining process all specifications will be checked with one of the 3D measuring machines. Protective close outs have been developed, they will be glued into apertures where cabling has to be guided through.

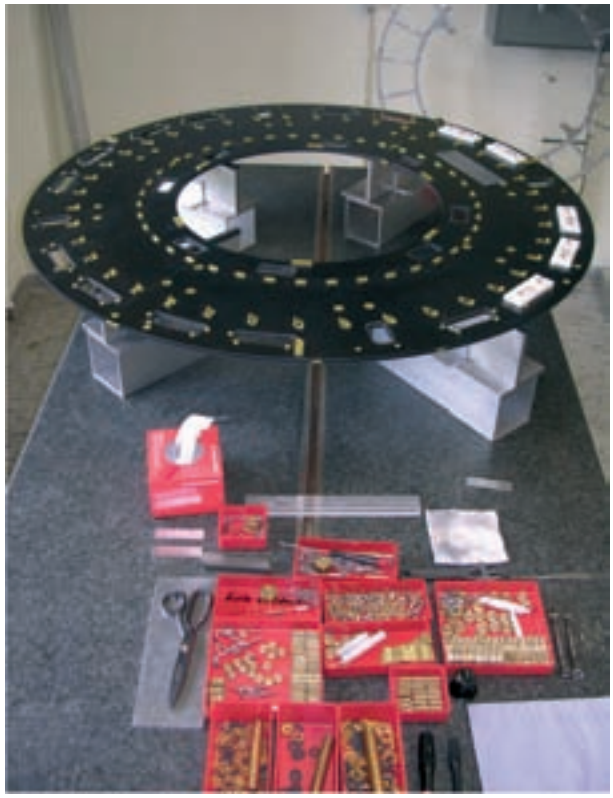

Figure 4.1: *Production of discs for the ATLAS Semi-Conductor Tracker. Here, inserts and close-outs are being glued-on.*

Some of the services, consisting of cooling pipes, wiggly tapes, shielding, fibers and connectors, have arrived from Rutherford Appleton Laboratory, which also participates in the SCT project. In the beginning of 2004 tooling will be made to build up a disc with all of its services. Wire bonding of the modules has been started. Although a variety of problems have been encountered solutions for all of them have been found.

A 'module to disc' setup has been built; it will be used to mount a single module onto a disc. This has to be done very cautiously because of the breakable modules. Therefore a camera system has been integrated in the setup, in order to position the module very accurately and then slide it on. It is equipped with small grippers to fetch the modules and keep the tiny screws before fixing.

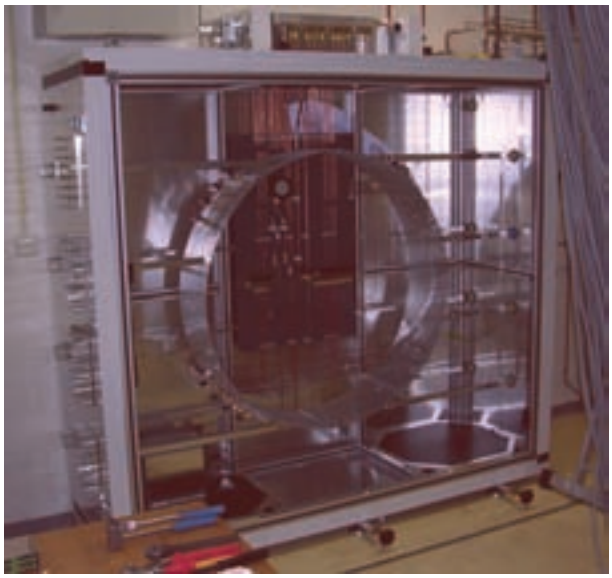

Figure 4.2: *Test box for testing completed discs of the ATLAS Semi-conductor Tracker.*

A prototype transport- and storage box for complete discs has been produced; it has springs and damping to protect the disc. After tests with the the prototype 9 boxes were ordered at an outside firm. For testing the complete discs, including the modules, a test box with cooling and dry air is being built (see Fig. 4.2). Another test- and buildup facility is being built, it will be used to mount the 9 discs in its support cylinder and test the whole assembly (also including cooling and dry air).

Production of the SCT discs has been started and is proceeding now, 50% of the discs have been machined, 40% of the discs have their inserts glued on and 20% of these inserts have been machined flat.

LHCb Vertex Detector

Some changes have been made to the wakefield suppressors of the LHCb Vertex Detector. Prototypes of various attachment pieces to the vacuum box have been produced. At the VU-workshop a welding mold was made for the aluminum, thin walled, vacuum box. With the help of molds all parts (foils) have been produced by Hot Metal Gas Forming, and then welded, using the welding mold. Especially welding of the box (0.3 mm thickness) to the flange (20 mm thickness) is quite difficult; nevertheless, the first Detector Vacuum Box has been welded successfully (see Fig. 4.3).

The center-frame of the LHCb Vertex detector has been constructed at the mechanical workshop (see Fig. 4.4).

Figure 4.3: *The first complete Detector Vacuum Box for the LHCb Vertex detector is ready.*

In a later stage the completed frame has been machined again to comply with the very tight tolerances necessary for the accurate movement of the detector towards the beam.

The production of prototype bellows by soldering was not successful; it has therefore been decided to weld the

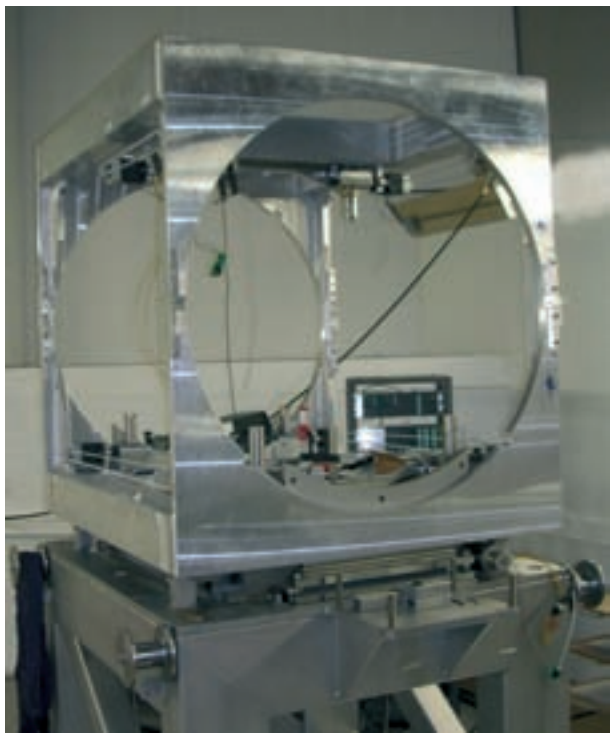

Figure 4.4: *The Center-frame of the LHCb Vertex Detector. The frame will accurately move the detector halves towards the beam.*

Figure 4.5: *Setup for the assembly of LHCb Outer Tracker modules. From left to right: tables for the assembly of the modules, wiring the modules and the straw preparation station.*

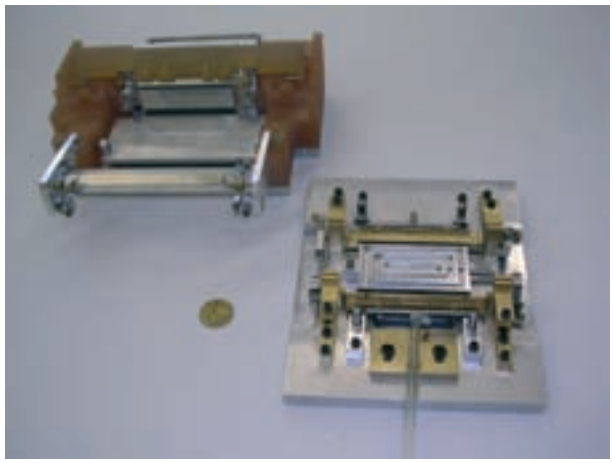

Figure 4.6: *Two prototypes of a production tool for folding and gluing kapton cable to the read-out modules of the ALICE detector.*

bellow parts together. We use molds to lead away the heat in the 0.15 mm thick stainless steel shells. To produce this bellow two flat shells are welded at the interior side. Next all five packages are pressed in the hollow shape that a bellow needs to make motion possible and the outer sides are welded together. The first rectangular bellow is now ready and vacuum tight. Welding itself runs smoothly, but preparation (removal of oxides due to laser cutting, matching tolerances for opposite sides) requires a large amount of time. Although the procedure is strenuous (welding-testing-welding-testing etc.) it was demonstrated that it is possible to make 70 meter of such a difficult joint vacuum tight.

LHCb Outer Tracker

A 1000 mm and a 5000 mm prototype module have been made with the final parts and methods. Also a scan table was built; it consists of a moving source and a slit that makes it possible to check the position of the wires in the module and see through the module to verify whether all parts are in place. A setup has been made for testing the gas tightness of a produced module.

A new complete mechanical mock-up module of the Front-End Electronics has been built. Some adaptations have been made. At the end of 2003 the engineering work for the electronics housing was completed. The housing is now ready for production; a first small quantity of parts will be produced and ordered.

At the VU-workshop a tool has been made to prepare the straws. It cuts them at the right length, makes a connection for grounding, and inserts wire locators and end-pieces that hold the wire in its right position. Approximately 30000 straws have to be produced in total. The templates that hold the straws during gluing, are produced at Philips and finished at NIKHEF. They are now ready for use. Production in 2004 of module zero is being prepared by collecting all components. It will take place in the cleanroom that is ready for the production process (see Fig. 4.5). Of the 185 long modules (5000 mm) 125 will be produced at NIKHEF.

ANTARES

For ANTARES we made several fiber trays that guide the fibers to prevent them from breaking. After finishing the prototype work several series have been laser cut at an outside firm. We also produced several cooling blocks that will hold and cool electronics boards.

ALICE

Prototype work has been done for the tool that pulls all cooling blocks in one movement onto the cooling circuit. The production of the complete unit will take place in the beginning of the year 2004. A first prototype for the end-cap mechanics has been produced. The development of a production tool for folding and gluing the kapton cable to the read-out modules for the detector has been completed; two successive prototypes have been developed (see Fig. 4.6) and 10 units will be manufactured at an outside firm.

A Data Acquisition System for the ANTARES Neutrino Telescope

Mieke Bouwhuis, on behalf of the ANTARES collaboration
NIKHEF, Amsterdam
mieke.bouwhuis@nikhef.nl

The ANTARES collaboration is building a neutrino telescope in the Mediterranean sea. High energy muon-neutrinos are detected indirectly via the Cherenkov light emitted from the muon produced in a charged current interaction. The light is detected by photo-multiplier tubes (PMTs) which are supported by vertical strings. From the arrival times of the photons on the PMTs the muon trajectory can be reconstructed. A data acquisition (DAQ) system has been designed for the readout and the processing of the data.

Detector

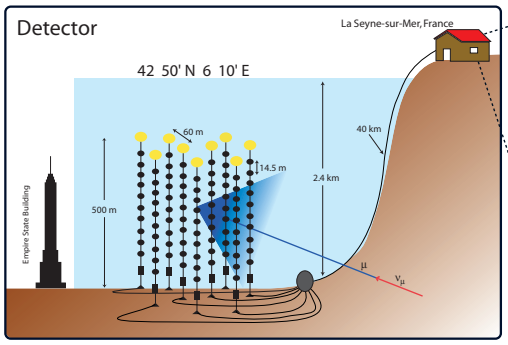

On-shore data processing system

The on-shore data processing system consists of 100 PCs, each running the DataFilter program. All data produced by the readout system in a certain time window are sent to a single processor. The DataFilters filter the physics events from the data online.

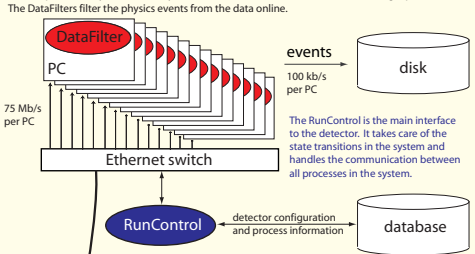

Off-shore readout system

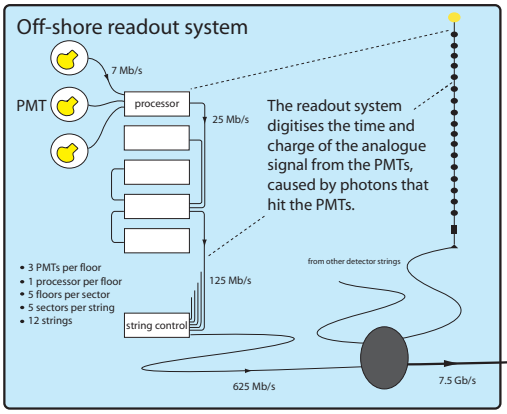

All data are sent to shore via an electro-optical cable which is also used to power the detector.

Neutrinos from gamma ray bursts

The gamma ray burst coordinates network (GCN) distributes information obtained from satellites that detect gamma ray bursts (GRBs). By using this network as an external trigger, the detection efficiency for neutrinos from GRBs can be increased.

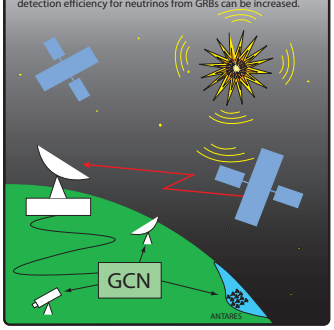

Detection of neutrinos from GRBs

The DataFilter is based on a cluster algorithm that looks for space-time correlations in the data. By connecting the DAQ system to the GCN, directional information of GRBs is obtained. The data can then be filtered using a different cluster algorithm that looks for time correlated hits from muons from the given direction. Such a specialised data filter algorithm is implemented in the FlashBack program. FlashBack can also be used online to track known astrophysical sources that may produce neutrinos, e.g. the Sun and the centre of the Galaxy.

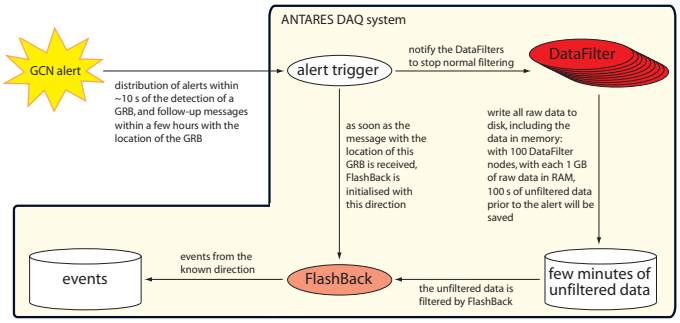

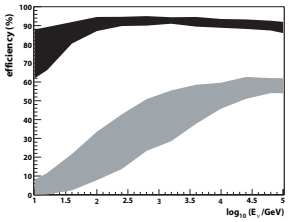

Efficiency of FlashBack (black area) and DataFilter (grey area) as a function of the neutrino energy. The areas cover the results for neutrinos that come from different upward directions.

Poster presented by Mieke Bouwhuis at ICRC 2003 (International Cosmic Ray Conference).

E Publications, Theses and Talks

1 Publications

ALICE

[1] STAR collaboration, Adams, J. *et al.*; Botje, M.; Snellings, R.; Tang, A.H.
Evidence from d+Au measurements for final state suppression of high p_T hadrons in Au+Au collisions at RHIC.
Phys. Rev. Lett. 91 (2003) 072304

[2] STAR collaboration, Adams, J. *et al.*; Botje, M.; Snellings, R.; Tang, A.H.
Transverse-momentum and collision-energy dependence of high p_T hadron suppression in Au+Au collisions at ultrarelativistic energies.
Phys. Rev. Lett. 91 (2003) 172302

[3] STAR collaboration, Adams, J. *et al.*; (Botje, M.; Snellings, R.; Tang, A.H.
Net charge fluctuations in Au + Au collisions at $\sqrt{s_{NN}} = 130$ GeV.
Phys. Rev. C 68 (2003) 044905

[4] STAR collaboration, Adams, J. *et al.*; Botje, M.; Snellings, R.; Tang, A.H.)
Three-Pion Hanbury Brown-Twiss correlations in relativistic heavy-ion collisions from the STAR experiment.
Phys. Rev. Lett. 91 (2003) 262301

[5] STAR Collaboration, Adams, J. *et al.*; Botje, M.; Snellings, R.; Tang A.H.
Pion-Kaon correlations in Au+Au collisions at $\sqrt{s_{NN}} = 130$ GeV.
Phys. Rev. Lett. 91 (2003) 262302

[6] NA49 collaboration, Alt, C. *et al.*; Botje, M.; Leeuwen, M. van
Directed and elliptic flow of charged pions and protons in Pb + Pb collisions at 40-A-GeV and 158-A-GeV.
Phys. Rev. C 68 (2003) 034903

[7] NA49 collaboration, Leeuwen M. van,
Recent results on spectra and yields form NA49.
Nucl. Phys. 715 (2003) 161-170c

[8] STAR Collaboration, Ackermann K.H. *et al.*; Botje, M.; Snellings, R.; Tang, A.)
Star detector overview.
Nucl. Instr. Meth. A 499 (2003) 624-632

[9] STAR Collaboration, Anderson M. *et al.*; Botje, M.; Snellings, R.; Tang, A.
The star time projection chamber: a unique tool for studying high multiplicity events at RHIC.
Nucl. Instr. Meth. A 499 (2003) 659-678

[10] STAR Collaboration J. Adams *et al.*; Botje, M.; Snellings, R.; Tang, A.
Narrowing of the balance function with centrality in au + au collisions at $\sqrt{s_{NN}} = 130$ GeV.
Phys. Rev. Lett. 90 (2003) 172301

[11] STAR Collaboration; Botje M.; Snellings, R.; Tang, A.
Heavy ions collisions.
eConf C030626:SAAT03 (2003)

[12] Lutz J.R. *et al.*; van den Brink, A.; de Haas, A.P.; Kuijer, P.; Nooren, G.J.L.; Oskamp, C.J.; Sokolov, A.
Front-end modules for ALICE SSD
Proceedings of 9th workshop on electronics for LHC experiments, Amsterdam, September 2003.

[13] Peitzmann T.
Hydrodynamic Description of Spectra at High Transverse Mass in Ultrarelativistic Heavy Ion Collisions
Eur. Phys. J. C 26 (2003) 539-549

[14] WA98 Collaboration, Aggarwal M.M. *et al.*; Geurts, F.; Kamermans, R.; Peitzmann, T.; Van der Pijll, E.; Van Eijndhoven, N.
One-, two-, and three-particle distributions from 158A GeV/c central Pb+Pb collisions
Phys. Rev. C 67 (2003) 014906

[15] WA98 Collaboration, Aggarwal M.M. *et al.*; Geurts, F.; Kamermans, R.; Peitzmann, T.; Van der Pijll, E.; Van Eijndhoven
Centrality dependence of charge-neutral fluctuations in 158 A GeV 208Pb + 208Pb Collisions
Phys. Rev. C 67 (2003) 044901

[16] PHENIX Collaboration, Adcox K. *et al.*; Peitzmann, T.
Centrality dependence of the high pt charged hadron suppression in Au+Au collisions at $\sqrt{s_{NN}} = 130$ GeV.
Phys. Lett. B 561 (2003) 82-92

[17] Peitzmann, T.
Influence of hydrodynamics on the interpretation of the high pt hadron suppression at RHIC
Nucl. Phys. A 727 (2003) 179-192

[18] Andronic, A. *et al.*; Peitzmann, T.
Pulse height measurements and electron attachment in drift chambers operated with Xe,CO2 mixtures.
Nucl. Instr. Meth. A 498 (2003) 143-154

[19] PHENIX Collaboration, Adler S.S. *et al.*; Peitzmann, T.
Suppressed pi0 production at large transverse momentum in central Au + Au collisions at $\sqrt{s_{NN}} =$ 200 *GeV.*
Phys. Rev. Lett. 91 (2003) 072301

[20] PHENIX Collaboration, Adler S.S. *et al.*; Peitzmann, T.
Scaling properties of proton and anti-proton production in $\sqrt{s_{NN}} = 200$ *GeV Au+Au collisions.*
Phys. Rev. Lett. 91 (2003) 172301

[21] PHENIX Collaboration, Adler S.S. *et al.*; Peitzmann, T.
Elliptic flow of identified hadrons in Au+Au collisions at $\sqrt{s_{NN}} = 200$ *GeV.*
Phys. Rev. Lett. 91 (2003) 182301

[22] PHENIX Collaboration, Adcox K. *et al.*(Peitzmann T.)
PHENIX detector overview.
Nucl. Instr. Meth. A 499 (2003) 469-479

[23] Aphecetche L. *et al.*; Peitzmann, T.
PHENIX calorimeter.
Nucl. Instr. Meth. A 499 (2003) 521-536

[24] WA98 collaboration; Van Eijndhoven, N.J.A.M.; Kamermans, R.; Peitzmann, T.
Photon flow in 158A GeV $^{208}Pb+^{208}Pb$ *collisions.*
Nucl. Phys. A 715 (2003) 579

[25] NA57 collaboration; Van Eijndhoven, N.J.A.M.; Kamermans, R.; Kuijer, P.G.; Sokolov, A.
Results on 40 A GeV/c Pb-Pb collisions from the NA57 experiment.
Nucl. Phys. A 715 (2003) 514

[26] NA57 collaboration; Van Eijndhoven, N.J.A.M.; Kamermans, R.; Kuijer, P.G.; Sokolov, A.
Hyperon yields in Pb-Pb collisions from the NA57 experiment.
Nucl. Phys. A 715 (2003) 140

[27] WA98 collaboration; Van Eijndhoven, N.J.A.M.; Kamermans, R.; Peitzmann T.
One-, Two- and Three-Particle Distributions from 158A GeV/c Central Pb+Pb Collisions.
Phys. Rev. C67 (2003) 014906

ANTARES

[28] Amran, P. *et al.*; Carloganu, C.; Dantzig, R. van; Engelen, J.J.; Heijboer, A.; Jong, M. de; Kooijman, P.; Nooren, G.J.; Oberski, J.E.J.; Witt Huberts, P. de; Wolf, E. de; ANTARES collaboration
Sedimentation and fouling of optical surfaces at the ANTARES site
Astropart. Phys. 19 (2003) 253-267

ATLAS

[29] A. Abazov, V.M. *et al.*; Balm, P.W.; Blekman, F.; Bos, K.; Peters, O.; Ahmed, S.N.; Jong, S.J. de; Duensing, S.; Filthaut, F.; Wijngaarden, D.A.; D0 collaboration
T Observation of diffractively produced W and Z bosons in pbar-p collisions at root-s = 1800 GeV
Phys. Lett. B 574 (2003) 169-179

[30] Abazov, V.M. *et al.*; Balm, P.W.; Blekman, F.; Bos, K.; Peters, O.; Ahmed, S.N.; Jong, S.J.; Duensing, S.; Filthaut, F.; Wijngaarden, D.A.; D0 collaboration
T t(t)over-bar production cross section in p(p)over-bar collisions at root s=1.8 TeV
Phys. Rev. D 67 (2003) 012004

[31] Abazov, V.M. *et al.*; Balm, P.W.; Blekman, F.; Bos, K.; Peters, O.; Ahmed, S.N.; Jong, S.J.; Duensing, S.; Filthaut, F.; Wijngaarden, D.A.; D0 collaboration
T Multiple jet production at low transverse energies in p(p)over-bar collisions at root s=1.8 TeV
Phys. Rev. D 67 (2003) 052001

[32] *Proceedings of the 31st International Conference, ICHEP 2002, Amsterdam, Netherlands, July 25-31, 2002.*
S. Bentvelsen, (ed.), P. de Jong, (ed.), J. Koch, (ed.), E. Laenen, (ed.), Nucl. Phys. B, Proc. Suppl. 117 (2003).

[33] Abazov, V.M. *et al.*; Balm, P.W.; Blekman, F.; Bos, K.; Peters, O.; Ahmed, S.N.; Jong, S.J.; Duensing, S.; Filthaut, F.; Wijngaarden, D.A.; D0

collaboration
T Search for large extra dimensions in the monojet + missing E(T) channel at D0
Phys. Rev. Lett. 90 (2003) 251802

[34] Keil, M. *et al.*; Eijk, B. van; Hartjes, F.; Noomen, J.
New results on diamond pixel sensors using ATLAS frontend electronics
Nucl. Instr. Meth. 501 (2003) 153-159

[35] Peeters, S.J.M.
The development and performance of silicon strip modules for the ATLAS forward semi-conductor tracker
Nucl. Instr. Meth. A513 (2003) 74-78

B-Physics

[36] B. Aubert *et al.*; G. Raven; BABAR Collaboration
Measurement of $B^0 \to D_s^{*+} D^{*-}$ branching fractions and $B^0 \to D_s^{*+} D^{*-}$ polarization with a partial reconstruction technique
Phys. Rev. D **67** (2003) 092003

[37] B. Aubert *et al.*; G. Raven; BABAR Collaboration
Measurement of the B^0 meson lifetime with partial reconstruction of $B^0 \to D^{*-}\pi^+$ and $B^0 \to D^{*-}\rho^+$ decays
Phys. Rev. D **67** (2003) 091101

[38] B. Aubert *et al.*; G. Raven; BABAR Collaboration
Simultaneous measurement of the B^0 meson lifetime and mixing frequency with $B^0 \to D^{*-} l^+ \nu l$ decays
Phys. Rev. D **67** (2003) 072002

[39] B. Aubert *et al.*; G. Raven; BABAR Collaboration
Study of inclusive production of charmonium mesons in B decays
Phys. Rev. D **67** (2003) 032002

[40] B. Aubert *et al.*; M.A. Baak; G. Raven; BABAR Collaboration
Measurement of the branching fraction for inclusive semileptonic B meson decays
Phys. Rev. D **67** (2003) 031101

[41] B. Aubert *et al.*; G. Raven; BABAR Collaboration
Measurement of the branching fractions for the exclusive decays of B^0 and B^+ to anti-$D^{(*)} D^{(*)} K$
Phys. Rev. D **68** (2003) 092001

[42] B. Aubert *et al.*; G. Raven; BABAR Collaboration
Measurement of the $B^0 \to J/\psi \pi^+ \pi^-$ Branching Fraction
Phys. Rev. Lett. **90** (2003) 091801

[43] B. Aubert *et al.*; G. Raven; BABAR Collaboration
Measurement of the CKM matrix element $|V_{ub}|$ with $B \to \rho e \nu$ decays
Phys. Rev. Lett. **90** (2003) 181801

[44] B. Aubert *et al.*; G. Raven; BABAR Collaboration
Study of the Rare Decays $B^0 \to D_s^{(*)+}\pi$ - and $B^0 \to D_s^{(*)-} K^+$
Phys. Rev. Lett. **90** (2003) 181803

[45] B. Aubert *et al.*; G. Raven; BABAR Collaboration
Measurement of the Branching Fraction, and Bounds on the i CP-Violating Asymmetries, of Neutral B Decays to $D^{*\pm} D^{\pm}$
Phys. Rev. Lett. **90** (2003) 221801

[46] B. Aubert *et al.*; M.A. Baak; G. Raven; BABAR Collaboration
Evidence for $B^+ \to J/\psi p \overline{\Lambda}$ and search for $B^0 \to J/\psi p \overline{p}$
Phys. Rev. Lett. **90** (2003) 231801

[47] B. Aubert *et al.*; M.A. Baak; G. Raven; BABAR Collaboration
Observation of a narrow meson decaying to $D_s^+ \pi^0$ at a mass of 2.32-GeV/c^2
Phys. Rev. Lett. **90** (2003) 242001

[48] B. Aubert *et al.*; M.A. Baak; G. Raven; BABAR Collaboration
Observation of the decay $B^{\pm} \to \pi^{\pm}\pi^0$, study of $B^{\pm} \to K^{\pm}\pi^0$, and search for $B^0 \to \pi^0\pi^0$
Phys. Rev. Lett. **91** (2003) 021801

[49] B. Aubert *et al.*; M.A. Baak; G. Raven; BABAR Collaboration
Measurements of the branching fractions and charge asymmetries of charmless three-body charged B decays
Phys. Rev. Lett. **91** (2003) 051801

[50] B. Aubert *et al.*; M.A. Baak; G. Raven; BABAR Collaboration
Study of time-dependent CP asymmetry in neutral B decays to $J/\psi \pi^0$
Phys. Rev. Lett. **91** (2003) 061802

[51] B. Aubert *et al.*; G. Raven; BABAR Collaboration
Rare B decays into states containing a J/ψ meson and a meson with s anti-s quark content
Phys. Rev. Lett. **91** (2003) 071801

[52] B. Aubert *et al.*; M.A. Baak; G. Raven; BABAR Collaboration
Limits on $D^0 - \overline{D^0}$ mixing and CP violation from the ratio of lifetimes for decay to $K^-\pi^+$, K^-K^+ and $\pi^-\pi^+$
Phys. Rev. Lett. **91** (2003) 121801

[53] B. Aubert *et al.*; M.A. Baak; G. Raven; BABAR Collaboration
Measurement of time-dependent CP asymmetries and the CP-odd fraction in the decay $B^0 \to D^{*+}D^{*-}$
Phys. Rev. Lett. **91** (2003) 131801

[54] B. Aubert *et al.*; M.A. Baak; G. Raven; BABAR Collaboration
Measurements of CP-violating asymmetries and branching fractions in B meson decays to $\eta' K$
Phys. Rev. Lett. **91** (2003) 161801

[55] B. Aubert *et al.*; M.A. Baak; G. Raven; BABAR Collaboration
Search for $D^0 - \overline{D^0}$ mixing and a measurement of the doubly Cabibbo-suppressed decay rate in $D^0 \to K\pi$ decays
Phys. Rev. Lett. **91** (2003) 171801

[56] B. Aubert *et al.*; M.A. Baak; G. Raven; BABAR Collaboration
Rates, polarizations, and asymmetries in charmless vector-vector B meson decays
Phys. Rev. Lett. **91** (2003) 171802

[57] B. Aubert *et al.*; M.A. Baak; G. Raven; BABAR Collaboration
Measurements of branching fractions and CP-violating asymmetries in $B^0 \to \rho^{+-}h^{-+}$ decays
Phys. Rev. Lett. **91** (2003) 201802

[58] B. Aubert *et al.*; M.A. Baak; G. Raven; BABAR Collaboration
Evidence for the rare decay $B \to K^* l^+ l^-$ and measurement of the $B \to K l^+ l^-$ branching fraction
Phys. Rev. Lett. **91** (2003) 221802

[59] B. Aubert *et al.*; M.A. Baak; G. Raven; BABAR Collaboration
Observation of the decay $B^0 \to \pi^0\pi^0$
Phys. Rev. Lett. **91** (2003) 241801

[60] O. Long; M. Baak; R.N. Cahn; D. Kirkby
Impact of tag side interference in time dependent CP asymmetry measurements using coherent B^0 anti-B^0 pairs
Phys. Rev. D68 (2003) 034010, hep-ex/0303030

[61] N. van Bakel; D. Baumeister; M. van Beuzekom; H.J. Bulten; M. Feuerstack-Raible; E. Jans; T. Ketel; S. Klous; S. Lochner; E. Sexauer; N. Smale; H. Snoek; U. Trunk; H. Verkooijen
Characterisation of a radiation hard front-end chip for the vertex detector of the LHCb experiment at CERN
Nucl. Instr. Meth. A509 (2003) 176-182.

[62] R.Antunes-Nobrega *et al.*
LHCb Technical Design Report 9: "LHCb Reoptimized Detector Design and Performance
CERN preprint CERN/LHCC/2003-030; September 2003.

[63] R.Antunes-Nobrega *et al.*
LHCb Technical design Report 10: "LHCb Trigger System"
CERN preprint CERN/LHCC/2003-031; September 2003.

DATAGRID

[64] Antony, A. *et al.*
IGrid2002 demonstration: bandwidth from the low lands
Future Generation Computer Science 19 (2003) 825-837

[65] Antony, A.
Microscopic examination of TCP flows over transatlantic links
Future Generation Computer Science 19 (2003) 1017-1029

[66] Belloum, A.S.Z.; Groep, D.L. *et al.*
VLAM-G: a grid-based virtual laboratory
Future Generation Computer Systems 19 (2003) 209-217

[67] Brook, N.; Bulten, H.
LHCb distributed computing and the GRID
Nucl. Instr. Meth. 502 (2003) 334-338

HERMES

[68] Airapetian, A. *et al.*; Blok, H.P.; Bouhali, O.; Garutti, E.; Heesbeen, D.; Hesselink, W.H.A.; Lapikas, L.; Laziev, A.; Mexner, V.; Reischl, A.; Simani, M.C.; Steijger, J.J.M.; Nat, P. van der; Steenhoven, G. van der; Visser, J.; Zihlmann, B.; HERMES collaboration

The Q^2-dependence of the generalised Gerasimov-Drell-Hearn integral for the deuteron, proton and neutron
Eur. Phys. J. C 26 (2003) 527-538

[69] Airapetian, A. *et al.*; Blok, H.P.; Garutti, E.; Heesbeen, D.; Hesselink, W.H.A.; Lapikas, L.; Laziev, A.; Mexner, V.; Reischl, A.; Simani, M.C.; Steijger, J.J.M.; Nat, P. van der; Steenhoven, G. van der; Visser, J.; Zihlmann, B.; HERMES collaboration
Measurement of single-spin azimuthal asymmetries in semi-inclusive electroproduction of pions and kaons on a longitudinally polarised deuterium target
Phys. Lett. B 562 (2003) 182-192

[70] Airapetian, A. *et al.*; Blok, H.P.; Garutti, E.; Heesbeen, D.; Hesselink, W.H.A.; Lapikas, L.; Laziev, A.; Mexner, V.; Reischl, A.; Simani, M.C.; Steijger, J.J.M.; Steenhoven, G. van der; Visser, J.; Zihlmann, B.; HERMES collaboration
Double spin asymmetries in the cross-section of ρ^0 and ϕ production at intermediate-energies
Eur. Phys. J. C 29 (2003) 171-179

[71] Airapetian, A. *et al.*; Blok, H.P.; Garutti, E.; Heesbeen, D.; Hesselink, W.H.A.; Lapikas, L.; Laziev, A.; Mexner, V.; Reischl, A.; Simani, M.C.; Steijger, J.J.M.; Nat, P. van der; Steenhoven, G. van der; Zihlmann, B.; HERMES collaboration
Quark fragmentation to $\pi^{\pm}, \pi^0, K^{\pm}$, p and $\bar{p}$ in the nuclear environment
Phys. Lett. B 577 (2003) 37-46

[72] Airapetian, A. *et al.*; Blok, H.P.; Garutti, E.; Heesbeen, D.; Hesselink, W.H.A.; Lapikas, L.; Laziev, A.; Mexner, V.; Reischl, A.; Simani, M.C.; Steijger, J.J.M.; Nat, P. van der; Steenhoven, G. van der; Visser, J.; Zihlmann, B.; HERMES collaboration
The Q^2 dependence of nuclear transparency for exclusive ρ^0 production
Phys. Rev. Lett. 90 (2003) 052501

[73] Airapetian, A. *et al.*; Blok, H.P.; Garutti, E.; Heesbeen, D.; Hesselink, W.H.A.; Laziev, A.; Mexner, V.; Reischl, A.; Simani, M.C.; Steijger, J.J.M.; Nat, P. van der; Steenhoven, G. van der; Visser, J.; Zihlmann, B.; HERMES collaboration
Evidence for quark-hadron duality in the proton spin asymmetry A_1
Phys. Rev. Lett. 90 (2003) 092002

[74] Airapetian, A. *et al.*; Blok, H.P.; Bouhali, O; Garutti, E.; Heesbeen, D.; Hesselink, W.H.A.; Lapikas, L.; Laziev, A.; Mexner, V.; Reischl, A.; Simani, M.C.; Steijger, J.J.M.; Steenhoven, G. van der; Visser, J.; Zihlmann, B.; HERMES collaboration
Erratum to: "Nuclear Effects on $R = \sigma_L/\sigma_T$ in Deep-Inelastic Scattering" Phys. Lett. B 475 (2000) 386
Phys. Lett. B 567 (2003) 339

[75] Baumgarten, C. *et al.*; Garutti, E.; Kolster, H.
The storage cell of the polarized H/D internal gas target of the HERMES experiment at HERA
Nucl. Instr. Meth. A 496 (2003) 277-285

[76] Baumgarten, C. *et al.*; Kolster, H.
Measurements of atomic recombination in the HERMES polarized hydrogen and deuterium storage cell target
Nucl. Instr. Meth. A 496 (2003) 263-276

[77] Baumgarten, C. *et al.*; Kolster, H.; Simani, M.C.
gas analyzer for the internal polarized target of the HERMES experiment
Nucl. Instr. Meth. A 508 (2003) 268-275

[78] Beuzekom, M.G. van; Bouhali, O.; Mexner, V.; Mos, S.; Reischl, A.; Steijger, J.J.M.
The HERMES silicon project: the radiation protection system
Nucl. Instr. Meth. A 512 (2003) 44-51

[79] Beuzekom, M.G. van; Steenhoven, G. van der; Steijger, J.J.M.
Recoil detection at future QCD facilities
Nucl. Instr. Meth. A 513 (2003) 79-83

[80] Garutti, E.
Hadron formation in nuclei in deep-inelastic lepton scattering
Proc. 9^{th} Int. Conf. on the Structure of Baryons (Baryons 2002), Newport News 2002, Eds. C. Carlson, B.A. Mecking, World Scientific (2003) p. 558

[81] Nass, A. *et al.*; Kolster, H.; Simani, M.C.
The HERMES polarized atomic beam source
Nucl. Instr. Meth. A 505 (2003) 633-644

[82] Steenhoven, G. van der; HERMES collaboration
The (spin) structure of the nucleon
Eur. Phys. J. 18 (2003) 377-381

[83] Steenhoven, G. van der
Polarized Structure Functions
Proc. 9^{th} Int. Conf. on the Structure of Baryons (Baryons 2002), Newport News 2002, Eds. C. Carlson, B.A. Mecking, World Scientific (2003) p. 78

LEP-DELPHI

[84] Abdallah, J. *et al.*; Blom, H.M.; Kluit, P.; Montenegro, J.; Mulders, M.; Reid, D.; Timmermans, J.; Dam, P. van; Vulpen, I. van; DELPHI Collaboration
T Search for supersymmetric particles in light gravitino scenarios and sleptons NLSP
Eur. Phys. J. C 27 (2003) 153-172

[85] Abdallah, J. *et al.*; Blom, H.M.; Kluit, P.; Montenegro, J.; Mulders, M.; Reid, D.; Timmermans, J.; Dam, P. van; Vulpen, I. van; DELPHI Collaboration
T Search for an LSP gluino at LEP with the DELPHI detector
Eur. Phys. J. C 26 (2003) 505-525

[86] Abdallah, J. *et al.*; Blom, H.M.; Kluit, P.; Montenegro, J.; Mulders, M.; Reid, D.; Timmermans, J.; Dam, P. van; Vulpen, I. van; DELPHI Collaboration
T Inclusive b decays to wrong sign charmed mesons
Phys. Lett. B 561 (2003) 26-40

[87] Abdallah, J. *et al.*; Blom, H.M.; Kluit, P.; Montenegro, J.; Mulders, M.; Reid, D.; Timmermans, J.; Dam, P. van; Vulpen, I. van; DELPHI Collaboration
T Study of inclusive J/psi production in two-photon collisions at LEP II with the DELPHI detector
Phys. Lett. B 565 (2003) 76-86

[88] Abdallah, J. *et al.*; Blom, H.M.; Kluit, P.; Montenegro, J.; Mulders, M.; Reid, D.; Timmermans, J.; Dam, P. van; Vulpen, I. van; ALEPH, DELPHI, OPAL and L3 Collaborations,
Search for the standard model Higgs boson at LEP
Phys. Lett. B 565 (2003) 61-75

[89] Abdallah, J. *et al.*; Blom, H.M.; Kluit, P.; Montenegro, J.; Mulders, M.; Reid, D.; Timmermans, J.; Dam, P. van; Vulpen, I. van; DELPHI Collaboration
Search for resonant $\tilde{\nu}$ production at $\sqrt{s}$= 183 to 208 GeV
Eur. Phys. J. C 28 (2003) 15-26

[90] Abdallah, J. *et al.*; Blom, H.M.; Kluit, P.; Montenegro, J.; Mulders, M.; Reid, D.; Timmermans, J.; Dam, P. van; DELPHI Collaboration
T Study of the energy evolution of event shape distributions and their means with the DELPHI detector at LEP
Eur. Phys. J. C 29 (2003) 285-312

[91] Abdallah, J. *et al.*; Blom, H.M.; Kluit, P.; Montenegro, J.; Mulders, M.; Reid, D.; Timmermans, J.; Dam, P. van; DELPHI Collaboration
T Measurement of inclusive f(1) (1285) and f(1) (1420) production in Z decays with the DELPHI detector
Phys. Lett. B 569 (2003) 129-139

[92] Abdallah, J. *et al.*; Blom, H.M.; Kluit, P.; Montenegro, J.; Mulders, M.; Reid, D.; Timmermans, J.; Dam, P. van; DELPHI Collaboration
T ZZ production in e + e - interactions at $\sqrt{s}$ = 183-209 GeV
Eur. Phys. J. C 30 (2003) 447-466

[93] Abdallah, J. *et al.*; Blom, H.M.; Kluit, P.; Montenegro, J.; Mulders, M.; Reid, D.; Timmermans, J.; Dam, P. van; DELPHI Collaboration
T measurement of the branching fractions of the b-quark into charged and neutral b-hadrons
Phys. Lett. B 576 (2003) 29-42

[94] Abdallah, J. *et al.*; Blom, H.M.; Kluit, P.; Montenegro, J.; Mulders, M.; Reid, D.; Timmermans, J.; Dam, P. van; DELPHI Collaboration
T Measurement of the $e^+e^- \to W^+W^-\gamma$ cross-section and limits on anomalous quartic gauge couplings with DELPHI
Eur. Phys. J. C 31 (2003) 139-147

[95] Abdallah, J. *et al.*; Blom, H.M.; Kluit, P.; Montenegro, J.; Mulders, M.; Reid, D.; Timmermans, J.; Dam, P. van; DELPHI Collaboration
T The η_c(2980) formation in two-photon collisions at LEP energies
Eur. Phys. J. C 31 (2003) 481-489

[96] Abdallah, J. *et al.*; Blom, H.M.; Kluit, P.; Montenegro, J.; Mulders, M.; Reid, D.; Timmermans, J.; Dam, P. van; Vulpen, I. van; DELPHI Collaboration
T Search for doubly charged Higgs bosons at LEP2
Phys. Lett. B 552 (2003) 127-137

[97] Kluit, P. *et al.*
Proceedings of the worskhop on 'The CKM matrix and the Unitarity Triangle'
yellow report CERN-2003-002 (2003), hep-ph/0304132.

LEP-L3

[98] Achard, P. *et al.*; Baldew, S.V.; Bobbink, G.J.; Dalen, J.A. van; Dierckxsens, M.; Filthaut, F.; Gulik, R. van; Hakobyan, R.S.; Hu, Y.; Jong, P. de; Kittel, W.; König, A.C.; Linde, F.L.; Mangeol, D.; Metzger, W.J.; Muijs, A.J.M.; Petersen, B.; Roux, B.; Sanders, M.P.; Schotanus, D.J.; Timmermans, C.; Van de Walle, R.T.; Wilkens, H.; L3 collaboration
Inclusive charged hadron production in two photon collisions at LEP
Phys. Lett. B 554 (2003) 105–114

[99] Achard, P. *et al.*; Baldew, S.V.; Bobbink, G.J.; Dalen, J.A. van; Dierckxsens, M.; Filthaut, F.; Gulik, R. van; Hakobyan, R.S.; Hu, Y.; Jong, P. de; Kittel, W.; König, A.C.; Linde, F.L.; Mangeol, D.; Metzger, W.J.; Muijs, A.J.M.; Petersen, B.; Roux, B.; Sanders, M.P.; Schotanus, D.J.; Timmermans, C.; Van de Walle, R.T.; Wilkens, H.; L3 collaboration
Measurement of W polarisation at LEP Phys. Lett. B 557 (2003) 147–156

[100] Achard, P. *et al.*; Baldew, S.V.; Bobbink, G.J.; Dalen, J.A. van; Dierckxsens, M.; Filthaut, F.; Gulik, R. van; Hakobyan, R.S.; Hu, Y.; Jong, P. de; Kittel, W.; König, A.C.; Linde, F.L.; Mangeol, D.; Metzger, W.J.; Muijs, A.J.M.; Petersen, B.; Roux, B.; Sanders, M.P.; Schotanus, D.J.; Timmermans, C.; Van de Walle, R.T.; Wilkens, H.; L3 collaboration
Study of the $e^+e^- \to Ze^+e^-$ process at LEP
Phys. Lett. B 561 (2003) 73–81

[101] Achard, P. *et al.*; Baldew, S.V.; Bobbink, G.J.; Dalen, J.A. van; Dierckxsens, M.; Filthaut, F.; Gulik, R. van; Hakobyan, R.S.; Hu, Y.; Jong, P. de; Kittel, W.; König, A.C.; Linde, F.L.; Metzger, W.J.; Muijs, A.J.M.; Petersen, B.; Schotanus, D.J.; Timmermans, C.; Van de Walle, R.T.; Wang, Q.; Wilkens, H.; L3 collaboration
Search for colour reconnection effects in $e^+e^- \to W^+W^- \to$ hadrons through particle-flow studies at LEP
Phys. Lett. B 561 (2003) 202–212

[102] Heister, A. *et al.*; Baldew, S.V.; Bobbink, G.J.; Buijs, A.; Dalen, J.A. van; Dierckxsens, M.; Dierendonck, D. van; Duinker, P.; Filthaut, F.; Gulik, R. van; Hu, Y.; Jong, P. de; Kittel, W.; König, A.C.; Linde, F.L.; Mangeol, D.; Metzger, W.J.; Muijs, A.J.M.; Petersen, B.; Roux, B.; Sanders, M.P.; Schotanus, D.J.; Timmermans, C.; Van de Walle, R.T.; Wilkens, H.; ALEPH, DELPHI, L3, OPAL collaborations and The LEP Working Group for Higgs Boson Searches
Search for the Standard Model Higgs boson at LEP
Phys. Lett. B 565 (2003) 61–75

[103] Achard, P. *et al.*; Baldew, S.V.; Bobbink, G.J.; Dalen, J.A. van; Dierckxsens, M.; Filthaut, F.; Gulik, R. van; Hu, Y.; Jong, P. de; Kittel, W.; König, A.C.; Linde, F.L.; Metzger, W.J.; Muijs, A.J.M.; Novak, T.; Petersen, B.; Schotanus, D.J.; Timmermans, C.; Van de Walle, R.T.; Wang, Q.; Wilkens, H.; L3 collaboration
Measurement of exclusive ρ^0 ρ^0 production in two photon collisions at high Q^2 at LEP
Phys. Lett. B 568 (2003) 11–22

[104] Achard, P. *et al.*; Baldew, S.V.; Bobbink, G.J.; Dalen, J.A. van; Dierckxsens, M.; Filthaut, F.; Gulik, R. van; Hakobyan, R.S.; Hu, Y.; Jong, P. de; Kittel, W.; König, A.C.; Linde, F.L.; Metzger, W.J.; Muijs, A.J.M.; Schotanus, D.J.; Timmermans, C.; Van de Walle, R.T.; Wang, Q.; Wilkens, H.; L3 collaboration
Search for excited leptons at LEP
Phys. Lett. B 568 (2003) 23–34

[105] Achard, P. *et al.*; Baldew, S.V.; Bobbink, G.J.; Dalen, J.A. van; Dierckxsens, M.; Filthaut, F.; Gulik, R. van; Hakobyan, R.S.; Hu, Y.; Jong, P. de; Kittel, W.; König, A.C.; Linde, F.L.; Mangeol, D.; Metzger, W.J.; Muijs, A.J.M.; Petersen, B.; Roux, B.; Sanders, M.P.; Schotanus, D.J.; Timmermans, C.; Van de Walle, R.T.; Wilkens, H.; L3 collaboration
Search for a Higgs boson decaying to weak boson pairs at LEP
Phys. Lett. B 568 (2003) 191–204

[106] Achard, P. *et al.*; Baldew, S.V.; Bobbink, G.J.; Dalen, J.A. van; Dierckxsens, M.; Filthaut, F.; Gulik, R. van; Hakobyan, R.S.; Hu, Y.; Jong, P. de; Kittel, W.; König, A.C.; Linde, F.L.; Metzger, W.J.; Muijs, A.J.M.; Petersen, B.; Schotanus, D.J.; Timmermans, C.; Van de Walle, R.T.; Wang,

Q.; Wilkens, H.; L3 collaboration
Proton anti-proton pair production in two photon collisions at LEP
Phys. Lett. B 571 (2003) 11–20

[107] Achard, P. *et al.*; Baldew, S.V.; Bobbink, G.J.; Dalen, J.A. van; Dierckxsens, M.; Filthaut, F.; Gulik, R. van; Jong, P. de; Kittel, W.; König, A.C.; Linde, F.L.; Metzger, W.J.; Muijs, A.J.M.; Novak, T.; Petersen, B.; Roux, B.; Schotanus, D.J.; Timmermans, C.; Van de Walle, R.T.; Wang, Q.; Wilkens, H.; L3 collaboration
Z boson pair-production at LEP
Phys. Lett. B 572 (2003) 133–144

[108] Achard, P. *et al.*; Baldew, S.V.; Bobbink, G.J.; Dalen, J.A. van; Dierckxsens, M.; Filthaut, F.; Gulik, R. van; Hu, Y.; Jong, P. de; Kittel, W.; König, A.C.; Linde, F.L.; Metzger, W.J.; Muijs, A.J.M.; Novak, T.; Petersen, B.; Schotanus, D.J.; Timmermans, C.; Van de Walle, R.T.; Wang, Q.; Wilkens, H.; L3 collaboration
Search for charged Higgs bosons at LEP
Phys. Lett. B 575 (2003) 208–220

[109] Achard, P. *et al.*; Baldew, S.V.; Bobbink, G.J.; Dalen, J.A. van; Dierckxsens, M.; Filthaut, F.; Gulik, R. van; Hu, Y.; Jong, P. de; Kittel, W.; König, A.C.; Linde, F.L.; Metzger, W.J.; Muijs, A.J.M.; Novak, T.; Petersen, B.; Schotanus, D.J.; Timmermans, C.; Van de Walle, R.T.; Wang, Q.; Wilkens, H.; L3 collaboration
Search for doubly-charged Higgs bosons at LEP
Phys. Lett. B 576 (2003) 18–28

[110] Achard, P. *et al.*; Baldew, S.V.; Bobbink, G.J.; Buijs, A.; Dalen, J.A. van; Dierckxsens, M.; Dierendonck, D. van; Duinker, P.; Filthaut, F.; Gulik, R. van; Hu, Y.; Jong, P. de; Kittel, W.; König, A.C.; Linde, F.L.; Mangeol, D.; Metzger, W.J.; Muijs, A.J.M.; Petersen, B.; Roux, B.; Sanders, M.P.; Schotanus, D.J.; Timmermans, C.; Van de Walle, R.T.; Wilkens, H.; L3 collaboration
Measurement of charged-particle multiplicity distributions and their Hq moments in hadronic Z decays at LEP
Phys. Lett. B 577 (2003) 109–119

Transition Program
(AmPS, CHORUS, Medipix)

[111] Fornaini, A. *et al.*; Boerkamp, T.; Visschers, J.
Multi-chip board for X-ray imaging in build-up technology
Nucl. Instr. Meth. 509 (2003) 206-212

[112] Jakubek, J. *et al.*; Visschers, J.L.
Resolution and stability tests of a Medipix-1 pixel detector for X-ray dynamic defectoscopy
Nucl. Instr. Meth. 509 (2003) 294-301

[113] San Segundo Bello, D.; Beuzekom, M. van; Jansweijer, P.; Verkooijen, H.; Visschers, J.
An interface board for the control and data acquisition of the Medipix2 chip
Nucl. Instr. Meth. 509 (2003) 164-170

[114] Vavrik, D.; Jakubek, J.; Pospisil, S.; Visschers, J.L.; Zemankova, J.
X-Ray Dynamical Defectoscopy: A Way to Study Damage Processes
Proc. of the 14th Biennal Conference on Fracture - ECF14, Cracow, Poland, 8-13 September 2002. ISBN 1 901537 35 8 (2003)

[115] Vavrik, D.; Jakubek, J.; Pospisil, S.; Visschers, J.L.;
Non-desctructive Observation of Damage Processes by X-Ray Dynamic Defectoscopy
Mechanical Behaviour of Materials, Switzerland, Geneva , 25-29 May, 2003.

[116] Vavrik, D.; Jakubek, J.; Pospisil, S.; Visschers, J.L.; Zemankova, J
Non-desctructive Observation of Damage Processes in precracked specimens by X-Ray Dynamic Defectoscopy
Proc. of the conference Engineering Mechanics 2003, Czech Republic, 12-15 May, 2003

[117] Adamovich, M.I. *et al.*; Scheel, C.; WA89 collaboration
V0, anti-Xi+ and Omega- inclusive production cross-sections measured in hyperon experiment WA89 at CERN
Eur. Phys. J. C 26 (2003) 357-370

[118] Adam, W. *et al.*; Eijk, B. van; Hartjes, F.; Noomen, J.
Status of the R&D activity on diamond particle detectors
Nucl. Instr. Meth. 511 (2003) 124-131

[119] Adam, W. *et al.*; Eijk, B. van; Hartjes, F.; Noomen, J.
The development of diamond tracking detectors for the LHC
Nucl. Instr. Meth. 514 (2003) 79-86

[120] Atayan, M.R. *et al.*; Kittel, W.; EHS-NA22 collaboration
Erraticity analysis of multiparticle production in π^+p and K^+p collisions at 250 GeV/c
Phys. Lett. B 558 (2003) 22-28

[121] Atayan, M.R. *et al.*; Kittel, W.; EHS-NA22 collaboration
Erraticity of rapidity gaps in p+p and K+p collisions at 250 GeV/c
Phys. Lett. B 558 (2003) 29-33

[122] Audi, G. *et al.*; Wapstra, A.H.
The NUBASE evaluation of nuclear and decay properties
Nucl. Phys. 729 (2003) 3-128

[123] Audi, G. *et al.*Wapstra, A.H.
The AME2003 atomic mass evaluation (II). Tables, graphs and references
J. Nucl. Phys 729 (2003) 337 - 676

[124] Boer, J. de; Schalm, K.
General covariance of the non-abelian DBI-action
JHEP (2003) 02041

[125] Blume, C.
Results on correlations and fluctuations from NA49
Nucl. Phys. 715 (2003) 55-64c

[126] Eskut, E. *et al.*; Dantzig, R. van; Jong, M. de; Konijn, J.; Melzer, O.; Oldeman, R.G.D .; Pesen, E.; Poel, C.A.F.J. van der; Uiterwijk, J.W.E.; Visschers, J.L.; CHORUS collaboration
Cross-section measurement for quasi-elastic production of charmed baryons in nu N interactions
Phys. Lett. B 575 (2003) 198-207

[127] Hansen, J.E.; Ven E.G.
Some unexpected proportionalities between components of the spin-other-orbit interaction in the f shell
Mol. Phys. 101 (2003) 997-1000

[128] Kayis-Topaksu, A. *et al.*; Dantzig, R. van; Jong, M. de; Melzer, O.; Oldeman, R.G.C.; Pesen, E.; Spada, F.R.; Visschers, J.L.; CHORUS collaboration
Measurement of the Z/A dependence of neutrino charged-current total cross-sections
Eur. Phys. J. C 30 (2003) 159-167

[129] Kayis-Topaksu, A. *et al.*; Dantzig, R. van; Jong, M. de; Melzer, O.; Oldeman, R.G.C.; Pesen, E.; Spada, F.R.; Visschers, J.L.; CHORUS collaboration
Measurement of Lambda(+)(c) production in neutrino charged-current interactions
Phys. Lett. B 555 (2003) 156-166

[130] Manzari, V.
Hyperon yields in Pb-Pb collisions from NA57 experiment
Nucl. Phys. 715 (2003) 140-150c

[131] Mischke, A.
Energy dependence of Lambda and (Lambda)overbar production at CERN-SPS energies
Nucl. Phys. 715 (2003) 453-457c

[132] Mohanty, B.
Particle density fluctuations
Nucl. Phys. 715 (2003) 339-348c

[133] Nikolaev, S.; WA98 Collaboration
Photon flow in 158 GeV Pb+Pb collisions
Nucl. Phys. 715 (2003) 579-582c

[134] Nikolenko, D.M. *et al.*; Jager, C.W. de; Vries, H. de,
Measurement of the tensor analyzing powers T_{20} and T_{21} in elastic electron-deuteron scattering
Phys. Rev. Lett. 90 (2003) 072501

[135] Nikolenko, D.M. *et al.*; Vries, H. de
Measurement of tensor analyzing power in elastic electron-deuteron scattering at momentum transfer range 2.8-4.6 fm^{-1}.
Nucl. Phys. 721 (2003) 409-412C

[136] Putte, M.J.J. van den *et al.*
The Amsterdam quintuplet nuclear microprobe
Nucl. Instr. Meth. B 210 (2003) 21-26

[137] Riccioni, F.
Truncations of the D9-brane action and type-I strings
Phys. Lett. B 560 (2003) 223-231

[138] Wapstra, A.H. *et al.*
The AME2003 atomic mass evaluation (I). Evaluation of input data, adjustment procedures
Nucl. Phys. 729 (2003) 129-336

[139] West, J.B. *et al.*; Hansen, J.E.
Revised interpretation of the photoionization of Cr+ in the 3p excitation region
J. Phys. B 36 (2003) L327-L333

Theory

[140] Banfi, A.; Marchesini, G.; Smye, G.E.
Azimuthal correlation in DIS
Nucl.Phys. B (Proc.Suppl.) 121: (2003) 137-140

[141] Eynck, T.O.; Laenen, Eric; Magnea, Lorenzo
Exponentiation of the Drell-Yan cross section near partonic threshold in the DIS $\overline{MS}$-schemes
JHEP (2003) 06057

[142] Groot Nibbelink, S.; Nyawelo, T.S.; Riccioni, F.; Holten, J.W. van
Singular supersymmetric sigma models
Nucl. Phys. B 663 (2003) 60-78

[143] Heide, J. van der *et al.*; Lutterot, M.; Koch, J.H.
The pion form factor in improved lattice QCD
Phys. Lett. B 566 (2003) 131-136

[144] Kidonakis, N.; Laenen, E.; Moch, S.; Vogt, R.
Threshold effects in charm hadroproduction
Phys. Rev. D 67 (2003) 074037

[145] Kidonakis, N.; Laenen, E.; Moch, S.; Vogt, R.
Understanding bottom production
Nucl. Phys. 715 (2003) 549-552c

[146] Nyawelo, T.S.
T Supersymmetric hydrodynamics
Nucl. Phys. B 672 (2003) 87-100

[147] Nyawelo, T.S.; Holten, J.W. van; Groot Nibbelink, S.
Relativistic fluid mechanics, Kaehler manifolds and supersymmetry
Phys. Rev. D 68 (2003) 125006

[148] Riccioni, F.
Truncations of the D9-brane action and type-I strings
Phys. Lett. B560 (2003) 223-231

[149] Sousa, N.; Schellekens, A.N.
Orientation matters for NIMreps
Nucl. Phys. B 653 (2003) 339-368

[150] Vermaseren, J.A.M.
Tuning FORM with large calculations
Nucl. Phys. B (Proc. Suppl.) 116 (2003) 343-347

[151] Vermaseren, J.A.M.; Moch, S.; Vogt, A.
First results for three-loop deep-inelastic structure functions in QCD
Nucl. Phys. B (Proc. Suppl.) 116 (2003) 100-104

ZEUS

[152] S. Chekanov *et al.*; N. Coppola; S. Grijpink; E. Koffeman; P. Kooijman; E. Maddox; A. Pellegrino; S. Schagen; H. Tiecke; J.J. Velthuis; L. Wiggers; E. de Wolf; ZEUS Collaboration
Measurement of the open-charm contribution to the diffractive proton structure function
Nucl. Phys. B 672 (2003) 3-35

[153] S. Chekanov *et al.*; N. Coppola; S. Grijpink; E. Koffeman; P. Kooijman; E. Maddox; A. Pellegrino; S. Schagen; H. Tiecke; J.J. Velthuis; L. Wiggers; E. de Wolf; ZEUS Collaboration
Measurement of high-Q^2 charged current cross sections in e+p deep inelastic scattering at HERA
Eur. Phys. J. C32 (2003) 1-16

[154] S. Chekanov *et al.*; N. Coppola; S. Grijpink; E. Koffeman; P. Kooijman; E. Maddox; A. Pellegrino; S. Schagen; H. Tiecke; J.J. Velthuis; L. Wiggers; E. de Wolf; ZEUS Collaboration
Measurement of deeply virtual Compton scattering at HERA
Phys. Lett. B 573 (2003) 46-62

[155] S. Chekanov *et al.*; N. Coppola; S. Grijpink; E. Koffeman; P. Kooijman; E. Maddox; A. Pellegrino; S. Schagen; H. Tiecke; J.J. Velthuis; L. Wiggers; E. de Wolf; ZEUS Collaboration
Jet production in charged current deep inelastic e^+p scattering at HERA
Eur. Phys. J. C 31 (2003) 149-164

[156] S. Chekanov *et al.*; N. Coppola; S. Grijpink; E. Koffeman; P. Kooijman; E. Maddox; A. Pellegrino; S. Schagen; H. Tiecke; J.J. Velthuis; L. Wiggers; E. de Wolf; ZEUS Collaboration
A search for resonance decays to lepton+jet at HERA and limits on leptoquarks
Phys. Rev. D 68 (2003) 052004

[157] S. Chekanov *et al.*; N. Coppola; S. Grijpink; E. Koffeman; P. Kooijman; E. Maddox; A. Pellegrino; S. Schagen; H. Tiecke; J.J. Velthuis; L. Wiggers; E. de Wolf; ZEUS Collaboration
Dijet angular distributions in photoproduction of charm at HERA
Phys. Lett. B 565 (2003) 87-10

[158] S. Chekanov *et al.*; N. Coppola; S. Grijpink; E. Koffeman; P. Kooijman; E. Maddox; A. Pellegrino; S. Schagen; H. Tiecke; J.J. Velthuis; L. Wiggers; E. de Wolf; ZEUS Collaboration

Search for single-top production in ep collisions at HERA
Phys. Lett. B 559 (2003) 153 - 170

[159] S. Chekanov *et al.*; N. Coppola; S. Grijpink; E. Koffeman; P. Kooijman; E. Maddox; A. Pellegrino; S. Schagen; H. Tiecke; J.J. Velthuis; L. Wiggers; E. de Wolf; ZEUS Collaboration
Scaling violations and determination of α_s from jet production in γp interactions at HERA
Phys. Lett. B 560 (2003) 7-23

[160] S. Chekanov *et al.*; N. Coppola; S. Grijpink; E. Koffeman; P. Kooijman; E. Maddox; A. Pellegrino; S. Schagen; H. Tiecke; J.J. Velthuis; L. Wiggers; E. de Wolf; ZEUS Collaboration
Measurement of subjet multiplicities in neutral current deep inelastic scattering at HERA and determination of α_s
Phys. Lett. B 558 (2003) 41-58

[161] S. Chekanov *et al.*; N. Coppola; S. Grijpink; E. Koffeman; P. Kooijman; E. Maddox; A. Pellegrino; S. Schagen; H. Tiecke; J.J. Velthuis; L. Wiggers; E. de Wolf; ZEUS Collaboration
Measurement of event shapes in deep inelastic scattering at HERA
Eur. Phys. J. C 27 (2003) 531-545

[162] S. Chekanov *et al.*; N. Coppola; S. Grijpink; E. Koffeman; P. Kooijman; E. Maddox; A. Pellegrino; S. Schagen; H. Tiecke; J.J. Velthuis; L. Wiggers; E. de Wolf; ZEUS Collaboration
Observation of the strange sea in the proton via inclusive c-meson production in neutral current deep inelastic scattering at HERA"
Phys. Lett. B 553 (2003) 141-158

[163] S. Chekanov *et al.*; N. Coppola; S. Grijpink; E. Koffeman; P. Kooijman; E. Maddox; A. Pellegrino; S. Schagen; H. Tiecke; J.J. Velthuis; L. Wiggers; E. de Wolf; ZEUS Collaboration
Study of the azimuthal asymmety of jets in neutral current deep inelastic scattering at HERA
Phys. Lett. B 551 (2003) 3-4

[164] S. Chekanov *et al.*; N. Coppola; S. Grijpink; E. Koffeman; P. Kooijman; E. Maddox; A. Pellegrino; S. Schagen; H. Tiecke; J.J. Velthuis; L. Wiggers; E. de Wolf; ZEUS Collaboration
Leading proton production in e^+p collisions at HERA
Nucl. Phys. B 658 (2003) 3-46

[165] S. Chekanov *et al.*; N. Coppola; S. Grijpink; E. Koffeman; P. Kooijman; E. Maddox; A. Pellegrino; S. Schagen; H. Tiecke; J.J. Velthuis; L. Wiggers; E. de Wolf; ZEUS Collaboration
Measurement of high-Q^2 e^-p neutral current cross sections at HERA and the extraction of xF_3
Eur. Phys. J. C 28 (2003) 2, 175-201

[166] S. Chekanov *et al.*; N. Coppola; S. Grijpink; E. Koffeman; P. Kooijman; E. Maddox; A. Pellegrino; S. Schagen; H. Tiecke; J.J. Velthuis; L. Wiggers; E. de Wolf; ZEUS Collaboration
A ZEUS next-to-leading-order QCD analysis of data on deep inelastic scattering
Phys. Rev. D 67 (2003) 012007

[167] L.A.T. Bauerdick *et al.*
Beam test of silicon strip sensors for the ZEUS micro vertex detector
Nucl. Instr. Meth. A 501 (2003) 340

[168] D. Dannheim *et al.*
Design and tests of the silicon sensors for the ZEUS micro vertex detector
Nucl. Instr. Meth. A 505 (2003) 663

2 PhD Theses

[1] Garutti, E.
Nuclear effects in semi-inclusieve deep-inelastic scattering off ^{84}Kr and other nuclei
Universteit van Amsterdam, 14 Mar. 2003

[2] Visser, E.J.
Muon tracks through ATLAS
Katholieke Universiteit Nijmegen, 21 Mar. 2003

[3] Mevius, M.
Beauty at HERA-B - Measurement of the $b\overline{b}$ production cross section in pN collisions at $\sqrt{s} = 41.6$ GeV
Universiteit Utrecht, 2 Apr., 2003.

[4] Willering, H.W.,
The 2H(e,e'p)n reaction at large energy transfers
Universiteit Utrecht, 7 Apr. 2003

[5] Velthuis, J.J.
Radiation hardness of the ZEUS MVD frontend chip and strangeness production in ep scattering at HERA
Universiteit van Amsterdam, 9 Apr. 2003.

[6] Peeters, S.J.M.,
The ATLAS semiconductor tracker endcap
Universiteit van Amsterdam, 15 Apr. 2003

[7] Blom, H.M.
Single W measurement at DELPHI
Universiteit van Amsterdam, 22 Apr. 2003

[8] Wilkens, H.G.S.
Experimental study of high energy muons from Extensive Air Showers in the energy range 100 TeV to 10 PeV
Katholieke Universiteit Nijmegen, 19 May 2003

[9] Leeuwen, M. van
Kaon and open charm production in central lead-lead collisions at the CERN SPS
Universiteit Utrecht, 19 May 2003

[10] Schillings, E.
Λ Polarization in Lead-Lead Collisions
Universiteit Utrecht, 28 May 2003

[11] Heesbeen, D.
Quasi-real photo-production of hyperons on polarized ^{1,2}H targets
Rijksuniversiteit Groningen, 06 Jun. 2003

[12] Vos, M.A.
The ATLAS inner tracker and the detection of light supersymmetric Higgs bosons
Universiteit Twente, 1 Oct. 2003

[13] Sousa, Nuno Miguel Marques de
Open descendants at c = 1;
Katholieke Universiteit Nijmegen, 13 Oct. 2003

[14] Hierck, R.
Optimisation of the LHCb detector
Vrije Universiteit Amsterdam, 21 Oct., 2003.

[15] Peters, O.,
Measurement of the b-jet cross section at $\sqrt{s} =$ 1.96 TeV
Universiteit van Amsterdam, 24 Oct. 2003

[16] Scholte, R.C.
Data read-out and Bc production in ATLAS
Universiteit Twente, 19 Nov. 2003

[17] Eynck, T.O.
Soft gluons and hard scales in QCD - heavy quarks at finite and all orders;
Universiteit Utrecht, 20 Nov. 2003

[18] Buuren, L.D. van,
Double-polarized electron-proton scattering and the N-delta transition
Vrije Universiteit Amsterdam, 25 Nov. 2003

3 Invited Talks

ALICE

[1] Peitzmann T.
Lessons from SPS and future perspectives
GSI Future Workshop 2003, Darmstadt.

[2] Peitzmann T.
Heavy Ion Physics in the RHIC Era - Results from the PHENIX Experiment
Physics Colloquium, Heidelberg University, 3 Feb 2003

[3] Peitzmann T.
The Search for the Quark-Gluon-Plasma at the Relativistic Heavy Ion Collider
ITP Theory Colloquium, Utrecht University, 5 Feb. 2003.

[4] Peitzmann T.
The Search for the Quark-Gluon-Plasma at the Relativistic Heavy Ion Collider
SRON Colloquium, Utrecht University, 13 Feb. 2003.

[5] Snellings R.
Heavy-Ion Physics at RHIC
Cornell, Ithaca, New York, USA, 2003

[6] Snellings R.
Event anisotropy at RHIC 'Rhein-Necker-Main' seminar at GSI, Germany, 2003.

[7] Snellings R.
Anisotropic flow and azimuthally sensitive HBT at RHIC
CERN Heavy Ion Forum, Geneva, Switzerland, 2003.

[8] Snellings R.
Heavy-Ion Physics
XXIII Physics in Collision, DESY, Zeuthen, Germany, 2003.

[9] Snellings R.
Physics Status and Goals of Relativistic Heavy Ion Experiments Beyond the Desert '03
Castle Ringberg, Tegernsee, Germany, 2003.

[10] Snellings R.
Flow in STAR
19th Winter Workshop on Nuclear Dynamics Breckenridge, Colorado, USA, 2003.

[11] Van Eijndhoven N.J.A.M.: *Astrophysics report of the Astro-Alice workshop*
Alice physics forum, CERN, Geneva, 17 juni 2003.

[12] Peitzmann T.
Hard Scattering and Hydrodynamics - Heavy Ion Reactions Studied at the Relativistic Heavy Ion Collider
Lecture in the European Graduate School "Complex Systems of Hadrons and Nuclei", Giessen University, 20 Feb. 2003.

[13] Peitzmann T.
Influence of Hydrodynamics on the Interpretation of the High pT Hadron Suppression at RHIC
STAR Collaboration Meeting, MSU East Lansing

[14] Peitzmann T.: *Ultrarelativistic Heavy Ion Collisions - the search for the quark gluon plasma*
Summer School on Particle and Nuclear Astrophysics, Nijmegen, 18-19 Aug. 2003.

[15] Snellings R.
v2 measurements at RHIC
Transverse Dynamics at RHIC, Brookhaven, USA, 2003

[16] Van Eijndhoven N.J.A.M.
The Astrophysics Arena
Astro-Alice workshop, CERN, Geneva, 15 Jun. 2003.

[17] Van Eijndhoven N.J.A.M.
The Alice (Physics Analysis) Toolbox
Offline analysis workshop, Mons, Belgium, 16-22 Oct. 2003.

[18] Van Eijndhoven N.J.A.M.
The AliRoot Offline Framework
Workshop on simulation and analysis techniques, Uppsala, Sweden, 9-14 november 2003.

[19] Mischke A.
Lambda and PHI production in heavy ion collisions
Erice workshop.

[20] Mischke A.
Strangeness production in heavy ion collisions at SPS energies
European Physical Society, Aken, Jul. 17-23 2003.

[21] Mischke A.
Recent results from STAR
NNV fall meeting, Lunteren, Oct. 10, 2003

ANTARES

[22] A.J. Heijboer
ICRC 2003, Tsukuba, Japan

[23] M.C. Bouwhuis
UHENT workshop 2003, Chiba, Japan

[24] A.J. Heijboer
UHENT workshop 2003, Chiba, Japan

[25] A.J. Heijboer
VLVNT workshop 2003, NIKHEF, Amsterdam

[26] M. de Jong
VLVNT workshop 2003, NIKHEF, Amsterdam

[27] M. de Jong
FANTOM, Amsterdam

[28] M. de Jong
Wessel Knoops genootschap, Arnhem

ATLAS

[29] P.W. Balm
Towards CP violation results from DØ
International Europhysics Conference on High Energy Physics, Jul. 2003

[30] H.P. Beck *et al.*
The base-line DataFlow system of the ATLAS Trigger & DAQ
13th IEEE-NPSS Real Time Conference 2003 RT 03, Montreal, Canada ,18 - 23 May 2003

[31] Barisonzi, M. *et al.*
The MROD: the read out driver for the ATLAS MDT Muon Precision Chambers
Proceedings 8th Workshop on Electronics for LHC Experiments, Colmar, France, 9-13 Sep. 2002

[32] H. Boterenbrood *et al.*
Design and Implementation of the ATLAS Detector Control System
13th IEEE-NPSS Real Time Conference 2003 RT 03 ,Montreal, Canada ,18 - 23 May 2003

[33] R. Cranfield *et al.*(J. Vermeulen)
Computer modeling the ATLAS Trigger/DAQ system performance
13th IEEE-NPSS Real Time Conference 2003 RT 03 ,Montreal, Canada ,18 - 23 May 2003

[34] M. Abolins *et al.*(M. Barisonzi, H. Boterenbrood, P. Jansweijer, G. Kieft, J. Vermeulen)
The Second Level Trigger of the ATLAS Experiment at CERN's LHC
IEEE Nuclear Science Symposium and Medical Imaging Conference, Part 1, NSS-MIC 2003 ,Portland, OR, USA ,19 - 24 Oct 2003

[35] H. Boterenbrood, B. Hallgren
The Development of Embedded Local Monitor Board (ELMB)
9th Workshop On Electronics For Lhc Experiments LECC 2003 ,Amsterdam, The Netherlands ,29 Sep - 03 Oct 2003

[36] M. Abolins *et al.*(M. Barisonzi, H. Boterenbrood, P. Jansweijer, G. Kieft, J. Vermeulen)
The Baseline DataFlow System of the ATLAS Trigger & DAQ
9th Workshop On Electronics For LHC Experiments - LECC 2003 ,Amsterdam, The Netherlands ,29 Sep - 03 Oct 2003

[37] G. Lehmann *et al.*(M. Barisonzi, H. Boterenbrood, P. Jansweijer, G. Kieft, J. Vermeulen)
The DataFlow System of the ATLAS Trigger and DAQ
2003 Conference for Computing in High-Energy and Nuclear Physics CHEP 2003 ,La Jolla, CA, USA ,24 - 28 Mar 2003

[38] S. Gadomski *et al.*(M. Barisonzi, H. Boterenbrood, P. Jansweijer, G. Kieft, J. Vermeulen)
Experience with multi-threaded C++ applications in the ATLAS DataFlow software
2003 Conference for Computing in High-Energy and Nuclear Physics CHEP 2003 ,La Jolla, CA, USA ,24 - 28 Mar 2003

[39] S. Bentvelsen
Tests of the Standard Model at Particle Colliders
Colloquium Ehrenfestii, Leiden, Feb 5th, 2003

[40] S. Bentvelsen
'Velvet revolution' in neutrino physics
Nijmegen Colloquium, Nijmegen, Dec 2003

[41] A.P. Colijn
X-Ray Computed Tomography
Nikhef Colloquium, Amsterdam, Dec 12, 2003

[42] F. Linde
The Large Hadron Collider & the Atlas Experiment
Colloquium TUE, Eindhoven, Oct 28, 2003

B-Physics

[43] S. Klous
The LHCb Vertex Detector
Vertex 2003, Cumbria, United Kingdom, Sep. 14-19, 2004.

[44] G. Raven
sin(2beta): Status and prospects
Invited talk at 2nd Workshop on the CKM Unitarity Triangle, Durham, England, 5-9 Apr. 2003.

[45] N. van Bakel
Vertex detection in LHCb
SLAC Experimental Seminar Thursday, Dec. 4, 2003

[46] N. van Bakel
Vertex detection in LHCb
Research Progress Meeting at LBNL (Lawrence Berkeley National Lab) Tuesday, December 9, 2003

[47] M.Baak,
Current Status and Prospects for sin(2beta+gamma) with fully reconstructed B to D(*)h (h=pi,rho,a1)
SLAC CKM angles workshop (2 Oct. 2003).

[48] M. Baak
Impact of Tag Side Interference on sin(2beta+gamma) measurements
APS, division particles and fields(Philadelphia), 8 Apr 2003

[49] M. Baak
$B \rightarrow$ J/psi K wrong flavour amplitude*
APS, division particles and fields(Philadelphia), 8 Apr 2003

[50] G. Raven
LHCb reoptimization and tracking performance
Beauty 2003 (CMU, Pittsburgh), 14-18 Oct. 2003:

[51] G. Raven
CP violation: the difference between matter and antimatter
VU studiedag (Amsterdam), 8 Oct. 2003.

[52] J. van den Brand
Elementary Particle Physics: Perspectives
VU studiedag (Amsterdam), 8 Oct. 2003.

[53] G. Raven
CP Violation
Joint Belgian-Dutch-German Graduate school (Bonn), 22-25 September 2003.

[54] G. Raven
From observerving matter-antimatter asymmetries to testing the unitarity triangle
KVI Colloquium (KVI, Groningen), 24 Jun. 2003.

[55] A. Pellegrino
The outer tracker of the LHCb tracking system
2nd Workshop of NSFC-CERN, Oct. 30, 2003, Weihai, China

[56] M. Merk
Performance Studies for the LHCb Experiment
19-th Int Workshop on Weak Interactions and neutrinos Lake Geneva, Wisconsin, USA, 6-11 Oct. 2003

[57] J. van Hunen
LHCb performance for Bs -¿ J/psi phi and Bd -¿ J/psi KS decays
Physics at the LHC, Prague, Czech Republic, Jul. 11, 2003

[58] J. van Tilburg
LHCb Tracking Performance
IVth International Symposium on LHC Physics and Detectors, Fermilab, Chicago, 3 May 2003

[59] T. Bauer
Status of the HERA-B pentaquark search
Pentaquark Forum at Desy, Nov. 25, 2003

[60] A. Sbrizzi
Physics Results at HERA-B
Lunteren, NNV Meeting 2003

DATAGRID

[61] K. Bos
DataGrid Infrastructure and First Results
Vrije Universiteit van Brussel, 20 Jan. 2003

[62] K. Bos
D0 and NIKHEF
Fermilab, Chicago, Ill., USA, 12 Feb. 2003

[63] K. Bos
The DataGrid Project
KNMI, De Bilt, 17 Apr. 2003

[64] K. Bos
D0 Computing in the LCG Environment
Beaune, France, 17 Jun. 2003

[65] I. Augustin *et al.*; K. Bos; J. Templon
HEP applications evaluation of the EDG testbed and middleware
Computing in High Energy and Nuclear Physics, CHEP03, La Jolla, CA, USA, 24-28 Mar. 2003

[66] D. Bonacorsi *et al.*; J. Templon,
Running CMS software on GRID testbeds
Computing in High Energy and Nuclear Physics, CHEP03, La Jolla, CA, USA, 24-28 Mar. 2003

[67] D.L. Groep
DutchGrid
Vrije Universiteit van Brussel, 20 Jan. 2003

[68] R. Alfieri *et al.*; D.L. Groep; M. Steenmakkers
Managing Dynamic User Communities in a Grid of Autonomous Resources.
Computing in High Energy and Nuclear Physics, CHEP03, La Jolla, CA, USA, 24-28 Mar. 2003

[69] D.L. Groep
Grid Security for Site Authorization in EDG
HEPiX/HEPNT Conference, Amsterdam, NL, 20 May 2003

[70] D.L. Groep
VOMS and LCMAPS: on Global Permissions and Local Credentials
6th EU DataGrid Conference, Barcelona, SP, 12-15 May 2003

[71] D.L. Groep
Grids - achtergronden en praktijk in het EU DataGrid
ICT Kenniscongres 2003, The Hague, NL, 5-6 Sep 2003

HERMES

[72] G. van der Steenhoven
Summary of the working group on spin physics
Summary talk at the workshop on Deep Inelastic Scattering (DIS03), St. Petersburg, Russia, Apr. 27, 2003

[73] G. van der Steenhoven
The quark-gluon structure of hadrons
Opening talk at the Euresco Conference on Electromagnetic Interactions with Nucleons and Nuclei, Santorini, Greece, Oct. 7, 2003

[74] E. Garutti
Electroproduction of $f_0(980)$ Scalar Mesons at HERMES
Workshop on Deep Inelastic Scattering (DIS03), St. Petersburg, Russia, Apr. 24-29, 2003

[75] V. Mexner
Contribution of gluons to the nucleon spin
Symposium on Quarks in Hadrons and Nuclei II, Oberwoelz, Austria, Sep. 15-20, 2003

[76] P.B. van der Nat
Attenuation of hadrons in nuclei
Int. Symposium on Multiparticle Dynamics (ISMD), Cracow, Poland, Sep. 5-11, 2003

[77] G. van der Steenhoven
QCD and the origin of the proton spin
Natuurkundig colloquium, Rijksuniversiteit Groningen, Mar. 6, 2003

LEP-DELPHI

[78] J. Timmermans
Recent LEP results
XVIIth Int. Workshop on High Energy Physics and Quantum Field Theory, Samara-Saratov, Russia, Sep. 2003

LEP-L3

[79] P. de Jong
Final state correlations at LEP2: Bose Einstein correlations and the W mass
Int. Europhysics Conf. on High Energy Physics, Aachen, 17–23 Jul. 2003

[80] W. Kittel
Recent Developments on Correlations and Fluctuations
University of Bologna and INFN, Seminar Jun. 25, 2003

[81] W. Kittel
Festvortrag on Multiparticle Dynamics
Festkolloquium Prof. N.Schmitz, Oct. 28, 2003

[82] C. Timmermans
Results from the L3+C detector
Int. Europhysics Conf. on High Energy Physics, Aachen, 17–23 July 2003

Transition Program
(AmPS, CHORUS, Medipix)

[83] J.H.R. Schrader, E.A.M. Klumperink, J.L. Visschers, B. Nauta
Data communication in Read-Out systems: How fast can we go over copper wires?
Int. Workshop on Radiation Imaging Devices, Riga Latvia, Sep. 2003

[84] D. Vavrik, J. Jakubek, S. Pospisil, J.L. Visschers
Present Status of X-ray Dynamic Defectoscopy
NSS-IEEE Portland, Oct. 2003, USA.

[85] A. Fornaini, T. Boerkamp, R. De Oliveira, J.L. Visschers
A Tiled Array of Hybrid Pixel Detectors for X-ray Imaging
NSS-IEEE Portland, Oct. 2003, USA.

[86] J.L. Visschers
Workshop Summary Talk
Int. Workshop on Radiation Imaging Devices, Riga, Latvia, Sep. 2003

[87] L. Lapikás
Spectroscopic Strength and the Reaction (e,e'p) : an overview
Workshop on Contributions of Short- and Long-range Correlations to Nuclear Binding and Saturation, Trento (Italy), Jun. 2003

[88] E. Jans
Results from ^{3}He(e,e'pp) and ^{3}He(e,e'pn) experiments at AmpS and MAMI
6th Workshop on electromagnetically induced Two-Hadron Emission, Pavia (Italy), Sep. 2003

[89] C. Barbieri, W.H. Dickhoff, L. Lapikás, H. Müther and D. Rohe
Rescattering contributions to final-state interactions in (e,e'p) reactions
Second Int. Conf. on Nuclear and Particle Physics with CEBAF at JLab (NAPP 2003), Dubrovnik, 2003.

[90] P.J. Barneo González *et al.*
Investigation of the electron-induced proton-neutron knockout reaction in ^{3}He
Proc. Int. Workshop on Probing Nucleons and Nuclei via the (e,e'p) Reaction, Grenoble, France, 2003.

[91] C. Barbieri and L. Lapikás
Rescattering contributions to final-state interactions in (e,e'p) reactions at high (p_m,E_m)
Proc. 6^{th} Workshop on Electromagnetically induced Two-hadron Emission, Pavia, Italy, 2003.

Theory

[92] A. Banfi
Jet observables in hadronic dijet production
DIS 2003, St. Petersburg (Russia)

[93] A. Banfi
Automated resummation of jet observables in QCD
23rd Int. Symp. on Multiparticle Dynamics (ISMD 2003) Cracow (Poland)

[94] Bentvelsen, S.; Jong, P. de; Koch, J.; Laenen, E. (eds.)
Proc. 31st Int. Conference on High-Energy Physics (ICHEP 2002)
(North Holland, Amsterdam; 2003); Nucl. Phys. B, Proc. Suppl. 117 (2003)

[95] T.O. Eynck, E. Laenen, L. Magnea
Exponentiation ar partonic threshold for Drell-Yan cross section
DIS 2003, St. Petersburg (Russia)

[96] J.W. van Holten
Kaehler manifolds and supersymmetry
Lectures 43rd Cracow School of Theoretical Physics, Zakopane, Poland, Jun. 2003

[97] E. Laenen
Top quark production dynamics
38th Rencontres de Moriond, Les Arcs (France)

[98] S. Moch, J.A.M.Vermaseren, A. Vogt,
Three loop results and soft gluon efects in DIS
DIS 2003, St. Petersburg (Russia)

[99] J. van der Heide
The pion form factor from first principles
10th Int. Conf. on Hadron Spectroscopy (Hadron 03) Aschaffenburg (Germany)

[100] J.W. van Holten
Singular supersymmetric sigma models
Workshop *Beyond the standard model* Bad Honnef (Germany)

[101] J.W. van Holten
Kosmische straling en deeltjesfysica
Gastlezingen op 5 middelbare scholen in het kader van het HISPARC project

[102] A.N. Schellekens
Orientation matters for NIMreps
Workshop *Beyond the standard model* Bad Honnef (Germany)

ZEUS

[103] M. Vasquez
Inclusive Jet cross sections
EPS-HEP03, 07/2003

[104] A. Pellegrino
Structure functions
Int. Workshop on QCD theory and experiment, 06/2003

[105] E. Maddox
Analysis of the ZEUS 2002/2003 data using the new vertex detector
NNV Najaarsvergadering, 10/2003

[106] E.Maddox
Vertex Fitting
DESY student Seminar, 05/2003

[107] N. Coppola
Charm Production at HERA
Vergadering Italiaanse natuurkundige vereniging, 05/2003.

[108] J. Velthuis
Radiation hardness of silicon chips
Seminar Univ. Bonn, 02/2003

F Resources and Personnel

1 Resources

In 2003 the NIKHEF income was 19.6 million Euro. The budget figures of the NIKHEF partners were: FOM-institute 12.6 M Euro, universities 4.0 M Euro of which 1.2 M Euro through the FOM working groups. A further 3.1 M Euro was contributed to the NIKHEF income of which 1.1 M Euro earmarked for the completion costs of Atlas. Expenses for the largest program, Atlas, consumed almost 30% of the total budget. Capital investments in 2003 (1.6 M Euro) were allocated for the Atlas, Alice and LHCb detectors and for the technical infrastructure of the institute (i.e. Transition Program).

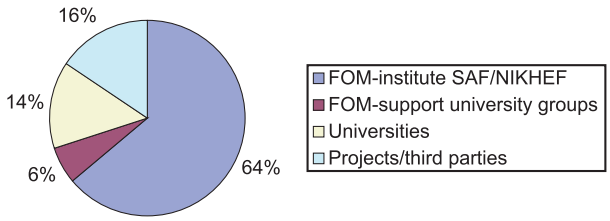

Figure 1.1: *Income 2003: 19.6 M Euro.*

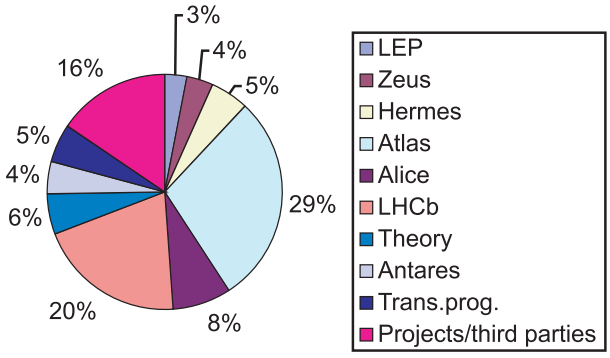

Figure 1.2: *Expenses 2003: 19.6 M Euro.*

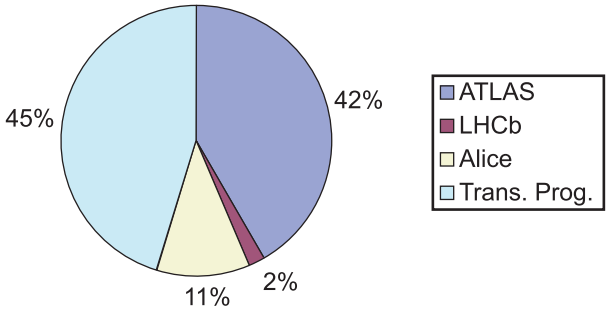

Figure 1.3: *Capital Investments 2003: 1.6 M Euro.*

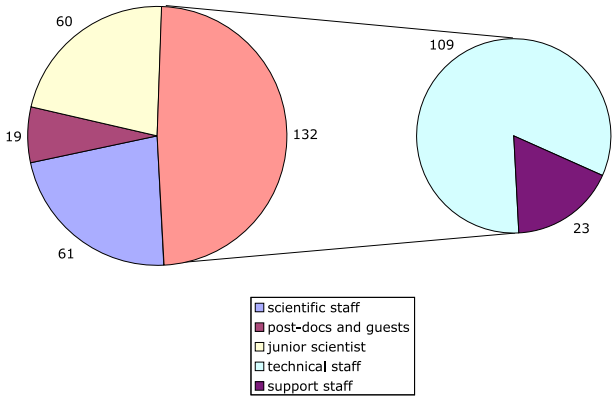

Figure 1.4: *NIKHEF personnel as of December 31, 2003.*

2 Membership of Councils and Committees during 2003

NIKHEF Board

F.T.M. Nieuwstadt (FOM, chairman)
K.H. Chang (FOM)
P.F. van der Heijden (UvA)
S. Groenewegen (VU)
S.E. Wendelaar Bonga (KUN)
J.G.F. Veldhuis (UU)
H.G. van Vuren (secretary, FOM)

Scientific Advisory Committee NIKHEF

G. Goggi (CERN)
K. Pretzl (Bern)
G. Ross (Univ. Oxford)
M. Spiro (IN2P3)
J. Stachel (Univ. Heidelberg)
J. Dainton (Univ. Liverpool)

NIKHEF Works Council

P. de Jong (chairman)
L. Wiggers (2nd chairman, COR representative)
G. Venekamp (1st secretary)
R. Kluit (2nd secretary)
A. Boucher
H. Boer Rookhuizen (COR representative)
F. Bulten
S. Muijs
P.B. van der Nat (COR representative)
K. Rijksen
F. Schimmel

Wetenschappelijke Advies Raad NIKHEF

J.W. van Holten (chairman)
P. de Jong (observer from works council)
M. de Jong
F. Linde
K.J.F Gaemers
G. van der Steenhoven
S.J. de Jong
A.J. van Rijn
J.J. Engelen
R. Snellings
J.F.J. van den Brand
W. Hoogland

FOM Board

S.J. de Jong

Raad voor de Natuur- en Sterrenkunde

J.J. Engelen

Contactcommissie in CERN aangelegenheden

J.J. Engelen
K.J.F. Gaemers
G. van Middelkoop (until Dec. 2003)
S.J. de Jong
R. Kamermans

Stichting voor de Hoge-energiefysica

J.J. Engelen (chairman)
A.J. van Rijn (treasurer)

Stichting beta-plus

J.J. Engelen

NNV Sectie H

K.J.F. Gaemers

NNV Sectie Onderwijs en Communicatie

S.J. de Jong (vice-chairman)

Restricted ECFA

J.J. Engelen

ECFA

K.J.F. Gaemers
G. van Middelkoop
S.J. de Jong

Linear Collider Steering Group in Organisational Matters

J.J. Engelen

Extended Scientific Council DESY

J.J. Engelen

Astroparticle Physics European Coordination (ApPEC) Steering Committee

J.J. Engelen (dep. chairman)

INFN Comitato di Valutatione Interna

J.J. Engelen

OECD Global Science Forum's Consultative Group on High Energy Physics

J.J. Engelen

LHCC-CERN

H. Tiecke

SPSC-CERN

M. de Jong

NuPECC

G. van der Steenhoven

EPAC Organizing Committee and EPAC Scientific Committee

G. Luijckx

Beleidsadvies college KVI

G. Luijckx
P.J.G. Mulders

Wetenschappelijke Adviescommissie (WAC) KVI

G. van der Steenhoven

Physical Review Letters

G. van der Steenhoven (Divisional Associate Editor)

Nuclear Physics News International

G. van der Steenhoven (Correspondent)

Scientific Committee Frascati Laboratory

G. van Middelkoop

Scientific Council JINR, Dubna

G. van Middelkoop

Scientific Advisory Committee DFG Hadronen Physik

J.H. Koch

Program Advisory Committee, Jefferson Laboratory

E. Jans

NNV Board

J. Konijn (treasurer)
E. de Wolf

Peer Review Committee of the Astro-particle Physics European Coordination

M. de Jong

Stichting Physica Board

G. van der Steenhoven
J. Konijn

Stichting Conferenties en Zomerscholen over de Kernfysica

G. van der Steenhoven
J. Konijn
G. van Middelkoop
P.J.G. Mulders

Summerschool on Particle and Nuclear Astrophysics, Nijmegen 2003

P.J.G. Mulders (chair)
G. van der Steenhoven

High Energy Physics Computing Coordination Committee (HEPCCC)

A.J. van Rijn

Advisory Comittee of CERN Users (ACCU)

M. Merk

Gebiedsbestuur Exacte Wetenschappen NWO

R. Kamermans (vice-chair)

NWO-GBE VENI commissie

S.J. de Jong (chairman)

Standing Committee for Physical and Engineering Sciences of the European Science Foundation

R. Kamermans

Nederlands Tijdschrift voor Natuurkunde, redactie

P.J.G. Mulders
S.J. de Jong

Computer Algebra Nederland, Board

J. Vermaseren

Linear Collider workshop 2003 Amsterdam, Local Organizing Committee

J. Timmermans (chair)
P. Kluit (secretary)
A.J. van Rijn (finances)
F. Linde
S.J. de Jong
M. Pohl

FOm/v committee

E. de Wolf (chair)

Board GridForum Nederland

A.J. van Rijn (treasurer)

Steering Group NCF Grid infrastructure project

A.J. van Rijn (chairman)

Other committees

DIS03 (St. Petersburg 2003): G. van der Steenhoven (convenor spin physics)
ESRF Purchasing committee: G. Luijckx (advisor for NWO)
ACAT 2003 advisory committee: J. Vermaseren
ECOS-exact, KNAW: G. van Middelkoop
IWORID Scientific Committee: J.L. Visschers
Medipix2: J.L. Visschers (deputy spokesperson)
Second workshop on the CKM Unitarity triangle 2003 Durham, Local Organizing Committee: P. Kluit
HTASC: E. de Wolf
EGEE Project Technical Forum: J. Templon, D. Groep
EGEE Middleware Design Team: D. Groep
LCG Phase 2 Planning Team: K. Bos
WCW Board: A.J. van Rijn
Steering group Development Science Park Amsterdam: A.J. van Rijn

3 Personnel as of December 31, 2003

1. Experimental Physicists

Apeldoorn, Dr. G.W. van	UVA	B-Phys.
Baak, Drs. M.	VU	B-Phys.
Bai, Drs. Mw. Y.	FOM	Alice
Bakel, Drs. N.A. van	FOM	B-Phys.
Baldew, Drs. S.V.	GST	L-3
Balm, Drs. P.W.	FOM	ATLAS
Barisonzi, Drs. M.	UT	ATLAS
Barneo González, Drs. P.J.	FOM	Other Projects
Bauer, Dr. T.S.	FOM-UU	B-Phys.
Bentvelsen, Dr. S.C.M.	FOM	ATLAS
Berg, Drs. P.J. van den	FOM	ATLAS
Blekman, Drs.Mw. F.	FOM	ATLAS
Blok, Dr. H.P.	VU	HERMES.
Bobbink, Dr. G.J.	FOM	L-3
Bos, Dr. K.	FOM	ATLAS
Botje, Dr. M.A.J.	FOM	ALICE
Boudreault, Dr. G.	FOM	Other Projects
Bouwhuis, Drs. Mw. M.C.	FOM	ANTARES
Brand, Prof.dr. J.F.J. van den	VU	Other Projects
Bruin, Drs. R.	UVA	ANTARES
Bruinsma, Ir. P.J.T.	GST	ANTARES
Bulten, Dr. H.J.	FOM-VU	B-Phys.
Colijn, Dr. A.P.	FOM	ATLAS
Colnard, Drs. Mw. C.M.M.	FOM	ANTARES
Coppola, Dr. N.	FOM	ZEUS
Cornelissen, Drs. T.G.	FOM	ATLAS
Crijns, Dipl.Phys.F.J.G.H.	FOM-KUN	ATLAS
Dantzig, Dr. R. van	GST	Other Projects
Demey, Drs. M.	FOM	HERMES
Diddens, Prof.Dr. A.N.	GST	DELPHI
Dierckxsens, Drs. M.E.T.	FOM	L-3
Djordevic, Drs. M.	KUN	Other Projects
Dreschler, Drs. J.	FOM	HERMES
Duinker, Prof.dr. P.	GST	L-3
Eijk, Prof.dr. B. van	FOM	ATLAS
Eldik, Dipl. Phys. N. van	FOM	ATLAS
Engelbertink, Dr., G.A.P.	FOM	Other Projects
Engelen, Prof.dr. J.J.	UVA	DIR
Eyndhoven, Dr. N. van	FOM-UU	Other Projects
Fabbri, Dr. R.	FOM	HERMES
Ferreira Montenegro, Drs. Mw. J.	FOM	DELPHI
Filthaut, Dr. F.	KUN	ATLAS
Fornaini, Drs. A.	FOM	ATLAS
Galea, Mw. Drs. C.F.	FOM	ATLAS
Gorfine, Dr. G.	FOM	ATLAS
Graaf, Dr.Ir. H. van der	FOM	ATLAS
Grebenyuk, Drs. O.	FOM	ALICE
Griffioen, Prof.dr. K.A.	GST	HERMES
Grigorescu, Drs. G.T.	FOM	ZEUS
Grijpink, Drs. S.J.L.A.	GST	ZEUS
Groep, Dr. D.L.	FOM	Other Projects
Hartjes, Dr. F.G.	FOM	ATLAS
Heijboer, Drs. A.J.	UVA	ANTARES
Hesselink, Dr. W.H.A.	VU	HERMES
Hessey, Dr. N.P.	FOM	ATLAS
Hommels, Ir. L.B.A.	FOM	B-Phys.
Houben, Drs. P.W.	FOM	ATLAS
Hunen, Dr. J.J. van	FOM	B-Phys.
Jans, Dr. E.	FOM	AmPS-Phys.
Jong, Dr. M. de	FOM	ANTARES
Jong, Dr. P.J.	FOM	ATLAS
Jong, Prof.dr. S.J.	KUN	ATLAS
Kamermans, Prof.dr. R.	FOM-UU	ALICE
Keramidas, Drs. A.A.	FOM	ZEUS
Ketel, Dr. T.J.	FOM-VU	B-Phys.
Klok, Drs. P.F.	FOM-KUN	ATLAS
Klous, Drs. S.	FOM-VU	B-Phys.
Kluit, Dr. P.M.	FOM	ATLAS
Koffeman, Dr. Ir. Mw. E.N.	FOM	ZEUS
König, Dr. A.C.	KUN	ATLAS
Kooijman, Prof.dr. P.M.	UVA	ZEUS
Kuijer, Dr. P.G.	FOM	ALICE
Laan, Dr. J.B. van der	FOM	Other Projects
Lapikás, Dr. L.	FOM	HERMES
Laziev, Drs. A.E.	FOM-VU	HERMES
Linde, Prof.dr. F.L.	UVA	ATLAS
Luijckx, Ir. G.	FOM	ATLAS
Maas, Dr. R.	FOM	Other Projects
Maddox, Drs. E.	UVA	ZEUS
Massaro, Dr. G.G.G.	FOM	ATLAS
Merk, Dr. M.H.M.	FOM	B-Phys.
Metzger, Dr. W.J.	KUN	L-3
Mexner, Drs. Mw. I.V.	FOM-BR	HERMES
Middelkoop, Prof.dr. G. van	GST	Other Projects
Mischke, Dr. A.	FOM-UU	ALICE
Muijs, Mw. Dr., A.J.M.	FOM	ATLAS
Nardulli, Drs. J.	FOM-VU	B-Phys
Nat, Drs. P.B.	FOM	HERMES
Naumann, Drs. A.	FOM	ATLAS
Nooren, Dr. Ir. G.J.L.	FOM-UU	ALICE
Novak, Drs. T.	KUN	L-3
Peitzmann, Prof.dr. T.	UU	ALICE
Pellegrino, Dr. A.	FOM	B-Phys
Phaf, Drs. L.K.	FOM	ATLAS
Pohl, Prof.dr. M.	KUN	Other Projects
Putte, Dr. Ir. M.J.J. van den	FOM	Other Projects
Raven, Dr. H.G.	VU	B-Phys.
Reischl, Drs. A.J.	FOM	HERMES
Rens, Drs. B.A.P. van	FOM	ANTARES
Rijke, Drs. P. de	FOM-UU	ALICE
Sbrizzi, Drs. A.	FOM	B-Phys.
Schagen, Drs. S.E.S.	FOM	ZEUS
Schotanus, Dr. D. J.	KUN	L-3
Schrader, Ir. J.H.R.	FOM	Other Projects
Snellings, Dr. R.J.M.	FOM	ALICE
Snoek, Drs. Mw. H.L.	FOM	B-Phys.
Sokolov, Drs. A.	UU	ALICE
Steenhoven, Prof.dr. G. van der	FOM	HERMES
Steijger, Dr. J.J.M.	FOM	HERMES
Templon, Dr. J.A.	FOM	B-Phys
Tiecke, Dr. H.G.J.M.	FOM	ZEUS
Tilburg, Drs. J.A.N.	FOM	B-Phys.

Timmermans, Dr. C.W.J.P.	FOM	ATLAS
Timmermans, Dr. J.J.M.	FOM	DELPHI
Tvaskis, Drs. V.	VU	HERMES
Vankov, Drs. P.H.	FOM	B-Phys.
Vázquez Acosta, Dr. Mw. M.L.	FOM	ZEUS
Vermeulen, Dr.Ir. J.C.	UVA	ATLAS
Visschers, Dr. J.L.	FOM	Other Projects
Vos, Drs. M.A.	UT	ATLAS
Vreeswijk, Dr. M.	FOM	ATLAS
Vries, Drs. G. de	UU	ANTARES
Vries, Dr. H. de	FOM	B-Phys.
Wahlberg, Drs. H.	UU	B-Phys.
Wang, Drs. Q.	KUN	L-3
Wiggers, Dr. L.W.	FOM	ZEUS
Wilden, Dr. L.H.	FOM	B-Phys.
Wijngaarden, Drs. D.A.	GST	ATLAS
Witt Huberts, Prof.Dr. P.K.A.	FOM	ANTARES
Wolf, Dr. Mw. E. de	UVA	ZEUS
Woudstra, Dr. Ir. M.J.	FOM	ATLAS
Ybeles Smit, Drs. G.V.	FOM	HERMES
Zupan, Drs. M.	FOM	B-Phys.

2. Theoretical Physicists

Banfi, Dr. A.	FOM
Dijkstra, Drs. T.P.T.	FOM
Fuster, Drs. Mw. A.	GST
Gaemers, Prof.dr. K.J.F.	UVA
Gato-Rivera, Dr. Mw. B.	GST
Heide, Drs. J. van der	FOM
Holten, Prof.dr. J.W. van	FOM
Kleiss, Prof.dr. R.H.P.	KUN
Koch, Prof.Dr. J.H.	FOM
Koers, Drs. H.B.J.	UVA
Laenen, Dr. E.	FOM
Motylinski, Drs. P.	FOM
Mulders, Prof.dr. P.J.G.	VU
Nyawelo, B.Sc. T.S.	FOM
Pijlman, Drs. F.	VU
Schellekens, Prof.dr. A.N.J.J.	FOM
Veltman, Prof.dr. M.J.G.	GST
Vermaseren, Dr. J.A.M.	FOM
Vogt, Dr. A.	Other
Warringa, Drs. H.	VU
Wit, Prof.dr. B.Q.P.J. de	UU

3. Computer Technology Group

Akker, T.G.M. van den	FOM
Antony, A.T.	FOM
Blokzijl, Dr. R.	FOM
Boterenbrood, Ir. H.	FOM
Damen, Ing. A.C.M.	FOM
Eijk, Dr. R.M. van der	FOM
Geerts, M.L.	FOM
Harapan, Drs. D.	FOM
Hart, Ing. R.G.K.	FOM
Heubers, Ing. W.P.J.	FOM
Huyser, K.	FOM
Koeroo, Ing. O.A.	FOM
Kuipers, Drs. P.	FOM
Leeuwen, Drs. W.M. van	FOM
Li, H.	FOM
Oudolf, J.D.	Other
Salomoni, Drs. D.	FOM
Schimmel, Ing. A.	FOM
Steenbakkers, Ir. M.F.M.	FOM
Tierie, Mw. J.J.E.	FOM
Venekamp, Drs. G.M.	FOM
Wijk, R.F. van	FOM

4. Electronics Technology Group

Balke, D.	FOM-UU
Berkien, A.W.M.	FOM
Beuzekom, Ing. M.G.van	FOM
Boer, J. de	FOM
Boerkamp, A.L.J.	FOM
Born, E.A. van den	FOM
Evers, G.J.	FOM
Fransen, J.P.A.M.	FOM
Gotink, G.W.	FOM
Groen, P.J.M. de	FOM
Groenstege, Ing. H.L.	FOM
Gromov, Drs. V.	FOM
Haas, Ing. A.P. de	FOM
Heine, Ing. E.	FOM
Heutenik, B.	FOM
Hogenbirk, Ing. J.J.	FOM
Jansen, L.W.A.	FOM
Jansweijer, Ing. P.P.M.	FOM
Kieft, Ing. G.N.M.	FOM
Kluit, Ing. R.	FOM
Koopstra, J.	UVA
Kroes, Ir. F.B.	FOM
Kruijer, A.H.	FOM
Kuijt, Ing. J.J.	FOM
Mos, Ing. S.	FOM
Peek, Ing. H.Z.	FOM
Reen, A.T.H. van	FOM
Reus, D.P.	FOM
Schipper, Ing. J.D.	FOM
Sluijk, Ing. T.G.B.W.	FOM
Stolte, J.	FOM
Timmer, P.F.	FOM
Verkooijen, Ing. J.C.	FOM
Vink, Ing. W.E.W.	FOM
Yona, Y.	FOM
Zevering, J.	FOM-VU
Zwart, Ing. A.N.M.	FOM
Zwart, F. de	FOM

5. Mechanical Engineering Group

Arink, R.P.J.	FOM
Band, H.A.	FOM
Boer Rookhuizen, H.	FOM
Boucher, A.	FOM
Buskop, Ir. J.J.F.	FOM
Doets, M.	FOM

Duisters, D.H.	Other
Kaan, Ir. A.P.	FOM
Klpping, Ir. R.	FOM
Korporaal, A.	FOM
Kraan, Ing. M.J.	FOM
Lassing, P.	FOM
Lefévere, Y.	FOM
Liem, Ing. A.M.H.	FOM
Munneke, Ing. B.	FOM
Riet, Ing. M.	FOM
Schuijlenburg, Ing. H.W.A.	FOM
Snippe, Ir. Q.H.C.	FOM
Thobe, P.H.	FOM
Verlaat, Ing. B.A.	FOM
Werneke, Ing. P.J.M.	FOM

6. Mechanical Workshop

Arends, Mw. W.	FOM
Berbee, Ing. E.M.	FOM
Beumer, H.	FOM
Boer, R.P. de	FOM
Boer, Ir. Y.R. de	FOM
Bozkus, B.	FOM
Bron, M.	Other
Brouwer, G.R.	FOM
Buis, R.	FOM
Burg, R.H. van der	Other
Ceelie, L.	UVA
Hagedorn, J.	Other
Homma, J.	FOM
Jaspers, M.J.F.	UVA
John, D.	FOM
Kok, J.W.	FOM
Kuilman, W.C.	FOM
Langedijk, J.S.	FOM
Leguyt, R.	FOM
Martis, J.	FOM
Mul, F.A.	FOM-VU
Oskamp, C.J.	FOM
Overbeek, M.G. van	FOM
Petten, O.R. van	FOM
Rem, Ing. N.	FOM
Rietmeijer, A.A.	FOM
Roeland, E.	FOM
Rövekamp, J.C.D.F.	UVA
Stoffelen, N.	FOM
Veen, J. van	FOM
Willemse, M.A.	FOM

7. Management and Administration

Berg, A. van den	FOM
Buitenhuis, W.E.J.	FOM
Bulten, F.	FOM
Doest, Mw. C.J.	FOM
Dokter, J.H.G.	FOM
Echtelt, Ing. H.J.B. van	FOM
Egdom, T. van	FOM
Faassen, Mw. N.F.	Other
Geerinck, Ir. J.	Other
Greven-v.Beusekom, Mw. E.C.L.	FOM
Heuvel, Mw. G.A. van den	FOM
Kerkhoff, Mw. E.H.M. van	FOM
Kesgin-Boonstra, Drs. Mw. M.J.	FOM
Kleinsmiede-van Dongen, Mw. T.W.J. zur	FOM
Langelaar, Dr. J.	UVA
Langenhorst, A.	FOM
Lemaire-Vonk, Mw. M.C.	FOM
Mors, A.G.S.	UVA
Mulders, Mw. S.A.M.P.	FOM
Pancar, M.	FOM
Rijksen, C.	FOM
Rijn, Drs. A.J. van	FOM
Schram - Post. Mw. E.C.	FOM
Spelt, Ing. J.B.	FOM
Vervoort, Ing. M.B.H.J.	FOM
Visser, J.	FOM
Vries, W. de	FOM
Willigen, E. van	FOM
Witlox, Ing. W.M.	Other
Woortmann, E.P.	FOM

8. Apprentices in 2003

Abou El Khair, M.M.	Computer Technology
Amrath, Mw. D.	Hermes
Bekkum, E.M.W. van	Mechanical Engineering
Blok, J.	Transition Program
Boer, Y.R. de	Atlas/D0
Bos, E.	Atlas/D0
Boukaiba, K.	Electronics Technology
Breukink, R.W.	Alice
Cuperus, M.	Electronics Technology
Dalhuizen, J.M.	Atlas/D0
Deng, Z.	B-Physics
Dernier, M.	Electronics Technology
Eijk, C.J.	Electronics Technology
Elbers, M.C.	Zeus
Groot, J.C.	Algemeen
Hegeman, J.G.	Atlas/D0
Henze, E.	Mechanical Workshop
Hoekstra, T.	Electronics Technology
Jansen, F.M.	Atlas/D0
Jansen, P.N.J.M.	Electronics Technology
Jimenez-Delgado, P.	B-Physics
Keiser, P.C.H.	Mechanical Workshop
Kemmers, P.	LEP / Delphi
Kerssens, R.	Electronics Technology
Kesteren, Z. van	Atlas/D0
Koek, M.	Mechanical Engineering
Koeroo, O.A.	Computer Technology
Koutsman, A.J.	Zeus
Kruijtzer, G.L.	Atlas/D0
Li, H.	Computer Technology
Limper, Mw. M.	Atlas/D0
Merencia, J.V.J.	Computer Technology
Micharek, Mw. B.	B-Physics
Nijenhuis, Mw. N.	ANTARES

Nowak, Mw. H.T.	Hermes
Otto, J.	Electronics Technology
Parker, A.	Atlas/D0
Pels, M.	Staff
Plas, B.A. van der	Zeus
Putten, S. van der	Zeus
Rashid, Z.	Technical Facilities
Reus, D.P.	Electronics Technology
Rijksen, K.M.	Mechanical Workshop

9. They left us

Adamus, Dr. M.	B-Physics
Akker, Drs. M. van den	LEP/L-3
Apel, A.W.	Mechanical Workshop
Bakel, Drs. ing. N.A. van	B-Physics
Baldew, Drs. S.V.	LEP/L-3
Blom, Dr. H.M.	LEP / Delphi
Boomgaard-Hilferink, Mw. J.G.	Mechanical Engineering
Brantjes, R.M.	Atlas/D0
Bron, M.	Mechanical Workshop
Cossee, Mw. N.	Secretariat / Reception
Dam, Dr. P.H.A. van	LEP / Delphi
Dantzig, Dr. R. van	Transition Program
Dierckxsens, Drs. M.E.T.	LEP/L-3
Dirks, Ir. B.P.F.	Atlas/D0
Doest, J.S.	Secretariat / Reception
Duensing, Mw. Drs. S.	Atlas/D0
Eynck, Dipl.Phys. T.O.	Theory
Garutti, Mw. dr. E.	Hermes
Grijpink, Drs. S.J.L.A.	Zeus
Hansen, Dr. J.E.	Theory
Harmsen, C.J.	Electronics Technology
Heesbeen, Dr. ing. D.	Hermes
Hegeman, J.G.	Mechanical Workshop
Hierck, Dr. R.H.	B-Physics
Hollenberg, P.A.M.	Mechanical Workshop
Hover, Ing. J.P.	Mechanical Engineering
Iersel, Mw. drs. M. van	Theory
Joosten, Mw. dr. K.	Computer Technology
Kittel, Prof.dr. E.W.	Atlas/D0
Koek, M.	Mechanical Engineering
Kok, Ing. E.	Electronics Technology
Langedijk, J.S.	Mechanical Workshop
Leeuwen, Dr. M. van	Alice
Li, H.	Computer Technology
Limper, Mw. M.	Atlas/D0
Louwrier, Dr. P.W.F.	Staff
Luigjes, J.A.	Atlas/D0
Mevius, Mw. dr. M.	B-Physics
Mulders, Mw. P.N.	Personnel Department
Nawrot, Dr. A.	B-Physics
Ouchrif, Dr. M.	B-Physics
Peeters, Dr.ir. S.J.M.	Atlas/D0
Peters, Dr. O.	Atlas/D0
Pijll, Drs. E.C. van der	Transition Program
Rewiersma, Ing. P.A.M.	† 28/2/03 Electronics Technology
Riccioni, Dr. F.	Theory
San Segundo Bello, Ir. D.	Transition Program
Schagen, Dr. S.E.S.	Zeus
Schillings, Drs. E.	Alice
Scholte, Dr. ir. R.C.	Atlas/D0
Som de Cerff, N.	Atlas/D0
Stoffelen, N.	Mechanical Workshop
Syryczynski, Dr. K.	B-Physics
Tump, I.	Mechanical Workshop
Velthuis, Dr. ir. J.J.	Zeus

FOM, and the universities UVA, VU, KUN and UU are partners in NIKHEF (see colofon). UL and UT denote the universites of Leiden and Twente. GST stands for guest. Other abbreviations refer to the experiments, projects and departments.